

THERAPEUTIC POTENTIAL OF SOME HERBS AND STRUCTURE OF BERBERRUBINE-DNA COMPLEX

A THESIS

*Submitted in partial fulfilment of the
requirements for the award of the degree*

of
DOCTOR OF PHILOSOPHY
in
BIOTECHNOLOGY

by

SYED ASIF HASSAN



DEPARTMENT OF BIOTECHNOLOGY
INDIAN INSTITUTE OF TECHNOLOGY ROORKEE
ROORKEE-247 667 (INDIA)

NOVEMBER, 2010

©INDIAN INSTITUTE OF TECHNOLOGY ROORKEE, ROORKEE 2010
ALL RIGHT RESERVED



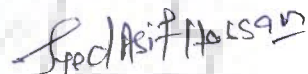


INDIAN INSTITUTE OF TECHNOLOGY ROORKEE ROORKEE


CANDIDATE'S DECLARATION

I hereby certify that the work which is being presented in the thesis entitled "Therapeutic potential of some herbs and structure of berberrubine-DNA complex" in partial fulfilment of the requirements for the award of the Degree of Doctor of Philosophy and submitted in the Department of Biotechnology of the Indian Institute of Technology Roorkee, Roorkee is an authentic record of my own work carried out during a period from July 2005 to Oct 2010 under the supervision of Prof. Ritu Barthwal, Professor & Head, Department of Biotechnology, Indian Institute of Technology Roorkee, Roorkee, India.

The matter embodied in this thesis has not been submitted by me for the award of any other degree of this or any other Institute.


(SYED ASIF HASSAN)

This is to certify that the above statement made by the candidate is correct to the best of my knowledge.


(Ritu Barthwal)
Supervisor

Date: 08.11.10

The Ph.D. Viva-Voce examination of **Mr. SYED ASIF HASSAN**, Research Scholar, has been held on.....

Signature of Supervisor

Signature of External Examiner

ACKNOWLEDGEMENT

“Allah understands our prayers even when we can't find the words to say them.”

This piece of work would have been never accomplished without Almighty Allah's blessings and His power that work within me. I thank god for everything with which I am blessed with.

This thesis is the end of my long journey in obtaining my degree but I have not traveled in a vacuum in this journey. There are some people who made this journey easier with words of encouragement and their contribution in assorted ways to the research and the making of the thesis deserved special mention. It is a pleasure to convey my gratitude to them all in my humble acknowledgment.

In the first place I would like to record my gratitude to my supervisor, Prof. Ritu Barthwal, Head, Department of Biotechnology for her supervision, advice, and guidance from the very early stage of this research as well as giving me extraordinary experiences through out the work. Above all and the most needed, she provided me unflinching encouragement and support in various ways which always encouraged me to do hard work. Her involvement with her originality has nourished my intellectual maturity and enriched my growth as a student and a researcher.

Special thanks are due to Prof. Sudha Mahajan Cowsik, Prof. Aparna Dixit, Dr. Naveen Navani, Dr. Partha Roy and Dr. Maya S. Nair, for taking intense interest in this study as well as providing valuable suggestions that improved the quality of this study.

I am also thankful to the faculty members and staff of the Department of Biotechnology, IIT Roorkee for their support and help.

I would also like to gratefully acknowledge my respected seniors Dr. Manpreet, Dr. Prashansa, Dr. Durai Raj, Dr. Amit Kumar, Dr. Kushuma Bist and Dr. Sulaxana. Special thanks are due to my friend and senior colleague Dr. Lata Chauhan for always being my side during the toughest times. I was lucky to have such a good friend and partner at work.

This thesis would have been a distant dream without care and support of my wife Arshiya Hassan. She has been a pillar of support during the stressful periods, a great listener and has always been available for me. Her wonderful sense of humor helped me to see the positive sides of even the most difficult moments. Her beautiful smile was always being powerful source of liveliness in monotonous life.

This thesis would not be in its present state without the support of my dearest friends and colleague Dhruv Kumar, Pradeep T.P and Sweta Tripathi. They always encouraged me to grow and to expand my thinking. This helped me to concentrate on completing my thesis and supported intectually and mentally during the course of this

work. I would also like to thank my junior colleagues, Miss Jyoti Tomor, Miss Gouri Sharma, Mr. Naresh Kumar and Mr. Amit Dubey for their support during my thesis.

“Wherever you are its your friends who make your world” its true because of the direct and indirect support and help from my friends Mr. Vivekanand Malviya, Mr. Hari Narayan, Mr. Vikrant, Mr. Anuj Aroora, Mr. Kishore, Mr. Imran, Mr. Tabish Alam, Mr. Kuldeep, Mr. Rizwan, Mr. Omkar, Mr. Sahag, Mr. D K, Mr. Sanjay Dudawad, Mr. Ajith, Mr. Gaurav Sharma, Mr. Sharukh, Mr. Guru, Mr. Dabbu and Mr. Pushkar. They provided me the joyful, affectionate and healthy environment during my stay at Roorkee for accomplishing my goal.

“Family is the compass that guide us”, Where would I be without my family? My respected parent Mr. Syed Zubair Alam and Mrs Ishrat Nasreen deserve special mention for their unending love, inseparable support and prayers during my Ph.D. experience. I feel deep sense of gratitude for my mummy and papa. They always encouraged me in all my endeavours and felt proud of my every achievement. I would like to extend my sincere thanks to my Majhlae Abbi–Mr. Saeed Alam for his indirect support to make this journey so congenial and easy. I am thanking him for his memorable concern, affection and constant care. Thanks to my loving sister Shahina Afroz and my brother in law for their affection and moral boost up whenever needed. I am grateful to my in-laws whose faith on me has always inspired me in this venture.

How can I forget to mention the support of my sweet cousin sisters and brothers Saba Alam, Sadaf Alam, Sana Alam, Shefa, Saif, Atif and Arif Alam. Last but not the least I am thankful to my sweet sister-in-law Miss Tarbiya Jamil for her support and prayers for my career.

And to the rest, I extremely thankful to those people, whose names have been unknowingly left, thank you very much for your prayers. It really helped a lot. I apologize and believe, they will be always with me as they were there in the time of need.

Last but not the least; I would like to thank G. B. Pant Institute of Himalayan environment and Development (GBPIHED) for providing financial support for my research work.

Syed Asif Hassan

ABSTRACT

Over the last two decades many strategies have been developed to design drugs to control diseases like cancer and diabetes mellitus. Advancement of in our understanding of these diseases at the molecular level has provided us with new effective armors to diagnose, combat and control the spread of these diseases. In this regard the understanding of the interaction of small molecules with macromolecules like protein or DNA has opened the doors for rational drug design against cancer and type 1 and 2 diabetes mellitus. Although it is type 2 diabetes which is more prevalent and the main driver of the diabetes epidemic in India, it is noted that prevalence of type 1 diabetes in India is also on the rise. In spite of the introduction of hypoglycemic agents, diabetes and the related complications continue to be a major medical problem. Several bioactive molecules have been studied and employed for their antidiabetic activity but have shown toxic effects which cannot be bypassed. Recently the role of herbal remedies is in focus due to the side effects associated with oral hypoglycemic agents and insulin. More than 400 plants with glucose-lowering effects are known in India. Some of them have been tested and the active components are being isolated. In this context similar cytotoxicity of synthetic drugs are observed for antineoplastic agents prevalent in cancer treatment. Thus there is continuing search for new antidiabetic and anticancer drugs of herbal origin. A substantial body of research has been directed towards screening of drugs acting as stimulator of insulin (insulinotropic agent) or drugs which regenerate the injured pancreatic beta cells. At the same time, focus is on for developing and improvising the existing methodology to screen potent anticancer drugs from herbal origin. The present research work is directed towards screening components which shows insulinotropic

properties. As well as screen phytochemical enriched fractions which targets topoisomerases and bind to specific nucleic acid sequences of oncogenes. Therefore, this work will allow us to screen both antidiabetic and antitumor agents. To achieve the goal of screening drugs from herbal origin; we have used both *in vitro* and *in vivo* method to screen active insulinotropic agents phytochemical from *Cinnamomum zeylanicum* and antitumor components through topoisomerase I and II inhibition assay and restriction inhibition assay using specific restriction endonucleases. In order to gain understanding of the mode of action berberrubine-a protoberberine analogue which is known to have antitumor potential, we present here the structure-conformation of berberrubine d-(CCAATTGG)₂ complex based on 1D, 2D ¹H and ³¹P NMR spectroscopy measurements followed by restrained Molecular Dynamics simulations based on observed NOEs.

The present work is a significant step in screening and understanding the molecular basis of action of the active phytochemical rich fractions and berberrubine. The PhD thesis work has been reported in the form of 6 chapters.

Chapter 1 contains introduction of the subject, a comprehensive review of the literature and scope of thesis.

Chapter 2 deals with materials, methods, results and discussion of the antidiabetic study of *Cinnamon zeylanicum*. The methodology employed for preparation of methanol and aqueous extract, selection of animals used for *in vivo* studies, induction of type 1 diabetes mellitus in male wistar rats, estimation of blood glucose level of extract treated of both normal and induced type 1 fasted rats, estimation of OGTT (oral glucose tolerance test) of both normal and induced type 1 diabetic fasted rats, estimation of lipid, glycogen, SGOT, SGPT, alkaline phosphatase, urea, creatinine and insulin level of both normal and treated rats is satisfied.

Preparation of different phytochemical rich fractions from the aqueous extract of *Cinnamomum zeylanicum*, estimation of in vitro release of insulin from normal and treated rat pancreas and also methodology employed for semiquantitative reverse transcriptase-PCR, histopathological studies, toxicity study and statistical analysis is also given. The present study showed better hypoglycemic and antihyperglycemic property of 200 mg/kg body weight aqueous extract than methanol extract of *cinnamomum zeylanicum* in normal and streptozotocin induced type 1 diabetic mellitus (T1DM) animals. In case of treated animals, the hepatic glycogen increased by 63.27 % and serum SGOT, SGPT, ALKP, creatinine and urea levels were reduced by 68.04, 64.42, 47.05, 52.63 and 62.03 % respectively, after 15 days of oral administration of the extract. While small change towards normalcy was observed in the lipid profile of experimental animals. In order to understand the molecular mechanism of action, the expression profile of enzymes involved in glucose homeostasis was analyzed. The role of saponins as an antidiabetic and insulinotropic agent from *Cinnamomum zeylanicum* was identified. The results indicate the favorable effect of saponin rich fractions of the aqueous extract of *cinnamomum zeylanicum* in bringing down the severity of T1DM.

Chapter 3 deals with materials, methods, results and discussion of the qualitative and quantitative study of drug-DNA interaction by inhibition of restriction endonucleases and its application in screening DNA interacting components from herbal plants. This includes methodology for transformation of bacterial cells, plasmid isolation, quantification of DNA using UV visible spectrophotometer, DNA fragment isolation from pBCKS+ plasmid DNA for restriction inhibition assay, transformation and isolation and linearization of pQE32 plasmid DNA, preparation of phytochemical rich fractions from aqueous extract of *Cinnamomum zeylanicum*, binding studies,

screening for the presence of *EcoRI* and *HindIII* recognition sequence in the mRNA, STS and ESTs of breast oncogene and agarose gel electrophoresis. The present study showed the use of the restriction inhibition assay, using *HindIII*, *EcoRI* and *EcoRV* restriction enzymes, to evaluate the binding specificity of DNA with anticancer drugs (mitoxantrone, berberine and palmitine). The inhibition of endonuclease *HindIII* at 220 μM concentration was observed with mitoxantrone giving a direct evidence of the co-existence of concentration and sequence specificity for drug-DNA interaction. The present study showed that a simple and rapid method can be used to screen, plant extracts and the active phytochemicals involved in binding with restriction sequences of *EcoRI* and *HindIII* in a relatively qualitative and quantitative manner. The results show that among; Fraction I- anthraglycosides, bitter principles, flavonoids and arbutin, Fraction II-saponins, Fraction III- Cardiac glycosides and Fraction IV- terpenes, coumarins, phenol carboxylic acids, valepotriates. The Fraction II, saponins rich fraction from *Cinnamomum zeylanicum* shows inhibition at minimum concentration 15 $\mu\text{g/ml}$ and 2.1 $\mu\text{g/ml}$ for *EcoRI* and *HindIII* restriction endonucleases, respectively. Secondly, the *EcoRI* and *HindIII* restriction sites were found repeatedly in the cDNA and ESTs of BRCA2 early onset oncogene. These observations project the possible use of the screened phytochemical as an anticancer agent, targeting the expression of an oncogene (BRCA2). Through this study we postulate for the first time the use of restriction inhibition assay as a rapid and simple method to screen possible anticancer phytochemical from herbal plants.

Chapter 4 deals with materials, methods, results and discussion of anti topoisomerases activity of *Picrorrhiza kurroa*. This includes the methodology employed for preparation of the *Picrorrhiza kurroa* extract, inhibition of catalytic activity of human, topoisomerase I (relaxation assay), stabilization of DNA–enzyme

covalent complex studies, preincubation studies, human topoisomerase II α inhibition assay and agarose gel electrophoresis. The present study describes the inhibitory effect of the aqueous extract of *Picrorrhiza kurroa* on human topoisomerases by measuring the relaxation of superhelical plasmid pBR322 DNA. The aqueous extract inhibited topoisomerase I and II α in a concentration-dependent manner (Inhibitory concentration (IC) \approx 25 and 50 μg , respectively). From the stabilization studies of topoisomerase I-DNA complex and preincubation studies of topoisomerase I and II α with the extract, we conclude that the possible mechanism of inhibition is both; 1) stabilization of covalent complex of topoisomerase I-DNA complex and 2) direct inhibition of the enzyme topoisomerases. These findings might explain the antineoplastic activity of *Picrorrhiza kurroa* and encourage new studies to elucidate the usefulness of the extract as a potent antineoplastic agent.

Chapter 5 deals with the materials, methods, result and discussion of the NMR studies of interaction of berberrubine with DNA. The detailed structural analysis is carried out using Nuclear Magnetic Resonance 1D NMR, 2D Nuclear Overhauser Enhancement Spectroscopy (NOESY) and ^{31}P - ^{31}P NOESY exchange techniques. The following experiments were performed on the berberrubine-DNA complex - ^1H and ^{31}P NMR titration studies at various drug (D)/DNA duplex (N) ratios up to 1.0 at 278, 283 K and 298 K in 90% H_2O and 10% D_2O , temperature dependence of ^{31}P and ^1H NMR of the berberrubine-DNA complex having D/N = 1.0 in the range of 278 – 313 K; 2D ^{31}P - ^{31}P exchange spectra of drug-DNA complex by phase sensitive NOESY using mixing time of 200 ms at 278 K, 283 K and 298 K for D/N=1.0; 2D NOESY ^1H - ^1H at D/N = 1.0 using mixing time $\tau_m = 200$ ms at 278 K, 283 K, 298 K in 90 % H_2O and 10 % D_2O . The ^{31}P NMR shows a maximum downfield shift of 0.29 ppm for the A3pA4 resonance contrary to that observed for

intercalating drugs e.g., Adriamycin or daunomycin) which show downfield shift upto 1.6 ppm at the interaction site due to changes in the phosphodiester angle of the DNA. The 2 D proton spectra of the 1:1 berberrubine-d-(CCAATTGG)₂ complex at 298 K shows no significant shift in DNA base, sugar or the NH protons. The drug protons H 19, 20 and H 24 showed upfield shift of 0.24 ppm and 0.18 ppm, respectively and H 14 showed an upfield shift of 0.14 ppm upon binding to the DNA. The inter-drug cross peaks: H 10-H 5, H 10-H 14, H 10-H 24, H 10-H 31, 32, H 28-H 24 indicates that two drug molecules are stacked over each other in a possible antiparallel orientation in the complex. Drug protons H 10, H 16, 17 and H 31, 32 gave strong NOEs with C2NH₂^b, C2NH₂^{nb}, A4H₂, T5H₂' and T5H₂'', respectively. The observed 19 inter-molecular NOEs connectivities of the drug with the sugar H1', H2'/2'' and NH₂^{nb/b}, CH₃ and the A3/A4H₂ region of the DNA supports the minor groove mode of binding of berberrubine in the complex. The restrained molecular dynamics approach using INSIGHT II and DISCOVER showed that the two drug molecules with their aromatic region stacked in an antiparallel pattern lies at the upper minor groove region (5'-CAATT-3') of the DNA. The interaction of the drug at this site of the DNA was stabilized by van der Waals, electrostatic and hydrogen bonding forces. The specific drug-DNA structure thus obtained spells out exact contacts the drug makes with DNA, which is important for formation of ternary complex with enzyme and hence the molecular basis of topoisomerase II poisoning.

Chapter 6 summarizes the result obtained and their implication in understanding the therapeutic potential of *Picrorrhiza kurroa* and *Cinnamom zeylanicum* against cancer and streptozotocin induced type 1 diabetes mellitus as well as role of berberrubine as topoisomerase II poison.

LIST OF PUBLICATIONS

To be communicated:

1. Hassan S A, Chauhan L, Gupta P, Dixit A, Cowsick S M, Barthwal R. A Qualitative and Quantitative assay to study anticancer drug-DNA Interactions based on the sequence Selective Inhibition of Restriction Endonucleases.
2. Syed Asif Hassan, Maya S Nair, Sulaxna Sharma and Ritu Barthwal “Saponins from aqueous extract of *Cinnamomum zeylanicum*: A potential therapeutic agent for Streptozotocin induced type I (T1DM) diabetic rats”. Structure determination of promoter site containing Octamer d-(CCAATTGG)₂ using Nuclear Magnetic Resonance and restrained molecular dynamics and comparison with the crystal structure.
3. Hassan S A and Barthwal R Aqueous extract of *Picrorrhiza kurroa Royle ex Benth*- a potent inhibitor of human topoisomerases.
4. Hassan S A, Tripathi S, Pradeep T.P, Maya S. N and Barthwal R. Berberrubine binding studies with promoter site sequence d-(CCAATTGG)₂ using nuclear magnetic resonance and molecular modeling technique.

Papers in National Conference

- Hassan S A, Gupta P, Cowsick S M, **Chauhan L**, Dixit A, Barthwal R (2007). DNA – Anticancer Drug Interaction Studies Using Sequence Selective Inhibition of Restriction Endonucleases. *National Symposium on Biophysics: Trends in Biomedical Research IBS 2007, Department of NMR and MRI facility AIIMS, New Delhi India, 13-15 February 2007, entitled “” pg no. 181 Abs. no. pp-118.*

| CONTENTS | | PAGE NO. |
|---|---|---------------------|
| CHAPTER 1 | | |
| 1.0 | Introduction and review of literature | 1 |
| 1.8 | Scope of thesis | 39 |
| CHAPTER 2 | | |
| “Saponins from aqueous extract of <i>Cinnamomum zeylanicum</i>: A potential therapeutic agent for streptozotocin induced agent for streptozotocin induced type 1 (T1DM) diabetic rat”. | | |
| 2.1 | MATERIALS AND METHOD | |
| 2.2.1 | Preparation of the bark extract in solvents of increasing polarity | 47 |
| 2.2.2 | Experimental model (animals) | 47 |
| 2.2.3 | Induction of type 1 diabetes mellitus | 48 |
| 2.2.4 | <i>In-Vivo</i> study | 49-54 |
| 2.2.5 | Preparation of the various phytochemical rich fractions from aqueous extract of <i>Cinnamomum zeylanicum</i> | 54 |
| 2.2.6-10 | Effect of aqueous and its phytochemical-rich fractions of cinnamon on the release of insulin by <i>in vivo</i> and <i>in vitro</i> methods, respectively; Semiquantitative reverse transcriptase-PCR; Histopathology of Pancreatic Tissue and Toxicity study; Statistical analysis | 55-58 |
| 2.3 | RESULTS | 58 |
| 2.3.1 | Hypoglycemic test in normal Male Wistar Rats | 58 |
| 2.3.2 | Oral Glucose Tolerance Test (OGTT) in normal Male Wistar Rats | 59 |
| 2.3.3 | Oral Glucose tolerance test (OGTT) in streptozotocin induced type 1 diabetic rats | 60 |
| 2.3.4 | Activity of the aqueous extract for short duration | 61 |
| 2.3.5 | Antidiabetic activity of aqueous extract for long duration | 62 |
| 2.3.6 | Acute Toxicity studies | 63 |
| 2.3.7 | Body weight levels | 63 |
| 2.3.8 | Estimation of lipid profile | 64 |
| 2.3.9 | Glycogen level in liver | 65 |
| 2.3.10 | Liver function tests serum SGOT, SGPT, ALKP, Creatinine and Urea | 65 |
| 2.3.11 | Effect of aqueous extract of cinnamon on serum insulin level | 66 |
| 2.3.12 | Effect of fraction (I to IV) on the <i>in vitro</i> release of insulin | 67 |
| 2.3.13 | Gene expression profile | 68 |
| 2.3.14 | Histopathological studies | 69 |
| 2.4 | DISCUSSION | 70 |
| CHAPTER 3 | | |
| A qualitative and quantitative assay to screen the DNA interacting component based on the sequence selective inhibition of restriction endonucleases | | |
| 3.1 | MATERIALS AND METHOD | |
| 3.2.1 | Transformation of bacterial cells | 78 |
| 3.2.2 | Plasmid Isolation | 78 |
| 3.2.3 | Quantification of DNA using spectrophotometer | 79 |
| 3.2.4 | DNA fragment for restriction inhibition assay | 79 |
| 3.2.5 | Transformation and Isolation and linearization of pQE32 plasmid DNA | 80 |

| | | |
|--|--|-------|
| 3.2.6 | Binding Studies | 80 |
| 3.2.7 | Preparation of aqueous extract of <i>Picrorrhiza kurroa</i> and <i>Cinnamomum zeylanicum</i> | 81 |
| 3.2.8 | Screening of DNA-extract binding studies of <i>Cinnamomum zeylanicum</i> and <i>Picrorrhiza kurroa</i> by restriction inhibition assay | 81 |
| 3.2.9 | Preparation of phytochemical rich fractions from aqueous extract of <i>Cinnamomum zeylanicum</i> | 82 |
| 3.2.10 | Screening of restriction inhibition activity of phytochemical rich fractions from aqueous extract of <i>Cinnamomum zeylanicum</i> | 82 |
| 3.2.11 | Screening for the minimum inhibitory concentration of the active inhibitory phytochemical rich fractions | 83 |
| 3.2.12 | Screening for the presence of <i>EcoRI</i> and <i>HindIII</i> recognition sequence in the mRNA, STS and ESTs of the oncogene | 83 |
| 3.3 | RESULTS and DISCUSSION (A) | 84-95 |
| 3.4 | RESULT (B) | |
| 3.4.1 | Screening of DNA-Extract binding studies of <i>Cinnamomum zeylanicum</i> and <i>Picrorrhiza kurroa</i> by restriction inhibition assay | 95 |
| 3.4.2 | Screening of restriction inhibition activity of phytochemical rich fractions from aqueous extract of <i>Cinnamomum zeylanicum</i> | 97 |
| 3.4.3 | Screening for the minimum inhibitory concentration of the active inhibitory phytochemical rich fractions (I to III) | 99 |
| 3.4.4 | Screening for the presence of <i>EcoRI</i> and <i>HindIII</i> recognition sequence in the mRNA and STS and ESTs of the oncogenes | 103 |
| 3.5 | DISCUSSION (B) | 104 |
| CHAPTER 4 | | |
| Aqueous extract of <i>Picrorrhiza kurroa</i> Royle ex Benth-A potent inhibitor of human topoisomerases | | |
| 4.1 | MATERIALS AND METHOD | |
| 4.2.1 | Preparation of the <i>Picrorrhiza kurroa</i> extract | 108 |
| 4.2.2 | Inhibition of catalytic activity of Human Topoisomerase I (relaxation assay) | 109 |
| 4.2.3 | Stabilization of DNA-enzyme covalent complex studies | 109 |
| 4.2.4 | Preincubation analysis | 109 |
| 4.2.5 | Human Topoisomerase II α inhibition assay | 109 |
| 4.2.6 | Agarose gel electrophoresis | 110 |
| 4.3 | RESULTS AND DISCUSSION | |
| 4.3.1 | Inhibition of topoisomerase I | 111 |
| 4.3.2 | Preincubation analysis | 112 |
| 4.3.3 | Effect of aqueous extract on the Relaxation Activity of Topoisomerase II α | 114 |
| 4.4 | CONCLUSION | 115 |
| CHAPTER 5 | | |
| Studies on complex of berberrubine with promoter site containing octamer d-(CCAATTGG)₂ by using phosphorous-31 and proton nuclear magnetic resonance spectroscopy and restrained molecular dynamics approach | | |

INTRODUCTION AND REVIEW OF LITERATURE

1.0 INTRODUCTION AND REVIEW OF ANTIDIABETIC STUDY

1.1 INTRODUCTION TO TYPE 1 DIABETES MELLITUS (T1DM)

Every year, thirty thousand people worldwide are diagnosed with type 1 diabetes mellitus (T1DM). T1DM, also called autoimmune diabetes, is a multi factorial disease affecting predisposed individuals and involving genetic susceptibilities, environmental triggers, as well as unbalanced immune responses. The detail of the same is discussed in the following section.

1.2 CAUSES

- Patients with type 1 diabetes are believed to have a genetic susceptibility to developing the disease. Genetic predisposition has traditionally been considered to originate from the Class II major histocompatibility complex (MHC) genes on chromosome 6p21, and is associated with HLA-DR and DQ. Approximately 30 % of the type 1 diabetic patients are heterozygous for the high risk HLA-DR3/4 or HLA-DQ2/Dq8. Some also lack the protective HLA-DR2 or HLA-DQ6 which increases type 1 diabetes susceptibility (Resic-Lindehammer et al., 2008; Morran et al., 2008).
- Autoimmunity–type 1 diabetes caused due to autoimmunity, is a type of self-allergy that induces the T-Lymphocytes of the immune system to attack the pancreatic islets, as if they are a foreign invader.

- Immune cells such as macrophages and T cells have been identified as the mediators of the pancreatic islet β -cell destruction and have been shown to act by releasing cytotoxic molecules including cytokines, oxygen free radicals and NO (Reijonen and Concannon, 2006). Perforin and granzymes released from the granules of cytotoxic T-cells are toxic to the β -cells resulting in their destructions.

- Environmental factors have also been suggested as inducers of autoimmunity since several studies showed its involvement in the pathogenesis of type 1 diabetes. The environmental factors can be classified into three major groups: viral infections (e.g., Enterovirus, Cytomegalovirus and Rubella Virus), early infant diet (e.g., breast feeding versus early introduction of cow's milk components), and toxins (e.g., N-nitroso derivatives).

1.2 GLUCOSE METABOLISM

Glucose provides a major energy supply for cells. The blood glucose concentration is maintained within narrow limits (4-7 mM) by the regulated production of glucose by liver from glycogenolysis and gluconeogenesis, which is counterbalanced by the glucose absorption from the intestine and regulated peripheral clearance of glucose by tissues such as skeletal muscle, adipose tissue, and the splanchnic bed (intestine and liver tissues are collectively referred as splanchnic bed), including the liver (DeFronzo, 1981; Yki-Jarvinen, 1993). The liver produces glucose by glycogenolysis or via de novo gluconeogenesis mainly from lactate, alanine, pyruvate and glycerol (Wahren et al., 1972; Joseph et al., 1996; Patel, 1989). Insulin decreases endogenous glucose production primarily by suppressing glycogenolysis and by decreasing the glucose synthesis via gluconeogenesis.

| | | |
|------------|--|---------|
| 5.1 | MATERIALS AND METHOD | |
| 5.2.1-4 | Sample Preparation | 118 |
| 5.2.5 | Chemical Shift | 122 |
| 5.2.6 | Spin-Spin Coupling Constant (J) | 122 |
| 5.2.7 | Relaxation Process | 124 |
| 5.2.8 | Two-Dimensional (2D) NMR Techniques | 126 |
| | Nuclear Overhauser Effect Spectroscopy (NOESY) | 128 |
| 5.2.9 | Experimental Parameters | 129 |
| 5.3 | RESULTS AND DISCUSSION | |
| 5.3.1 | Phosphorous-31 NMR Studies of Berberrubine-d-(CCAATTGG) ₂ Complex | 130 |
| 5.3.2 | 2D ³¹ P - ³¹ P Exchange Spectra | 135 |
| 5.3.3 | Temperature Dependence Studies | 137 |
| 5.3.4 | Proton NMR Spectra | 139 |
| | Chemical Shift | 139 |
| 5.3.5 | Structure of Berberrubine-d-(CCAATTGG) ₂ Complex | 142 |
| 5.4 | Restrained Molecular Dynamics Simulations | 161 |
| 5.5 | CONCLUSION | 170 |
| | CHAPTER 6 | |
| 6.0 | Summary and Conclusions | 173-175 |
| | REFERENCES | i-xxvii |

Insulin dramatically inhibits the transcription of the gene encoding phosphoenolpyruvate carboxykinase (PEPCK), the rate-limiting step in gluconeogenesis. Insulin also decreases transcription of the genes encoding fructose 1,6-bisphosphatase (FBP1) and glucose 6-phosphatase (G6Pase) and increase transcription of those encoding glycolytic enzymes such as Glucokinase (GK) and pyruvate kinase and lipogenic enzymes such as fatty acid synthase (FAS) and acetyl CoA carboxylase (ACC).

Hexokinase (HK) catalyzes glucose phosphorylation, which is the first step in glucose uptake in skeletal muscles. Two HK isoforms, HK-1 and Hk-II, are expressed in human skeletal muscle, but only HK-II is regulated by insulin (Vogt et al., 2000), which is a physiological regulator of HK-II mRNA expression in skeletal muscle in-vivo (Shulman et al., 1995). The balance between GS and glycogen phosphorylase activities determines in vivo net glycogen synthesis.

1.3 LIPID METABOLISM

In the type 1 diabetic patient, the consequences of insulin deficiency and glucagon excess provide a hormonal milieu that favors ketogenesis and in the absence of appropriate treatment, may lead to ketonemia and acidosis. Insulin also enhances the transcription of lipoprotein lipase in the capillary endothelium, which hydrolyzes triglycerides present in VLDL and chylomicrons, resulting in release of intermediate-density lipoprotein (IDL) particles (Bellomo et al., 2007). In absence of insulin IDL particles are converted by the liver to more cholesterol rich LDL, resulting in hypertriglyceridemia and hypercholesterolemia. In addition, deficiency of insulin may be associated with increased production of VLDL (Hartge et al., 2007).

1.4 CURRENT THERAPIES

1.4.1 INSULIN THERAPY

By definition, patients with type 1 diabetes require lifelong treatment with insulin to promote glucose utilization. Rapid-, short-, intermediate-, and long-acting insulin preparations are available.

1.4.2 PANCREAS TRANSPLANT IN TYPE 1 DIABETES MELLITUS:

Pancreas transplant is a widely viable option. It requires a dedicated and experienced team. Long term immunosuppression is required and quite expensive.

1.4.3 ISLET CELL TRANSPLANT IN TYPE 1 DIABETES MELLITUS:

There is a resurgent interest in islet transplantation due to recent successes reported by a group in Edmonton, Canada. Over 400 islet cell allografts were performed worldwide within the past decade. Although the simplicity of administration (intra portal injection of islets) makes it attractive, patients require islets from at least two donor pancreas (an average 11,000 islet equivalents per kilogram body weight). The necessary islet cell mass required to achieve normoglycemia in the recipient and difficulties in recovering islet tissue from donor pancreas can be limiting factors.

1.4.4 ENGINEERING OTHER CELLS TO PRODUCE INSULIN

In last few years a new era has dawned, exploring the ability to engineer non-islet cells to produce insulin through forced expression of the insulin gene (Flier, 2001; Cheung, 2000; Lee, 2000). So far duodenal K cells, hepatocytes and pituitary cells have been successfully transfected.

1.4.5 TRADITIONAL HERBAL THERAPY FOR DIABETES MELLITUS

Advances in biomedical research have unraveled complex and nonlinear physiological, biochemical and pathological processes involved in causing/fostering diabetes, along with the multiple cross talk of signaling pathways. Therefore this warrants the use of multiple drugs for different target potency for the reversal of all or majority of aspects of the diabetes. At the same time conventional therapeutic measurement available for the treatment are associated with severe side effects along with the development of resistance towards a particular treatment across the prolonged administration of the drugs. Also the present conventional therapeutic approach deals with a symptoms or a specific target for a particular disease or disorders not the root cause (Wagner, 2005). All these drawbacks associated with conventional therapy have triggered the search for a safe and effective alternative source of cure for this disorder. Traditional therapy with a holistic approach and thousand years of experience has come up as the right answer. Traditional therapy comprises lifestyle management and medicinal preparation, which includes medicinal plants, minerals and organic matters (Tiwari, 2005; Tiwari and Madhusudana, 2005). Medicinal plants are the most important component of these medicinal preparations, used by Indian, Chinese, Egyptian, Greek and Roman system of traditional medicines. The plants provide an effective and potential source of hypoglycemic drug. More than 400 plants with glucose-lowering effects are known in India (Grover, Yadav, Vats, 2002; Maiti, Jana, Das, Ghosh, 2004) and some of them have been tested and the active components are being isolated. In spite of having enormous potential to cure many diseases, traditional medicines could not achieve the expected popularity among the scientific community due to some or other reasons. This necessitates a rigorous scientific validation of any drug for the treatment of a particular disease. The probable reasons for

lesser use of these medicines are lack of authentication, identification and qualitative as well as quantitative standardization (Samy and Gopalakrishnakone, 2007; Wagner, 2005). Thus there is continuing, search for new antidiabetic drug by initial purification of medicinal products of herbal origin, so as to eliminate any kind of detrimental components before using herbal preparation. This step is followed by a sequential activity and toxicity analysis along with the identification as well as standardization of active principles using certain modern analytical procedures.

1.4.5.1 *Cinnamomum zeylanicum*- A HERBAL APPROACH IN TYPE 1 DIABETES

MELLITUS CONTROL

Cinnamon is one of the traditional herbs used as a remedy for diabetes. Cinnamon tree (*Cinnamomum zeylanicum*) is a native in South-West Asia, e.g. Sri Lanka, and the bark is sold in powder, scrapings and branches. The main components of cinnamon are reported as cinnamaldehyde (Wijesekera, 1978), cinnamic acid (Hiromu, Katudi, Nenokichi, 1974), tannin (Inokuchi, Okabe, Yamauch, Nagamatsu, 1984) and methylhydroxychalcone polymer (MHCP) (Jarvill-Taylor, Anderson, Graves, 2001). The insulin sensitizing effect of cinnamon has been established in *in vitro* cell lines with adipocytes using rat epididymal adipocyte assay (Broadhurst, Polansky, Anderson, 2000). The insulin mimicking property of hydroxychalcone from cinnamon is reported in 3T3-L1 Adipocytes. In addition, MHCP activated glycogen synthase, inhibited glycogen synthase kinas-3 β and phosphorylated the IR, mimicking the known effect of insulin (Jarvill-taylor et al., 2001).

In this context the aqueous soluble polyphenol-type A polymers are the most active components that increases insulin-dependent *in vitro* glucose metabolism

(Anderson et al., 2004). Cinnamon extract have also shown to enhance the glucose utilization *in vivo*, in a dose dependent manner and also potentiates the insulin-stimulated tyrosine phosphorylation of IR- β and IRS-1 and IRS-1 association with PI 3-kinase, without affecting their protein content in skeletal muscle (Qin, Nagasaki, Ren, Bajotto, Oshida, Sato, 2003). A comparative antidiabetic study of *Cinnamomum cassia* and *Cinnamomum zeylanicum* in normal wistar rat showed higher potency of *Cinnamomum cassia* to (1) control glucose level when challenged with excess of glucose; (2) and stimulate both *in vitro* and *in vivo* insulin release (Verspohl, Bauner and Neddermann, 2005). Cinnamon extract has a regulatory role in a type 2 diabetic animal model (C57BIKsj db/db). It was found to reduce the blood glucose in a dose dependent manner and reduce the triglyceride, total cholesterol and intestinal α -glycosidase activity and enhance serum insulin and HDL-cholesterol levels. It also showed blood glucose-suppressing effect by improving insulin sensitivity or slowing absorption of carbohydrates in the small intestine (Kim and Choung, 2006).

The aim of the present study was to investigate the dose dependence activity of aqueous and methanol extracts of *Cinnamomum zeylanicum* on fasting blood glucose, Oral Glucose Tolerance Test (OGTT), short and long term effects of extracts on blood glucose levels of normal and streptozotocin-induced type 1 diabetic male wistar rats. Out of methanol and aqueous extract of *Cinnamomum zeylanicum* the study was narrowed down to aqueous extract of *Cinnamomum zeylanicum* as it was found to be the most effective for hypoglycemic and antidiabetic effects. To understand the molecular mechanism behind the hypoglycemic and antidiabetogenic nature of the aqueous extract of *Cinnamomum zeylanicum*, lipid profiling, *in vivo* and *in vitro* insulin secretion,

glycogen content and enzyme activity from liver and serum were analyzed to evaluate its effect on biochemical parameters of glucose homeostasis and liver function respectively.

Further its actions at cellular and molecular levels were analyzed by determining its effects on expression of various target genes, e.g. Glucokinase (GK), glucose-6-phosphatase (G6Pase), Phosphoenol pyruvate carboxykinase (PEPCK), Insulin II and Glucose-6-phosphate dehydrogenase (Gpdh) in different target tissues, such as liver and pancreas. Finally, we attempted to identify the hypoglycemic and antihyperglycemic phytochemical group in the aqueous extract of *Cinnamomum zeylanicum*. To the best of our knowledge, this is the first ever report on the role of saponin demonstrating both hypoglycemic, antidiabetic and insulintropic effects at cellular levels for the treatment of streptozotocin induced type I diabetes (T1DM) from the aqueous extract of *Cinnamomum zeylanicum*.

1.5 INTRODUCTION AND REVIEW-INTERACTION OF DRUG AND NUCLEIC ACID

1.5.1 STURCTURE OF NUCLEIC ACID

DNA (deoxyribonucleic acid) and RNA (ribonucleic acid) are polymers of nucleotides linked in a chain through phosphodiester bonds. Each nucleotide consists of three distinct chemical groups, a nitrogenous base, a five-carbon sugar, and a phosphate group. Two different heterocyclic aromatic bases with a purine ring (adenine and guanine) and one heterocyclic aromatic base with pyrimidine ring—thymine and cytosine (composed of carbon and nitrogen) are found in DNA (Fig. 1.1 a-b). In RNA thymine is replaced by uracil. Ribose sugar is found in all RNA molecules while a slightly different sugar, α -D-2-deoxyribose is found in DNA. This is a derivative of β -D-ribose in which

the hydroxyl (–) the 2' position is replaced by hydrogen (–OH) (Fig. 1.1 c). The sugar moiety of DNA is one of the more flexible and dynamic parts of the molecule. The sugar base combination is called nucleoside unit. A nucleotide is a nucleoside phosphorylated at one of the free sugar hydroxyls.

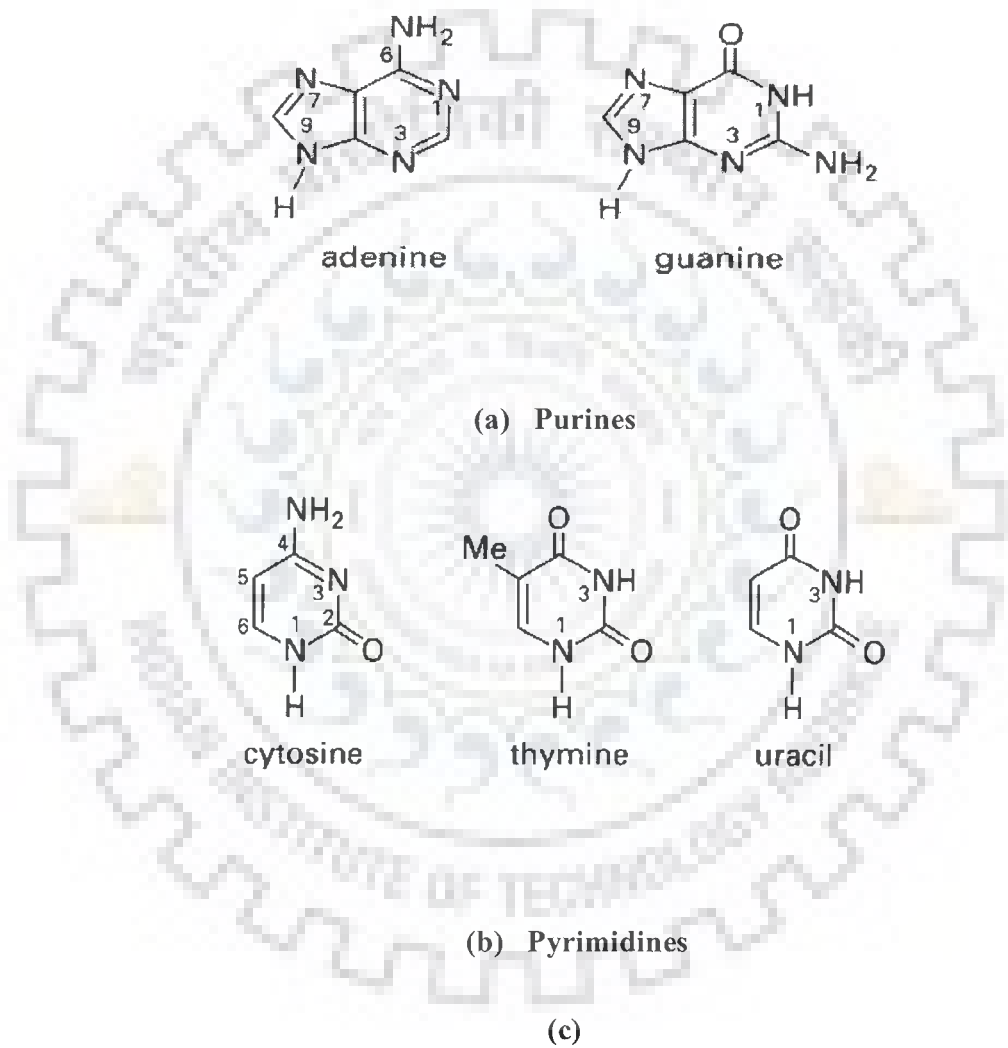


Fig. 1.1: (a) Structural formulae of purines and (b) pyrimidines

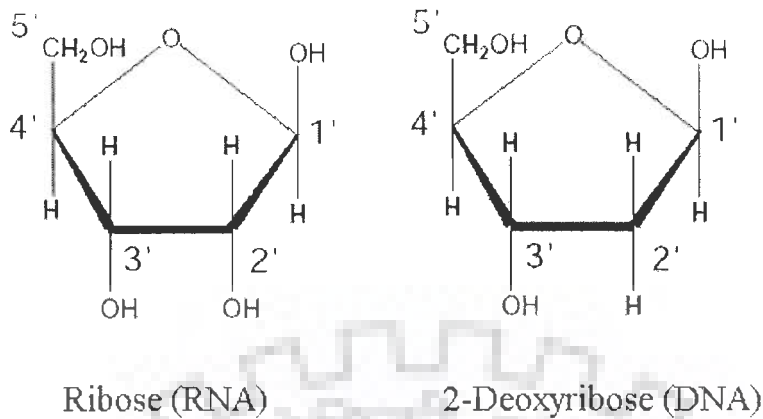


Fig. 1.1: (c) Five membered furanose ring of deoxyribose and ribose sugar

1.5.1.1 CONFORMATION OF SUGAR PHOSPHATE BACKBONE AND FURNOSE SUGAR RING

The conformation of the sugar- phosphate backbone, following the sequential numbering of atoms P –O5'–C5' –C4'etc., is defined by torsional angles $\alpha, \beta, \gamma, \delta, \epsilon$ and ζ . Angles $\nu_0, \nu_1, \nu_2, \nu_3$ and ν_4 decide the geometry of sugar ring (Figure 1.2 (a-b)). The different families of DNA structures are characterized by the values of these torsion angles.

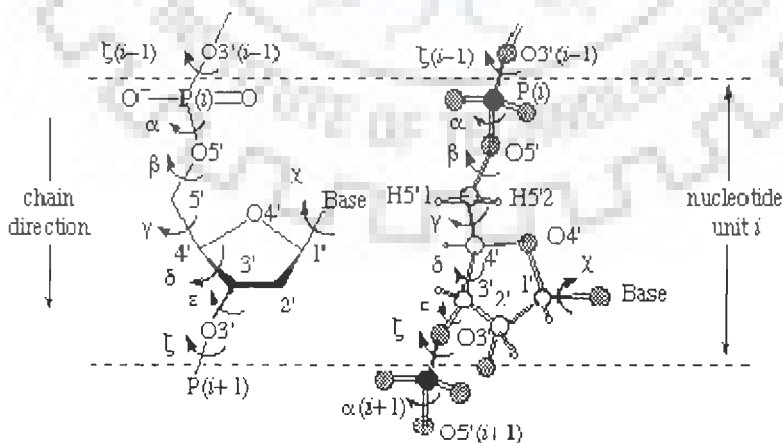


Figure 1.2 (a): Section of a polynucleotide backbone showing the atom numbering and the notation for torsion angles

The ribose sugar geometry is defined by the following five endocyclic torsion angles: ν_0 , ν_1 , ν_2 , ν_3 , ν_4 are denoted by the symbols, respectively. The sequence of atoms used to define each backbone torsion angle is shown in e.g. ν_0 , ν_1 , ν_2 , ν_3 , ν_4 refers to the torsion angle of the sequence of atoms C4'-O4'-C1'-C2', etc.

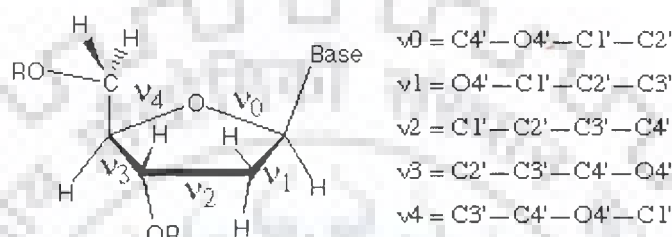


Figure 1.2 (b): Endocyclic torsional angles in the sugar ring

The magnitudes of such angles are all interrelated and, therefore, the geometry of the ribose ring can be defined from two parameters: the pseudorotation phase angle (P) and the pucker amplitude. The ribose ring is not a planar and usually presents C2'-endo (South) or C3'-endo (North) conformation. For the sugar pucker conformation, homonuclear $^3J_{\text{H-H}}$ coupling constant serve as the most direct determinant. These constants can be measured in a qualitative way from 2D ^1H - ^1H TOCSY, 2D ^1H - ^{13}C TOCSY-HMQC or 2D ^1H - ^{13}C TOCSY-HSQC experiments:

- Very weak $J_{\text{H1}'-\text{H2}'}$ and strong $J_{\text{H3}'-\text{H4}'}$ cross-peaks correspond to *pure N-type conformation* (preferred conformation in RNA).
- Strong $J_{\text{H1}'-\text{H2}'}$ and weak $J_{\text{H3}'-\text{H4}'}$ cross-peaks correspond to *pure S-type conformation*.
- $J_{\text{H2}'-\text{H3}'}$ is similar in both states.
- Intermediate intensities indicate equilibrium between N and S states.

1.5.1.2 SUGAR PUCKER

The five-membered ring is generally non planar and its conformation is designated as follows. If four atoms lie in the plane, this plane is chosen as reference plane and the conformation is designated as envelope (E) and if they do not, the reference plane is then that of the three atoms that are closest to the five-atom, least-squares plane, and the conformation is described as twist (T).

a) The present *E* and *T* notations for puckered forms of the sugar ring confirm to those recommended for the conformational nomenclature of five and six-membered rings of monosaccharide and their derivatives.

b) The *E/T* notation has superseded the *endo/exo* description in which atoms now designated by superscripts were called *endo*, and those now designated by subscripts were called *exo*. They are shown by both systems of designation (Figure 1.2 (c)).

Examples: C3'-*endo*/C2'-*exo* has become 3T_2 and C3'-*endo* has become 3E .

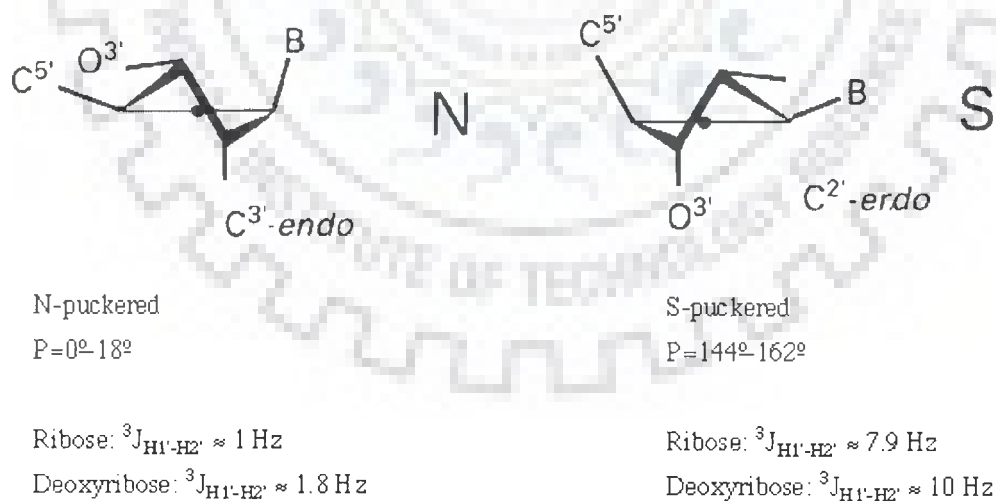


Figure 1.2 (c): Preferred conformation of sugar pucker C2' endo and C3' endo of sugar

1.5.1.3 PSEUDO ROTATION CYCLE

Sugar conformation can only be approximately defined by sugar pucker if intermediate twist modes are considered and hence inadequate. In furanose ring maximum pucker rotates virtually without any potential energy barriers, giving rise to infinite number of conformations. Each conformation of the furanose ring can be unequivocally described by two pseudorotational parameters: the phase angle of pseudorotation, P , and the degree of pucker, ψ_{\max} . In nucleotides, the pseudorotation phase angle P is calculated from the endocyclic sugar torsion angles according to Altona C. and Sundaralingam M.

$$\tan P = \frac{(v_4 + v_1) - (v_3 + v_0)}{2 \cdot v_2 (\sin 36^\circ + \sin 72^\circ)}$$

Given the phase angle P , the five torsional angles are related by:

$$v_j = v_{\max} \cdot \cos(P + j \cdot \psi)$$

Where $j = 0$ to 4 and $\psi = 720^\circ / 5 = 144^\circ$. The maximum torsion angle, v_{\max} is derived by setting $j = 0$.

$$v_{\max} = v_0 / \cos P$$

At every phase angle P , the sum of the positive torsional angles is equal to the sum of the negative torsional angles, i.e. the sum of the five angles is zero.

$$v_0 + v_1 + v_2 + v_3 + v_4 = 0$$

Standard conformation ($P=0^\circ$) is defined with a maximally positive $C1'-C2'-C3'-C4'$ torsion angle [i.e. the symmetrical 2_3T form], and P has value $0-360^\circ$ (Figure 1.2 d).

Conformations in the upper or northern half of the circle ($P = 0 \pm 90^\circ$) are denoted *N* and those in the southern half of the circle ($P = 180 \pm 90^\circ$) are denoted *S* conformation. It is seen that the symmetrical twist (*T*) conformations arise at even multiples of 18° of *P* and the symmetrical envelope (*E*) conformations arise at odd multiples of 18° of *P*. The symbols 'r' and 'd' represent the usual range of *P* values for *N* and *S* conformations of ribo- (r) and 2'-deoxyribo- (d) furanose rings of β -D-nucleosides and nucleotides. In B-DNA two ranges of pseudorotation phase angles are preferred C3' – endo at $0^\circ \leq P \leq 36^\circ$ (*N* conformer) and C2' endo at $144^\circ \leq P \leq 180^\circ$ (*S*- conformer).

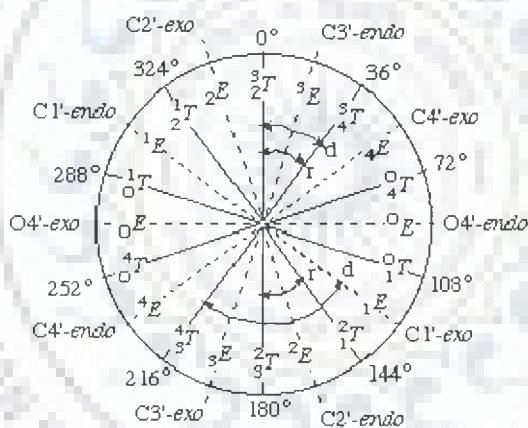


Figure 1.2 (d): Pseudorotation cycle of furanose ring in nucleosides (Altona and Sundarlingam)

1.5.1.4 GLYCOSYL TORSION ANGLE (χ)

The glycosyl torsion (χ) angle defines the orientation of the purine and pyrimidine bases relative to sugar ring. For pyrimidine nucleoside, χ is defined as torsion angle O4'-C1'-N1-C2 and for purines χ is O4'-C1'-N9-C4. Relative to the sugar moiety the base can adopt two main orientations about the glycosyl C1'-N link, called *syn* and *anti*

(Figure 1.2 e). Rotamers with χ values between -90° and $+90^\circ$ are called *syn* whereas *anti* refers to χ values from $+90^\circ$ to $+270^\circ$. In Watson-Crick double helices both bases of a base pair are in *anti* conformation. Bases in *syn* conformation indicate a distortion of the double helix due to base pair opening or mismatched base pairs.

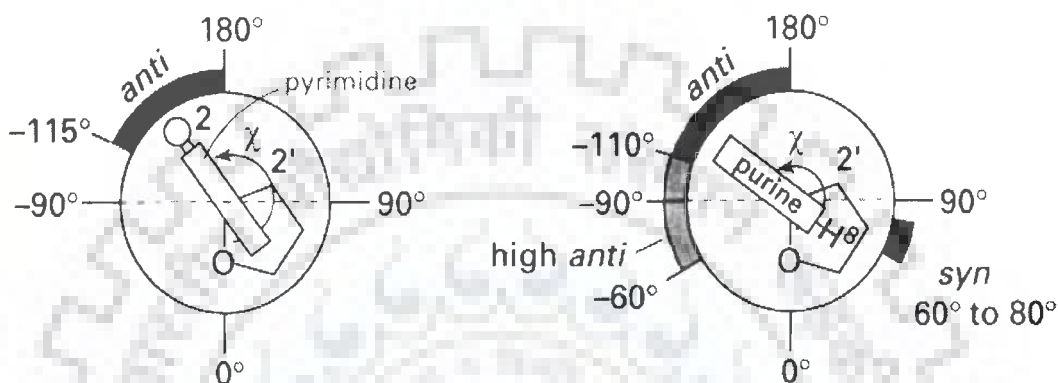


Figure 1.2 (e): Anti high, anti and syn orientations about the glycosidic

The *syn* conformation is also found with guanines in left-handed Z-DNA (zig-zag helix). In *anti*, the bulk of heterocyclic atoms i.e., the six-membered pyrimidine ring in purines and O2 in pyrimidines is pointing away from the sugar, and in *syn*, pyrimidine is over and toward the sugar. An *anti* conformation is located near $\chi = 0^\circ$, whereas in *syn* domain is around 210° . There is also a high *anti* which denotes a torsion angle lower than *anti*.

1.5.1.5 BACKBONE TORSIONAL ANGLES

The sugar phosphate backbone conformation is fixed by the values of six conformational angles. The sequential numbering of atoms $(n-1)P - O 5' - C5' - C4' - C3' - O3' - P - O5'_{(n+1)}$ is defined by torsion angles $\alpha, \beta, \gamma, \delta, \epsilon$ and ζ (Figure 1.2 f).

1.5.1.6 HELICAL PARAMETERS

The structure of DNA can be described by a number of parameters that define the helix (Dickerson et al, 1989) termed as Helical Parameters. The output from helix analysis program CURVES 5.1 version of Richard Lavery (Lavery and Sklenar, 1988), includes “global helical parameters” defined relative to a global helix axis, that is, it depends on all the atoms in the structure and “local helical parameters” defined relative to local helix axis at each base pair, that is, arises if only a subset of neighboring atoms is used to determine that quantity. The helicoidal parameters are classified into three categories: 1. Global base pair-axis parameters 2. Intra-base pair or global base-base parameters and 3. Inter-base pair or base pair-step parameters.

The global as well as the local inter-base pair parameters are related to particular base pair steps. These parameters are vector quantities, which have a defined location in 3-dimensional space and with respect to the nucleic acid sequence. In contrast, the average inter-base pair parameters are scalar values that are not related to any part of the structure. They characterize properties of the whole structure. Intra-base pair or global base-base parameters comprises of the translational components as stagger, stretch and shear, and the rotational components are propeller twist, buckle, opening. Propeller twist refers to the angle between the planes of two paired bases. A base pair is rarely a perfect flat plane with each aromatic base in the same plane. Rather, each base has a slightly different roll angle with respect to the other base. This makes two bases look like an aeroplane propeller. Twist or rotation per residue refers to the angle between two adjacent base pairs. Each step from one plate to the next can be described as a combination of a translational and a rotational movement.

The translational and the rotational displacements are three-dimensional vectors, which can be split into three orthogonal components. In inter-base pair or base pair-step parameters the three translational components are rise, shift and slide. Twist, roll and tilt are the three rotational components. Rise is the distance between adjacent planar bases in the DNA double helix i.e. it is a translation in the direction of the helical axis (z-axis), and shift is orthogonal to the helical axis and directs to the major groove side. Twist is a rotation about the helical axis (z-axis). Base pair roll refers to the angle of deflection of the base pair with respect to the helix axis along a line drawn between two adjacent base pairs relative to a line drawn perpendicular to the helix axis. A positive roll indicates that there is a cleft between two stacked base pairs, which opens towards the minor groove. A negative roll is related to an opening towards the major groove. Base pair tilt refers to the angle of the planar bases with respect to the helical axis. In the B-form DNA the bases are tilted by only -6° . In the A-form DNA the base pairs are significantly tilted at an angle of 20° . The sense of the base-pair tilt is associated with sugar pucker. In double helical polynucleotide, the normal to the base pair are not exactly parallel to the helix axis but inclined to it by up to 20° . The sense of tilt is positive in A-type and negative in B-type of helices, and hence is correlated with sugar pucker. Base tilt angle is correlated with rise per residue. If the bases in base pairs were coplanar and the base pairs exactly perpendicular to the helix axis, the axial rise per nucleotide should correspond to the van der Waal's distance, 3.4 \AA .

Global base pair–axis parameters: x- and y- displacement refers to the shift of bases in positive or negative x and y direction with respect to each other, besides this tip and inclination are also there (Figure 1.3 a).

Inter-base parameters (Base pair step parameters): The helical parameters are derived from the spatial location of the bases, while the sugar phosphate backbone is not taken into account.

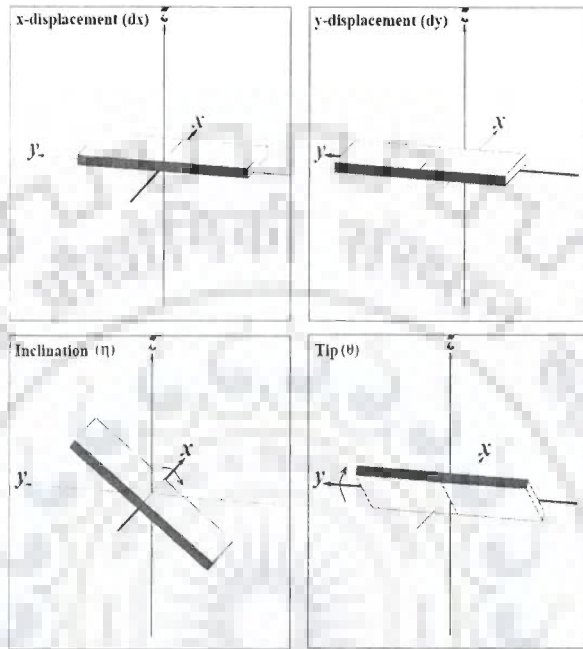


Figure 1.3(a): Pictorial representation of global base pair-axis parameters

The six inter base pairs parameters (*rise, twist, shift, roll, tilt, slide*) describe the local conformation of a double helix at every base pair step (Figure 1.3 b). In the below figure the base pairs are shown as planar plates. In a regular helix such planar elements are stacked on each other. Each step from one plate to the next can be described as a combination of a translational and a rotational movement. The translational and the rotational displacements are 3-dimensional vectors, which can be split into three orthogonal components. The three translational components are **rise, shift and slide**. **Rise** is a translation component in the direction of the helical axis (z- axis) and **shift** is orthogonal to the helical axis and directs to the major groove side. **Twist, roll and tilt** are

the three rotational components. **Twist** is a rotation about the helical axis (z -axis). A **positive roll** indicates that there is a cleft between two stacked base pairs which opens towards the minor groove. A **negative roll** is related to an opening towards the major groove. The definitions of the six inter base pair parameters are rigorous but the Cambridge convention does not define how to establish the reference coordinate system.

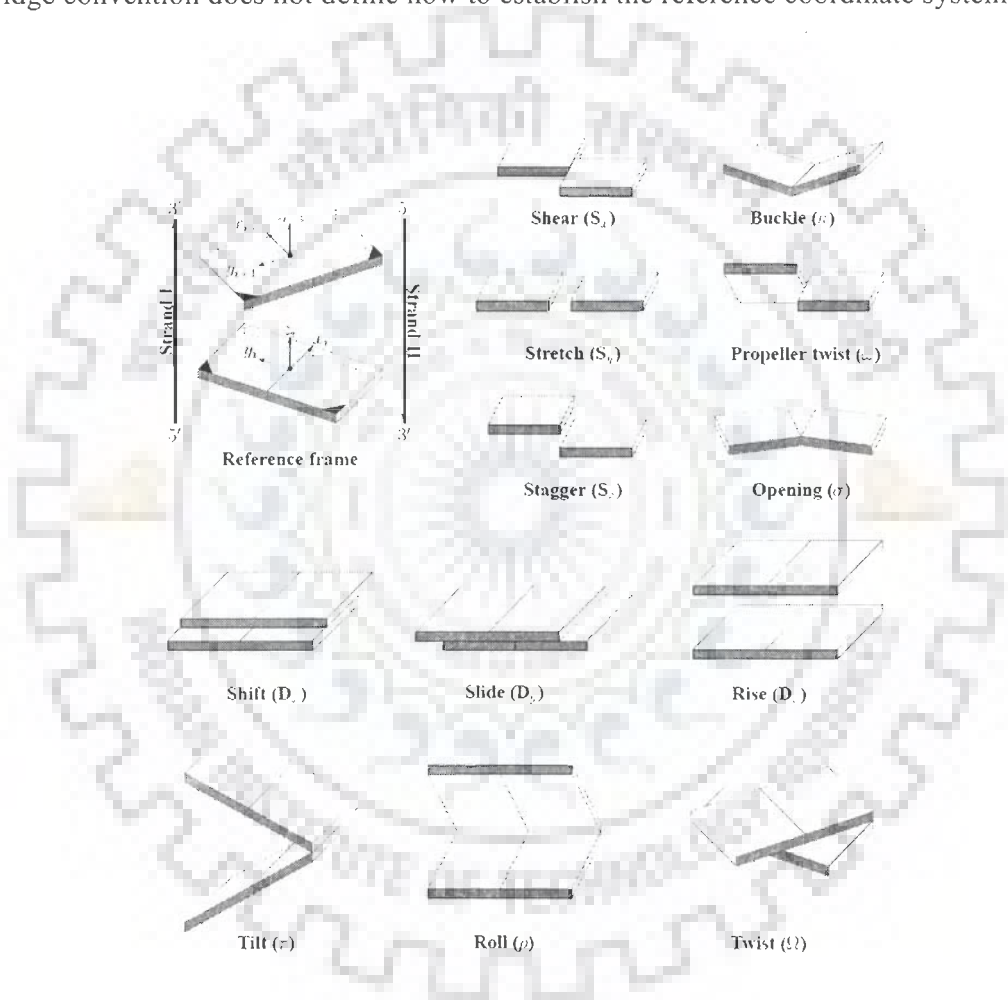


Figure 1.3 (b): Pictorial definitions of parameters that relate complementary base pairs and sequential base pair steps. The base-pair reference frame is constructed such that the x -axis points away from the (shaded) minor groove edge. Images illustrate positive values of the designated parameters (Dickerson et al., 1989).

The decomposition of the total translational and rotational movement into orthogonal components depends crucially on the reference system used. Several different algorithms and programs exist for calculating the helical parameters. The algorithms differ mainly in the methods used to derive the reference coordinate systems.

Intra-base pair step parameters (Base pair parameters): The base pairs in nucleic acid structures are not really planar. For example, the propeller twist of AT base pairs in B-DNA is usually in the range of -15° to -20° . If the base pairs are not planar, the six inter base pair parameters will give only a rough model of the helix. A more detailed picture is obtained if also the intra base pair parameters are taken into account. The Cambridge convention defines six base pair parameters which describe the deviation from planarity within a base pair. These six parameters describe the translational and rotational displacement between the two bases of a base pair. Again, the translational and rotational displacement is divided into orthogonal components. The translational components are *stagger*, *stretch* and *shear*, and the rotational components are *propeller twist*, *buckle*, *opening* (Figure 1.3 b). Instead of determining the (intra) base pair parameters, it is also possible to calculate the inter base pair separately for each strand.

1.6 TOOLS TO STUDY DRUG-DNA INTERACTION

1.6.1 RESTRICTION INHIBITION ASSAY-A QUALITATIVE AND QUANTITAVE TOOL FOR DRUG-DNA INTERACTION

1.6.1.1 INTRODUCTION AND LITERATURE REVIEW

DNA, as a carrier of genetic information is a major target for drug-DNA interaction because of the ability to interfere with the transcription and protein synthesis. DNA replication is a major step in cell growth and division, which is central for tumor genesis and pathogenesis. Interaction of the anti-tumor agent with DNA has been the subject of intensive research for two principle reasons. Firstly, this is most rapid era of drug discovery and development; Secondly, due to the current trend of chemotherapy against cancer. In this regard, considerable amount of effort has been made to elucidate the molecular basis of action of several drugs like adriamycin, daunomycin, distamycin A, mitoxantrone and berberine and palmatine, which are known to bind to DNA. All these drugs have shown good anti-tumor activity and there anti tumor activity has been correlated to sequence specific mode of binding to DNA.

Sequence specificity of these drugs has been attempted by DNA foot printing, in vitro transcription assay, restriction inhibition assay, absorption spectroscopy, fluorescence, circular dichromism spectroscopy, Nuclear Magnetic Resonance spectroscopy (NMR) and X ray crystallography. DNase foot printing experiments have shown preference for CpG, CpA, TpA sites in DNA with mitoxantrone (Fox et al., 1986; Bailly et al., 1986). Adriamycin and daunomycin have shown affinity for CpA rich sequences (Skorobogaty et al., 1988). Transcriptional inhibition assay have shown preferences for 5'-(A/T)CA and 5'-(A/T)CG sites on DNA for mitoxantrone (Panousis and Phillips, 1994) and 5'-TCA for adriamycin and GC flanked at 5' by AT sequences for daunomycin (Trist and Phillips, 1989). In this context restriction inhibition assay showed more specificity for CA than GC rich sequence for adriamycin and more affinity towards

GC than AT rich sequence for daunomycin (Chaires et al., 1987), distamycin A showed more specificity for AT rich sequence (Forrow et al., 1995).

Structures of complex of some of the drugs with specific oligonucleotide by X-ray and NMR have been studied in recent times. Structure of adriamycin with DNA by X-ray (Frederick et al., 1990) and by NMR (Quigley et al., 1980) has shown that in these complexes the chromophore is intercalated at the CpG. While in case of daunomycin by X-ray (Jain et al., 2005) and by NMR (Barthwal et al., 2006) have shown that daunomycin intercalates in the d(CpG) and d(TpG) sequences respectively. Structural studies of distamycin A with sequences such as d (CGCGAATTCGCG)₂ (Klevit et al., 1986) and d(CGCAAATTTGCG)₂ by using NMR (Pelton and Wemmer, 1990) and X-ray (Coll et al., 1987) respectively have shown that distamycin A prefers AT rich sequence in the minor groove of DNA.

Our Research group is working on structural studies of mitoxantrone-DNA complexes with specific sequences such as d(TGATCA)₂, d(CGTACG)₂ and d(TGTACG)₂ by ³¹P, ¹H NMR and restrained molecular dynamics studies have shown mitoxantrone to be an external binder (unpublished data). Similar structural studies are also in process for protoberberines alkaloids with some promoter sequences. In this context we have set out experiments to detect sequence specificity of berberine, palmatine and mitoxantrone whose sequence specific interaction with *HindIII*, *EcoRI* and *EcoRV* binding sites remained to be explored by restriction inhibition assay (Fig. 1.5). We have also confirmed daunomycin, adriamycin and distamycin-A sequence specificity using restriction inhibition assay (RIA), with the available literature and have standardize the protocol using them as standard for our experimental work.

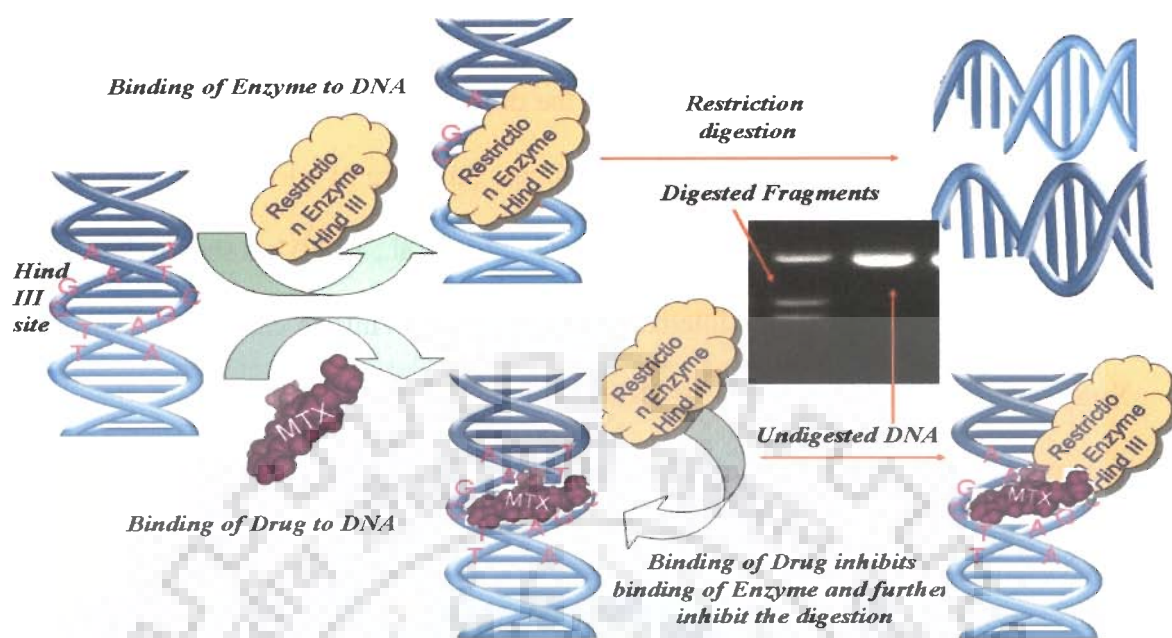


Fig. 1.4: A diagrammatic representation of restriction inhibition of mitoxantrone

1.6.2 APPLICATION OF RESTRICTION INHIBITION ASSAY FOR SCREENING DRUG-DNA INTERACTING COMPONENTS FROM HERBAL PLANTS

1.6.2.1 INTRODUCTION AND REVIEW OF LITERATURE

It is appreciated that DNA is a primary target for many potent anti-tumor agents; a substantial body of research has been directed towards understanding the molecular basis of DNA sequence specificity for binding, by identifying the preferred binding sequences of many key drugs with DNA. The mutual recognition of molecules is fundamental to all the biological processes. It is indeed thought to be decisive in enzyme catalysis and inhibition, DNA replication, gene expression and its control. Interaction of the anti-tumor agent with DNA has been the subject of intensive research for two principle reasons.

Firstly, this is most rapid era of drug discovery and development; secondly, due to the current trend of chemotherapy against cancer.

In recent years there has been a great deal of interest in the rational development of anticancer drug from plant origin. This changing inclination towards plant derived drug discovery is due to its lesser side effect as compared to the chemically synthesized counterpart. In this context the development of new inhibitors, natural products from plant sources can be valuable source of novel inhibitors and may also serve as a suitable lead for the production of semisynthetic active agents. In the past, techniques like DNA foot printing, in vitro transcription assay, restriction inhibition assay, absorption spectroscopy, fluorescence, circular dichromism spectroscopy were used to study the sequence specificity of anti-tumor drugs. DNase foot printing experiments have shown preference for CpG, CpA, TpA sites in DNA with mitoxantrone (Fox et al., 1986; Bailly et al., 1986). Transcriptional inhibition assay have shown preferences for 5'-(A/T) CA and 5'-(A/T) CG sites on DNA for mitoxantrone (Panousis and Phillips, 1994) and 5'-TCA for adriamycin and GC flanked at 5' by AT sequences for daunomycin (Trist and Phillips, 1989). In this context restriction inhibition assay showed more specificity for CA than GC rich sequence for adriamycin and more affinity towards GC than AT rich sequence for daunomycin (Chaires et al., 1987), distamycin A showed more specificity for AT rich sequence (Forrow et al., 1995).

Normally all these techniques are were used to study the sequence specificity of drug-DNA interaction and none were used for screening compound which bind to a specific sequence of DNA in a quantitative manner. In this context we have set out

experiments to screen extract binding of sequences having 5'-GC-3' and 5'-AT-3' in their binding domain. The restriction inhibition assay using restriction endonucleases as an agonist were used to screen extract/phytochemicals showing affinity for *EcoRI* (5'-GAATTC-3') and *HindIII* (5'-AAGCTT-3') restriction recognition sequences. Mitoxantrone and Distamycin-A were used as standard drugs interacting with *HindIII* and *EcoRI* restriction endonucleases. The current study is the first report of applying restriction endonuclease inhibition assay to screen phytochemical, from *Cinnamomum zeylanicum* bark and *Picrorrhiza kurroa* rhizome extracts, showing sequence affinity for *EcoRI* (5'-GAATTC-3') and *HindIII* (5'-AAGCTT-3'), respectively.

The clinical significance of the work is related to anticancer property, by searching for (5'-GAATTC-3') and (5'-AAGCTT-3') in the mRNA and their corresponding STS (Sequence Tag Sites) and ESTs (Expressed Sequence Tag) of BRCA 2 (oncogene). The STS are short tagged tracts of DNA sequence (200 to 500 base pairs) that are operationally unique and have a single occurrence in the human genome. Their location and base sequence are known and therefore they can be used as landmarks in genome mapping (Olson et al., 1989). The ESTs are short sub-sequence of a transcribed cDNA sequence (ESTs Factsheet). They may be used to identify gene transcripts, and are instrumental in gene discovery and gene sequence determination. Because these clones consist of DNA that is complementary to mRNA, the ESTs represent portions of expressed genes (Adams et al., 1991). The ESTs are present in the database as either cDNA/mRNA sequence or as the reverse complement of the mRNA, the template strand. These ESTs serve as markers for genetic and physical mapping of genes along the chromosome (Nagaraj, 2007). The presence of (5'-GAATTC-3') and (5'-AAGCTT-3')

sequences in the coding domain of an oncogene provides the necessary clinical relevance of the protocol to screen phytochemicals which bind to such sequences. Thereby interfering the transcription and protein expression of an oncogene; this is central for antitumorogenesis of an antitumor drug.

1.6.3 STUDIES OF BERBERRUBINE-d(CCAATTGG)₂ COMPLEX BY NMR SPECTROSCOPY

1.6.3.1 INTRODUCTION AND REVIEW OF LITERATURE

The specific and non covalent interaction of small organic molecules with DNA and RNA have attracted considerable interest, not only because they provide molecular basis for antitumor, antiviral, and antibiotic drugs to elucidate their structure-activity relationship but also because they provide rational design of sequence specific DNA binding molecules. Gene regulation is controlled by a complete interplay of numerous proteins - DNA interaction. Small molecules can interfere with these processes in a variety of ways e.g. by directly competing at regulatory sites or binding at adjacent site accompanied by deformation of DNA so that protein protein binding does not occur (Neidle S., 2001). Among the various molecules, natural products, particularly those having less toxic effects are a natural choice. Protoberberine analogues, representing an important class of quinoline alkaloids have been used as active constituents in Chinese herbal medicines. They exhibit multiple pharmacological activities such as antimicrobial (Schmeller et al., 1997), antimalarial (Rafatro et al., 2000; Wright et al., 2000), antifungal (Iwasa et al., 2000), anti-inflammatory, antipyretic and hepatoprotective (Kupeli et al., 2000) activity. It also exhibits in vitro cytotoxicity against cell lines derived from solid tumors SF 268 and HL 60 leukemic cells (Kuo et al., 1995).

Berberrubine (Figure 1.5 a) isolated from *Berberis Vulgaris* can be readily derived from berberine. The two compounds differ in chemical structure at 9-substituents in ring D, which is $-OH$ and $-OCH_3$ for berberrubine and berberine, respectively (Figure 1.5 b).

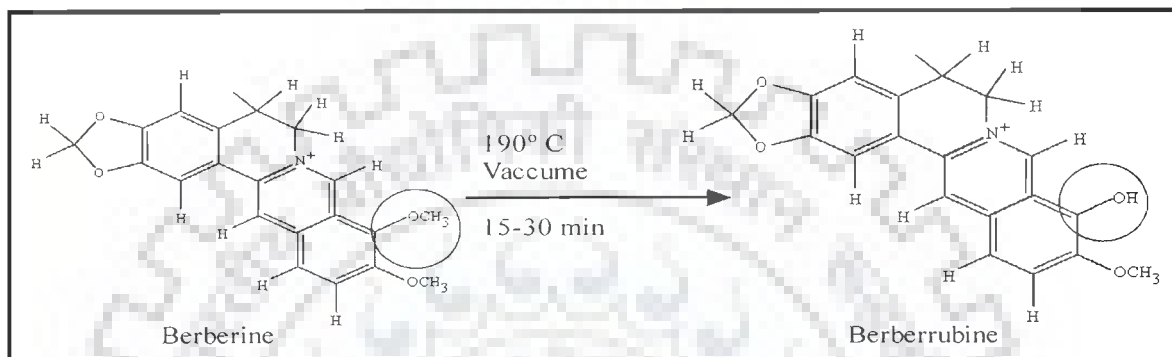


Figure 1.5 (a): Synthesis of berberrubine from berberine

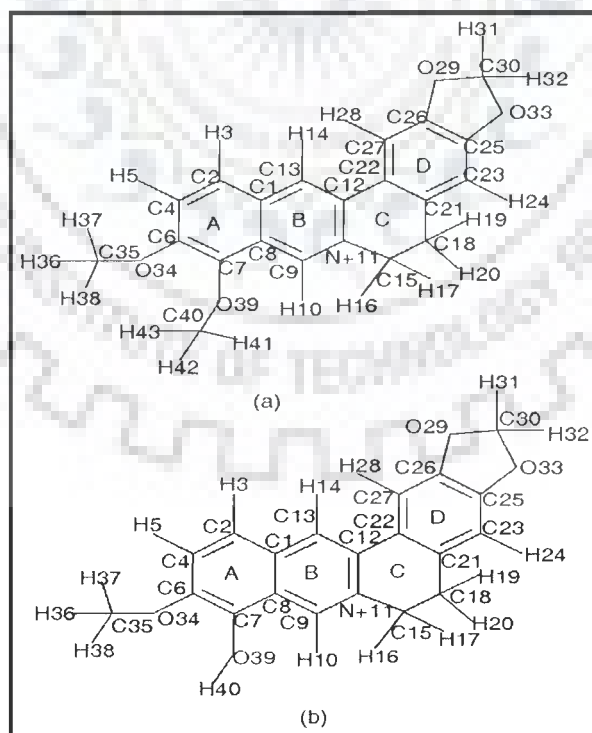


Figure 1.5 (b): Structure of (a) berberine and (b) berberrubine.

Earlier studies (Hoshi et al., 1976) have shown that berberine and its ester derivatives have a strong antitumor activity against Sarcoma -180 ascites cells and therapeutic index decreased in the order acetyl derivative > berberine > benzoyl derivative. It was consequently shown (Ikekawa et al., 1982) that hydroxyl group at 9-position of berberine is essential for the manifestation of antitumor activity in S-180, NF Sarcoma, Ehrlich carcinoma and L-1210 in mice. The 9-O-acyl and 9-O-benzoyl substituents increased antibacterial activity against several Gram +ve and Gram -ve bacteria (Hong et al., 2000). Alkyl analogs were found (Kim et al. 2002) to have still better antimicrobial activity against Gram +ve bacteria and fungus. The result suggested that the presence of lipophilic substituents of certain structures and sizes might be crucial for antimicrobial activity.

The ability of cytotoxic protoberberine alkaloids to acts as topoisomerase I and II poisons was report to be related to the antitumor activity in which the DNA binding process was of vital importance (Li et al., 2000; Pilsch et al., 1997). Berberrubine has been identified as specific poison of topoisomerase II by stabilization of the reversible enzyme-DNA cleavable complex. It induces DNA cleavage in a site specific and concentration dependent manner (Kim et al., 1998). Its DNA cleavage activity is found to be much higher than that of structurally similar berberine molecule (Jeon et al., 2000), which is a stronger DNA binding agent (Krishnan et al., 2000). That topoisomerase II is the cellular target of berberrubine in vivo has been confirmed (Kang et al., 2002) by the observed resistance to berberrubine in human colorectal carcinoma cells, which is associated with decreased level of catalytically active topoisomerase II. However the mechanism of action of these drugs that target topoisomerase II is much less clear.

The suggested mechanism of action-intercalation or minor groove binding is still controversial (Li et al., 1998; Ogiso et al., 2000; Ren et al., 1999; Pilsch et al., 2000; Li et al., 2000; Kim et al., 1998). A study of analogue having substituents at C9 position have shown (Kraishnan et al., 2000) that the proposed drug domain for DNA intercalation is not a major determinant of enzyme inhibition for specific berberine analogue. Rather the 9 substituents within the domain has a major influence, presumably by facilitating drug interaction with enzyme and/or enzyme-DNA complex.

The binding of five cytotoxic protoberberine alkaloids with several oligonucleotide duplex sequences by ESI-MS and fluorescence spectrometric methods showed that no remarkable sequence selectivity and a comparatively lower binding affinity for berberrubine. Significantly, all alkaloids except berberrubine bind like a typical DNA minor groove binder. It may be emphasized that only a molecular structure of drug-DNA complex derived from experimental geometrical parameters can resolve the DNA binding properties of protoberberine alkaloids. There are only three NMR solution structures reported so far in literature (Mazzini et al., 2003; Park et al., 2004^a; Park et al., 2004^b).

On the basis of observed 15 intermolecular NOEs between berberine and DNA protons in berberine d-(AAGAATTCTT)₂ complex, it has been shown (Mazzini et al., 2003) that the berberine molecule is located near AATTC segment in the minor groove, lying with the convex side on the helix groove and presenting the positively charged nitrogen atom close to the negative surface of the oligomer. Binding of berberine to d-(AAGAATTCTT)₂ resulted in steady shift in resonance positions as well as line broadening (Park et al., 2004^a) with increase in drug to DNA ratio from 0 to 6, which was

attributed to non specific interaction. On the other hand, berberrubine binds to the same sequence (Park et al., 2004^b) at molar ratio 1:1 specifically by partial intercalation. Intermolecular NOEs between drug and DNA protons have not been observed which would have given a more direct proof of the mode of binding. In order to gain understanding of the mode of action of these drugs, we have set out to determine the structure of berberrubine to an octamer sequence d-(CCAATTGG)₂ containing presumable AATT binding site as well as CCAAT segment, occurring at remarkably high frequency in the promoters of mRNA encoding genes (Borghini et al., 2006; Mantovani et al., 1998).

We present here the structure-conformation of berberrubine d-(CCAATTGG)₂ complex based on 1D, 2D ¹H and ³¹P NMR spectroscopy measurements followed by restrained molecular dynamics simulations based on observed NOEs. The significance of the conformation in relation to the biological activity is discussed.

1.6.3.2 SIGNIFICANCE OF THE PROMOTER SEQUENCE d-(CCAATTGG)₂

Regulation of transcription is a complex set of events controlled by DNA sequences positioned in proximity to these genes (promoters) and by elements acting at a distance (enhancers). Promoters and enhancers that activate polymerase II transcribed mRNA genes are formed by a combinational puzzle of short sequences recognized by sequence specific regulators. Some such as the TATA, GC and CCAAT box are encountered at extremely high frequency (Bucher, 1990; Bucher and Trifonov, 1988). The CCAAT box was the first element identified (Benoist et al., 1980; Efstratiadis et al., 1980). Later studies clearly established that such pentanucleotide sequence are present in a wide variety of vertebrate, yeast and plant promoters and are important for

transcription. All five nucleotides are almost invariably conserved. The CCAAT sequences can be found both in the direct and in the inverted orientation and it is present in both TATA containing (such as globins) and in TATA less (such as MHC class II) promoters. The frequency of CCAAT boxes appears to be relatively higher in TATA-less promoters (Mantovani, 1998). Borghini pointed out the lack of conventional TATA boxes and the presence of two identical CCAAT boxes as the crucial elements involved in the transcription regulation of the human TLX3 gene which is a gene over expressed in T-cell Acute Lymphocytic leukemia (Borghini et al., 2006). TLX3 is uniquely expressed in the developing medulla oblongata and is required for proper formation of first order relay visceral sensory neurons and of most of the (nor) adrenergic centres in the brain stem especially involved in the physiologic control of cardiovascular and respiratory systems (Qian et al., 2001), but expression of TLX3 has also been detected in leukemia samples from 20% of children's and 13% of adult affected with T-cell acute lymphocyte leukemia (Ballerini et al., 2002; Cave et al., 2004; Mauvieux et al., 2002) although this gene has never involved in normal T-cell differentiation (Ferrando et al., 2004), but based on its specific spatiotemporal expression and the correlation between upregulation and development of T-cell Acute Lymphocytic leukemia a role of this gene in either cell cycle, survival or differentiation can be postulated. These promoter sequences are rich in AT content and sequence of consecutive adenines and thymines, so called A-tracts also constitute an important class of naturally curved DNA (Boulikas, 1996; Crothers and Shakked, 1999; Marini et al., 1982). AT rich sequences, including A-tracts, are also strongly over-represented in origins of replication in many organisms (Boulikas, 1996).

Sequence dependent local DNA structure is correlated with all biological functions and also detailed stereochemical studies have shown that the helical parameters of a DNA double helix are strongly influenced by its base sequence (Dickerson, 1992) hence it is probable that structure of control sites (eg promoters and operators) in DNA are different from the structure of genomic DNA (Nussinov, 1985). Special structures like different cross linking, and pseudosquare knot structures are also identified by conformational studies, which shows critical importance in biological behavior of DNA elements (Paquet et al., 1999; Ulyanov et al., 1998). Special structure and conformation, of packaging signal of HIV-1 RNA contains a stem-loop, which is sequence dependent, SL1, serves as the dimerization initiation site for two identical copies of the genome and is important for packaging of the RNA genome into the budding virion and for overall infectivity (Ulyanov et al., 2006). The dependence of the local conformation on sequence may be involved in recognition by specific proteins involved in transcription and replication processes. Novel drugs, which can be oligonucleotide, peptides or small molecules, are currently being designed to target nucleic acids. In order to develop this new medicinal strategy in a rational way, there is a need for information regarding the structure, stability and dynamics of nucleic acids in the presence or in the absence of these drugs. Residues of the complementary octamer duplex were labeled and numbered according to the Figure 1.6 below:

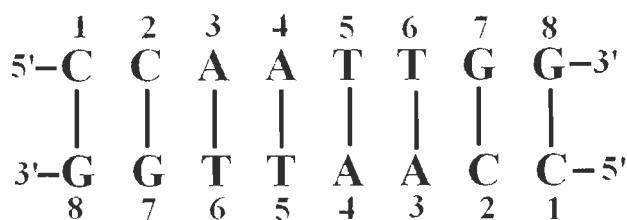


Figure 1.6: Complementary octamer duplex sequence

1.6.4 MOLECULAR MODELING IN DRUG-DNA INTERACTIONS

Molecular modeling is a broad term that encompasses ab initio quantum mechanical calculations, semi-empirical calculations, and empirical calculations (charge-dependent molecular mechanics force fields). These techniques can be used to study the three-dimensional structure, dynamics, and properties of a molecule of interest. Molecular modeling can identify and define the possible key details of the molecular interaction and, using the graphics/computational approach, decide on optimal structural modifications likely to enhance either general binding affinity or recognition of a particular nucleotide-binding site. A number of studies have revealed the converse, with the discovery that particular patterns of chemical modification on a given drug (e.g., doxorubicin) can result in both low biological activity and low-ranking interaction energy.

The molecular modeling, particularly molecular mechanics and dynamics, are highly complementary to macromolecular NMR and X-ray crystallography. Molecular dynamics simulation can, in principle, provide a complete theoretical description of DNA structure and motions, and are thus a valuable independent means of developing models and interpreting experimental data.

1.7 MODE OF ACTION OF ANTICANCER DRUGS

Drugs bind to DNA both covalently as well as non-covalently:

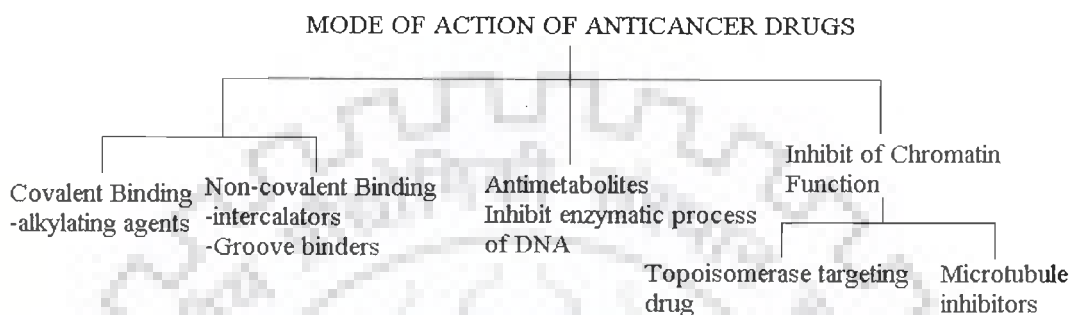


Figure 1.7: Graphical representation of modes of action of anticancer drugs

1.7.1 TOPOISOMERASE TARGEING DRUGS

1.7.1.1 INTRODUCTION AND REVIEW OF LITERATURE

Chromosomal DNA is extensively twisted and topoisomerases permit selected regions of DNA to untangle so as to allow transcription and replication. These enzymes temporarily break DNA, allowing for topological changes, and then reseal the breaks. DNA topoisomerases are essential cellular enzymes required for cell proliferation and have recently emerged as important cellular targets for chemical intervention in the development of anti-cancer agents. Studies of the subclass type I topoisomerases indicate that they act by a mechanism involving the introduction of temporary breaks in only one strand of the double-stranded DNA. The type II topoisomerases break and religate both strands of the double-stranded DNA. A catalytic intermediate stage involving a covalent linkage between the topoisomerase and the 3' end of the broken DNA strand has been

shown to be susceptible to interference by certain compounds which essentially prevent the religation of the broken strand and the release of the bound enzyme (Hertzberg et al., 1989; Hsiang et al., 1985).

Topoisomerases can be inhibited by two distinct mechanisms, and are divided into two classes accordingly: type I and II. Type I inhibitors stabilize the enzyme–DNA-covalent complex and block the subsequent rejoining of DNA break, enhance apoptosis through blocking the advancements of replication forks. Type II inhibitors prevent the enzyme and DNA from binding by interacting with either the topoisomerase enzyme or DNA (Yonezawaa et al., 2005, Pommier et al., 2009). Topoisomerase I and II inhibitors are very rare but instead attract much attention in biomedical research since they constitute important chemotherapeutic routes in combating cancer. A naturally occurring alkaloid, camptothecin, extracted from stem tissue of the Chinese tree *Camptotheca acuminata*, was the first topoisomerase I poison identified (Wall et al., 1966). Topoisomerase targeting drugs like etoposide stabilizes the topoisomerase II–DNA complex preventing it from making a topological change. This results in an irreversible double strand break, which is lethal to cells in S and G2 phases. Six anti-neoplastic drugs targeting topoisomerase II, i.e., several quinolones e.g., Lomefloxacin, Ciprofloxacin, Moxifloxacin and alkaloid such as etoposide, doxorubicin, daunorubicin, idarubicin, mitoxantrone, and teniposide are currently approved for clinical use in the United States. Synthetic topoisomerase inhibitory analogs are also studied (Singh, et al., 1992; Holden et al., 2001; Li et al., 2001).

DNA topoisomerase II is a ubiquitous enzyme that is essential for the survival of all eukaryotic organisms and plays critical roles in virtually every aspect of DNA

metabolism. The enzyme unknots and untangles DNA by passing an intact helix through a transient double-stranded break that it generates in a separate helix. Beyond its physiological functions, topoisomerase II is the target for some of the most active and widely prescribed anticancer drugs currently utilized for the treatment of human cancers. DNA is an extremely important target for drug action, with a wide range of biological activities (anti-tumor, antiviral and antimicrobial) arising from the ability of compounds to bind sequence specifically to DNA and interfere with DNA topoisomerases or with transcription binding factor (Lancelot and Paquet, 2003). These antibiotics act by intercalating between base pairs of DNA causing lengthening of the double helix and a decrease in the helical twist on unwinding, inducing mediated strand scission. These drugs act in an insidious fashion and kill cells by increasing levels of covalent topoisomerase II-cleaved DNA complexes that are normally fleeting intermediates in the catalytic cycle of the enzyme. The anti-tumor topoisomerase II inhibitors presently used in the clinic, poison the enzyme by stabilizing cleavable complexes, presumably by increasing the rate of forwards reaction i.e. more rate of DNA cleavage or by decreasing the rate of backward reaction i.e. slow rate of religation of cleaved DNA (Figure 1.8). Thus synthesis of DNA and RNA is blocked.

The success of camptothecin and etoposide and their analogues as anticancer agents has spurred a search for additional agents acting by inhibition of topoisomerases I and II in the past years. While the majority of topoisomerase (topo) inhibitors show selectivity against either topo I or topo II, a small class of compounds can act against both enzymes e.g., disulfiram, acridine DACA, the benzopyridoindole intoplicine, the indenoquinolinone TAS-103, the benzophenazine XR11576, NSC 366140, camptothecin-

epipodophyllotoxin, ellipticine-distamycin hybrids, modified camptothecin BN 80927, topopyrones A-D and the modified epipodophyllotoxin tafluposide F-11782 (Denny et al., 2003; Yakisich et al., 2001; Khan et al., 2008).

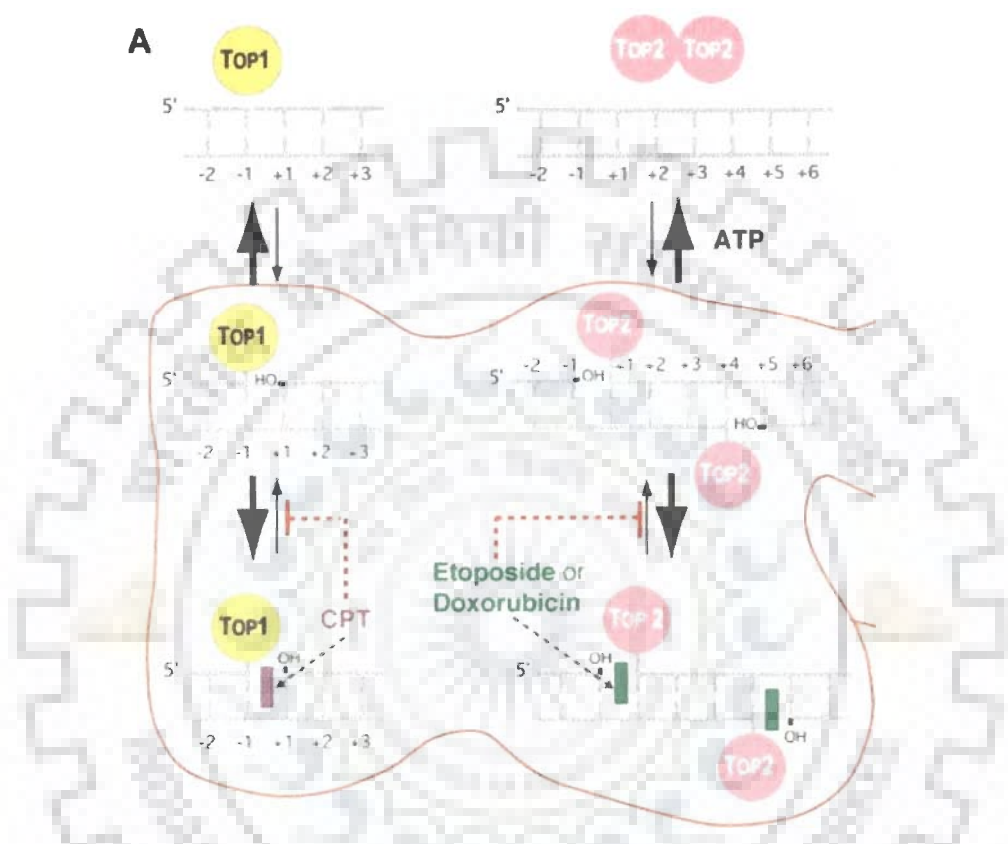


Figure 1.8: DNA damage induced by inhibition of Topoisomerase I & II.

In a recent development furanocoumarins from *Ruta graveolens L.* a medicinal plant, showed topo I inhibitory potential (Diwan et al., 2009). In this context the development of new inhibitors, natural products from plant sources can be a valuable source of novel inhibitors and may also serve as a suitable lead for the production of semisynthetic active agents. *Picrorrhiza kurroa* Royle ex Benth (family, Scrophulariaceae) is a hairy perennial herb growing wild in North Western Himalayan region. *P. kurroa* forms a major ingredient of many indigenous medical preparations

especially useful for the treatment of diseases of liver such as hepatitis (Mittal et al., 1978; Ansari et al., 1988), jaundice (Handa et al., 1986) as well as anaemia (Antarkar et al., 1988) and asthma (Langer et al., 1981). The extract was also reported to reduce the blood sugar in alloxan-induced diabetics in rats (Joy et al., 1999) and could scavenge superoxides and hydroxyl radicals and inhibits the lipid peroxidation in vitro (Joy et al., 1995).

Picrorrhiza kurroa 75 % methanol extract have also shown antineoplastic activity on transplanted tumors and chemical carcinogenesis in mice. In the same study the authors have also shown the anti yeast topoisomerases I and II activity, on *Saccharomyces cerevisiae* mutant cell cultures (Joy et al., 2000). Therefore in the current study the aqueous extract of *Picrorrhiza kurroa* was assessed for its human topoisomerase I and II inhibitory activity. To determine the exact mechanism of topoisomerase inhibition the enzyme and DNA were preincubated prior to addition of extract and to test the affinity of inhibitors with the enzyme, the enzyme and extract were preincubated before addition of substrate (DNA). The current study is the first report on the activity and mode of action of human topoisomerase I and II α inhibition from the aqueous extract of *Picrorrhiza kurroa* Royle ex Benth.

1.8 SCOPE OF THESIS

Medicinal plants are the most valuable assets nowadays due to presence of small doses of active compounds which produce physiological actions in human and animal body. Some of the important bioactive compounds are alkaloids, glycosides, resins, gums and mucilages which possess anticancer, antiviral, antidiabetic and antimicrobial activity. The medicinal value of *Picrorrhiza kurroa* and *Cinnamomum zeylanicum* has been

recognized since ancient times. Apart from their anti-cancerous property, it also displays a wide variety of biological and pharmacological activities e.g. antidiabetic, antimicrobial, antiplasmodial, antidiarrhoeal, cardiovascular, etc. The therapeutic potential of *Cinnamomum zeylanicum* in the control and management of type 1 diabetes mellitus was not well explored. Therefore the current study was stimulated towards understanding the therapeutic potential of *Cinnamomum zeylanicum* in the management of type 1 diabetes mellitus. *Picrorrhiza kurroa* another Himalayan herb known for its medical value was screened for antitopoisomerases activity using human topoisomerases I and II as targets.

The molecular basis for designing DNA binding drugs with improved specificity and affinity stems from the ability to identify the structural elements of the drug and DNA which are responsible for the specificity of the binding and the stabilization of the drug-DNA complex. An analytical technique to elucidate the mode of drug-DNA interaction could be essential for the design of new drugs. Restriction inhibition assay, Nuclear Magnetic Resonance (NMR) spectroscopy and restrained Molecular Dynamics (rMD) are some of the analytical techniques which have been used in this study; 1) the sequence specificity of anticancer drugs and screen phytochemical rich fraction from herbal plant which bind specific sequences, and 2) investigate the binding specificity and conformation of drug-DNA complexes.

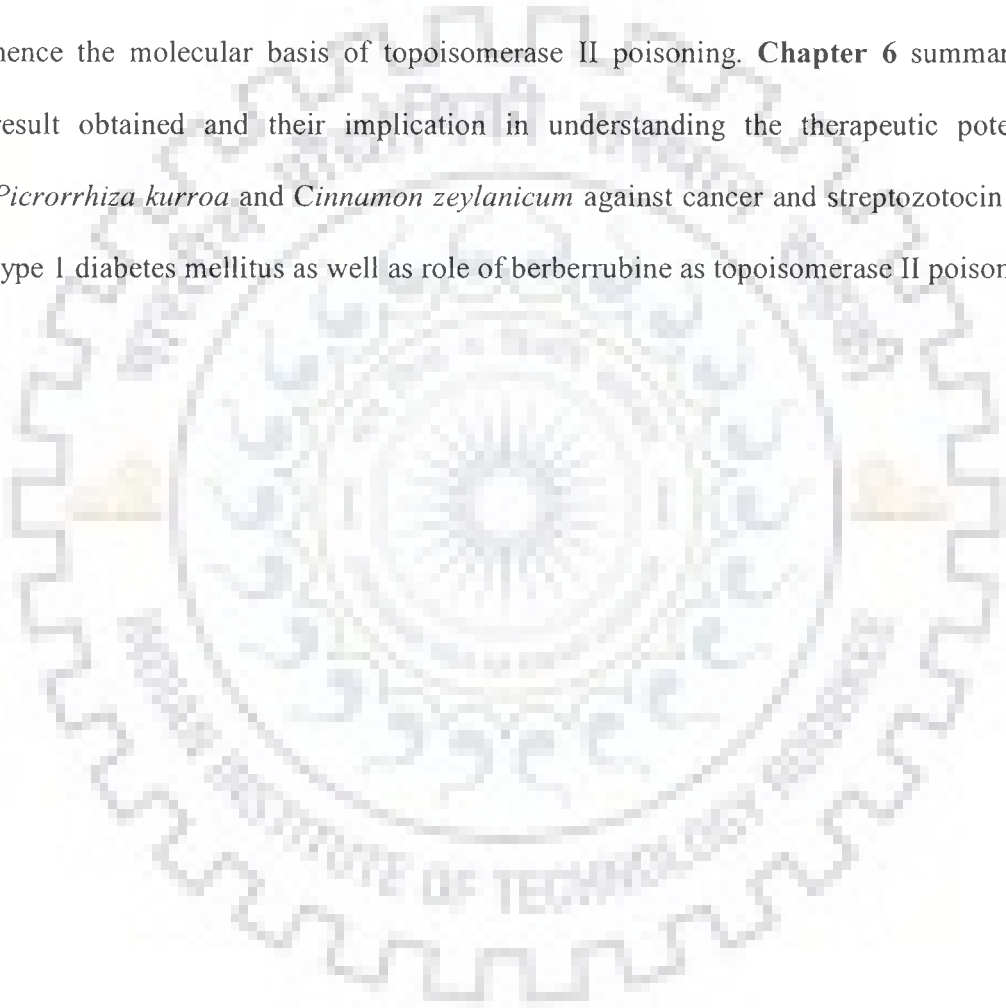
This thesis deals with (i) Screening of insulinotropic, antidiabetogenic and β -cell regenerating agent involved in the control and management of type 1 diabetes mellitus (ii) sequence specificity determination for anticancer drugs using restriction inhibition assay (iii) screening DNA binding phytochemical rich fraction from herbal plants and

postulating the anticancer potential of the screened phytochemical rich fractions, (iv) anticancer activity of *Picrorrhiza kurroa* using human topoisomerases I and II as targets. (iv) Structural studies of berberrubine- d-(CCAATTGG)₂ complex.

The PhD thesis work has been reported in the form of 6 chapters. **Chapter 1** contains introduction of the subject, a comprehensive review of the literature and scope of thesis. **Chapter 2** deals with materials, methods, results and discussion of antidiabetic or insulintropic property of the aqueous extract of *Cinnamomum zeylanicum*. The present study showed better hypoglycemic and antihyperglycemic property of 200 mg/kg body weight aqueous extract than methanol extract of *cinnamomum zeylanicum* in normal and streptozotocin induced type 1 diabetic mellitus (T1DM) animals. The role of saponin as an antidiabetic and insulintropic agent from *Cinnamomum zeylanicum* was identified. The results indicate the favorable effect of saponin rich fraction of the aqueous extract of *cinnamomum zeylanicum* in bringing down the severity of T1DM. **Chapter 3** deals with materials, methods, results and discussion of the qualitative and quantitative assay to screen the DNA interacting component based on the sequence selective inhibition of restriction endonucleases. The present study showed the use of the restriction inhibition assay using *Hind* III, *Eco*RI and *Eco*RV restriction enzymes to evaluate the binding specificity of DNA with anticancer drugs (mitoxantrone, berberine and palmatine) and phytochemical rich fractions from herbal plants. In the first study the inhibition of *Hind* III endonuclease at 220 μ M concentration with mitoxantrone gave a direct evidence of the co-existence of concentration and sequence specificity for drug-DNA interaction. The second study showed how a simple and rapid method can be used to screen plant extracts and the active phytochemicals involved in binding with restriction sequences of

EcoRI and *HindIII* in a relatively qualitative and quantitative manner. The *EcoRI* (5'-GAATTC-3') and *HindIII* (5'-AAGCTT-3') restriction sites were found repeatedly in the cDNA/mRNA and ESTs of BRCA2, early onset oncogene. These observation projects the possible use of the screened phytochemical as an anticancer agent, targeting the expression of an oncogene (BRCA2). Through this study, we propose for the first time the use of restriction inhibition assay as a rapid and simple method to screen possible anticancer phytochemical from herbal plants. **Chapter 4** deals with materials, methods, results and discussion of anti topoisomerases activity of the aqueous extract of *Picrorrhiza kurroa* Royle ex Benth. The present study describes the inhibitory effect of the aqueous extract of *Picrorrhiza kurroa* on human topoisomerases by measuring the relaxation of superhelical plasmid pBR322 DNA. By stabilization studies of topoisomerase I-DNA complex and preincubation studies of topoisomerase I and II α with the extract; we conclude that the possible mechanism of inhibition is both; 1) stabilization of covalent complex of topo I-DNA complex and 2) direct inhibition of the enzyme topoisomerases. These findings might explain the antineoplastic activity of *Picrorrhiza kurroa* and encourage new studies to elucidate the usefulness of the extract as a potent antineoplastic agent. **Chapter 5** deals with the materials, methods, results and discussion of NMR studies of berberrubine and DNA interaction. This chapter deals with Proton NMR and Phosphorus-31 on binding of berberine with DNA octamer sequence d-(CCAATTGG)₂. The observed 19 inter-molecular NOEs connectivities of the drug with the sugar H1', H2'/2'' and NH₂^{nb/b}, CH₃ and the A3/A4H2 region of the DNA supports the minor groove mode of binding of berberrubine in the complex. The restrained molecular dynamics approach using INSIGHT II and DISCOVER showed that

the two drug molecules with their aromatic region stacked in an antiparallel pattern lies at the upper minor groove region (5'-CAATT-3') of the DNA. The interaction of the drug at this site of the DNA was stabilized by van der waal, electrostatic and hydrogen bonding forces. The specific drug-DNA structure thus obtained spells out exact contacts the drug makes with DNA, which is important for formation of ternary complex with enzyme and hence the molecular basis of topoisomerase II poisoning. **Chapter 6** summarizes the result obtained and their implication in understanding the therapeutic potential of *Picrorrhiza kurroa* and *Cinnamon zeylanicum* against cancer and streptozotocin induced type I diabetes mellitus as well as role of berberrubine as topoisomerase II poison.



SAPONINS FROM AQUEOUS EXTRACT OF *Cinnamomum zeylanicum*: A POTENTIAL THERAPEUTIC AGENT FOR STREPTOZOTOCIN INDUCED TYPE 1 (T1DM) DIABETIC WISTAR RATS.

Cinnamon is one of the traditional herbs used as a remedy for type 2 diabetes mellitus. In the present study, the profiling of blood glucose level; short term and long term activity of herbal extract; serum insulin estimation; insulin, glycolytic and gluconeogenic gene expression profiling and histopathological examination of pancreatic tissue has been done to generate an overview on the effectiveness of the treatment of *Cinnamomum zeylanicum* extract in type 1 diabetic condition. The present investigation reports:

1. The dose dependence activity of aqueous and methanol extracts of *Cinnamomum zeylanicum* on fasting blood glucose, Oral Glucose Tolerance Test (OGTT), short and long term effects of extracts on blood glucose levels of normal and streptozotocin-induced type 1 diabetic male wistar rats.
2. The molecular mechanism behind the hypoglycemic and antidiabetogenic nature of the aqueous extract of *Cinnamomum zeylanicum*, lipid profiling, *in vivo* and *in vitro* insulin secretion, glycogen content and enzyme activity from liver and

serum to evaluate their effect on biochemical parameters of liver function and glucose homeostasis, respectively.

3. Actions at cellular and molecular levels by determining its effects on expression of various target genes, e.g. Glucokinase (GK), glucose-6-phosphatase (G6Pase), Phosphoenol pyruvate carboxykinase (PEPCK), Insulin II and Glucose-6-phosphate dehydrogenase (Gpdh) in different target tissues, such as liver and pancreas.
4. Identification of the hypoglycemic and antihyperglycemic phytochemical group in the aqueous extract of *Cinnamomum zeylanicum*.

To the best of our knowledge, this is the first ever report on the role of saponin demonstrating the hypoglycemic, antidiabetic and insulinotropic effects at cellular levels for the treatment of streptozotocin induced type 1 diabetes (T1DM) from the aqueous extract of *Cinnamomum zeylanicum*.

2.1 MATERIALS

2.1.1 Plant Material

The *Cinnamomum zeylanicum* bark was purchased from an ayurvedic store, Kannur, Kerala during December 2008. The plant material was identified as per the literature of Auyervada and by local expert of herbal gardens and also confirmed by Dr. H.S. Dhaliwal, Professor of Plant Biotechnology, Department of Biotechnology, Indian Institute of Technology Roorkee, India.

2.1.2 Animal Selection and Procurement

The diabetic study was conducted on 26 Male Wistar Rats, 8-10 weeks old, weighing 160-180 g, purchased from the animal facility centre at NIPER, Chandigarh-India.

2.1.3 Chemicals, Kits and Oligo primers

DEPC (Diethyl polycarbonate), DNase and RNase free Water, streptozotocin, glibenclamide were obtained from Sigma Aldrich Co. USA. Total lipid, tissue glycogen content, S.G.O.T, S.G.P.T, alkaline phosphatase, urea, and creatinine estimation kits were purchased from (Transasia Bio Medical Limited, Himachal Pradesh, India). Enzyme linked immunosorbant assay kits for insulin estimation from plasma was purchased from Boehringer Mannheim Diagnostic, Mannheim, Germany. Agarose, methanol, hank's balanced salt solution, collagenase, D-glucose, sucrose, xylene, bovine serum albumin (BSA pH 7.4), ficoll (Type-400), chromium hematoxylin phloxin stain, Krebs Ringer bicarbonate buffer (KRB), sodium hydrogen carbonate (NaHCO_3), HEPES and hematoxylin, eosin and paraffin wax were purchased from Hi-Media Mumbai, India. One step RT-PCR kit was purchased from Bangalore Genei (Bangalore, India). The primer pairs used for analysis were: GK-F5'-CAGACAGTCCTCACCTGCAA-3', GK-R5'-TTTGTCTTCACGCTCCACTG-3'; G6Pase-F5'-ACCCTGGTAGCCCTGTCTTT-3', G6Pase-R5'-ACTCATTACACGGGCTGGTC-3'; Ins II-F5'-CTGTGGATCCGCTTCCTG, Ins II F5'-AGAGAGAGCAGATGGTG-3', PEPCK-F5'-ATACGGTGGGAACTCACTGC-3', PEPCK-R5'-ACCCCATCACTTGTCTCAG-3'; Gapdh-F5'-AGACAGCCGCATCTTCTTGT-3', Gapdh-R5'-TACTCAGCACCAGCATCACC-3' and β -Actin-F5'-CAGCGGAACCGCTCATTGCCAATGG-3', β -Actin-R5'-TCACCCACAC

ATCACCCACACACTGTGCCCCATCTACGA-3' were purchased from Sigma genosys, Bangalore, India. Data obtained was analyzed using Statistical software - Origin 6.1 (Origin Lab Corporation, USA).

2.2 METHODOLOGY

2.2.1 Preparation of the bark extract in solvents of increasing polarity

Cinnamomum zeylanicum bark ~500 g was weighed, thoroughly powdered and kept airtight in cool, dry and dark conditions. Approximately 50 g was weighed and placed in a Soxhlet apparatus and extracted with solvents of increasing polarity (methanol and distilled water) for 60 h each. The methanol extract and aqueous extract were concentrated in a rotary evaporator at reduced pressure. The concentrated crude extract was lyophilized into powder and 10 mg/ml stock was used for the study.

2.2.2 Experimental Model

The study was conducted on adult 26 male wistar rats, *Rattus norvegicus* of age group 8-10 weeks old, weighing 160-180g. Animals were purchased from the animal facility centre at National Institute of Pharmaceutical Education & Research (NIPER), Chandigarh-India. They were housed in colony cages, maximum 5 rats/cage at an ambient temperature of 25 ± 2 °C with 12 h light and dark cycles. The rats were fed normal diet purchased from commercial vendors. The animals were then randomly divided into three groups (n = 5 rats per group) as given below: Group I—untreated (control); Group II –streptozotocin treated (diabetic); Group III -streptozotocin-induced diabetic rats treated with aqueous extract of *Cinnamomum zeylanicum* (diabetic treated). After randomization into various groups, the rats were acclimatized for a period of a further 2-3 weeks in the new environment before initiation of the experiment. Animals

described as fasting had been deprived of food for at least 16 h but were allowed free access to drinking water. All the experiments with animals were carried out according to the guidelines of the institutional animal ethical committee and had prior approval. The procedures were confirmed to the UFAW handbook on the care and Management of Laboratory Animals.

2.2.3 Induction of type 1 diabetes mellitus

2.2.3.1 Streptozotocin

Streptozotocin (STZ, 2-deoxy-2-(3-(methyl-3-nitrosourido)-D-glucopyranose) is a commonly used substance in development of diabetic animal models for the study of diabetes. Originally isolated from *Streptomyces achromogenes* as an effective broad spectrum antibiotic drug, STZ also possesses anti-tumour, diabetogenic and oncogenic properties. Rakieten and his associates first demonstrated the diabetogenic property of STZ in dogs and rats in 1963.

The STZ molecule consists of a glucose residue with a methylated nitrosourea linked to carbon-2 (Figure 2.1). Its nitosourea moiety especially at the O6 position of guanine is responsible for Beta cell toxicity, while deoxyglucose moiety facilitates transport across the cell membrane via Glut-2-glucose transporter. Inside the cell, STZ is decomposed and reactive methylcarbonium ions are produced, which may alkylate the DNA and cause cross links between the DNA strands. This leads to the activation of DNA repair mechanisms and increases in the activity of poly-ADP-ribose synthetase, which in turn depletes NAD in beta –cells. This causes a deficiency in cofactors for oxidative phosphorylation with subsequent lack of ATP, and causes diminished protein synthesis,

insulin release and reduced activity of the ion pumps, which ultimately lead to beta cell death.

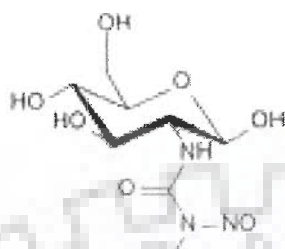


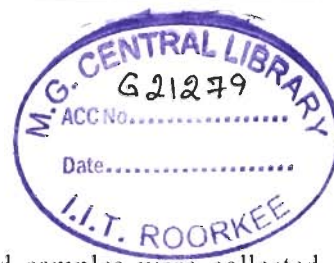
Figure 2.1: Chemical structure of Streptozotocin

For the induction of diabetes overnight starved rats were injected with a freshly prepared solution of streptozotocin (65 mg/kg bw) in 0.1M citrate buffer, pH 4.5 was injected intraperitoneally. The rats in control group were injected with sodium citrate buffer as vehicle control. Fasting blood glucose (FBG) was estimated at the time of induction of diabetes and postprandial glucose (PPG) was checked regularly until stable hyperglycemia was achieved. The rats having marked hyperglycemia (FBG > 250 mg/dl) were selected for the study as stable hyperglycemic animals (Brondum, Nilsson and Aalkjaer, 2005).

2.2.4 In-Vivo study

2.2.4.1 Effect of methanol and aqueous *Cinnamomum zeylanicum* extracts on blood glucose levels of normal fasted rats

Fasted rats were divided into five groups of five rats per group. The first group of animals was given distilled water through oral intubations and served as control (Group I). Groups II and III were given methanol extract orally at dose of 100 and 200 mg/kg body weight, respectively while group IV and V were given aqueous extract orally at



dose of 100 and 200 mg/kg body weight, respectively. Blood samples were collected from the tail vein at 0, 60, 120 and 180 min after the oral administration of the extracts.

2.2.4.2 Effect of methanol and aqueous *Cinnamomum zeylanicum* extracts on glucose tolerance in normal fasted rats

The Oral Glucose Tolerance Test (OGTT) is the gold standard for the diagnosis of diabetes mellitus. It is a useful epidemiological tool and has been used to determine the prevalence of diabetes. In this test following a standard glucose load, blood glucose levels is monitored at regular intervals.

OGTT was performed in all the groups over night fasted animals after completion of the treatment. During fasting, the animals were allowed to drink water. Fasted rats were divided into three groups of five rats in each group. Control rats (group I) were given distilled aqueous. Oral dose of 100 and 200 mg/kg body weight of methanol extracts were administered to second and third groups of rats respectively, while groups IV and V were given aqueous extract orally at dose of 100 and 200 mg/kg body weight, respectively. The rats of all the groups were given glucose (2 g/kg body weight; p.o.) 30 min after administration of the drug. Blood samples were collected from the tail vein just prior to glucose administration and at 30, 120 and 180 min after the glucose loading and blood glucose levels were measured immediately. The results were expressed in terms of milligram per deciliter (mg/dl) of blood.

2.2.4.3 Effect of methanol and aqueous *Cinnamomum zeylanicum* extract on streptozotocin-induced diabetic rats

The diabetic rats were divided into five groups, each containing five animals. Control rats (group I) were given distilled water orally, while dose of methanol extract

100 and 200 mg/kg body weight were given to the second and third groups, respectively while group IV and V were given aqueous extract orally at dose of 100 and 200 mg/kg body weight, respectively. Blood samples were collected just prior to and 30, 120, 180 and 240 min after drug administration. Thereafter OGTT assay was performed in the diabetic rats. The diabetic rats were divided into four groups, each containing five animals. The negative control group (group I) were given distilled water orally, while dose of methanol and aqueous extract at dose 200 mg/kg body weight were given to the second and third groups, respectively. Group IV which served as the positive control was given a dose of hypoglycemic agent Glibenclamide (10 mg/kg body weight). Blood samples were collected just prior to and 30, 120, 180 and 240 min after drug administration.

2.2.4.4 Long term effect of aqueous extract of *Cinnamomum zeylanicum* on streptozotocin induced diabetic rats

The effect of *cinnamomum zeylanicum* was also tested for a long duration of treatment. The male wistar rats (160 g) were divided into three groups of five rats each. The control diabetic group (group I) received distilled water instead of extract. The rats of groups II were orally given a dosage of 200 mg/kg body weight, of aqueous cinnamon extract for 15 days. Blood samples were collected through the tail vein just prior to and on days 0, 6, 10 and 15 days after the streptozotocin injection. The blood sugar and the body weights of the animals were measured.

2.2.4.5 Estimation of lipid profile in blood samples

On completion of the treatment, blood samples were collected and lipid profiles for all the three groups of animals were obtained by using commercially available kits. Total cholesterol, high density lipoprotein (HDL) cholesterol and triglyceride (TG) levels in serum were determined according to the instructions of the manufacturer (Transasia Bio Medical Limited, Himachal Pradesh, India). For the determination of very low density lipoprotein (VLDL) and low density lipoprotein (LDL) cholesterol, Friedwald's formula was used which states: $VLDL \text{ cholesterol} = \text{Triglyceride} / 5$ and $LDL \text{ cholesterol} = \text{Total cholesterol} - (VLDL + HDL \text{ cholesterol})$.

2.2.4.6 Biochemical estimation of tissue glycogen content

On completion of the treatment the estimation of tissue glycogen from liver, was carried out by the established method of (Sadasivam & Manikam, 1996). Samples were homogenized separately in warm 80 % ethanol at the concentration of 100 mg/ml and then centrifuged at 10, 000 rpm for 20 min. the residue was collected and allowed to dry over water bath. To each residue 5 ml of distilled water and 6 ml of perchloric acid was added and extracted further at 0 °C for 20 min. the collected extract was centrifuged at 10, 000 rpm for 15 min and 1 ml the supernatant was collected. From the supernatant, 0.2 ml was transferred to a graduated test tube and the volume was made up to 1 ml with distilled water. To each tube added 4 ml of anthrone reagent and incubated at 95 °C in a boiling water bath for 10 min. the absorbance of the sample was measured with UV/Visible spectrophotometer (Varian Cary Bio 100, USA) at 630 nm after cooling the tube at room temperature. The amount of glycogen in tissue sample was expressed in microgram of glucose per milligram wet weight of tissue.

2.2.4.7 Biochemical estimation of enzyme activity in serum samples

2.2.4.7.1 Estimation of S.G.O.T. in blood samples

On completion of the treatment, blood samples were collected and centrifuged at 5000 rpm for 10 minutes to obtain serum and S.G.O.T. levels for all the three groups of animals were obtained by using commercially available kits. S.G.O.T. levels in serum were determined according to the instructions of the manufacturer (Transasia Bio Medicals Limited, Himachal Pradesh, India).

2.2.4.7.2 Estimation of S.G.P.T. in blood samples

On completion of the treatment, blood samples were collected and centrifuged at 5000 rpm for 10 minutes to obtain serum and serum S.G.P.T. levels for all the three groups of animals were obtained by using commercially available kits. S.G.P.T. levels in serum were determined according to the instructions of the manufacturer (Transasia Bio Medicals Limited, Himachal Pradesh, India).

2.2.4.7.3 Estimation of alkaline phosphatase in blood samples

On completion of the treatment, blood samples were collected and centrifuged at 5000 rpm for 10 minutes to obtain serum and serum alkaline phosphatase levels for all the three groups of animals were obtained by using commercially available kits. Alkaline phosphatase levels in serum were determined according to the instructions of the manufacturer (Transasia Bio Medicals Limited, Himachal Pradesh, India).

2.2.4.7.4 Estimation of urea in blood samples

On completion of the treatment, blood samples were collected and centrifuged at 5000 rpm for 10 minutes to obtain serum and urea levels for all the three groups of animals were obtained by using commercially available kits. Urea levels in serum were determined according to the instructions of the manufacturer (Transasia Bio Medical Limited, Himachal Pradesh, India).

2.2.4.7.5 Estimation of creatinine in blood samples

On completion of the treatment, blood samples were collected and centrifuged at 5000 rpm for 10 minutes to obtain serum and creatinine levels for all the three groups of animals were obtained by using commercially available kits. Creatinine levels in serum were determined according to the instructions of the manufacturer (Transasia Bio Medical Limited, Himachal Pradesh, India).

2.2.5 Preparation of the various phytochemical rich fractions from aqueous extract of *Cinnamomum zeylanicum*

The aqueous extract which showed a better glucose lowering effect compared to methanol extract, was further screened to identify the phytochemical group of compounds in the extract using protocols reported (Wagner et al, 1984). Four groups of phytochemicals were prepared namely, (1) anthraglycosides, bitter principles, flavonoids and arbutin (Fraction I) (2) saponins (Fraction II) (3) Cardiac glycosides (Fraction III) and (4) terpenes, coumarins, phenol carboxylic acids, valepotriates (Fraction IV) were prepared using standard protocol (Wagner, Bladt, Zgainski, Scott, 1984). The fractions were further screened for their antihyperglycemic activity using *in vitro* method.

2.2.6 Effect of aqueous and its phytochemical-rich fractions of cinnamon on the release of insulin by *in vivo* and *in vitro* methods respectively

2.2.6.1 *In vivo* studies

In order to discover the active phytochemical group of compound involved in stimulating the release of insulin, serum insulin levels were measured in diabetic rats treated with the extract for 15 days. Serum insulin levels were estimated in each sample of blood using enzyme linked immunosorbant assay kits (Boehringer Mannheim Diagnostic, Mannheim, Germany).

2.2.6.2 *In vitro* studies

Isolation of pancreatic cells was done according to methods reported earlier (Gupta, Kesari, Watal, Murthy, Chandra and Maithal, 2005; Xia & Laychok, 1993) with slight modification. After removing the pancreas from the rats, they were perfused with Hank's balanced salt solution (HBSS) (pH 7.4) for about 15 min to remove blood and endogenous insulin. This was followed by finely mincing the tissue and then they were incubated for 30 min at 37°C with rapid magnetic stirring in a solution of crude collagenase (4 mg/ml) in HBSS containing 0.3% glucose and 1% bovine serum albumin (BSA) pH 7.4. In the next step, the separation of the islet cells from acinar tissues was done with ficoll (Type-400) (Himedia, Mumbai, India) with varying gradients, followed by centrifugation. The islets were picked up from the interphase of 20–11% gradient by Pasteur pipette. The purity of the islet cells were checked by Gomori's chromium hematoxylin phloxin stain (Gomori, 1941). After dividing into 10 islets/batch they were pre-incubated with glucose – Krebs Ringer bicarbonate buffer (KRB), along with

NaHCO₃ (0.2%), HEPES (0.38%), insulin-free BSA (0.1%) and 10 mM glucose for 5 min at 37 °C in a CO₂ incubator. The incubation was continued for a further 1 h after adding 50 µl of plant extract (final concentration of 30 mg/l) or buffer for controls. Aliquots of 50 µl were removed from the incubation mixture at the end of incubation (i.e. 1 h) and were stored at -20 °C prior to insulin assay. Insulin was measured using commercially available ELISA kit.

2.2.7 Semiquantitative Reverse Transcriptase–PCR

This was performed in highly aseptic conditions and all the glassware used in the experiment was baked at 250 °C for 6 h and then treated with DEPC treated water before autoclaving. Total RNA was extracted from the liver of the rat treated with 200 mg/kg bw of aqueous extract of cinnamon and diabetic control rats according to Gen Elute™ Mammalian Total RNA Miniprep Kit from Sigma-Aldrich, USA. The isolated RNA samples were quantified and equal amount of it were reverse transcribed according to the manufacturer's instructions with the help of the one step RT–PCR kit purchased from Sigma Co. U.S.A. PCR was performed by denaturing at 94°C for 60 s, annealing at various temperatures (depending on primer pairs) and by extension at 72°C for 60 s and 35 additional cycles were used for amplification. The primer sequences were designed with the help of Primer3 software for Glucokinase (GK), PEPCK, Gapdh, Ins II, G6pase and β-Actin. On completion of the PCR reaction the samples were ran in 2 % agarose gels. Agarose gel was prepared by melting 2 gm agarose in 100 ml of 1x TAE (Tris acetate EDTA) buffer (50x stock having 242 gm of Tris base, 57.1 ml of glacial acetic acid and 100 ml of 0.5 M EDTA). The gel was allowed to cool up to a temperature of approximate 55 °C and ethidium bromide was added to a final concentration of 0.5 µg/ml.

the solution was poured into a tray and gel was allowed to set and finally dipped with sufficient amount of 1x TAE buffer. The PCR product were mixed with 0.2 volumes of 6x gel loading buffer (0.25 % bromophenol blue, 40 % sucrose w/v in water), loaded on the gel and electrophoresis was carried out. The intensity of the bands on gels was converted into a digital image with a gel analyzer documentation system (Bio Rad, USA).

2.2.8 Histopathology of Pancreatic Tissue

For histopathological staining, the basic protocol by Mukherjee, 2003 was followed with modification according to our laboratory conditions. Briefly the pancreatic tissue was separated and fixed in Bouins solution (saturated aqueous solution of picric acid, 75 %; formalin, 25 % glacial acetic acid, 25 %) for 4 h. Following the fixation; sections were washed thoroughly in 30 % alcohol until all the color of picric acid disappeared. This was followed by gradual dehydration of the samples by placing them in ascending series of alcohols (each change for 1 h) viz. 30 %-50 %-70 %-80 % (2 changes) - 100 % (3 changes) – xylene (3 changes). The tissues were then placed in wax, made into blocks and finally cut into sections of 5 micron thickness. Section were adhered on the slide treated with Mayer's solution (per 100 ml having 50 ml egg albumin, 50 ml glycerin, 1 gm sodium salicylate), stretched at approximately 40 °C temperatures and preserved at room temperature. The sections were then stained in haematoxylin and eosin by placing the slide in different solutions in a sequential manner as described below:

Xylene (2 changes, each 5 min) followed by 1 min change each in 1:1 (v/v) xylene and 100 % alcohol -100 % alcohol (2 changes)- 90 % alcohol – 80 % alcohol- 70 % alcohol- washing in tap water followed by gentle tapping of slide – haematoxylin

solution (5 min)- washing in running water- 3 to 4 dipping of slide in 0.5 % HCl- wash in distilled water (1 min)- several dipping in ammonia water (section changes to blue colour)- wash in distilled water (1 min)-80 % alcohol (1 min) – 95 % alcohol (1 min)- eosine staining (2 to 3 min) – 70 % alcohol – 95 % alcohol – 100 % alcohol (1 min each) – xylene (two changes, 1 min each). This was followed by mounting of tissues with Canada balsam and preservation with coverslip.

2.2.9 Toxicity study

The *Cinnamomum zeylanicum* aqueous extract was orally administered at a concentration of 100 200 and 300 mg/kg of body weight per day for a period of 15 days. The toxic effect of *Cinnamomum zeylanicum* aqueous extract was measured by body weight gain and morphological changes.

2.2.10 Statistical Analysis

All values are represented as means \pm SEM (standard error of mean). The statistical significance was evaluated by independent two population *t*-test using the statistical software Origin 6.1 (Origin Lab Corporation, USA).

2.3 RESULTS

2.3.1 Hypoglycemic test in normal Male Wistar Rats

The hypoglycemic effect of aqueous and methanol extracts at dose of 100 mg/kg body weight and 200 mg/kg body weight was evaluated in normal male wistar rats (Table 2.1 (a-b)). The groups of rats treated with 200 mg/kg body weight of aqueous and methanol extracts showed better hypoglycemic effect as compared to 100 mg/kg body

weight of the extracts. Therefore the concentration 200 mg/kg body weight was carried forward for glucose tolerance test in normal male wistar rats.

| Time (min) | Blood Glucose (mg/dl) | | |
|-------------|-----------------------|------------------|---------|
| | Aqueous extract | Methanol extract | Control |
| 0 | 100 ± 1* | 105 ± 5* | 104 ± 5 |
| 60 | 96 ± 1* | 94 ± 6* | 103 ± 3 |
| 120 | 81 ± 5* | 78 ± 6* | 101 ± 4 |
| 180 | 72 ± 3* | 71 ± 5* | 98 ± 5 |
| % Reduction | 28 | 32 | 5.8 |

Table 2.1 (a): Hypoglycemic effect of aqueous and methanol extracts of *Cinnamomum zeylanicum* (100 mg/kg body weight) in normal male wistar rats. Each value represent the mean ± S.E.M., n = 5. * Represent statistically significant result as compared to normal group (p< 0.05).

| Time (min) | Blood glucose(mg/dl) | | |
|-------------|-----------------------|------------------|---------|
| | Aqueous extract | Methanol extract | Control |
| 0 | 106 ± 2* | 112 ± 4 | 104 ± 5 |
| 60 | 97 ± 1* | 90 ± 7 | 103 ± 3 |
| 120 | 85 ± 4* | 84 ± 7 | 101 ± 4 |
| 180 | 69 ± 3* | 70 ± 3 | 98 ± 5 |
| % Reduction | 34.9 | 37.5 | 5.8 |

Table 2.1 (b): Hypoglycemic effect of aqueous and methanol extracts of *Cinnamomum zeylanicum* (200 mg/kg body weight) in normal male wistar rats. Each value represents the mean ± S.E.M., n = 5. * Represent statistically significant result as compared to normal group (p< 0.05).

2.3.2 Oral Glucose Tolerance Test (OGTT) in normal Male Wistar Rats

The aqueous extract (200 mg/kg body weight) showed remarkable activity and ability to normalize the hike in the blood glucose level when a glucose dose of 2 g/kg

body weight was given to all the groups (Table 2.2 a). The activity of methanol extract was not encouraging at the given concentration as compared to the aqueous extract treated animals.

| Time (min) | Blood Glucose (mg/dl) | | |
|------------|-----------------------|------------------|---------|
| | Aqueous extract | Methanol extract | Control |
| 0 | 104 ± 6* | 110 ± 5 | 108 ± 1 |
| 30 | 110 ± 2* | 131 ± 8 | 167 ± 5 |
| 120 | 106 ± 5* | 158 ± 2 | 135 ± 8 |
| 180 | 80 ± 4* | 118 ± 3 | 129 ± 1 |

Table 2.2(a): OGTT assay of aqueous and methanol extracts of *Cinnamomum zeylanicum* in normal male wistar rats. Each value represent the mean ± S.E.M., n = 5. * Represent statistically significant result as compared to normal group (p< 0.05).

2.3.3 Oral Glucose Tolerance Test (OGTT) in streptozotocin induced type 1 diabetic rats

In the OGTT assay conducted in diabetic rats, the aqueous extract (200 mg/kg body weight) showed similar profile of tolerance of blood glucose level as exhibited in normal rats (Table 2.2 b). The above data show a greater potency of the aqueous extract to tolerate the sudden rise in blood glucose than methanol extract in streptozotocin induced male wistar rats.

| Time (min) | Blood Glucose (mg/dl) | | | |
|------------|-----------------------|------------------|------------------|------------------|
| | Aqueous extract | Methanol extract | Positive control | Negative control |
| 0 | 274 ± 22* | 334 ± 17 | 244 ± 6 | 230 ± 8 |
| 30 | 371 ± 21* | 543 ± 12 | 299 ± 4 | 488 ± 10 |
| 120 | 335 ± 42* | 550 ± 24 | 287 ± 3 | 465 ± 5 |
| 180 | 276 ± 37* | 525 ± 25 | 231 ± 2 | 445 ± 8 |
| 240 | 230 ± 16* | 486 ± 23 | 229 ± 2 | 423 ± 7 |

Table 2.2 (b): OGTT assay of aqueous and methanol extracts of *Cinnamomum zeylanicum* conducted in type 1 diabetic male wistar rats. Each value represent the mean ± S.E.M., n = 5. * Represent statistically significant result as compared to diabetic group (p< 0.05).

2.3.4 Activity of the aqueous extract for short duration

The greater potency of the aqueous extract in reducing and normalizing the blood glucose level as compared to methanol extract attributes its further use in short and long duration treatment of streptozotocin induced type 1 diabetes in male wistar rats (Table 2.3 a). Both 100 and 200 mg/kg body weight concentration were considered for this study. It was observed that 200 mg/kg body weight showed higher ability (61 %) to reduce the blood glucose level of type-I diabetic rats as compared to 100 mg/kg body weight (47 %). The aqueous extract at the concentration of 200 mg/kg body weight remarkably reduced the glucose level to normal levels (70-120 mg/kg body weight).

| Time (min) | Blood Glucose (mg/dl) | | |
|-------------|---|---|------------------|
| | Aqueous extract (300 mg/kg body weight) | Aqueous extract (200 mg/kg body weight) | Diabetic control |
| 0 | 237 ± 6 | 303 ± 31* | 277 ± 10 |
| 60 | 240 ± 10 | 305 ± 33* | 320 ± 14 |
| 120 | 188 ± 16 | 299 ± 42* | 289 ± 18 |
| 180 | 132 ± 2 | 240 ± 33* | 272 ± 5 |
| 240 | 97 ± 11 | 209 ± 26* | 262 ± 11 |
| 300 | 92 ± 5 | 162 ± 38* | 289 ± 10 |
| % Reduction | 61.2 | 46.5 | - 4.3 |

Table 2.3 (a): Short term activity of aqueous extracts of *Cinnamomum zeylanicum* conducted in type 1 diabetic rats. Each value represent the mean ± S.E.M., n = 5. * Represent statistically significant result as compared to diabetic group (p < 0.05).

2.3.5 Antidiabetic activity of aqueous extract for long duration

Both 100 mg/kg body weight and 200 mg/kg body weight concentrations were used to determine the long-term effect of the aqueous extract on streptozotocin induced diabetic rats (Table 2.3 b). Upon daily treatment with aqueous extract the blood glucose level was measured on 0th, 6th, 10th and 15th day. The concentration of 200 mg/kg bodyweight was found to reduce the glucose level by 68.40 % from its initial value.

| Group | Blood Glucose(mg/dl) | | | | % age activity |
|------------------|----------------------|---------------------|----------------------|----------------------|----------------|
| | 0 th day | 6 th day | 10 th day | 15 th day | |
| Diabetic treated | 288 ± 5* | 237 ± 4* | 150 ± 12* | 107±8* | 68.40 |
| Diabetic control | 304 ± 14 | 312 ± 5 | 337 ± 4 | 321±14 | |

Table 2.3 (b): Long term activity of aqueous extract of *Cinnamomum zeylanicum* (200 mg/kg weight) conducted on type 1 diabetic male wistar rats. Each value represent the mean ± S.E.M., n = 5. * Represent statistically significant result as compared to diabetic group (p< 0.05).

2.3.6 Acute Toxicity studies

The Normal rats were treated with aqueous extract of *Cinnamomum zeylanicum* for a period of 15 days for toxicity study. The toxic studies revealed non toxic nature of *Cinnamomum zeylanicum* at a concentration of 100, 150 and 200 mg/kg body weight for a period of 15 days. There was no morphological change like respiratory distress, hair loss, restlessness, convulsion, laxative, coma, weight loss, etc. There was no lethality or any toxic reactions found at any of the doses selected till the end of the treatment period.

2.3.7 Body weight levels

There was a gradual increase in body weight in the normal controls while the diabetic controls continued to lose weight. However, treated diabetic group gained 31.6 % weight as compared to diabetic control and the bodyweights of diabetic treated animals were towards normal range (Table 2.4).

| Group | Before treatment | After treatment |
|------------------|------------------|-----------------|
| Normal | 159.0 ± 3.6 | 163 ± 2.4 |
| Diabetic control | 160.0 ± 4.4 | 120 ± 3.2 |
| Diabetic treated | 162.0 ± 2.8* | 158 ± 2.6* |

Table 2.4: Effect of 200 mg/kg body weight of the aqueous extract of *Cinnamomum zeylanicum* on body weight of diabetic and treated rats for 15 days. Each value represent the mean ± S.E.M., n = 5. * Represent statistically significant result as compared to diabetic group (p< 0.05).

2.3.8 Estimation of lipid profile

Various parameters of blood lipid profiles were tested in streptozotocin-induced diabetic rats before and after the treatment with the plant extract. A trend towards normalcy in the levels of TC, LDL, VLDL and TG in the treated animal was observed as compared to control (Table 2.5 a).

| Group | TC(mg/dl) | HDLC(mg/dl) | LDLC(mg/dl) | TG(mg/dl) | VLDLC (mg/dl) |
|----------|------------|-------------|-------------|------------|---------------|
| Normal | 141 ± 3.8 | 40 ± 2.1 | 78 ± 3.1 | 113 ± 3.7 | 23 ± 1.9 |
| Diabetic | 208 ± 8.2 | 25.6 ± 1.5 | 147 ± 7.4 | 176 ± 7.2 | 35 ± 1.4 |
| Treated | 182 ± 4.7* | 32 ± 2.8* | 125 ± 3.8* | 134 ± 6.6* | 28 ± 0.6* |

Table 2.5 (a): Serum levels of different lipids before and after the administration of aqueous extract of *Cinnamon zeylanicum* in streptozotocin-induced diabetic rats. Each value represent the mean ± S.E.M., n = 5. * Represent statistically significant result as compared to diabetic group (p< 0.05).

2.3.9 Glycogen level in liver

The treatment with aqueous extract of cinnamon led to an increase of 63.27 % in liver glycogen content in the diabetic treated animals when compared to the diabetic control (Table 2.5 b).

| <i>Group</i> | <i>Glycogen</i> |
|-------------------------|-----------------|
| Normal | 49.47 ± 3.41 |
| Diabetic control | 16.26 ± 2.34 |
| Diabetic treated | 44.28 ± 3.35* |

Table 2.5 (b): Glycogen level (μg of glucose per mg of tissue) of normal and experimental groups of rat liver before and after the administration of aqueous extract of *Cinnamom zeylanicum*. Each value represent the mean \pm S.E.M., n = 5. *

Represent statistically significant result as compared to diabetic group ($p < 0.05$).

2.3.10 Liver function tests serum SGOT, SGPT, ALKP, Creatinine and Urea

In the case of diabetic rats, the serum SGOT, SGPT and ALKP levels were reduced by 68.04, 64.4, and 47.05 % respectively, with respect to initial value. The serum urea and creatinine levels decrease in the diabetic animals by 68.02 and 52.63 %, respectively, as compared to initial values. The values of each parameter were in the normal range (Table 2.5 c-d).

| <i>Treatment Group</i> | <i>Alkaline Phosphatase(IU/L)</i> | <i>SGOT (IU/L)</i> | <i>SGPT (IU/L)</i> |
|------------------------|-----------------------------------|--------------------|--------------------|
| Normal | 73 ± 3.8 | 26 ± 2.9 | 30 ± 3.3 |
| Diabetic | 136 ± 4.4 | 97 ± 4.7 | 104 ± 7.5 |
| Treated | 72 ± 2.6* | 31 ± 2.5* | 37 ± 2.1* |

Table 2.5 (c): Serum levels of alkaline phosphatase, SGPT and SGOT before and after the administration of aqueous extract of *Cinnamon zeylanicum* in streptozotocin-induced diabetic rat. Each value represent the mean ± S.E.M., n = 5. * Represent statistically significant result as compared to diabetic group (p< 0.05).

| <i>Treatment Group</i> | <i>Urea(mg/dl)</i> | <i>Creatinine(mg/dl)</i> |
|------------------------|--------------------|--------------------------|
| Normal | 38.5 ± 2.5 | 1 ± 0.15 |
| Diabetic | 108 ± 3.15 | 1.9 ± 0.18 |
| Treated | 41 ± 1.7* | 0.9 ± 0.16* |

Table 2.5 (d): Serum levels of urea and creatinine before and after the administration of saponin-rich fraction of *Cinnamon zeylanicum* in streptozotocin-induced diabetic rat. Each value represent the mean ± S.E.M., n = 5. * Represent statistically significant result as compared to diabetic group (p< 0.05).

2.3.11 Effect of aqueous extract of cinnamon on serum insulin level

Serum insulin level was significantly decreased in diabetic rats with respect to control. After 15 days of plant extract supplementation to the diabetic rats, there was

significant elevation in serum insulin levels as compared to the diabetic group. Treatment with extract resulted in 15.96 % increase in insulin level and the serum insulin level of diabetic treated animals were towards normal range (Table 2.6 a).

| <i>Treatment group</i> | <i>Serum insulin(μIU/ml)</i> |
|------------------------|------------------------------|
| Normal | 21.6 ± 3.42 |
| Diabetic | 16.32 ± 3.6 |
| Treated | 19.42 ± 2.86* |

Table 2.6 (a): Serum insulin levels before and after the administration of aqueous extract of *Cinnamom zeylanicum* in streptozotocin-induced diabetic rats. Each value represent the mean ± S.E.M., n = 5. * Represent statistically significant result as compared to diabetic group (p< 0.05).

2.3.12 Effect of fraction (I to IV) on the *in vitro* release of insulin

In order to further understand the role of the each phytochemical rich fraction of aqueous extract of cinnamon as an insulinotropic agent based on insulin release *in vitro* from pancreatic islets of Langerhans of diabetic rats was investigated. The incubation of ten islets from normal rats with 10 mM glucose in the presence of fractions (I to IV) for 1 h .The fraction III showed a maximum of 11 % increase in stimulation of insulin, compared to the normal pancreatic secretion of insulin under the stimulation of 10 mM glucose (Table 2.6 b).

| <i>Fraction No</i> | <i>Conc. (μIU/ml)</i> |
|--------------------------|-----------------------|
| Control | 128.7±4.24 |
| FractionI (1ng) | 57.24±2.32 |
| FractionI (30ng) | 129.2±1.82 |
| FractionI (60ng) | 63.9±1.88 |
| FractionII (1ng) | 55.4±1.4 |
| FractionII (30ng) | 151.94±1.62* |
| FractionII (60ng) | 136.2±1.93 |
| FractionIII (1ng) | 13.2±0.6 |
| FractionIII (30ng) | 43.9±1.72 |
| FractionIII (60ng) | 46.05±1.86 |
| Fraction IV (1ng) | 18.12±1.49 |
| Fraction IV (30ng) | 36.1±1.77 |
| Fraction IV (60ng) | 35.72±1.57 |

Table 2.6 (b): *In vitro* results of insulin stimulation to determine the active phytochemical fraction from aqueous extract of *Cinnamon zeylanicum*. Each value represent the mean ± S.E.M., n = 5. * Represent statistically significant result as compared to normal (p< 0.05).

2.3.13 Gene expression profile

As shown in (Fig. 2.2), a marked change in expression profile of mRNA of all the glucose regulatory enzymes studied in liver was observed in diabetic treated groups (group III). The hepatic level of hexokinase and glucose-6-phosphate dehydrogenase was increased by 2.5-fold in diabetic treated rats; while the pancreatic insulin II expression showed several fold increase, when compared to the diabetic rat. At the same time there

was a clear reduction in the expression patterns of gluconeogenic enzymes, G6Pase and PEPCCK, by almost 2-fold as compared to diabetic rats (group II). In contrast the hepatic β -Actin showed uniform expression in each group's normal, diabetic and treated animals (Fig 2.2).

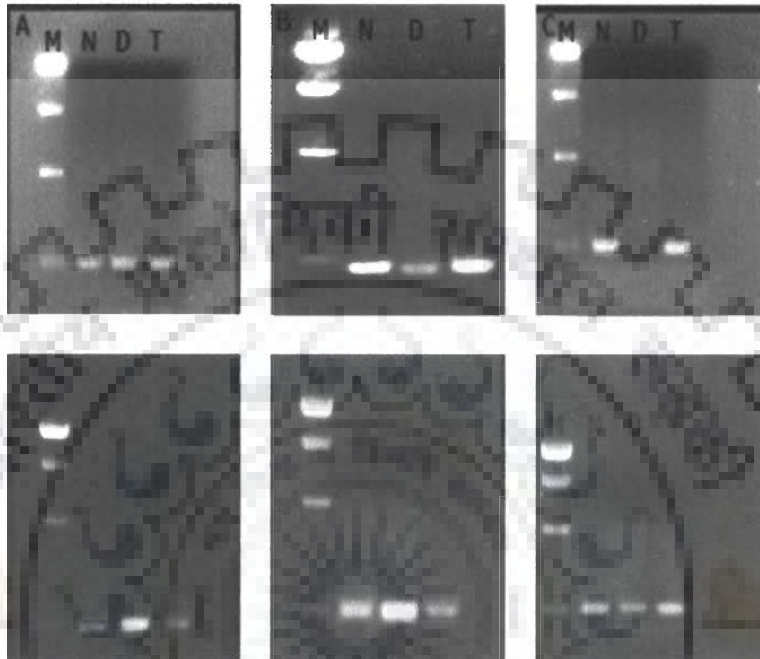


Fig. 2.2 (a-f): RT-PCR analysis of (A) liver mRNA expression of alpha Actin, (B) liver mRNA expression of glucokinase, (C) liver mRNA expression of glucose-6-phosphate dehydrogenase, (D) liver mRNA expression of glucose-6-phosphatase, (E) liver mRNA expression of Phosphoenol pyruvate carboxykinase, (F) liver mRNA expression of Insulin II. Where, M, N, D and T denote DNA ladder, Normal, Diabetic and Treated samples of RNA, respectively.

2.3.14 Histopathological studies

Sections of pancreas from the diabetic (group II) and diabetic treated (group III) rats had clearly shown the protective effect of the aqueous extract of cinnamon. A clear

decrease in the area occupied by the β cells was observed in the pancreatic sections, probably due to the reduction in the number of those cells in streptozotocin-induced diabetic rats (Fig. 2.3 a) which was again normalized in diabetic rats treated with aqueous extract of cinnamon (Fig. 2.3 b).

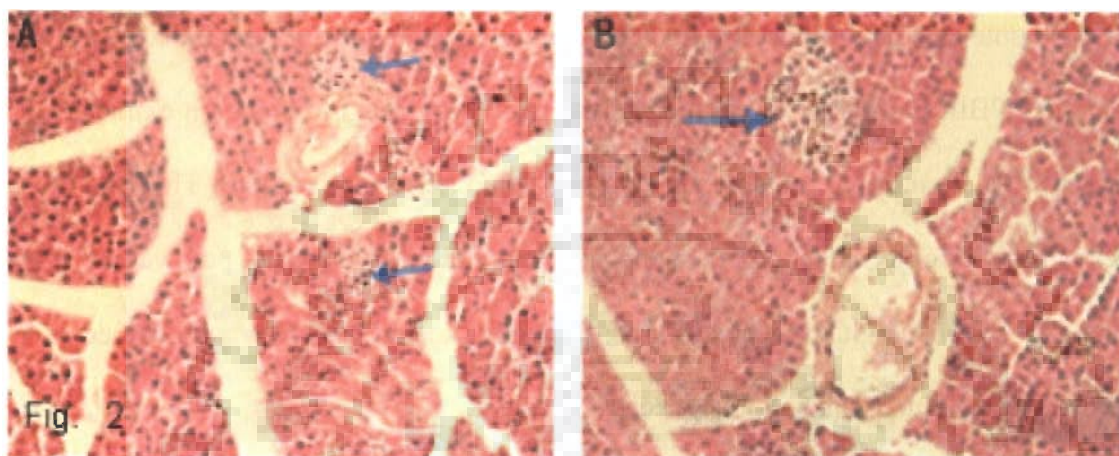


Fig. 2.3 (a-b) Photomicrograph of pancreas from (A) streptozotocin-induced diabetic rat and (B) diabetic rat treated with aqueous extract of *Cinnamom zeylanicum*. Hematoxylin and Eosin, 20 X objectives. The arrow indicates the islet region of the section.

2.4 Discussion

Streptozotocin has been shown to induce free radical production and cause tissue injury (Kolb, 1987). The pancreas is especially susceptible to the action of streptozotocin-induced free-radical damage. The single intraperitoneal injection of streptozotocin (65 mg/kg) induced damage, mimics the insulin dependent diabetic (T1DM) conditions to a greater extent (Brondum, et al., 2005; Kenneth and Youming, 2008). It was reported earlier that cinnamon extract could act as a free radical scavenger *in vitro* (Mathew &

Abraham, 2006). Cinnamon extract have been shown to improve insulin action via increasing glucose uptake, by enhancing insulin-signaling pathway in skeletal muscle in type 2 diabetes (Qin, Nagasaki, Ren, Bajotto, Oshida & Sato, 2003).

The comparative study of *Cinnamomum cassia* and *Cinnamomum zeylanicum* in normal wistar rat showed better reduction of blood glucose level in case of *Cinnamomum cassia* . In this context the anti-diabetic effect of *Cinnamomum cassia* in type 2 diabetic animal model (C57BIKsj db/db) was shown and the regulatory role of cinnamon extract in blood glucose level and lipid metabolism was suggested (Kim et al., 2006). Thus the past studies is limited to non insulin dependent diabetes (T2DM), where the pathway of glucose metabolism like glucose absorption through skeletal muscles and other alternative pathway of glucose metabolism becomes critical.

The present investigation reports anti-diabetogenic and hypoglycemic effects of the aqueous extract of *Cinnamomum zeylanicum* on streptozotocin- induce type 1 diabetic rats. The experimental results presented here could provide a basis for understanding the exact molecular mechanism of action of this plant's active principles. At a dose of 200 mg/kg bodyweight, cinnamon aqueous extract was found to reduce the blood glucose level and tolerate the challenge by glucose in OGTT assay in both normal and treated streptozotocin induced diabetic rats more efficiently than methanol extract. The significant stabilization of the blood glucose level in glucose loaded rats (OGTT) can be attributed to the potentiation of the insulin effect by increasing the pancreatic secretion of insulin from existing β -cells. The dosage of 200 mg/kg bw of *Cinnamomum zeylanicum* aqueous extract, showed excellent reduction of blood glucose level in long treatment In this context a number of other plants have been observed to have similar patterns of

hypoglycemic effects (Eidi, Eidi, & Esmaeili, 2006; Kasiviswanath, Ramesh, & Kumar, 2005). The increase in the serum insulin (*in vivo*) and the stimulated release of insulin, (*in vitro*) indicates the insulintropic property of aqueous extract and its saponin rich fraction, respectively. In past, the aqueous soluble polyphenol-type A polymers of cinnamon have shown to induce insulin release (Anderson et al., 2004). This supports our finding that aqueous extract and in particular its saponin rich fraction probably acts as an insulintropic agent as well.

Glycogen is the primary intracellular storable form of glucose and its level in liver is a direct reflection of insulin activity, which regulates glycogen deposition by stimulating glycogen synthase and inhibiting glycogen phosphorylase. Since streptozotocin causes selective destruction of β -cells of islets of Langerhans, resulting in marked decrease in insulin levels, it could be predicted that glycogen levels in liver decrease as the influx of glucose in the liver is inhibited in the absence of insulin (Golden, Wals, & Okakima, 1979). However, this alteration in hepatic glycogen content is normalized by insulin treatment (Yadav et al., 2002). Our study showed that, although the levels of glycogen in aqueous extract treated diabetic rats could not achieve the same level as that of non-diabetic control mice, yet the extract could significantly improve the hepatic glycogen contents. This indicates one of the possible ways the aqueous extract might act by improving the process of glycogenesis in liver.

Administration of aqueous extract improved the liver function by decreasing the serum SGPT, SGOT, ALKP, creatinine and urea levels in diabetic rats. The increase of SGOT and SGPT will increase the incidence of heart and liver diseases. SGOT is an enzyme found primarily in the cells of the liver, heart, skeletal muscles, kidneys, and

pancreas and to a lesser extent, in red blood cells. Its serum concentration is in proportion to the amount of cellular leakage or damage. It is released into serum in larger quantities when any one of these tissues is damaged. Its increased levels are usually associated with heart attacks or liver disease. *Cinnamomum zeylanicum* aqueous extract decreased the SGOT level, which is an indication of the protective effect on liver and heart. The significance of SGPT, an enzyme found primarily in the liver, is far greater. Its enhanced release into the bloodstream is the result of liver abnormality. It therefore serves as a fairly specific indicator of liver status and its elevated levels in serum indicate liver damage. An increased level of ALKP indicates bone disease, liver disease or bile tract blockage. *Cinnamomum zeylanicum* aqueous extract reduced the ALKP, creatinine and urea levels too, indicating its protective effect over liver and improvement in liver functional efficiency. There was a little change toward normalcy in the levels of TC, LDL, VLDL and TG in the treated animals.

In order to understand the molecular mechanism of action of *Cinnamomum zeylanicum* aqueous extract as anti-diabetogenic agent, the expression level of Glucokinase, glucose-6-phosphatase, glucose-6-phosphate dehydrogenase, Insulin II and Phosphoenol pyruvate carboxykinase was analyzed. These enzymes are directly linked to glucose homeostasis and production of glycogen. The glucokinase is involved in the phosphorylation step of glucose in glycolysis. Glucokinase was significantly reduced in the liver of diabetic rats. This possibly can be the reason for the decreased utilization of glucose and increased blood glucose level (Vestergaard, 1999). The *Cinnamomum zeylanicum* aqueous extract treated diabetic rats showed increased activity of glucokinase that may lead to activation of glycolysis and increased utilization of glucose for energy

production. The aqueous extract treated diabetic rats showed increased expression of insulin when compared to its diabetic control; this might be another possible reason for the normalcy of the blood glucose level. Glucokinase that may lead to reduction in the expression of the latter two enzymes (G6Pase and PEPCK) in response to extract treatment provides an additional clue to its role in carbohydrate metabolism.

In conclusion, the data obtained from the present study indicates that *Cinnamomum zeylanicum* aqueous extract contains bioactive molecules such as Saponins which may be beneficial as both hypoglycemic and anti-hyperglycemic agents. To the best of our knowledge, this is the first ever report on the role of Saponins from *Cinnamomum zeylanicum* aqueous extract in type 1 diabetes. It is necessary to identify and isolate the particular compound showing the desired effect from the *Cinnamomum zeylanicum* aqueous extract. However, the present study gives a preliminary indication that the Saponins rich fraction has potential to act at multiple sites of glucose regulatory pathways. Toxicity studies proved that the dose used in this investigation is safe for the animal as it did not show any change in morphological parameter. Considering all these facts, it is reasonable to undertake further studies on possible usefulness of saponin-rich *Cinnamomum zeylanicum* aqueous extract in the treatment of type 1 diabetes mellitus (T1DM).

A QUALITATIVE AND QUANTITATIVE ASSAY TO SCREEN THE DNA INTERACTING COMPONENT BASED ON THE SEQUENCE SELECTIVE INHIBITION OF RESTRICTION ENDONUCLEASES

The mutual recognition of molecules is fundamental to all the biological processes. It is indeed thought to be decisive in enzyme catalysis and inhibition, DNA replication, gene expression and its control and drug action. It is appreciated that DNA is a primary target for many potent anti-tumor agents; a substantial body of research has been directed towards understanding the molecular basis of DNA sequence specificity for binding, by identifying the preferred binding sequences of many key drugs with DNA. Despite the perception of the importance of this recognition as a whole, little is known about the details of both the sequence specific recognition as well as the relationship of concentration based affinity of anti-tumor drugs with their specific target sequences. This simple and rapid method (Restriction Inhibition Assay) was further used to screen, the plant extract and its active phytochemicals involved in binding with sequences *EcoRI* and *HindIII* with higher specificity in a relatively qualitative and quantitative manner. A compound bound at or near the restriction site inhibits enzymatic cleavage of DNA; inhibition of *HindIII* and *EcoRI* activity by preincubation of DNA-substrate (extract/phytochemical rich fraction) was assessed in this study using linearized pBR322 plasmid DNA.

The aim of the present study is.

1. To use the restriction inhibition assay, using *Hind*III, *Eco*RI and *Eco*RV restriction enzymes, to evaluate the binding specificity of DNA with anticancer drugs (mitoxantrone, berberine and palmatine). For this purpose both a 448bp DNA fragment derived from pBCKS+ plasmid (harboring the polylinker region with multiple restriction endonuclease sites) as well as a linearized pQE32 plasmid has been used as a template for sequence selective inhibition by the test drugs.
2. To screen for phytochemicals that inhibits *Eco*RI and *Hind*III restriction enzymes.
3. To search for *Eco*RI and *Hind*III restriction sequences in the library of cDNA/mRNA and ESTs of certain oncogenes.

The inhibition of endonuclease *Hind*III at 220 μ M concentration was observed with mitoxantrone giving a direct evidence of the co-existence of concentration and sequence specificity for drug-DNA interaction. We have also confirmed sequence specificity of daunomycin, adriamycin and distamycin-A using Restriction Inhibition Assay (RIA), with the available literature and have standardize the protocol using them as standard for our experimental work.

The second study was carried out to correlate the interaction of DNA with phytochemical having possible anticancer potential and hence as inhibitors of oncogene expression. The current study is the first report of applying restriction endonuclease inhibition assay to screen phytochemical, from *Cinnamomum zeylanicum* bark and *Picrorrhiza kurroa* rhizome extracts, showing sequence affinity for *Eco*RI (5'-GAATTC-3') and *Hind*III (5'-AAGCTT-3'), respectively. The clinical significance of the work is

related to anticancer property, by searching for (5'-GAATTC-3') and (5'-AAGCTT-3') in the mRNA and their corresponding STS (Sequence Tag Sites) and ESTs (Expressed Sequence Tag) of BRCA 2 (oncogene).

3.1 MATERIALS

3.1.1 Chemicals

Adriamycin, daunomycin, distamycin-A, mitoxantrone, berberine, palmitine, potassium acetate, sodium hydroxide, 6X loading dye, Tris-HCl, EDTA, chloroform, isoamyl alcohol and ethanol were purchased from Sigma Aldrich Co. USA. Restriction endonucleases *PvuII*, *Xba I*, *HindIII*, *EcoRI* and *EcoRV* supplied with NEB (10 X) restriction buffer (100 mM tris-HCl pH 7.5, 1 mM EDTA (Ehylene diamine tetra acetic acid), 100 mM magnesium acetate, 500 mM potassium acetate) was purchased from New England Biolab, UK. Distamycin-A and Mitoxantrone were purchased from Sigma Aldrich Co. USA. Restriction Endonucleases *PvuII*, *HindIII* and *EcoRI* supplied with NEB (10 X) restriction buffer (100 mM tris-HCl pH 7.5, 1 mM EDTA, 100 mM magnesium acetate, 500 mM potassium acetate) were purchased from New England Biolab, UK. Cesium chloride (CsCl) purified plasmid pBR322 DNA was purchased from Bangalore Gennei, India.

3.1.2 Plant Material

The *Cinnamomum zeylanicum* bark and the Rhizome of *Picrorrhiza kurroa* was obtained from Dr. A.N. Nautiyal (HNB Garhawal University, Utrakhand, India).

3.2 METHODOLOGY

3.2.1 Transformation of bacterial cells

All the procedures were strictly performed under sterile conditions. DH5 α bacterial cells were grown at 37 °C, 250 rpm to an OD₆₀₀ of 0.8. The culture was then allowed to chill at 4 °C in a pre-chilled falcon tube. These cells were pelleted at 5000 rpm for 10 min at 4 °C and re-suspended in 35 ml of pre-chilled 80 mM CaCl₂ and 20 mM MgCl₂ solution. The cells were re-pelleted and suspended in 2 ml of 0.1 M CaCl₂ to obtain the competent cells. An aliquot of these cells were added with 5 ng of pBCKS⁺ plasmid DNA, mixed well and incubated at 4 °C for 30 min. Proper negative and positive controls with no plasmid and known plasmids respectively were included. The cells were subjected to heat shock at 42 °C for 90 sec and immediately transferred to ice. Luria-Bertani (LB) broth was added to each tube and incubated at 37 °C for 45 min. The transformed cells were finally spread plated on antibiotic containing plates corresponding to the antibiotic resistant gene in the plasmid. The plates were incubated overnight at 37 °C.

3.2.2 Plasmid Isolation

The transformed bacteria was grown overnight at 37 °C, 250 rpm in LB broth containing an antibiotic. A small aliquot, 1.5 ml culture was pelleted by centrifugation at 5000 rpm for 10 min and the bacterial pellet was resuspended in 100 μ l of 50 mM glucose, 25 mM tris-Cl (pH 8.0), 10 mM EDTA (pH 8.0) solution. To the suspended cells, 200 μ l of freshly prepared 0.2 N NaOH, 1% SDS solution was added and mixed by inverting the tube gently and then incubated for 5 min at room temperature. After the

incubation, 150 μ l of ice-cold 5 M potassium acetate (pH 4.7) solution was added and the tubes were incubated on ice for 10 min. The solution was then centrifuged at 15,000 rpm for 15 min, at 4 °C and the supernatant was precipitated for the plasmid DNA by adding two volumes of ethanol. The DNA was pelleted at 14,000 rpm for 20 min at 4°C. Finally, the pellet was washed with 70% (v/v) ethanol, re-pelleted, air dried, suspended and stored at -20 °C in tris-HCl buffer (10 mM tris-HCl, pH 8.0) containing 1 mM EDTA. The quality of the plasmid DNA was confirmed by running the DNA on the agarose gel.

3.2.3 Quantification of DNA using spectrophotometer

2 μ l of the DNA/RNA sample was diluted in 1 ml of nuclease free water and its OD was determined at 260 nm and 280 nm against nuclease free water as blank. The ratio of the OD₂₆₀/OD₂₈₀ was calculated to check the purity of the nucleic acid. The quantity of DNA and RNA can be calculated using the standard value-

For DNA: 1 OD_{260nm} = 50 μ g/ml

For RNA: 1 OD_{260nm} = 33 μ g/ml

3.2.4 DNA fragment for restriction inhibition assay

The 448 bp fragment was obtained from pBCKS⁺ DNA by the following procedure. The 448 bp DNA fragment was derived from pBCKS⁺ plasmid (harboring the polylinker region with multiple restriction endonuclease sites) by restricting with *Pvu*II restriction enzyme and eluting the 448 bp fragment by gel elution and then purifying it further by phenol , chloroform and isoamyl alcohol method and ethanol precipitation. The 448 bp fragment was stored at -20 °C in Tris HCl buffer (10 mM Tris HCl, pH 8.0) containing 1 mM EDTA.

3.2.5 Transformation and Isolation and linearization of pQE32 plasmid DNA

The plasmid pQE32 DNA (kindly provided by Professor Aparna Dixit of School of Biotechnology, JNU, India) consists of an insert of 800 bp between the *EcoRI* and *HindIII* restriction site within the plasmid, was transformed in DH5 α as mentioned above. The plasmid DNA was isolated and stored at -20 °C in tris-HCl buffer (10 mM tris-HCl, pH 8.0) containing 1 mM EDTA. The plasmid pQE32 was linearized by restricting with *XbaI*. The linearized vector DNA sample was stored at -20 °C in Tris HCl buffer (10 mM Tris HCl, pH 8.0) containing 1 mM EDTA.

3.2.6 Binding Studies

The anti tumor drug–DNA complexes were prepared by pre incubating 4 μ l (300 ng) of the 448 bp DNA fragment, and 2 μ l (300 ng) of the linearized plasmid DNA with a range of concentration of the drugs in NEB restriction buffer (1 X), for 30 minutes at 37 °C. The restriction digestion carried out by incubating with *EcoRI*, *EcoRV* and *Hind III* respectively for a further 1 hr at 37 °C in a final volume of 20 μ l. A control setup with the DNA along with each restriction enzyme alone was kept to analyze the results of the restriction inhibition assay. Each digestion was stopped by incubation for 20 min at 65 °C followed by 10 min at 4 °C. A 20 μ l of the digestion mixture was added with 5 μ l of 6 X DNA loading dye (0.25 % bromophenol blue and 30 % glycerol) and loaded on to 2 % horizontal agarose gel in case of 448 bp DNA fragment, while 1 % horizontal agarose gel in case of linear plasmid DNA which was run in Tris-acetate EDTA buffer (40 mM Tris Base, pH 8.0, 18 mM glacial acetic acid and 1 mM EDTA) at 100 V for 2 hr. The gel was

exposed to 220 nm near UV region spectrum and then the DNA bands were visualized and analyzed for drug-DNA interaction studies.

3.2.7 Preparation of aqueous extract of *Picrorrhiza kurroa* and *Cinnamomum zeylanicum*

A routine procedure was followed for the preparation of aqueous extract (Saenphet et al. 2006). Approximately ~500 g of the rhizome and bark of *Picrorrhiza kurroa* and *Cinnamomum zeylanicum* respectively, was weighed thoroughly powdered and kept airtight in cool, dry and dark conditions. Approximately 50 g was weighed and placed in a Soxhlet apparatus and extracted with distilled water for 48 h. The aqueous extract was concentrated in a rotary evaporator at reduced pressure. The dried residue was dissolved in appropriate volume of DNase and RNase free water to obtained 10 mg/ml concentration and stored at -20 °C until use. The concentrated crude extract was lyophilized into powder and 10 mg/ml stock was used for the study.

3.2.8 Screening of DNA-extract binding studies of *Cinnamomum zeylanicum* and *Picrorrhiza kurroa* by restriction inhibition assay

The plasmid pBR322 was linearized using *PvuII*. The linearized plasmid (600 µg) was further incubated with standard drugs-distamycin-A (10 µM), mitoxantrone (220 µM) and aqueous extract of *Cinnamomum zeylanicum* and *Picrorrhiza kurroa* (5 µg to 1 mg/ml) in 20 µl of reaction volume for 30 mins at 37 °C. The reaction mixtures were further incubated with restriction digestion carried out by incubating with *EcoRI* and *HindIII* respectively for a further 1 hr at 37 °C in a final volume of 20 µl. A control setup with the DNA along with each restriction enzyme was kept to analyze the results of the

restriction inhibition assay. Each digestion was stopped by incubation for 20 min at 65 °C followed by 10 min at 4 °C. A 20 µl of the digestion mixture was added with 5 µl of 6 X DNA loading dye (0.25 % bromophenol blue and 30 % glycerol) and loaded on to 1 % horizontal agarose gel; which was run in Tris-acetate EDTA buffer (40 mM Tris Base, pH 8.0, 18 mM glacial acetic acid and 1 mM EDTA) at 100 V for 2 hr. The gel was exposed to 220 nm near UV region spectrum and then the DNA bands were visualized and analyzed for drug-DNA interaction studies.

3.2.9 Preparation of phytochemical rich fractions from aqueous extract of *Cinnamomum zeylanicum*

The aqueous extract of *Cinnamomum zeylanicum* which showed complete inhibition of restriction activity; was further fractionated into separate phytochemical enrich fraction using standardized protocol (Wagner et al, 1984). Four groups of phytochemicals were prepared namely, (1) anthraglycosides, bitter principles, flavonoids and arbutin (Fraction I); (2) saponins (Fraction II); (3) Cardiac glycosides (Fraction III) and (4) terpenes, coumarins, phenol carboxylic acids, valepotriates (Fraction IV) were prepared using standard protocol (Wagner, Bladt, Zgainski, Scott, 1984). The fractions were further screened for their restriction inhibition activity.

3.2.10 screening of restriction inhibition activity of phytochemical rich fractions from aqueous extract of *Cinnamomum zeylanicum*

The phytochemical rich fractions (I-IV) were further screened for inhibition of restriction endonucleases *EcoRI* and *HindIII* activity, at 100 µg/20 µl and 50 µg/20 µl concentrations, respectively. The individual fractions were preincubated with linearized

plasmid DNA (pBR322) at 37 °C for 30 min followed by addition of restriction endonuclease. Each digestion was stopped by incubation for 20 min at 65 °C followed by 10 min at 4 °C. Standard drugs mitoxantrone (220 µM) and distamycin-A (10 µM) were used as positive control for *Hind*III and *Eco*RI restriction inhibition activity, respectively. Each of the samples was electrophoresed in a 1 % agarose gel at 100 V for 2 hr. The gel was further exposed to 220 nm near UV region spectrum and then the DNA bands were visualized and analyzed for drug-DNA interaction studies.

3.2.11 Screening for the minimum inhibitory concentration of the active inhibitory phytochemical rich fractions

The Fraction I, II and III were further screened for minimum inhibitory concentrations. Each fraction was preincubated with the linearized DNA at 37 °C for 30 min followed by addition of restriction endonuclease. Each of the fractions was tested for its minimum inhibitory concentration against both *Eco*RI and *Hind*III, respectively. The samples were further electrophoresed in a 1 % agarose at 100 V for 2 hr. The gel was exposed to 220 nm near UV region spectrum and then the DNA bands were visualized and analyzed for drug-DNA interaction studies.

3.2.12 Screening for the presence of *Eco*RI and *Hind*III recognition sequence in the mRNA, STS and ESTs of the oncogene

The mRNA library of oncogene was screened for the presence of 5'-GAATTC-3' and 5'-AAGCTT-3' from Sanger.ac.uk/genetics/CGP/census. The oncogene with maximum hits of *Eco*RI and *Hind*III restriction sites, respectively was selected and

analyzed further for the presence of 5'-GAATTC-3' and 5'-AAGCTT-3' in the STS (Sequence Tagged Sites) and ESTs (Expressed Sequence Tag) of the oncogene.

3.3 RESULTS and DISCUSSION (A)

The principle of the RIA assay is based upon the ability of the different anti-tumor drugs to inhibit the cleavage activity of restriction endonucleases *Hind*III, *Eco*RI and *Eco*RV. Fig. 3.1 (a-c) shows the respective recognition and cleaving sites sequences of each restriction enzyme used in this study. The Fig. 3.2(a-f) shows structures of adriamycin, daunomycin, distamycin-A, mitoxantrone, palmatine and berberine.

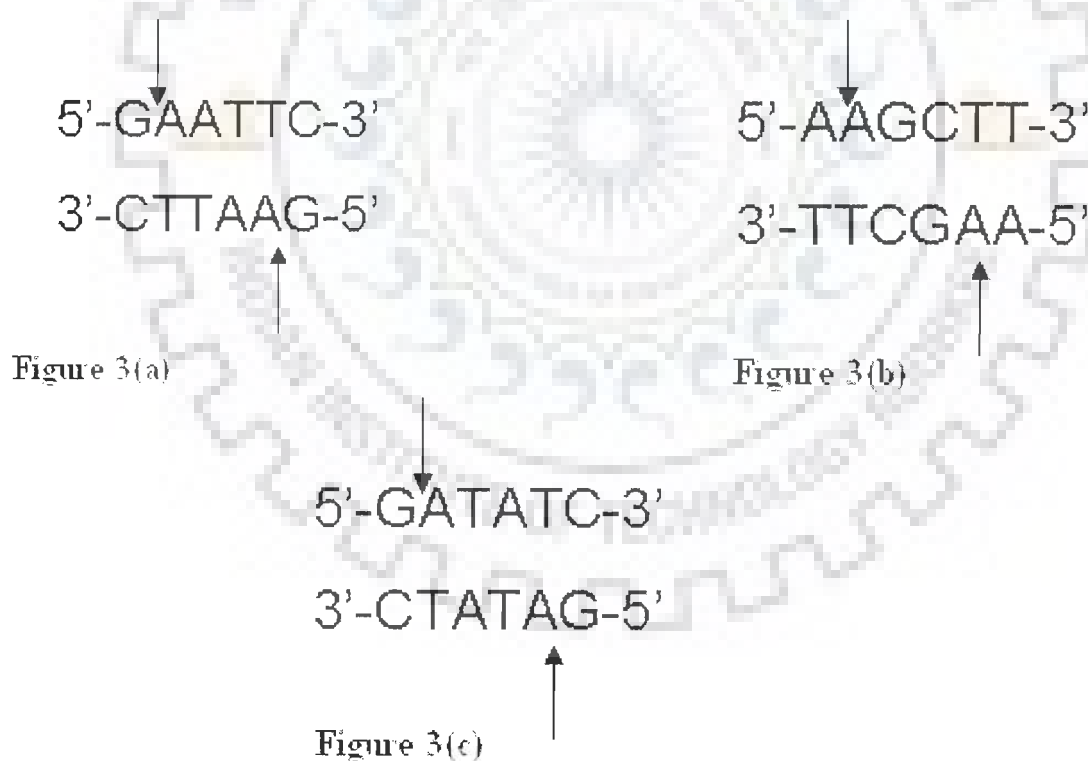


Figure 3.1 (a-c) shows the respective recognition and cleaving sites sequences of each restriction enzyme used in this study.

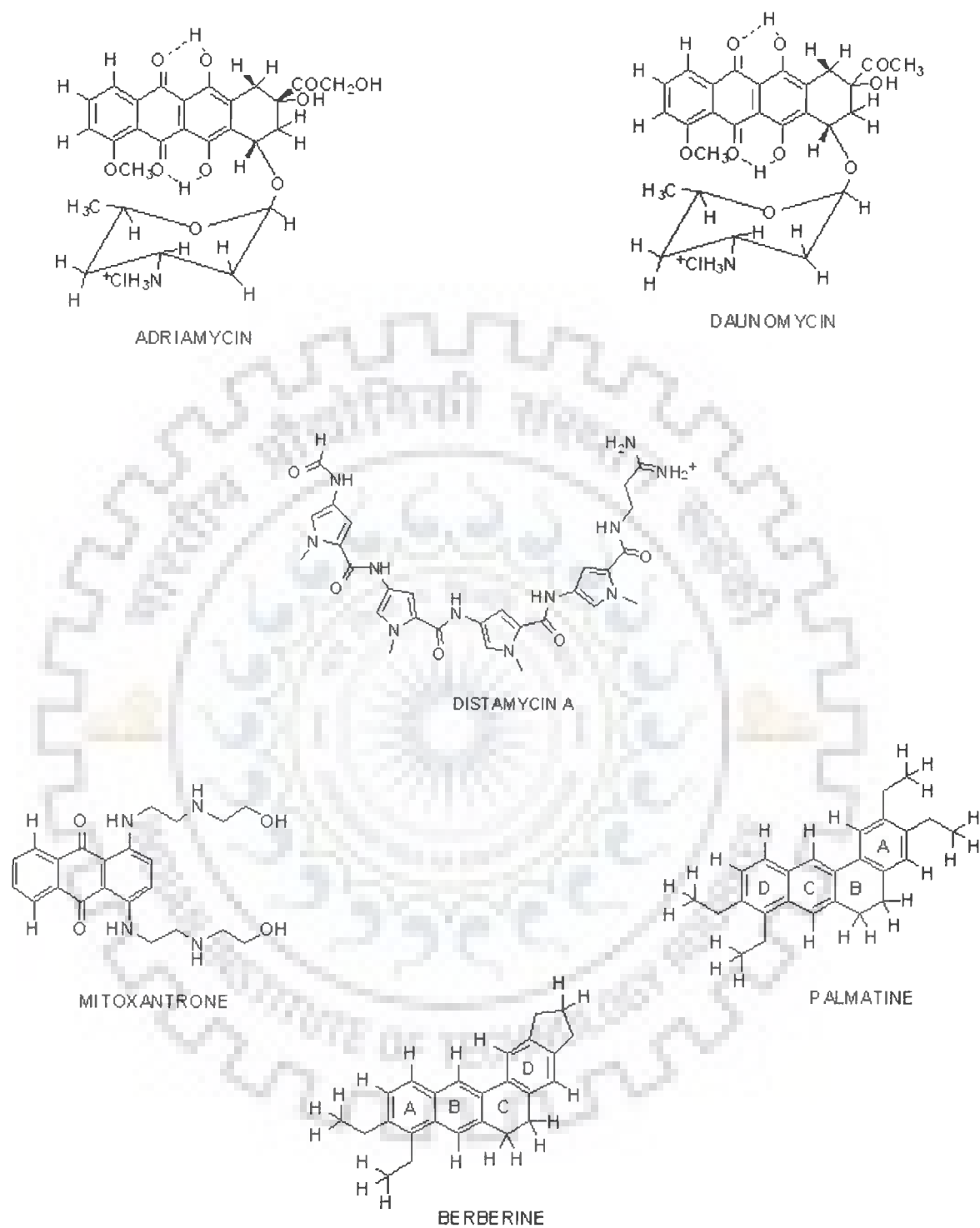


Fig. 3.2(a-f) shows structures of adriamycin, daunomycin, distamycin-A, mitoxantrone, palmatine and berberine.

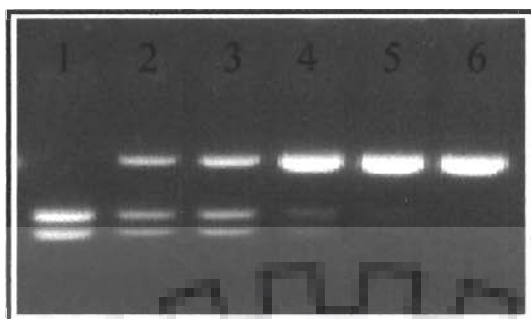


Figure 3.3 (a): 2 % agarose gel showing inhibition of *EcoRI* cleavage of 448 bp fragments of pBCKS⁺ by distamycin A. Lane 1: Control complete digest of 448 bp DNA fragment by *EcoRI*; Lane 2-6: distamycin A-448 bp complex digested by *EcoRI* with distamycin A concentration of 4, 6, 8, 10 and 12 μM , respectively.



Figure 3.3 (b): 2 % agarose gel showing inhibition of *HindIII* cleavage of 448 bp fragments of pBCKS⁺ by adriamycin. Lane 1: Control complete digest of 448 bp DNA fragment by *HindIII*; Lane 2-6: adriamycin-448 bp complex digested by *EcoRI* with adriamycin concentration of 3, 6, 12, 25, 30 50 and 100 μM , respectively.



Figure 3.3 (c): 2 % agarose gel showing inhibition of *Hind*III cleavage of 448 bp fragments of pBCKS⁺ by daunomycin. Lane 1: Control complete digest of 448 bp DNA fragment by *Hind*III; Lane 2-6: daunomycin-448 bp complex digested by *Hind*III with daunomycin concentration of 50, 80, 100, 150, 30 50 and 200 μ M, respectively.

The Figure (3.3 a-c) shows restriction inhibition assay gel for distamycin-A, adriamycin and daunomycin, each includes a control i.e. a 448 bp DNA fragment with the appropriate restriction enzyme and without the corresponding drug used for the test experiment. In each of the above case a gradual decrease in the intensity of the digested fragment was observed and finally a 100 % inhibition of restriction was observed. It was observed that distamycin inhibits the restriction digestion of *Eco*RI at 10 μ M concentration and shows its sequence specificity towards AT site present in *Eco*RI. This result was in accordance with the earlier studies done by Furrow *et al* 1986. They suggested that distamycin binds to AT rich sequences by restriction inhibition assay at 100 μ M. It was then further proved by structural studies that distamycin binds to AT base pair by minor groove binding (Klevit *et al.*, 1986; Pelton and Wemmer, 1990; Coll,

1987). Adriamycin which has been proved to bind at CA with higher affinity than GC rich sequences (Skorobogaty, 1988; Panousis and Phillips, 1994; Trist and Phillips, 1989; Chaires, 1987) using DNase foot printing assay, transcriptional and restriction inhibition assay. In our study using restriction inhibition assay adriamycin shows a complete inhibition for *Hind*III activity at 100 mM concentration and binding at GC rich sequences, which supports the sequence and structural studies done by a few authors by X-ray (Frederick, 1990) and NMR (Jain, 2005) methods which shows that, it intercalates between CG base pair. Our results also support daunomycin binding at GC rich sequence by 100 % inhibition of *Hind*III activity at 100 μ M concentration.

This result is in accordance with binding studies of daunomycin by foot printing and restriction inhibition assay (Chaires, 1987), which showed preference of daunomycin for GC base pair flanked by AT base pair. Therefore RIA can provide sequence specificity for these standard drugs used in this study. Structural studies of daunomycin complex with DNA by X-ray method showed that, it intercalates between CG base pair (Quigley, 1980). There are no conclusive reports available regarding structure and conformation of the mitoxantrone complexed to DNA. Therefore there is a need for the sequence specificity of mitoxantrone. In this context Fig. 3.4 (a), shows a typical restriction inhibition assay gel for mitoxantrone including a control: the 448 bp DNA fragment without drug. As the concentration of mitoxantrone was increased (lane 2-6), the intensity of the digested fragments decreased gradually. Finally 100 % inhibition in restriction was achieved at 220 μ M (lane 6), when compared to the control (lane 1). This shows mitoxantrone specificity for 5'-GC-3'.

This result supports the studies by (Fox, 1986; Bailly, 1986; Panousis and Phillips, 1994) using in vitro transcription assay and DNase foot printing assay respectively. These assays show sequence specificity towards CG, CA and TA (reading in the 5'-3' direction).

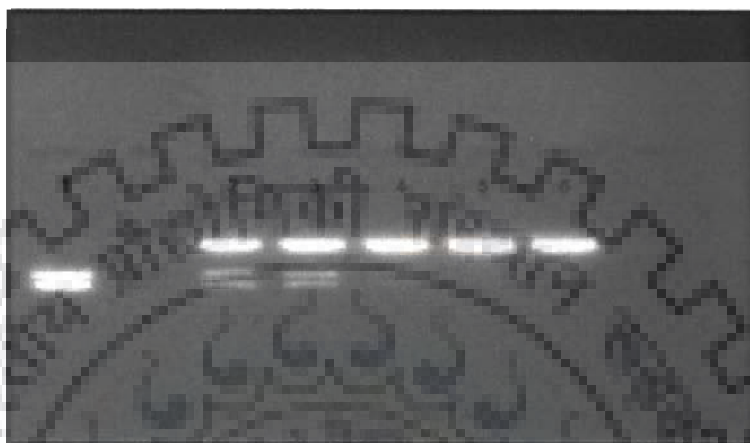


Figure 3.4 (a): 2 % agarose gel showing inhibition of *HindIII* cleavage of 448 bp fragments of pBCKS⁺ by mitoxantrone. Lane 1: Control complete digest of 448 bp DNA fragment by *HindIII*; Lane 2-6: daunomycin-448 bp complex digested by *HindIII* with daunomycin concentration of 50, 100, 150, 200 and 250 μM , respectively.

The Figure 3.4 (b) shows RIA assay gel of berberine and palmitine with *HindIII*. Restriction inhibitions due to palmatine and berberine were not observed irrespective of the concentration and restriction enzymes. Experimentally standardized binding specificity and the binding concentration of each distamycin-A, adriamycin, daunomycin, mitoxantrone, berberine and palmatine with 448 bp DNA fragment is summarized in (Table 3.1).

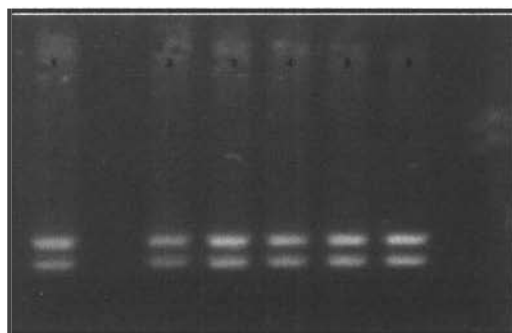


Figure 3.4 (b): 2 % agarose gel showing inhibition of *Hind*III cleavage of 448 bp fragments of pBCKS⁺ by berberine and palmatine. Lane 1: Control complete digest of 448 bp DNA fragment by *Eco*RI; Lane 2: berberine-448 bp complex digested by *Eco*RI with berberine concentration of 2 mM; Lane 3: palmatine-448bp fragment complexes digested by *Eco*RI with palmatine concentration of 2 mM; Lane 4: Control complete digest of 448 bp DNA fragment by *Eco*RV; Lane 5: Berberine-448 bp fragment complexes digested by *Eco*RV with berberine concentration of 2 mM; Lane 6: palmatine-448 bp fragment complexes digested by *Eco*RV with palmatine concentration of 2 mM.

| Drug | DNA fragment length | Binding concentrations ^a | Drugs sequence specificity ^b identified | Restriction enzyme used | Restriction enzyme restriction site |
|--------------|---------------------|-------------------------------------|--|---------------------------------|-------------------------------------|
| Mitoxantrone | 448 bp | 220 Mm | 5'-AAGCTT-3' | <i>Hind</i> III | 5'-AAGCTT-3' |
| Adriamycin | 448 bp | 100 μM | 5'-AAGCTT-3' | <i>Hind</i> III | 5'-AAGCTT-3' |
| Daunomycin | 448 bp | 100 μM | 5'-AAGCTT-3' | <i>Hind</i> III | 5'-AAGCTT-3' |
| Distamycin A | 448 bp | 10 Mm | 5'-GAATTC-3' | <i>Eco</i> RI | 5'-GAATTC-3' |
| Berberine | 448 bp | No Binding Observed at 2 mM | ----- | <i>Eco</i> RI & <i>Eco</i> R V | 5'-GAATTC-3', 5'-GATATC-3' |
| Palmatine | 448 bp | No Binding Observed at 2 mM | ----- | <i>Eco</i> R I & <i>Eco</i> R V | 5'-GAATTC-3' 5'-GATATC-3' |

Table 3.1: A summary of quantitative and qualitative binding studies of anticancer drugs

^a Concentration of different anti-tumor drugs required to inhibit restriction endonucleases cleavage by 100%.

^b Sequence selective binding of different anti-tumor drugs to the 448bp DNA fragment of pBCKS⁺ plasmid.

The specificity for each of the drugs was confirmed by performing a negative control experiment using *EcoRI* as negative control for drugs like mitoxantrone, adriamycin and daunomycin which bind to *HindIII* binding sites and conversely *HindIII* as control for drugs like distamycin A, berberine and palmatine which are known to bind at *EcoRI* binding region.

The control restriction experiment of mitoxantrone, berberine, distamycin-A and palmatine were positive i.e., showed no inhibition. But in case of adriamycin and daunomycin both the test as well as negative control experiments of adriamycin and daunomycin were found to be similar. It is known that *EcoRI* and *HindIII* sites are only 6 bp apart in the MCS (multiple cloning site) region of the pBCKS⁺ plasmid DNA.

Therefore the binding of the drug at the *HindIII* site in the negative control experiment might have caused a conformational change at the *EcoRI* binding site, thus inhibiting its activity. To confirm the above possibility, an alternative vector pQE32 plasmid DNA with an insert of 800 bp in between the *EcoRI* and *HindIII* restriction sites making *EcoRI* and *HindIII* restriction sites at least 800 bp apart was used. Figure 3.5 a, b, and c respectively, shows the standardized RIA assay gel for adriamycin and daunomycin in the linear 3.4 kb pQE32 plasmid DNA. As the concentration of adriamycin and daunomycin was increased, the intensity of the digested fragment showed a gradual decrease. Finally 100 % inhibition in restriction was achieved.

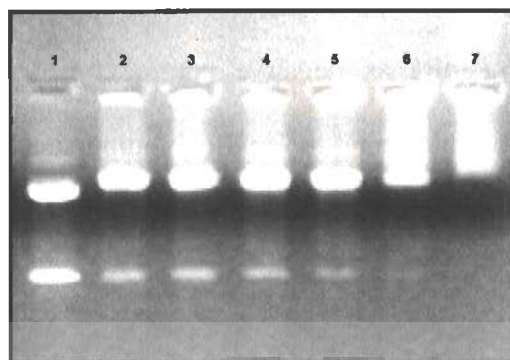


Figure 3.5 (a): 1 % agarose gel showing restriction inhibition assay of daunomycin in the linear 3.4 kb pQE32 plasmid DNA. Lane 1: Control complete digest of linear 3.4 kb pQE32 plasmid DNA by *HindIII*; Lane 2-7: daunomycin- linear 3.4 kb pQE32 plasmid DNA complexes digested by *HindIII* with daunomycin concentration of 600 μM , 700 μM , 800 μM , 900 μM , 1 mM and 2 mM, respectively.

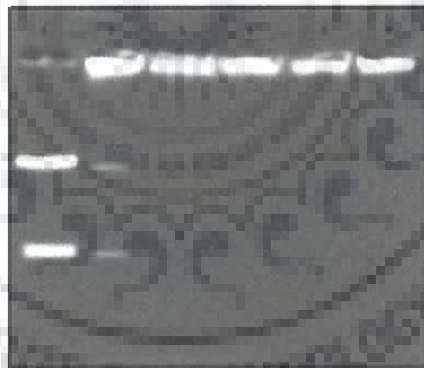


Figure 3.5 (b): 1 % agarose gel showing restriction inhibition assay of daunomycin in the linear 3.4 kb pQE32 plasmid DNA. Lane 1: Control complete digest of linear 3.4 kb pQE32 plasmid DNA by *HindIII*; Lane 2-6: daunomycin- linear 3.4 kb pQE32 plasmid DNA complexes digested by *HindIII* with daunomycin concentration of 1, 1.25, 1.50 and 2 mM respectively.

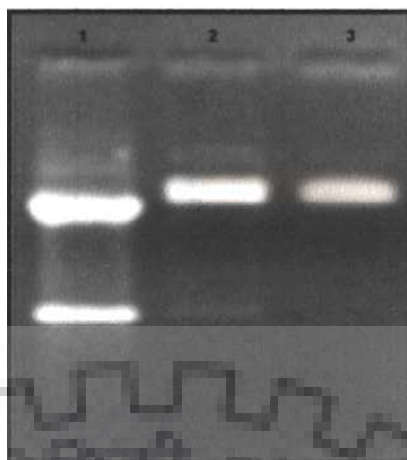


Figure 3.5 (c): 1 % agarose gel showing restriction inhibition assay of adriamycin in the linear 3.4 kb pQE32 plasmid DNA. Lane1: Control complete digest of linear 3.4 kb pQE32 plasmid DNA by *HindIII*; Lane 2-3: adriamycin-linear 3.4 kb pQE32 plasmid DNA complexes digested by *HindIII* with adriamycin concentration of 200 and 225 μM respectively.

In figure 3.6 (a) the RIA assay of adriamycin and daunomycin was performed using the linear 3.4 kb plasmid DNA. Partial inhibition at 100 μM concentration was observed compared to the complete inhibition observed at the same concentration for the 448 bp DNA fragment. However as the two restriction sites are separated by a large insert the digestion of the *EcoRI* restriction site was complete contrary to the results obtained with the 448 bp DNA fragment at 100 μM concentration. While, Table 3.2, shows the experimentally standardized sequence specificity and binding concentration of adriamycin and daunomycin in the linear 3.4 kb pQE32 plasmid DNA.

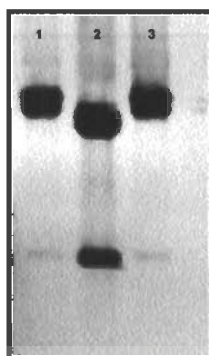


Figure 3.6 (a): 1 % agarose gel showing restriction inhibition assay of adriamycin and daunomycin in the linear 3.4 kb pQE32 plasmid DNA. Lane 1: adriamycin- linear 3.4 kb pQE32 plasmid DNA complexes digested by *Hind*III with adriamycin concentration of 100 μ M; Lane 2: control complete digest of linear 3.4 kb pQE32 plasmid DNA by *Hind*III; Lane 3: daunomycin- linear 3.4 kb pQE32 plasmid DNA complexes digested by *Hind*III with daunomycin concentration of 100 μ M.

| Drug | DNA fragment Length | Binding concentrations ^a | sequence specificity ^b Identified | Restriction enzyme used | Restriction enzyme restriction site |
|------------|-----------------------|-------------------------------------|--|-------------------------|-------------------------------------|
| Adriamycin | 3.4 kb linear plasmid | 225 μ M | 5'-AAGCTT-3' | <i>Hind</i> III | 5'-AAGCTT-3' |
| Daunomycin | 3.4 kb linear plasmid | 1.25 mM | 5'-AAGCTT-3' | <i>Hind</i> III | 5'-AAGCTT-3' |

Table 3.2: A summary of the qualitative and quantitative study of Adriamycin and daunomycin

^a Concentration of Adriamycin and Daunomycin to inhibit the restriction endonucleases cleavage by 100%.

^b Sequence specificity of different anti-tumor drugs to the linear 3.4kb pQE32 plasmid.

In the negative control experiment both adriamycin and daunomycin shows no restriction inhibition at 225 μ M and 1.25 mM concentrations, respectively at the *Eco*RI binding sites of pQE32 vector; in contrary to the results obtained with the 448 bp fragment of the pBCKS+ plasmid DNA (Figure 3.6 b).

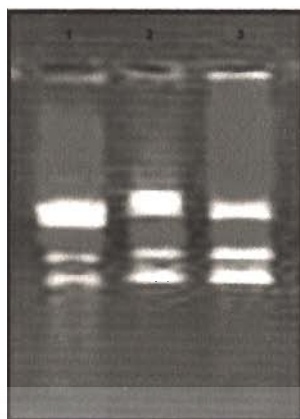


Figure 3.6 (b): 1 % agarose gel showing negative control experiment of adriamycin and daunomycin in the linear 3.4 kb pQE32 plasmid DNA. Lane 1: Control complete digest of linear 3.4 kb pQE32 plasmid DNA by *EcoRI*; Lane 2: Negative control experiment of adriamycin-linear 3.4 kb pQE32 plasmid DNA complexes digested by *EcoRI* with adriamycin concentration of 225 μM respectively; Lane 3: Negative control experiment of daunomycin-linear 3.4 kb pQE32 plasmid DNA complexes digested by *EcoRI* with daunomycin concentration of 1.25 mM.

The result obtained with modified pQE32 plasmid DNA supports the idea that a conformational change induced in the vicinity caused interference in the restriction activity of *EcoRI* in the 448 bp.

3.4 RESULTS (B)

3.4.1 Screening of DNA-Extract binding studies of *Cinnamomum zeylanicum* and *Picrorrhiza kurroa* by restriction inhibition assay

The DNA-extract binding was observed by measuring the inhibition of restriction endonucleases. Aqueous extract of *Cinnamomum zeylanicum* inhibited the activity of

restriction endonucleases *EcoRI* and *HindIII* in a concentration-dependent manner (5 µg to 1 mg/ml) in 20 µl working volume. The minimum inhibitory concentration of the aqueous extract of *Cinnamomum zeylanicum* was found to be 50 µg/ml and 100 µg/ml for *HindIII* and *EcoRI* restriction endonucleases, respectively. While the aqueous extract of *Picrorhiza kurroa* showed no binding at both the restriction sites *EcoRI* (5'-GAATTC-3') and *HindIII* (5'-AAGCTT-3'). Mitoxantrone (220 µM) and distamycin-A (10 µM) which binds to *EcoRI* and *HindIII* restriction sites, respectively were used as positive control (Figure 3.7a-b).



Figure 3.7 (a): 1 % agarose gel showing restriction inhibition assay of aqueous extract of *Cinnamomum zeylanicum* and *Picrorhiza kurroa* with *HindIII* restriction endonucleases. Lane 1: Linear plasmid (pBR322) + *HindIII*; Lane 2: Positive control-Linear plasmid (pBR322) + *HindIII* + Mitoxantrone (220 µM); Lane 3: Linear plasmid + *HindIII* + extract of *Cinnamomum zeylanicum* (10 µg); Lane 4: Linear plasmid + *HindIII* + extract (50 µg); Lane 5: Linear plasmid + *HindIII* + extract (100 µg); Lane 6: Linear plasmid + *HindIII* + extract (500 µg); Lane 7: Linear plasmid (pBR322) + *HindIII*; Lane 8: Positive control-Linear plasmid (pBR322) + *HindIII* + Mitoxantrone (200 µM); Lane 9: Linear plasmid + *HindIII* + extract of *Picrorhiza kurroa* (10 µg); Lane 10: Linear plasmid + *HindIII* + extract of (20 µg); Lane 11: Linear plasmid + *HindIII* + extract of *Picrorhiza kurroa* (100 µg); Lane 12: Linear plasmid + *HindIII* + extract of *Picrorhiza kurroa* (500 µg); Lane 13: Linear plasmid + *HindIII* + extract of *Picrorhiza kurroa* (1000 µg).

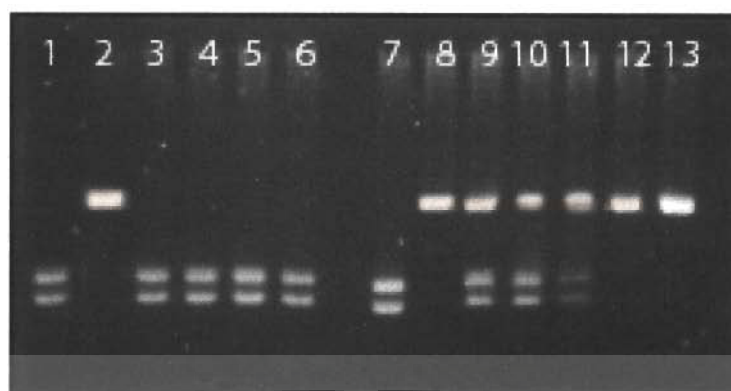


Figure 3.7 (b): 1 % agarose gel showing restriction inhibition assay of aqueous extract of *Cinnamomum zeylanicum* and *Picrorrhiza kurroa* with *EcoRI* restriction endonuclease. Lane 1: linear plasmid (pBR322) + *EcoRI*; Lane 2: Positive control-Linear plasmid (pBR322) + *EcoRI* + distamycin-A; Lane 3: Linear plasmid + *EcoRI* + aqueous extract of *Picrorrhiza kurroa* (10 μg); Lane 4: Linear plasmid + *EcoRI* + aqueous extract of *Picrorrhiza kurroa* (50 μg); Lane 5: Linear plasmid + *EcoRI* + aqueous extract of *Picrorrhiza kurroa* (100 μg); Lane 6: Linear plasmid + *EcoRI* + aqueous extract of *Picrorrhiza kurroa* (500 μg); Lane 7: Linear plasmid (pBR322) + *EcoRI*; Lane 8: Positive control-Linear plasmid (pBR322) + *HindIII* + Distamycin-A; Lane 9: Linear plasmid + *EcoRI* + aqueous extract of *Cinnamomum zeylanicum* (10 μg); Lane 10: Linear plasmid + *EcoRI* + aqueous extract of *Cinnamomum zeylanicum* (25 μg); Lane 11: Linear plasmid + *EcoRI* + aqueous extract of *Cinnamomum zeylanicum* (50 μg); Lane 12: Linear plasmid + *EcoRI* + aqueous extract of *Cinnamomum zeylanicum* (100 μg); Lane 13: Linear plasmid + *EcoRI* + aqueous extract of *Cinnamomum zeylanicum* (500 μg).

3.4.2 Screening of restriction inhibition activity of phytochemical rich fractions from aqueous extract of *Cinnamomum zeylanicum*

The binding of fractions (I-IV) to both *EcoRI* and *HindIII* restriction sites respectively, were examined by inhibition of restriction endonucleases (*EcoRI* and

HindIII). The fraction I, II and III of the aqueous extract of *Cinnamomum zeylanicum* showed complete inhibitory activity against *EcoRI* and *HindIII* restriction endonucleases at a concentration of 50 µg/ml and 5 µg/ml, respectively. The fraction IV (terpenes, coumarins, phenol carboxylic acids, and valepotriates) showed no inhibition at the given concentrations (5 µg/ml and 2.5 µg/ml) for both *EcoRI* and *HindIII* restriction endonucleases, respectively (Figure 3.7 c).



Figure 3.7 (c): 1 % agarose gel showing restriction inhibition assay of fraction I–IV of aqueous extract of *Cinnamomum zeylanicum* with both *EcoRI* and *HindIII* restriction endonucleases. Lane 1: Linear plasmid (pBR322) + *EcoRI*; Lane 2: Positive control-Linear plasmid (pBR322) + *EcoRI* + Distamycin-A (10 µM); Lane 3: Linear plasmid + *EcoRI* + Fraction I (100 µg); Lane 4: Linear plasmid + *EcoRI* + Fraction II (100 µg); Lane 5: Linear plasmid + *EcoRI* + Fraction III (100 µg); Lane 6: Linear plasmid + *EcoRI* + Fraction IV (100 µg); Lane 7: Linear plasmid (pBR322) + *HindIII*; Lane 8: positive control-Linear plasmid (pBR322) + *HindIII* + Mitoxantrone (220 µM); Lane 9: Linear plasmid + *HindIII* + fraction I (50 µg); Lane 10: Linear plasmid + *HindIII* + fraction III (50 µg); Lane 11: Linear plasmid + *HindIII* + fraction III (50 µg); Lane 12: Linear plasmid + *HindIII* + fraction IV (50 µg).

3.4.3 Screening for the minimum inhibitory concentration of the active inhibitory phytochemical rich fractions (I to III)

The binding efficiency of the fractions (I-III) was examined by measuring the minimum inhibitory concentration for both restriction endonucleases *EcoRI* and *HindIII*. The fraction I at concentrations of 40 $\mu\text{g} / \text{ml}$ and 5.6 $\mu\text{g} / \text{ml}$) inhibited the activity of restriction endonucleases, *HindIII* and *EcoRI* in a concentration dependent manner (Figure 3.8 a).

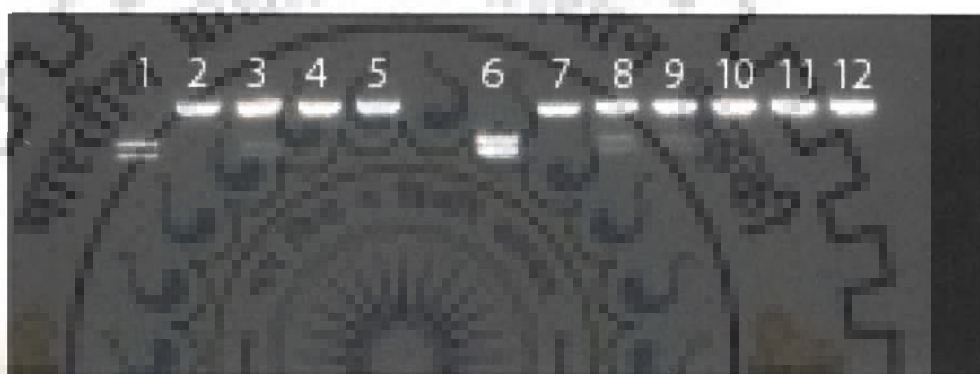


Figure 3.8 (a): 1 % agarose gel showing restriction inhibition assay of fraction I of *Cinnamomum zeylanicum* with both *EcoRI* and *HindIII* restriction endonucleases. Lane 1: Linear plasmid (pBR322) + *EcoRI*; Lane 2: Positive control-Linear plasmid (pBR322) + *EcoRI* + distamycin-A (10 μM); Lane 3: Linear plasmid + *EcoRI* + Fraction I (20 μg); Lane 4: Linear plasmid + *EcoRI* + Fraction I (40 μg); Lane 5: Linear plasmid + *EcoRI* + Fraction I (60 μg); Lane 6: Linear plasmid (pBR322) + *HindIII*; Lane 7: Positive control-Linear plasmid (pBR322) + *HindIII* + Mitoxantrone (220 μM) ; Lane 8: Linear plasmid + *HindIII* + Fraction I (0.7 μg); Lane 9: Linear plasmid + *HindIII* + Fraction I (1.4 μg); Lane 10: Linear plasmid + *HindIII* + Fraction I (2.8 μg); Lane 11: Linear plasmid + *HindIII* + Fraction I (4.2 μg); Lane 12: Linear plasmid + *HindIII* + Fraction I (7.6 μg).

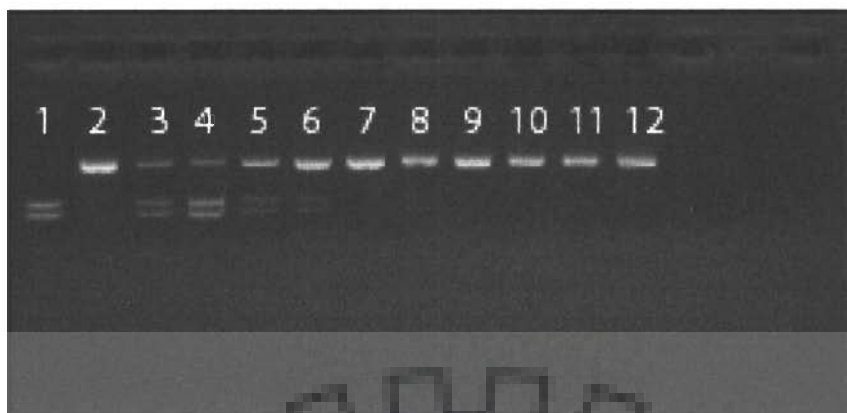


Figure 3.8 (b): 1 % agarose gel showing restriction inhibition assay of Fraction III of *Cinnamomum zeylanicum* with *Hind*III restriction endonuclease. Lane 1: Linear plasmid (pBR322) + *Hind*III; Lane 2: Positive control-Linear plasmid (pBR322) + *Hind*III + Mitoxantrone (220 μ M); Lane 3: Linear plasmid + *Hind*III + Fraction III (0.7 μ g); Lane 4: Linear plasmid + *Hind*III + Fraction III (1.05 μ g); Lane 5: Linear plasmid + *Hind*III + Fraction III of (1.4 μ g); Lane 6: Linear plasmid + *Hind*III + Fraction III (1.75 μ g); Lane 7: Linear plasmid + *Hind*III + Fraction III (2.1 μ g); Lane 8: Linear plasmid + *Hind*III + Fraction III (2.45 μ g); Lane 9: Linear plasmid + *Hind*III + Fraction III (2.8 μ g); Lane 10: Linear plasmid + *Hind*III + Fraction III (3.2 μ g).

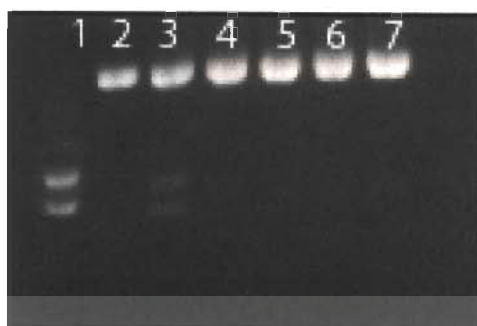


Figure 3.8 (c): 1 % agarose gel showing restriction inhibition assay of Fraction III of *Cinnamomum zeylanicum* with *EcoRI* restriction endonuclease. Lane 1: Linear plasmid (pBR322) + *EcoRI*; Lane 2: Positive control-Linear plasmid (pBR322) + *EcoRI* + mitoxantrone (220 μM); Lane 3: Linear plasmid + *EcoRI* + Fraction III of *Cinnamomum zeylanicum* (10 μg); Lane 4: Linear plasmid + *EcoRI* + Fraction III of *Cinnamomum zeylanicum* (15 μg); Lane 5: Linear plasmid + *EcoRI* + Fraction III of *Cinnamomum zeylanicum* (20 μg); Lane 6: Linear plasmid + *EcoRI* + Fraction III of *Cinnamomum zeylanicum* (25 μg); Lane 7: Linear plasmid + *EcoRI* + Fraction III of *Cinnamomum zeylanicum* (30 μg).

Like wise fraction II and III were evaluated for their binding efficiency at *EcoRI* and *HindIII* restriction sites 5'-GAATTC-3' and 5'-AAGCTT-3', respectively. The fraction II inhibited the restriction endonucleases, *EcoRI* and *HindIII* at 2.1 $\mu\text{g/ml}$ and 15 $\mu\text{g/ml}$ respectively in a concentration dependent manner (Figure 3.8 b-c). Similarly the minimum inhibitory concentration for fraction III was found to be 15 $\mu\text{g/ml}$ and 40 $\mu\text{g/ml}$, respectively for *HindIII* and *EcoRI* restriction endonucleases (Figure 3.8 d).



Figure 3.8 (d): 1 % agarose gel showing restriction inhibition assay of Fraction II of *Cinnamomum zeylanicum* with both *Eco*RI and *Hind*III restriction endonucleases. Lane 1: Linear plasmid (pBR322) + *Eco*RI; Lane 2: Positive control-linear plasmid (pBR322) + *Eco*RI + distamycin-A (10 μ M); Lane 3: Linear plasmid + *Eco*RI + Fraction II (5 μ g); Lane 4: Linear plasmid + *Eco*RI + Fraction II (10 μ g); Lane 5: Linear plasmid + *Eco*RI + Fraction II (15 μ g); Lane 6: Linear plasmid + *Eco*RI + Fraction II (20 μ g); Lane 7: Linear plasmid + *Eco*RI + Fraction II (25 μ g); Lane 8: Linear plasmid (pBR322) + *Hind*III; Lane 9: Positive control-Linear plasmid (pBR322) + *Hind*III + mitoxantrone (220 μ M); Lane 10: Linear plasmid + *Hind*III + Fraction II (5 μ g); Lane 11: Linear plasmid + *Hind*III + Fraction II (10 μ g); Lane 12: Linear plasmid + *Hind*III + Fraction II (30 μ g); Lane 13: Linear plasmid + *Hind*III + Fraction II (40 μ g); Lane 14: Linear plasmid + *Hind*III + Fraction II (50 μ g).

3.4.4 Screening for the presence of *EcoRI* and *HindIII* recognition sequence in the mRNA and STS and ESTs of the oncogenes

The library of oncogenes was screened for the presence of 5'-GAATTC-3' and 5'-AAGCTT-3' sequence, respectively. The oncogene Breast cancer 2, early onset mRNA (BRCA2) with, maximum hits of *EcoRI* and *HindIII* restriction sites was selected (Table 3.3). BRCA2 mRNA was screened for 5'-GAATTC-3' and 5'-AAGCTT-3' in the STS (Sequence Tagged Sites) and ESTs (Expressed Sequence Tag) of the same. The occurrence of 5'-GAATTC-3' and 5'-AAGCTT-3' in each STS and ESTs of the selected oncogene are shown (Table 3.3).

| | |
|--|---|
| NAME | BRCA 2 |
| GENE ID | 675 |
| Occurrence of <i>EcoRI</i> (5'-GAATTC-3') in mRNA | 5 |
| Occurrence of <i>HindIII</i> (5'-AAGCTT-3') in mRNA | 4 |
| Occurrence of <i>EcoRI</i> (5'-GAATTC-3') in STS of BRCA 2 | UniSTS-272209 (1) |
| Occurrence of <i>HindIII</i> (5'-AAGCTT-3') in STS of BRCA 2 | UniSTS-272803 (1); UniSTS-272880 (1); UniSTS-505289 (1) |
| Occurrence of <i>EcoRI</i> (5'-GAATTC-3') in ESTs of BRCA | dbEST Id: 1457605; dbEST Id: 27576196; dbEST Id: 37888790; dbEST Id:7737797; |
| Occurrence of <i>HindIII</i> (5'-AAGCTT-3') in ESTs of BRCA | dbEST Id: 6572441; dbEST Id: 37888790; dbEST Id: 22570003 |

Table 3.3: The occurrence of *HindIII* (5'-AAGCTT-3') and *EcoRI* (5'-GAATTC-3') in STS and ESTs of BRCA 2, breast cancer 2, early onset gene

3.5 Discussion (B)

In the initial screening, the aqueous extract of *Cinnamomum zeylanicum* showed inhibition of both *HindIII* and *EcoRI* endonucleases, respectively-in a concentration dependent manner. The minimum inhibitory concentration was found to be 50 µg/ml and 100 µg/ml, respectively for *HindIII* and *EcoRI* endonucleases (Figure 3.7 a-b). The above observation brings out the possible use of restriction inhibition assay in screening both qualitatively and quantitatively the sequence specific DNA binding components from plants. The assay was further used to screen phytochemical rich fraction from *Cinnamomum zeylanicum*, involved in interacting with *EcoRI* (5'-GAATTC-3') and *HindIII* (5'-AAGCTT-3') recognition sequences at 100 µg/ml and 50 µg/ml, respectively (Figure 3.7 c). The fraction I showed inhibition at 40 µg/ml and at 5.6 µg/ml) inhibited the activity of restriction endonucleases *HindIII* and *EcoRI* in a concentration dependent manner (Figure 3.8 a). The fraction II (saponin) showed inhibition at concentrations 15 µg/ml and 2.1 µg/ml, respectively for *EcoRI* and *HindIII* endonucleases (Figure 3.8 b-c). The fraction III at concentrations of 15 µg/ml and 40 µg/ml showed inhibition of *EcoRI* and *HindIII*, respectively (Figure 3.8 d).

The inhibitory concentration of saponins for both endonucleases was comparatively lower, when compared with other phytochemical rich fractions. Therefore this report brings out for the first time the possible application of restriction inhibition assay in screening particular phytochemical from herbal plants; binding specifically to a DNA sequences in concentration dependent manner.

The clinical significance of this novel screening protocol was evaluated by, screening the presence of 5'-GAATTC-3' and 5'-AAGCTT-3' in the cDNA or mRNA of

oncogenes from oncogene database of Sangers Laboratory, United Kingdom. The oncogene-BRCA 2 showed maximum repeats of 5'-GAATTC-3' and 5'-AAGCTT-3', respectively. To be more specific we analyzed the STS and ESTs, for the occurrence of 5'-GAATTC-3' and 5'-AAGCTT-3, respectively in the BRCA 2 early onset oncogene. The 5'-GAATTC-3' and 5'-AAGCTT-3 sequences were observed in the STS and ESTs of BRCA 2 cDNA/mRNA breast cancer 2, early onset oncogene (Table 3.3).

The STS are DNA sequences which are unique for a gene which may or may not be the coding region of the same (Olson, 1989). On the other hand ESTs are unique coding sequences of any gene (ESTs Factsheet; Adams, 1991; Nagaraj, 2007). Therefore presence of drug specific sequence in the ESTs and STS may provide us with a unique target for cancer therapy. Therefore targeting the ESTs can directly provide us with a site directed attack to inhibit the expression of the oncogene by the screened phytochemical component. This clearly proves the application of RIA to screen compound which bind to specific sequences (5'-GAATTC-3' and 5'-AAGCTT-3) present in the STS and ESTs of any oncogene.

Therefore the scope of the study is huge in perspective of its potential in screening plant derived components which binds to certain set of sequences unique for an oncogene.

**AQUEOUS EXTRACT OF *Picrorrhiza kurroa* Royle ex Benth-A
POTENT INHIBITOR OF HUMAN TOPOISOMERASES**

The topoisomerases I and II α , plays a crucial role in the DNA-maintenance in all living cells. For this reason inhibitors of this enzyme have been studied. In this chapter we have described the inhibitory effect of the aqueous extract of *Picrorrhiza kurroa* on human topoisomerases by measuring the relaxation of superhelical plasmid pBR322 DNA. In the current study:

1. The aqueous extract of *Picrorrhiza kurroa* was assessed for its human topoisomerase I and II inhibitory activity.
2. The exact mechanism of topoisomerase inhibition was determined by preincubating the enzyme and DNA with the aqueous extract of *Picrorrhiza kurroa* extract.
3. The affinity of extract with the enzyme was evaluated by preincubating the topoisomerases with the extract before the addition of substrate (DNA).

The current study is the first report on the activity and mode of action of human topoisomerase I and II α inhibition from the aqueous extract of *Picrorrhiza kurroa* Royle ex Benth.

4.1 MATERIALS

4.1.1 Plant Material

The Rhizome of *Picrorrhiza kurroa* was obtained from Dr. A.N. Nautiyal (Prof., HNB Garhawal University, Uttrakhand, India).

4.1.2 Chemicals

Etoposide, Camptothecin, Ethidium bromide, Dimethyl sulphoxide (DMSO), human topoisomerase I and II α were purchased from Sigma Aldrich Co. USA. Plasmid pBR322 DNA, protein kinases and DNase and RNase free water, were purchased from Bangalore Gennai, India. All other reagents were of analytical grade or the highest grade available.

4.2 METHODOLOGY

4.2.1 Preparation of the *Picrorrhiza kurroa* extract

A routine procedure was followed for the preparation of aqueous extract (Saenphet et al. 2006). The rhizome approximately ~500 gm was weighed, thoroughly powdered and kept airtight in cool, dry and dark conditions. Approximately 50 gm was weighed and placed in a Soxhlet apparatus and extracted with distilled water for 48 hr. The aqueous extract was concentrated in a rotary evaporator at reduced pressure. The dried residue was dissolved in appropriate volume of DNase and RNase free water to obtained 10 mg/ml concentration and stored at -20 °C until use.

4.2.2 Inhibition of catalytic activity of Human Topoisomerase I (relaxation assay)

Human Topoisomerase I activity was measured by the relaxation of superhelical plasmid pBR322 DNA. The 20- μ l assay mixture contained 50 mM tris-Cl (pH 8), 120 mM KCl, 10 mM MgCl₂, 0.5 mM EDTA, 0.01% (w/v) bovine serum albumin, pBR322 DNA (20 mg/ml) and the plant extract at the proper concentrations (see results) or vehicle alone (for controls). The appropriate inhibitor was added, and the reaction was initiated by the addition of 1.5 units of topoisomerase I. Reactions were carried out at 37 °C for 60 min.

4.2.3 Stabilization of DNA–enzyme covalent complex studies

Relaxation of plasmid was carried out as mentioned earlier. After 60 min incubation at 37 °C, SDS–proteinase K was added. Following 30 min incubation at 37 °C, samples were electrophoresed on a 1 % agarose gel. Presence of nicked form of DNA was recorded as a DNA-covalent complex.

4.2.4 Preincubation analysis

Enzyme (topoisomerase I) was preincubated with either extract or substrate (pBR322 DNA) at 37 °C for 30 min followed by addition of substrate or inhibitor respectively. The samples were electrophoresed on a 1 % agarose gel. Intercalating agent, ethidium bromide was used as a control for enzyme–substrate preincubation studies.

4.2.5 Human Topoisomerase II α inhibition assay

Topoisomerase II α activity was also determined by measuring the relaxation of superhelical plasmid pBR322 DNA (protocol from (Sigma)). The reaction was started by the addition of 5 U topoisomerase II α and allowed to proceed at 30 °C for 15 min. The

reactions of both assays were stopped by the addition of 5 μ l loading buffer (glycerol 30% (v/v), bromophenol blue 0.125% (w/v), xylene cyanol 0.125 (w/v), sodium dodecyl sulfate (SDS) 5% (w/v)). DNase and RNase free water was used as vehicle for aqueous extract of *Picrorrhiza kurroa*, and camptothecin.

4.2.6 Agarose gel electrophoresis

On completion of reactions the samples were run in 1 % agarose gels. Agarose gel was prepared by melting 1 gm agarose in 100 ml of 1x TAE (Tris acetate EDTA) buffer (50X stock having 242 gm of Tris base, 57.1 ml of glacial acetic acid and 100 ml of 0.5 M EDTA). The gel was allowed to cool up to a temperature of approximate 55 °C and ethidium bromide was added to a final concentration of 0.5 μ g/ml. the solution was poured into a tray and gel was allowed to set and finally dipped with sufficient amount of 1x TAE buffer. The reaction product were mixed with 0.4 volumes of 6X gel loading buffer (0.25 % bromophenol blue, 40 % sucrose w/v in water), loaded on the gel and electrophoresis was carried out. Gel electrophoresis was performed at 4 V/cm for 5 h in TAE (Tris + acetic acid + EDTA) buffer on a 1 % agarose gel. Gel was stained with 0.5 mg/ml ethidium bromide and destained in distilled water for 10 min. The intensity of the bands on gels was converted into a digital image with a gel analyzer documentation system (Bio Rad, USA). Plasmid DNA pBR322 alone (line 1 in all gels) and plasmid DNA pBR322 relaxed by topoisomerase (line 2 in all gels) were taken as blanks and controls (100 % activity), respectively.

4.3 RESULT & DISCUSSION

4.3.1 Inhibition of topoisomerase I

Effect of *Picrorrhiza kurroa* extracts on human topoisomerase I inhibition was determined by measuring relaxation of supercoiled pBR322 DNA using camptothecin (200 μM) as a positive control. *Picrorrhiza kurroa* aqueous extract at the concentration range (10–40 $\mu\text{g/ml}$) inhibited the activity of topoisomerase I in a concentration-dependent manner (Figure 4.1). The inhibitory concentration of the aqueous extract was found to be 25 $\mu\text{g/ml}$ for topoisomerase I. The Human topoisomerase I inhibitory activity for *Picrorrhiza kurroa* is being reported for the first time. In addition, it is of interest to know whether a novel topoisomerase I inhibitor likely exerts its cytotoxic effect by stabilizing complexes containing strand-cleaved DNA, as does camptothecin. This information can be inferred from the ability of the test compound to stabilize the covalent enzyme–DNA complex. Camptothecin is known to stabilize the covalent enzyme–DNA binary to a greater extent; even at much lower concentration (Ma, et al., 2005). The ability of extract to stabilize the topoisomerase I–DNA covalent binary complex was also assessed. The binary complex was converted to nicked, circular form after enzyme denaturation and degradation with SDS and proteinase K. Stabilization of covalent complex was observed in the tested extract (Figure 4.1).

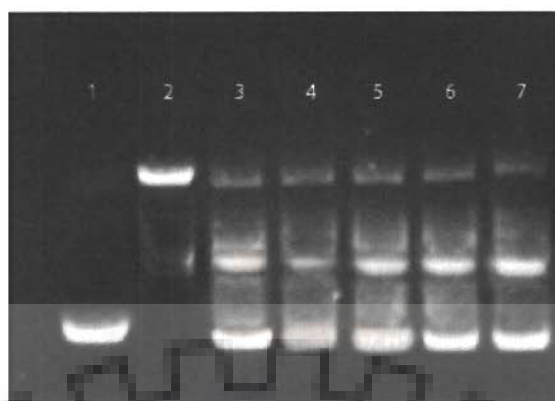


Figure 4.1: Topoisomerase I inhibition by aqueous extract of *Picrorrhiza kurroa*. Lane 1: Supercoiled pBR322 DNA, lane 2: DNA and topoisomerase I enzyme, lane 3: DNA and topoisomerase I enzyme + camptothecin (200 μM), lane 4: DNA + topoisomerase I + 10 μg aqueous extract, lane 5: DNA + topoisomerase I + 25 μg aqueous extract, lane 6: DNA + topoisomerase I + 50 μg aqueous extract, lane 7: DNA + topoisomerase I + 100 μg aqueous extract.

4.3.2 Preincubation analysis

Topoisomerases can be inhibited by two distinct mechanisms, either by stabilization of the enzyme–DNA covalent complex or by preventing the enzyme and DNA from binding by interacting with either the topoisomerase enzyme or DNA (Wang et al., 2001; Sehested et al., 1996). Topoisomerases inhibition seen by the aqueous extract at 40 μg concentration could be due to catalytic inhibition by test compound or indirectly through DNA-intercalation. To determine the exact mechanism of topoisomerase inhibition preincubation studies were conducted. When pBR322 DNA was first completely relaxed by topoisomerase I and then incubated with extracts, the relaxed plasmid did not revert back to its supercoiled form, indicating that extract constituents did

not inhibit the topoisomerase activity through intercalation into the DNA (Figure 4.2). On the contrary, the reaction containing ethidium bromide (positive control) showed slight change in relaxation state of plasmid (Figure 4.2, lane 4). Increase in inhibition of topoisomerase activity was observed after preincubation of enzyme with extract (Figure 4.3). Complete inhibition of topoisomerase I was observed at 25 $\mu\text{g/ml}$ concentration of the extract (lane 8). Extract by itself did not relax DNA. To test this supercoiled plasmid was incubated with extract without addition of enzyme. No relaxation was observed in after incubation of extract with DNA (data not shown).

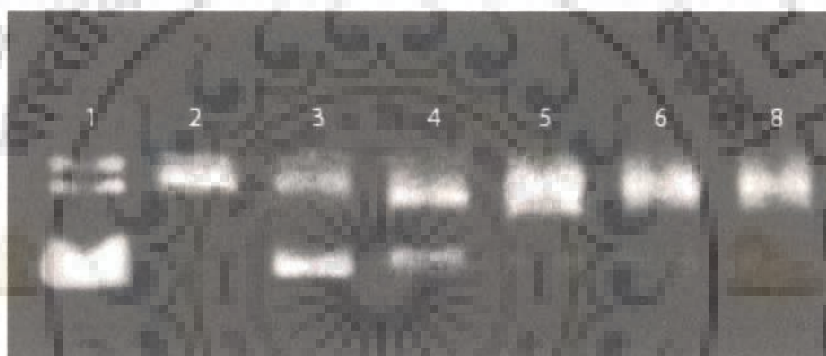


Figure 4.2: Effect of preincubation of relaxed DNA with aqueous extract of *Picrorrhiza kurroa*. Lane 1: Supercoiled pBR322 DNA, lane 2: DNA and topoisomerase I enzyme, lane 3: DNA and topoisomerase I enzyme + camptothecin (200 μM), lane 4: DNA and topoisomerase I enzyme + ethidium bromide (200 μM), 5: DNA + topoisomerase I + 10 μg aqueous extract, lane 6: DNA + topoisomerase I + 25 μg aqueous extract, lane 7: DNA + topoisomerase I + 50 μg aqueous extract, lane 8: DNA + topoisomerase I + 100 μg aqueous extract.



Figure 4.3: Effect of preincubation of enzyme and aqueous extract on inhibition of catalytic activity. Lane 1: Supercoiled pBR32 DNA, lane 2: DNA and topoisomerase I enzyme, lane 3: DNA and topoisomerase I enzyme + camptothecin (200 μ M), lane 4: DNA + topoisomerase I + 5 μ g aqueous extract, lane 5: DNA + topoisomerase I + 10 μ g aqueous extract, lane 6: DNA + topoisomerase I + 15 μ g aqueous extract, lane 7: DNA + topoisomerase I + 20 μ g aqueous extract; lane 8 DNA + topoisomerase I + 25 μ g aqueous extract.

4.3.3 Effect of aqueous extract on the Relaxation Activity of Topoisomerase II α

The effect of aqueous extract on topoisomerase activity was examined by measuring the relaxation of supercoiled plasmid pBR322 DNA. *Picrorrhiza kurroa* aqueous extract at the concentration range 10-50 μ g inhibited the activity of topoisomerase II α in a concentration-dependent manner (Figure 4.4). The inhibitory concentration was found to be 50 μ g/ml for topoisomerase II. Etoposide (200 μ M) is selective for topoisomerase II enzyme, and was used as positive control.

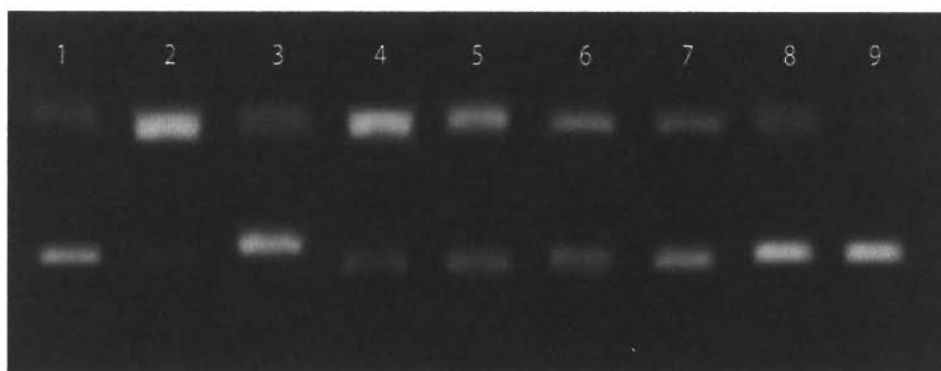


Figure 4.4: Effect of preincubation of topoisomerase II and the aqueous extract on inhibition of catalytic activity. Lane 1: Supercoiled pBR32 DNA, lane 2: DNA and topoisomerase I enzyme, lane 3: camptothecin (200 μ M), lane 4: DNA + topoisomerase I + 1 μ g aqueous extract, lane 5: DNA + topoisomerase I + 10 μ g aqueous extract, lane 6: DNA + topoisomerase I + 20 μ g aqueous extract, lane 7: DNA + topoisomerase I + 30 μ g aqueous extract, lane 8: DNA + topoisomerase I + 40 μ g aqueous extract, lane 9: DNA + topoisomerase I + 50 μ g aqueous extract.

4.4 CONCLUSION

Topoisomerase (topo) I and II are nuclear enzymes, which play a major role in the topological rearrangement of DNA during replication and transcription processes. In the course of years, many different agents have been found which can inhibit the topos and thereby exploit cytotoxicity, also against tumour cells. Selective inhibition of the topo I enzyme can, however, induce a reactive increase in topo II levels, and vice versa. This mechanism is associated with the development of drug resistance. Dual inhibition of both topo I and II may, theoretically, overcome this resistance problem. In this study the dual

inhibition of both topo I and II by the aqueous extract of *Picrorrhiza kurroa* is shown and discussed.

The aqueous extract of *Picrorrhiza kurroa* was effective in inhibiting both topoisomerases I and II α activity. The inhibition was dose dependent for the aqueous extract with IC values 25 $\mu\text{g/ml}$ and 50 $\mu\text{g/ml}$ for topoisomerase I and II α , respectively. Our results support the earlier report of anti topoisomerase I and II α activity of *Picrorrhiza kurroa* (Joy et al., 1995). In this context we are reporting for the first time the anti human topoisomerases I and II activity of the aqueous extract of *Picrorrhiza kurroa*. The current study demonstrates that the inhibitory mechanism of the extract can be attributed to its ability to stabilize the covalent topoisomerase I-DNA complex and inhibit the topoisomerase I and II α enzyme activity by interacting with the enzymes as observed in Preincubation studies. These mechanisms restrict the reversal of intermediate niked and relaxed form of plasmid to its native supercoiled form as observed for topoisomerases poison- *Picrorrhiza kurroa*.

Thus far, only the indolyl quinoline derivative TAS-103, the 7H-benzo [e] pyrido [4,3-b] indole derivative intopicine, and the acridine derivative PZA have been shown to be dual topo inhibitors with high cytotoxicity. In this regard the screening of herbs for topoisomerase I and II inhibitors may do well in cancer chemotherapy due to their less cytotoxic property Therefore our result provides the lead and encourages additional studies to identify and isolate the active principle involved in dual topo I and II inhibition with no cytotoxicity from *Picrorrhiza kurroa*.

Studies on Complex of Berberrubine with promoter site containing octamer d-(CCAATTGG)₂ by using Phosphorous-31 and Proton Nuclear Magnetic Resonance Spectroscopy and Restrained Molecular Dynamics Approach

The molecular basis for designing DNA binding drugs with improved specificity and affinity stems from the ability to identify the structural elements of the drug and DNA which are responsible for the specificity of the binding and the stabilization of the drug-DNA complex. In this chapter we have studied the structure of the berberrubine and d-(CCAATTGG)₂ complex. The information obtained on the conformational change occurring in DNA and drug during complex formation is reported. The following sets of studies were performed:

- 1D ¹H and ³¹P NMR titration studies of berberrubine-d-(CCAATTGG)₂ complex at drug (D) / DNA duplex (N) ratios of 0.25, 0.50, 0.75, 1.0 at 298 K in 90% H₂O and 10% D₂O.
- Temperature dependence of ³¹P and ¹H NMR of the berberrubine-d-(CCAATTGG)₂ complex having D/N = 1.0 in the range of 278 - 313 K.
- 2D ³¹P - ³¹P exchange spectra of berberrubine-DNA complex by a phase-sensitive NOESY using mixing time of 200 ms at 298 K for D/N = 1.0
- 2D NOESY ¹H - ¹H at D/N = 1.0 using mixing time $\tau_m = 200$ ms at 278, 283 and 298 K in 90 % H₂O and 10 % D₂O.

- Restrained molecular dynamics (rMD) studies on the solution structure of berberrubine- d-(CCAATTGG)₂ complex using inter-proton distances obtained from 2D NOESY as restraints.
- Analysis of the converged structures in terms of time average for the various conformational and helical parameters.

5.1 Materials

The deoxyribonucleic sequence d-(CCAATTGG)₂, berberine, Deuterium Oxide (D₂O), Dimethyl sulfoxide (DMSO) with isotopic purity 99.96% and (Trimethylsilyl) propionic-2, 2, 3, 3-d₄ acid sodium salt (TSP) were purchased from Sigma Chemical Co., USA. All other chemicals like sodium di hydrogen phosphate, di sodium hydrogen phosphat, sodium chloride (NaCl), etc. used for phosphate buffer preparation were purchased from Sigma Chemical Co., USA. All HPLC grade reagents like water, triethyl amine, acetonitrile, glacial acetic acid, ammonium acetate etc. were from Qualigens, Ltd. Berberine and oligonucleotides sample were used without further purification. Berberrubine was not available in the market, so it was synthesized using standard protocol reported in literature.

5.2 METHODOLOGY

5.2.1 Preparation of Berberrubine

Berberrubine was synthesized by heating 1g of berberine (1 g) at 190⁰C in a dry oven under vacuum (20-30 mm Hg) for 30 minutes. Then yellow color of berberine changed to dark reddish brown. Then berberrubine was separated from this brown mixture through silica gel (60-200 mesh size) Coolum chromatography using CHCl₃/ MeoH in 7:1 to 5:1 (v/v) solvent system. Separated dark red powder was then dissolved in BPES buffer to make a stock solution of (20.90 mM) for titration studies.

Molar extinction coefficient was obtained to be $29,950 \text{ M}^{-1}\text{cm}^{-1}$ at 377 nm in aqueous buffer.

5.2.2 Preparation of DNA Samples

The concentration of DNA samples was prepared in 10 mM BPES buffer containing 10 mM NaCl and concentration was determined using the standard values of the molar extinction coefficients tabulated in Table 5.1 by the UV-vis Spectrophotometer. The concentration of the stock solution was calculated by the formula of Beer Lambert's law-

$$\text{O.D} = \log T_0/T = \epsilon.c.l$$

Where,

c = Concentration of solution (in moles/ liter)

ϵ = Molar extinction coefficient (in $\text{M}^{-1}\text{cm}^{-1}$)

l = Path length of quartz cuvette (in cm)

From the stock solution of the known concentration, the solution of desired concentration was prepared by diluting the sample suitably, in BPES buffer and scanning the sample within the range 200-800 nm for berberine and berberrubine and 200-400 nm for DNA. The absorbance at the λ_{max} is noted from each scan and the concentration is calculated with the Lambert-Beer's equation considering the known molar extinction coefficient of berberrubine and DNA. The path length of the cuvette is fixed in each case i.e., 1 cm.

5.2.3 Sample Preparation for NMR

Stock solution of berberrubine (**Mol. Wt.-322.334640 g/mol**) 25.00 mM was prepared by dissolving a known quantity of sample in 10 mM BPES buffer having 10 mM NaCl concentration. The final concentration was checked by absorbance measurements at wavelength of 344 nm using Cary 100 Bio Spectrophotometer. The

extinction coefficient (ϵ) value used for berberubine was $\epsilon = 29950 \text{ M}^{-1}\text{cm}^{-1}$. Solution of deoxyoligonucleotide, d-(CCAATTGG)₂ (2.80 mM duplex concentration) was prepared by dissolving a known quantity of sample in 100 % D₂O for recording spectrum only for nonexchangeable protons. DNA sample was lyophilized and further dissolved in 90 % H₂O and 10 % D₂O BPES buffer (10 mM, of pH = 7.0 having 10 mM Na salt for exchangeable protons spectrum. Concentrations was determined by absorbance measurements at 260 nm using the **extinction coefficient (ϵ) value, 76300 M⁻¹cm⁻¹ and molecular weight 2409.6 Dalton for d-(CCCAATTGG)₂**. Ethylene diamine tetra acetic acid (EDTA), 0.1 mM, was added to suppress paramagnetic impurity, which may cause line broadening during NMR measurements. Typically 1 μ l of 0.1 M solution of DSS was added to the berberrubine, d-(CCAATTGG)₂ and complex of berberrubine d-(CCAATTGG)₂ as an internal reference.

| DNA | Extinction coefficient (ϵ) (M ⁻¹ cm ⁻¹ at 260 nm) |
|-------------------------------|--|
| CT DNA | 6600 |
| Poly d(A-T) | 8600 |
| Poly d(G-C) | 7750 |
| d-(CGATCG) ₂ | 57200 |
| d-(CGTACG) ₂ | 57600 |
| d-(TGCGCA) ₂ | 55600 |
| d-(CGTACGCGTACG) ₂ | 97200 |
| d-(CGATCGCGATCG) ₂ | 97200 |
| d-(ATATATAT) ₂ | 111200 |
| d-(CGCGCGCG) ₂ | 84800 |
| d-(TGCGCATGCGCA) ₂ | 109900 |
| d-(CCAATTGG) ₂ | 76300 |

Table 5.1 Extinction coefficient (ϵ) of various DNA and oligonucleotides

5.2.4 Preparation of Berberrubine- d-(CCAATTGG)₂ Complex

A complex of d-(CCAATTGG)₂ and berberrubine was prepared by titration. 119 μ l of 25.00 mM berberrubine was added in steps of 6 μ l to 530 μ l of 2.80 mM d-

(CCAATTGG)₂ sample during titration in order to make 1:1 complex of berberrubine: d-(CCAATTGG)₂.

The concentration of d-(CCAATTGG)₂ in this solution is determined as follows:

$$N_1V_1 = N_2V_2$$

$$N_1 \times 536 = 2.80 \times 530$$

$$N_1 = 2.77 \text{ mM}$$

The concentration of berberrubine in this solution is determined as follows:

$$N_3V_3 = N_4V_4$$

$$N_3 \times 536 = 25 \text{ mM} \times 6$$

$$N_3 = 0.28 \text{ mM}$$

The concentration of berberrubine (D), d-(CCAATTGG)₂ (N) and drug/ nucleic acid (D/N) ratio are shown in Table 5.2.

Table 5.2: Various concentration ratios (D/N) for the complex formed between berberrubine and d-(CCAATTGG)₂

| Nucleotide | Drug | D/N |
|---------------------------|---------------------------|------|
| Concentration (mM) = N | Concentration (mM) = D | |
| 2.80 | 0.00 | - |
| 2.77 | 0.28 | 0.10 |
| 2.73 | 0.55 | 0.20 |
| 2.70 | 0.83 | 0.30 |
| 2.67 | 1.13 | 0.40 |
| 2.47 | 1.49 | 0.60 |
| 2.45 | 1.68 | 0.70 |
| 2.43 | 1.68 | 0.70 |
| 2.41 | 1.91 | 0.80 |
| 2.39 | 2.13 | 0.90 |
| 2.36 | 2.35 | 1.00 |

5.2.5 Chemical Shift

The magnetic field at the nucleus is not equal to the applied magnetic field, B_0 ; electrons around the nucleus shield it from the applied field. The difference between the applied magnetic field and the field at the nucleus is termed the nuclear shielding. The induced field is directly proportional to B_0 . This is represented by the equation:

$$B_{\text{eff}} = B_0 (1 - \sigma)$$

where σ is the shielding constant which depends on the nature of electrons around the nucleus. Chemical shift is a function of the nucleus and its environment. It is measured relative to a reference compound. For ^1H NMR, the reference is usually tetramethylsilane, $\text{Si}(\text{CH}_3)_4$. Chemical shift is expressed in parts per million (ppm) is given as:

$$\delta = 10^6 \times \frac{\delta_{\text{obs}} - \delta_{\text{ref}}}{\delta_{\text{ref}}}$$

where, δ_{ref} is the position observed for a reference compound and δ_{obs} is the position of the signal of interest. There are useful general conclusions that can be drawn from specific chemical shift value, or changes due to the binding of the ligand

5.2.6 Spin-Spin Coupling Constant (J)

Nuclei experiencing the same chemical environment or chemical shift are called equivalent. Those nuclei experiencing different environment or having different shifts are nonequivalent. Nuclei, which are close to one another, exert an influence on each other's effective magnetic field. This effect shows up in the NMR spectrum when the nuclei are nonequivalent. If the distance between non-equivalent nuclei is less than or equal to three bond lengths, this effect is observable (Figure 5.1).

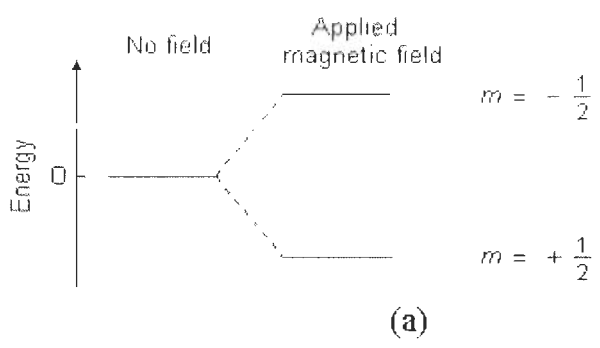


Figure 5.1: Energy levels for a nucleus with spin quantum number $\frac{1}{2}$ (b) Precessional motions by nucleus spinning on its axis in presence of the external magnetic field (c) Flipping of the magnetic moment on absorption of the radiations

This effect is called spin-spin coupling or J coupling and is expressed in Hertz. This coupling causes splitting of lines. The appearance of multiplet patterns depends on relative magnitude of δ and J for coupled nuclei. Vicinal couplings (3J) display a characteristic dependence upon the involved dihedral angle according to the relation dihedral couplings;

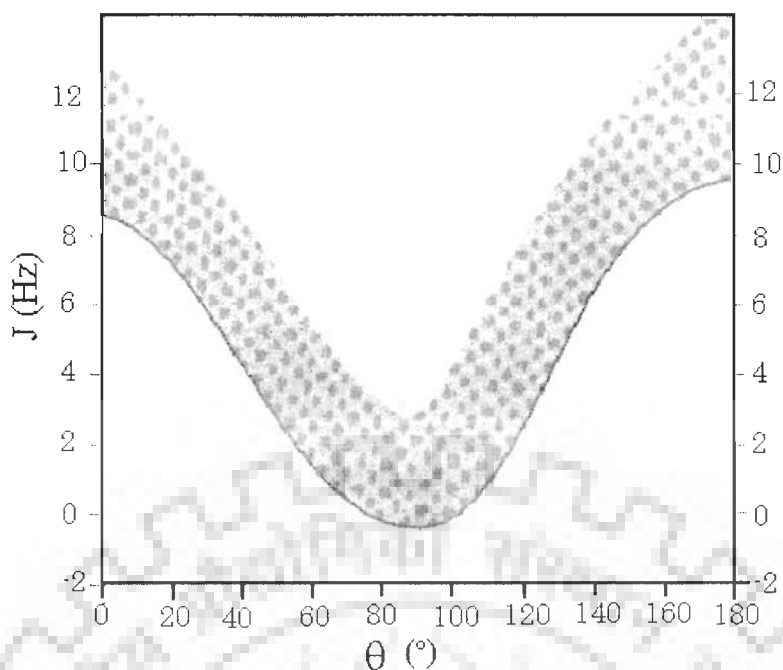
$$^3J = 8.5 \cos^2\theta - 2.8$$

$$^3J = 9.5 \cos^2\theta - 2.8$$

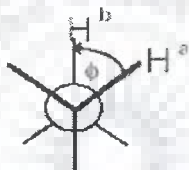
This relationship is known as the Karplus relation. Figure 5.2a and 5.2b shows the definition of dihedral angle and relationship between J couplings and dihedrals.

5.2.7 Relaxation Process

The magnetization does not precess infinitely in the transverse plane but turns back to the equilibrium state. This process is called relaxation. Two different time-constants describe this behaviour. The importance of these phenomena is in the nuclear Overhauser effect (NOE), which can be used to probe internuclear distances in a molecule. There are two major relaxation processes namely, Spin-lattice (longitudinal) relaxation (T_1) and spin-spin (transverse) relaxation (T_2). The relaxation time T_1 represents the "lifetime" of the first order rate process that returns the magnetization to the Boltzman equilibrium along the +Z axis.



(a)



(b)

Figure 5.2: (a) Karplus Curve showing relationship between J couplings and dihedral angle (b) definition of the dihedral angle

The components of the lattice field can interact with nuclei in the higher energy state, and cause them to lose energy (returning to the lower state). The energy that a nucleus loses increases the amount of vibration and rotation within the lattice. The relaxation time, T_1 depends on the motion of the molecule. As mobility increases, the vibrational and rotational frequencies increase, making it more likely for a component of the lattice field to be able to interact with excited nuclei. T_1 spin-lattice relaxation rate is then measured by plotting M as a function of τ :

$$M(\tau) = M_0 (1 - 2\exp^{-\tau/T_1})$$

T_2 represents the lifetime of the signal in the transverse plane (XY plane) and it is this relaxation time that is responsible for the line width. In Solution NMR, very often T_2 and T_1 are equal. The very fast spin-spin relaxation time provides very broad signals. The transverse relaxation constant T_2 is related to the linewidth of the signals. The width of the signal at half height is given by:

$$\Delta\omega_{1/2} = 1 / \pi T_2$$

Fast decay leads to broad signals, slow decay to sharper lines. The transverse relaxation constant T_2 of spin $I=1/2$ nuclei is mainly governed by the homogeneity of the magnetic field and the strength of the dipolar interaction with other $I=1/2$ nuclei depending on the number and the distance of neighbouring nuclei the overall tumbling time of the molecule which is related to its size. Transverse relaxation (T_2) is faster than longitudinal relaxation. T_2 spin-spin relaxation rate is measured by plotting M as a function of τ :

$$M(\tau) = M_0 \exp(-\tau/T_2)$$

5.2.8 Two-Dimensional (2D) NMR Techniques

In one-dimensional pulsed Fourier transform NMR the signal is recorded as a function of one time variable and then Fourier transformed to give a spectrum, which is a function of one frequency variable. In two-dimensional NMR the signal is recorded as a function of two time variables, t_1 and t_2 , and the resulting data Fourier transformed twice to yield a spectrum, which is a function of two frequency variables. The two-dimensional signal is recorded in the following way. First, t_1 is set to zero, the pulse sequence is executed and the resulting free induction decay recorded. Then the nuclear spins are allowed to return to equilibrium, t_1 is then set to Δt , the sampling

interval in t_1 , the sequence is repeated and free induction decay is recorded and stored separately from the first. Again the spins are allowed to equilibrate. t_1 is set to $2\Delta I$. the pulse sequence repeated and a free induction decay recorded and stored. The whole process is repeated again for $t_1 = 3\Delta I$, $4\Delta I$ and so on until sufficient data is recorded, typically 50 to 500 increments of t_1 . Thus recording a two-dimensional data set involves repeating a pulse sequence for increasing values of t_1 and recording a free induction decay as a function of t_2 for each value of t_1 . The general scheme for two-dimensional spectroscopy is (Figure 5.3):

Preparation time: The sample is excited by one or more pulse. This consists of a delay time or a sequence of pulses separated by fixed time intervals saturation sequences. Thermal equilibrium is attained during this period.

Evolution Period (t_1): The resulting magnetization is allowed to evolve for the first time period, t_1 . The evolution period is the pulse sequence element that enables frequency labelling in the indirect dimension. Further, one or several radiofrequency pulses may be applied to create coherence.

Mixing time (τ_m): During this period coherence is transferred between spins. Mixing sequences utilize two mechanisms for magnetization transfer: scalar coupling or dipolar interaction (NOE). After the mixing period the signal is recorded as a function of the second time variable, t_2 . This sequence of events is called a pulse sequence.

Detection Period: The signal is recorded during the time t_2 at the end of the sequence, detection, often called direct evolution time; during this time the magnetization is labelled with the chemical shift of the second nucleus. The data is recorded at regularly spaced intervals in both t_1 and t_2 .

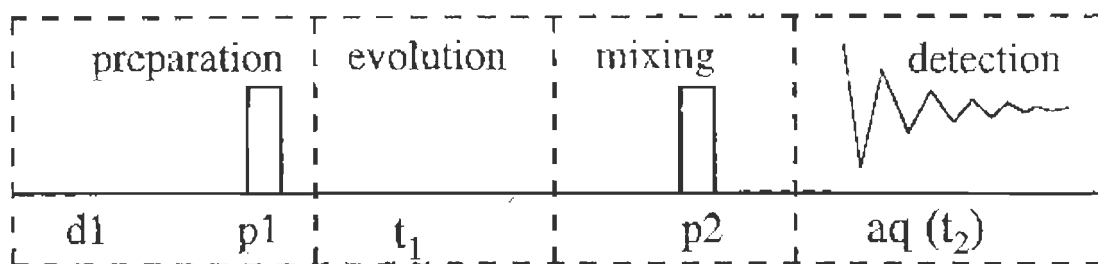


Figure 5.3: Four different time segments of a 2D NMR experiment namely (i) preparation period (ii) evolution period (t_1) (iii) mixing period (iv) detection period (t_2)

5.2.8.1 Nuclear Overhauser Effect Spectroscopy (NOESY)

NOESY is one of the most useful techniques as it allows correlating nuclei through space (distance smaller than 5\AA). By measuring cross peak intensity, distance information can be extracted. The pulse sequence starts as usual with a 90° pulse followed by an evolution time t_1 (Figure 2.4). This delay is varied systematically as usual to provide chemical shift information in the F1 domain. Then 90° pulse transmits some of the magnetization to the Z-axis and during the following mixing period, the non-equilibrium Z component will exchange magnetization through relaxation (dipole-dipole mechanism). This exchange of magnetization is known as Nuclear Overhauser Effect (NOE). After some time (shorter than the relaxation time T_1), the transverse magnetization is restored and detected. If relaxation exchange (or chemical exchange) has taken place during the mixing time, cross peaks will be observed in the spectra. The phase cycling ensures proper detection of NOESY signal.

5.2.9 Experimental Parameters

All NMR experiments were recorded on Bruker Avance 500 MHz FT-NMR spectrometer at Central NMR Facility located at Indian Institute of Technology Roorkee.

5.2.9.1 Study of drug berberrubine

Berberrubine has been studied in detail in DMSO at 298 K. ^1H NMR experiments was acquired with 128 K data points; number of scans = 128 and digital resolution = 0.25–0.5 Hz / point.

5.2.9.2 Study of berberrubine–DNA complex

^{31}P and ^1H NMR experiments were recorded for d-(CCAATTGG)₂ and its complex with berberrubine on successive addition of drug (Table 5.2) at 298 K in H₂O + D₂O (90:10) solvent.

The parameters were as follows:

1D ^1H NMR experiments were acquired with 128 K data points; number of scans = 128 and digital resolution = 0.15–0.3 Hz / point. Receiver gain was optimized in each instance to obtain the best signal to noise ratio.

1D ^{31}P NMR experiments were acquired with 128 K data points, number of scan = 128 and digital resolution 0.12 Hz / point.

^1H – ^1H 2D NOESY experiment were recorded with mixing times (τ_m) 200 ms at 298 K. Number of data points = 2048 data points along t_2 dimension; 256 induction decays in t_1 dimension; no. of scans = 56, digital resolution 1.495 Hz / point in t_1 dimension and relaxation delay of 2.0 secs.

^{31}P – ^{31}P 2D NOESY experiment for D / N = 1.0 at 298 K was recorded with mixing time of 200 ms; 2048 data points along t_2 dimension; 300 free–induction

decays in t_1 dimension; no. of scans = 56 ; digital resolution 1.495 Hz / point in t_1 dimension and relaxation delay of 2.0 secs.

5.3 RESULTS AND DISCUSSION

5.3.1 Phosphorous-31 NMR Studies of berberrubine-d-(CCAATTGG)₂ Complex

³¹P NMR experiments were performed to check for the mode of binding of berberrubine with d-(CCAATTGG)₂ because variation of phosphate resonances can provide a unique evidence of an intercalation process. The main factor which determines ³¹P chemical shift variations in phosphodiester groups at the level of the P-O (5') and P-O (3') bonds, i.e., the values of the angles $\alpha = \text{O}(3')\text{-P-O}(5')\text{-C}(5')$ and $\xi = \text{C}(3')\text{-O}(3')\text{-P-O}(5')$. Widening of ester O-P-O angle is expected to produce an upfield shift [Gorenstein and Kar, 1975; Gorenstein et al., 1984] while narrowing of this bond angle causes a downfield shift. For a nucleotide in a B-DNA type conformation, the phosphate groups are normally found in the gauche-gauche conformation with the angles of -60 and -90, respectively. Even small changes in these angles are reflected in the values of the phosphorus chemical shifts. The intercalating molecule induces a conformation with the angles of ca. -60 and 180 degree; this is associated with a low-field shift of ca. 1.5 ppm (Gorenstein 1994). Such transition from g^-, g^- to g^-, t on intercalation of drug chromophore by opening of adjacent base pairs at intercalation site from a distance of 3.4 to 6.8 Å have been reported in X-ray crystallographic structure of adriamycin and daunomycin binding to d-CGATCG, d-TGATCA, d-CGTACG sequences [Frederick et al., 1990] as well in similar NMR structures [Mazzini et al., 1998]. The pyridopurine [Favier et al., 2001] and berberine [Mazzini et al., 2003], which does not show such large shifts in the

phosphorus resonances on binding to DNA, have been shown to bind externally in the restrained molecular dynamics structures obtained by using inter molecular inter proton distances from NOESY spectra (Table 5.3-5.4).

Table 5.3: Chemical shift of free (δ^f), bound (δ^b), and change in chemical shift due to binding, $\Delta\delta = \delta^b - \delta^f$ in phosphate groups of some of the drug-DNA complexes taken from literature.

| Phosphate Group | [Mazzini et al., 1998], d-(CGATCG) ₂ + Adriamycin | | | [Mazzini et al., 1998], d-(CGTACG) ₂ + Adriamycin | | | [Searle et al., 1988] d-(GCATGC) ₂ + Nogalamycin | | |
|----------------------|--|------------|----------------|---|------------|----------------|---|---------------|----------------|
| | δ^f | δ^b | $\Delta\delta$ | δ^f | δ^b | $\Delta\delta$ | δ^f | δ^{b*} | $\Delta\delta$ |
| C1pG2/ G1pC2 | -0.91 | -0.48 | +0.43 | -1.03 | -0.58 | +0.45 | -3.30 | -2.90 | +0.20 |
| G2pA3/ C2pA3 | -0.86 | 0.67 | +1.53 | -1.40 | -0.56 | +0.84 | -3.00 | -2.50 | +0.50 |
| A3pT4/ T3pA4 | -1.26 | -1.28 | ≤-0.2 | -1.12 | -1.26 | -0.14 | -3.40 | -3.20 | +0.20 |
| T4pC5/T4pG6 | -1.06 | -1.12 | -0.06 | -1.20 | -1.34 | -0.14 | -3.10 | -1.60 | +1.50 |
| C5pG6/G5pC6 | -0.73 | 0.84 | +1.57 | -0.90 | +0.63 | +1.53 | -3.00 | -3.00 | +0.00 |
| | [Mazzini et al., 1998] d-(CGATCG) ₂ + Morpholinodoxorubicin | | | [Mazzini et al., 1998] d- (CGTACG) ₂ + Morpholinodoxorubici n | | | [Ragg et al., 1988] d-(CGTACG) ₂ + Daunorubicin | | |
| | | | | | | | | | |
| C1pG2 | -0.91 | -0.32 | +0.59 | -1.03 | -0.56 | +0.47 | -1.02 | -1.45 | -0.43 |
| G2pA3 / G2pT3 | -0.86 | 0.19 | +1.05 | -1.40 | -0.50 | +0.90 | -1.42 | -1.95 | -0.53 |
| A3pT4/T3pA4 | -1.26 | -1.36 | -0.10 | -1.12 | -1.45 | -0.33 | -1.08 | -1.28 | -0.20 |
| T4pC5/A4pC5 | -1.06 | -1.11 | -0.05 | -1.20 | -1.46 | -0.26 | -1.28 | -1.48 | -0.20 |
| C5pG6 | -0.73 | 0.52 | +1.25 | -0.90 | +0.22 | +1.12 | -0.88 | +0.44 | +1.32 |

+ve $\Delta\delta$ indicates downfield shift.

-ve $\Delta\delta$ indicates upfield shift

*Tentative assignment

Table 5.4: Chemical shift of free (δ^f), bound (δ^b), and the change in chemical shift due to binding, $\Delta\delta = \delta^b - \delta^f$ in phosphate resonances of some of the drug-DNA complexes taken from literature.

| Phosphate Group | [Lown and Hanstock, d-(CGCG) ₂ + mitoxantrone | | | [Kotovych et al., 1986] d-(CGATCG) ₂ + mitoxantrone | | | [Favier et al., 2001] d-(CGATCG) ₂ + pyridopurine | | | [Mazzini et al., 2003] d-(AAGAATTCTT) ₂ + berberine | | | | | |
|--|--|------------|----------------|---|------------|------------|--|---|------------|--|----------------|---------------|------------|------------|----------------|
| | δ^f | δ^b | $\Delta\delta$ | | δ^f | δ^b | $\Delta\delta$ | | δ^f | δ^b | $\Delta\delta$ | | δ^f | δ^b | $\Delta\delta$ |
| C1pG2 | -3.46 | -3.31 | +0.15 | C1pG2 | -1.71 | -1.70 | +0.01 | C1pG2 | 1.2 | 1.1 | -0.1 | A1pA2 | -1.31 | -1.19 | +0.12 |
| G2pA3 | -3.30 | -3.40 | -0.10 | G2pA3 | -1.71 | -1.70 | +0.01 | G2pA3 | 1.1 | 1.1 | 0.0 | A2pG3 | -1.00 | -0.98 | +0.02 |
| C3pG4 | -3.46 | -3.31 | +0.15 | A3pT4 | -2.19 | -2.21 | -0.02 | A3pT4 | 0.7 | 0.8 | -0.1 | G3pA4 | -1.14 | -1.12 | +0.02 |
| | | | | T4pC5 | -1.95 | -1.97 | -0.02 | T4pC5 | 0.4 | 0.5 | -0.1 | A4pA5 | -1.40 | -1.23 | +0.17 |
| | | | | C5pG6 | -1.59 | -1.25 | +0.34 | C5pG6 | 1.2 | 1.2 | 0.0 | A5pT6 | -1.37 | -1.40 | +0.03 |
| [Mazzini et al., 2004] Topotecan+d(CGTAACG)₂ | | | | [Mazzini et al., 2004] Camptothecin+d(CGTAACG)₂ | | | | [Mazzini et al., 2004] Camptothecin+d(CGTAACG)₂ | | | | T6pT7 | -1.18 | -1.10 | +0.08 |
| C1pG2 | -1.00 | -1.00 | 0.00 | C1pG2 | -0.88 | -0.95 | +0.07 | C1pG2 | -0.94 | -0.96 | +0.02 | T7pC8 | -1.11 | -1.07 | +0.04 |
| G2pT3 | -1.29 | -1.35 | -0.06 | G2pT3 | -1.32 | -1.33 | +0.01 | G2pT3 | -1.33 | -1.33 | +0.00 | C8pT9 | -1.14 | -1.10 | +0.04 |
| T3pA4 | -1.08 | -1.10 | -0.02 | T3pA4 | -1.14 | -1.17 | -0.03 | T3pA4 | -1.03 | -1.03 | +0.00 | T9pT10 | -1.04 | -1.07 | +0.03 |
| A4pC5 | -1.12 | -1.20 | -0.08 | A4pC5 | -1.14 | -1.17 | -0.03 | A4pC5 | -1.33 | -1.33 | +0.00 | | | | |
| C5pG6 | -0.90 | -1.00 | -0.10 | C5pG6 | -0.78 | -0.85 | +0.07 | T5pA6 | -1.10 | -1.13 | -0.03 | | | | |
| | | | | | | | | A6pC7 | -1.09 | -1.11 | +0.02 | | | | |
| | | | | | | | | C7pG8 | -0.82 | -0.84 | -0.02 | | | | |

+ve $\Delta\delta$ indicates downfield shift
 -ve $\Delta\delta$ indicates upfield shift

Currently ^1H - ^{31}P HMBC spectrum was used to assign the position of phosphate resonances for uncomplexed DNA. For the purpose of this discussion, the position of the bases in the octamer were designated as follows: d-(C1pC2pA3pA4pT5pT6pG7pG8)₂. The assignment of ^{31}P nucleotide resonances were quite straightforward using the three bond scalar coupling of ^{31}P with (H3')_n of the sugar residue. In addition ^4J couplings of phosphorous to (H4')_{n+1} protons of the sugar residues are also clearly evident. The positions for phosphate resonances for uncomplexed DNA were assigned as C1pC2, C2pA3, A3pA4, A4pT5, T5pT6, T6pG7, G7pG8 at -1.35, -1.01, -1.61, -1.73 and -1.71, -1.41 and -1.06 ppm respectively at 283 K (Figure 5.4).

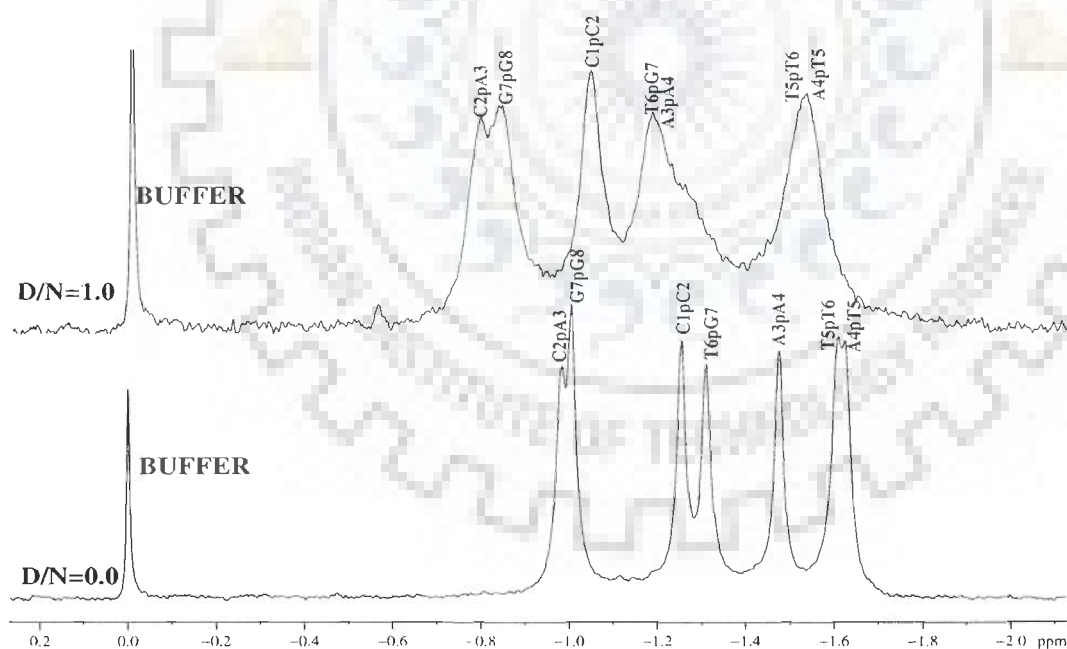


Figure 5.4: Proton decoupled ^{31}P NMR spectra of 2.76 mM d-(CCAATTGG)₂ in uncomplexed state and complexed with berberubine with increasing drug (D) to nucleic acid duplex (N) ratio, D/N, at 298 K.

Successive addition of berberrubine to d-(CCAATTGG)₂ was investigated by titrating a known concentration of berberrubine (25 mM) to a fixed concentration of 2.80 mM d-(CCAATTGG)₂. To arrive at Drug to Nucleic acid (D/N) stoichiometric ratios from 0 to 1.0 at 283 K an increment of 0.25 D/N was done. On binding of berberrubine to d-(CCAATTGG)₂ the resonances broadened considerably but no additional peaks appeared. Chemical shift values for all the phosphorus signals at different D/N ratio are tabulated in Table 5.5. It shows that a downfield shift ($\Delta\delta = \delta_b - \delta_f$) for all phosphorus resonance signals of complex DNA.

Table 5.5: chemical shift of ³¹P resonances of the phosphate groups of DNA octamer, in complex of berberrubine with d-(CCAATTGG)₂ at 298 K with different drug (D) to nucleic acid duplex (N) ratios (D/N). $\Delta\delta = (\delta_{D/N=1.0} - \delta_{D/N=0})$.

| D/N | C1pC2 | C2pA3 | A3pA4 | A4pT5 | T5pT6 | T6pG7 | G7pG8 |
|----------------|-------|-------|-------|-------|-------|-------|-------|
| 0.0 | -1.19 | -0.92 | -1.41 | -1.56 | -1.55 | -1.25 | -0.94 |
| 1.0 | -0.98 | -0.73 | -1.12 | -1.46 | -1.46 | -1.12 | -0.77 |
| $\Delta\delta$ | +0.21 | +0.19 | +0.29 | +0.10 | +0.09 | +0.13 | +0.17 |

+ve $\Delta\delta$ indicates downfield shift

-ve $\Delta\delta$ indicates upfield shift

C1pC2, C2pA3 and A3pA4 showed a downfield shift of 0.21, 0.19 and 0.29 ppm, respectively. While A4pT5, T5pT6, T6pG7 and G7pG8 shifted by lesser magnitude of 0.10 and 0.09, 0.13 and 0.17 ppm, respectively. C1pC2, C2pA3 and A3pA4 showed a downfield of 0.21, 0.19 and 0.29 which was maximum among all phosphorus signals observed and can be attributed due to the marginal opening of C1-G8, C2-G7 and A3-T6 base pairs and narrowing of ester O-P-O angles of C1pC2, C2pA3 and A3pA4

due to binding of berberrubine. Large downfield shift of ~ 1.5 ppm characteristic of opening of base pairs due to change in backbone torsional angles of DNA were clearly absent in any of the ^{31}P resonances. As discussed previously that pyridopurine [Favier et al., 2001] and berberine [Mazzini et al., 2003], which does not show such large shifts in the phosphorus resonances on binding to DNA, have been shown to bind externally by rMD (Restrained Molecular Dynamics) using intermolecular inter proton distances from NOESY spectra. Thus, it may be inferred that binding of berberrubine to d-(CCAATTGG)₂ does not lead to opening of base pairs, which is generally associated with large down field shifts of ^{31}P resonance of the order of 1.6-2.6 ppm [Gorenstein, 1992; Patel, 1974; Patel and Canuel, 1976; Patel et al., 1982]. Since, we also found that change in the chemical shifts was less (< 0.50) as compared to other DNA binding drug, intercalative mode can be excluded and the external mode or minor groove mode of binding of berberrubine can be suggested. But still predicting the binding site of berberine on the basis of alone ^{31}P chemical shift variation can be more imaginary.

5.3.2 2D ^{31}P - ^{31}P Exchange Spectra

Figure 5.5 shows 2D ^{31}P NMR exchange spectrum of the complex of berberrubine with d-(CCAATTGG)₂ at drug to DNA (D/N) ratio of 1.0 at 298 K. The one dimensional ^{31}P spectra are shown along both axes. In 2D ^{31}P NMR exchange spectrum each of the 7 phosphorus signals seen in uncomplexed DNA is expected to give cross peak due to chemical exchange with its respective bound resonance. On binding of berberrubine to d-(CCAATTGG)₂, only considerable broadening was observed with no additional cross peaks due to exchange between the bound and free phosphate resonances.

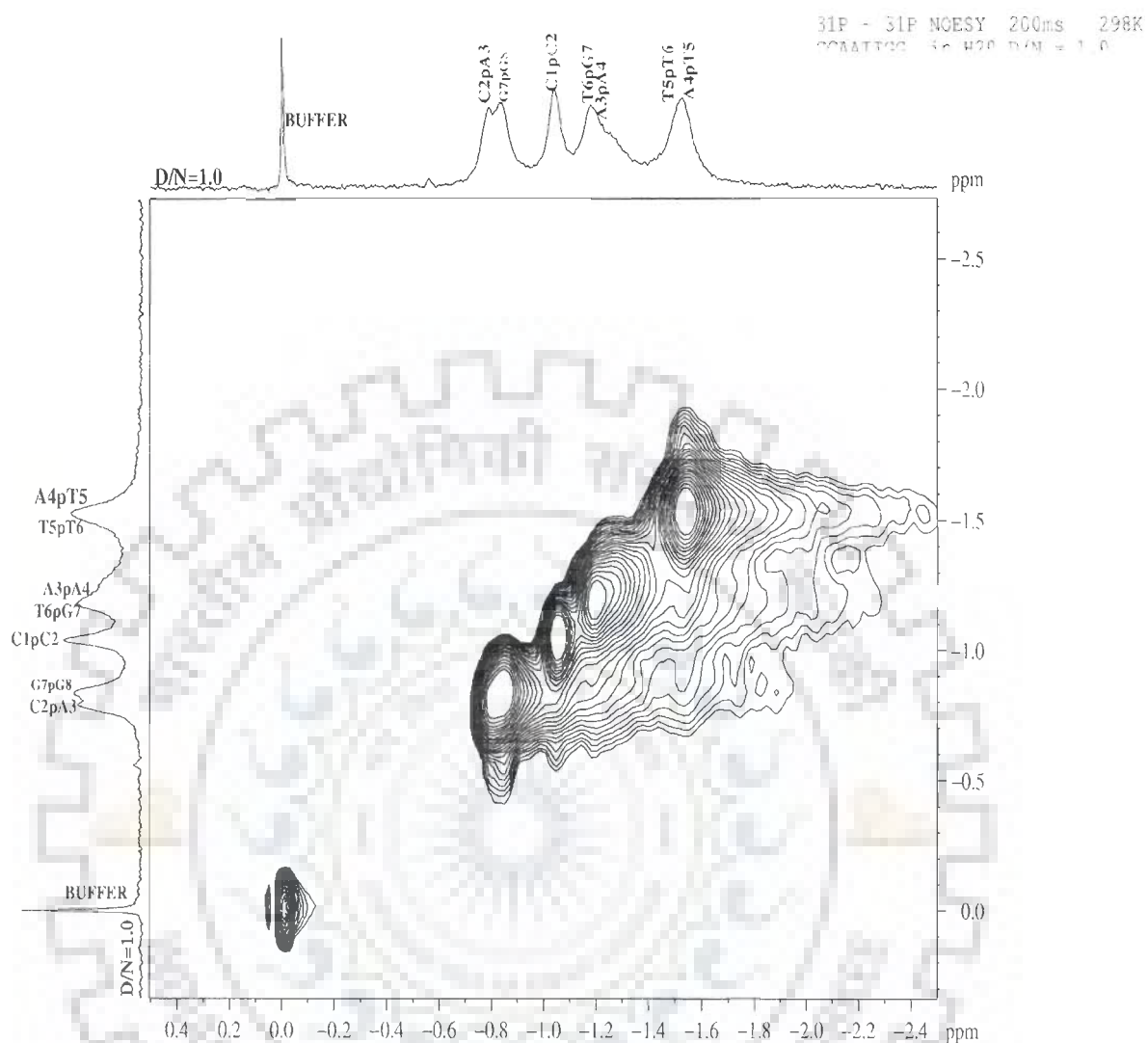


Figure 5.5: 2D ^{31}P NMR exchange spectrum of the complex of berberubine with d-(CCAATTGG) $_2$ at drug (D) to nucleic acid duplex (N) ratio, D/N=1.0 at 298 K

Since, only one set of resonances were observed for the complexes at different D/N ratios for free octamer and octamer bound to berberubine, it is expected that ^{31}P signals from the bound DNA were in fast exchange with the corresponding signals from free DNA to be followed individually at 298 K on NMR time scale.

5.3.3 Temperature Dependence Studies

We have also monitored the variation of chemical shift in complex (D/N=1) with temperature. The signals were found to vary with temperature, which may be due to shift in equilibrium of duplex to single strand transition as well as dissociation of duplex-berberine complex to free duplex and free berberrubine. The shift in ^{31}P resonances in the range 278-328 K was very gradual and not abrupt at D/N = 1.0. It can be noted from the Table 5.6 that a maximum downfield effect of 0.438 on chemical shift due to temperature at D/N 1.0 on berberrubine binding was found at A3pA4. It suggests that berberrubine binds to A3-A4 site and DNA becomes more resistant to temperature perturbation.

Table 5.6: ^{31}P chemical shift d-(CCAATTGG)₂-berberrubine complex (D/N =1.0) as a function of temperature in the range 278-328 K where $\Delta\delta = \delta_{328\text{ K}} - \delta_{278\text{ K}}$.

| Temp. | D/N 1.0 | | | | | | |
|----------------|---------|--------|---------------|--------|--------|--------|--------|
| | C1pC2 | C2pA3 | A3pA4 | A4pT5 | T5pT6 | T6pG7 | G7pG8 |
| 278 | -1.144 | -0.794 | -1.723 | -1.723 | -1.396 | -1.155 | -0.794 |
| 283 | -1.135 | -0.796 | -1.518 | -1.699 | -1.699 | -1.35 | -0.796 |
| 288 | -1.132 | -0.816 | -1.446 | -1.672 | -1.672 | -1.299 | -0.816 |
| 293 | -1.135 | -0.851 | -1.288 | -1.642 | -1.642 | -1.288 | -0.905 |
| 298 | -1.136 | -0.886 | -1.275 | -1.622 | -1.622 | -1.275 | -0.933 |
| 303 | -1.136 | -0.925 | -1.275 | -1.604 | -1.604 | -1.275 | -0.966 |
| 308 | -1.138 | -0.995 | -1.282 | -1.581 | -1.581 | -1.282 | -0.995 |
| 313 | -1.140 | -1.024 | -1.285 | -1.556 | -1.556 | -1.285 | -1.024 |
| $\Delta\delta$ | +0.004 | -0.23 | +0.438 | +0.167 | -0.16 | +0.27 | -0.23 |

+ve $\Delta\delta$ indicates downfield shift

-ve $\Delta\delta$ indicates upfield shift

The addition of berberrubine to d-(CCAATTGG)₂ did not induce significant chemical shift variation of the phosphate signals in the ³¹P NMR spectra ($\delta < 0.5$ ppm), which excludes directly the intercalation mode of the berberrubine binding. It has been reported earlier by Mazzini et al that berberine and its analog (berberrubine) binds to d-(AAGAATTCTT)₂ at the minor groove [Mazzini et al., 2003]. Most of the minor groove binding drugs binds to A_nT_n regions and require 4-5 base pair length for good binding [Neidle, 2001]. Our results shows that berberrubine affects other phosphorus signals temperature dependence in the order of A3pA4 > T6pG7 > A4pT5 (downfield shift) and C2pA3 > G7pG8 > T5pT6 > C1pC2 (upfield shift) (Figure 5.6) which supports the finding that berberrubine binds at A3pA4 site of d-(CCAATTGG)₂ and significantly effect the neighboring residues.

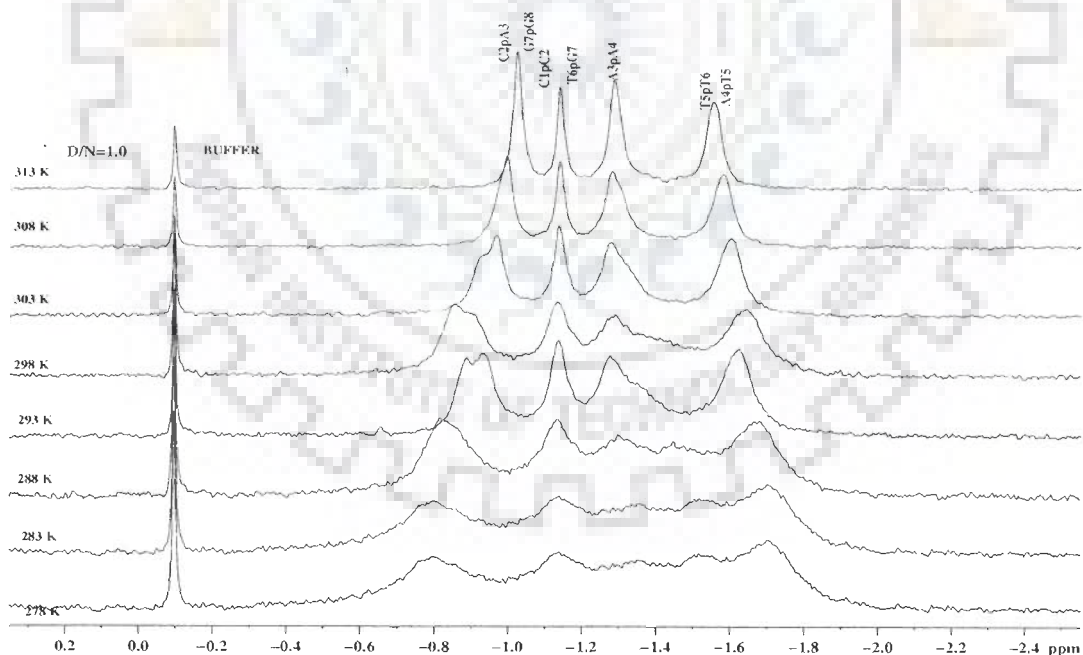


Figure 5.6: Proton decoupled ³¹P NMR spectra of d-(CCAATTGG)₂ as a function of temperature at D/N=1.0

Although ^{31}P NMR studies provide information on the conformation of the phosphate ester backbone and the mode of binding of berberrubine but it is unable to provide detailed information on the overall conformation of the sugar rings and bases of oligonucleotides. Direct inter-proton distances (NOE) which are available through ^1H NMR studies will be discussed further in this chapter.

5.3.4 Proton NMR Spectra

The assignment of nucleotide protons was carried out by following the strategies available in literature (Gronenborn et al., 1985; Hosur et al., 1988; Wüthrich, 1986) for sequential assignment in right handed B-DNA with sugar in predominantly S conformation and glycosidic angle in anti domain. The assignment of spectral lines to specific protons of berberrubine was made by following the strategies used for assignment in NMR spectra of uncomplexed berberrubine (Tripathi et al., 2007). Each resonance of drug and DNA were unambiguously assigned in the spectra of complex and are listed in Table 5.7 and 5.8, respectively.

5.3.4.1 Chemical Shift

Chemical shift perturbations often accompany the binding of the two biomolecules due to changes in the chemical environments of the atom in the interface. Consequently one goal of the chemical shift analysis is to identify, in the absence of detailed structural information, the site of local interactions between the two molecules. If the resonances that shift upon binding correspond to the residues directly involved in recognition, chemical shift changes can provide valuable insights into the structural basis for recognition, and should serve to guide design or screening efforts focused on the discovery of novel ligands.

Upon addition of berberrubine to d-(CCAATTGG)₂ in small steps up to drug/nucleic acid (D/N) ratio 1.0, a set of new signals corresponding to NMR resonances of berberrubine protons appear (Figure 5.7 a-d). The resonances of berberrubine were considerably broad and showed both upfield and downfield shift with respect to free berberrubine (Table 5.7). Maximum upfield shift of -0.24, -0.24 and -0.18 ppm in berberrubine protons was found in H 14, H 19, 20 and H 24, respectively. While a maximum downfield shift of 0.16 and 0.14 ppm was found for H 3 and H 31, 32, respectively. The change in chemical shift (δ) of d-(CCAATTGG)₂ protons with increasing D/N ratio was small in magnitude. Imino protons of d-(CCAATTGG)₂ shifted upfield up to 0.26 ppm by binding to berberrubine (Table 5.8). All the spectral lines of DNA were somewhat uniformly broadened on binding as the internal motions are affected and the protons get immobilized.

Table 5.7: Chemical shift table of berberrubine (ppm) protons from NOESY spectra of berberrubine alone (δ_f) and berberrubine-d-(CCAATTGG)₂ complex (δ_b) at D/N = 1.0, at 298 K.

| Berberrubine Proton | δ_f | δ_b | $\Delta\delta$ |
|---------------------|------------|------------|----------------|
| | D/N 0.0 | D/N 1.0 | |
| H10 | 9.07 | 8.93 | -0.14 |
| H14 | 7.99 | 7.75 | -0.24 |
| H5 | 7.22 | 7.24 | -0.02 |
| H3 | 6.37 | 6.53 | +0.16 |
| H28 | 7.65 | 7.55 | -0.10 |
| H24 | 6.96 | 6.79 | -0.18 |
| H31,32 | 6.09 | 6.23 | +0.14 |
| H16, 17 | 4.48 | 4.42 | -0.06 |
| H36,37,38 | 3.73 | 3.64 | -0.09 |
| H19,20 | 3.03 | 2.806 | -0.24 |

+ve $\Delta\delta$ indicates downfield shift
 -ve $\Delta\delta$ indicates upfield shift

Table 5.8: Chemical shift (ppm) of d-(CCAATTGG)₂ protons in uncomplexed state (δ_f) and that bound to berberine (δ_b) at drug (D) to nucleic acid duplex (N) ratio D/N=1.5 at 298 K. Also shown here is the change in chemical shift on binding, that is.

$$\Delta\delta = \delta_b (D/N=1.5) - \delta_f (D/N=0.0).$$

| Protons | C1 | | | C2 | | | A3 | | | A4 | | |
|-------------------------------|------------|------------|----------------|------------|------------|----------------|------------|------------|----------------|------------|------------|----------------|
| | δ_b | δ_f | $\Delta\delta$ | δ_b | δ_f | $\Delta\delta$ | δ_b | δ_f | $\Delta\delta$ | δ_b | δ_f | $\Delta\delta$ |
| H8/H6 | 7.49 | 7.77 | -0.28 | 7.43 | 7.60 | -0.17 | 8.23 | 8.32 | -0.09 | 8.18 | 8.23 | -0.05 |
| H1' | 5.73 | 5.94 | -0.19 | 5.18 | 5.38 | -0.20 | 5.92 | 6.02 | -0.10 | 6.15 | 6.22 | -0.07 |
| H2' | 1.94 | 2.06 | -0.12 | 2.05 | 2.07 | -0.02 | 2.82 | 2.84 | -0.01 | 2.60 | 2.62 | -0.02 |
| H2'' | 2.43 | 2.51 | -0.08 | 2.28 | 2.37 | -0.09 | 2.88 | 2.97 | -0.09 | 2.87 | 2.93 | -0.04 |
| H3' | 4.59 | 4.67 | -0.08 | 4.78 | 4.81 | -0.03 | 5.04 | 5.10 | -0.06 | 4.99 | 5.05 | -0.06 |
| H4' | 4.04 | 4.04 | 0.00 | 4.05 | 4.06 | -0.01 | 4.39 | 4.42 | -0.03 | 4.74 | 4.51 | +0.23 |
| H5' | 3.79 | 3.77 | +0.02 | 4.02 | 4.02 | 0.00 | 4.23 | 4.29 | -0.06 | 4.40 | 4.31 | +0.09 |
| H5'' | | 3.64 | --- | --- | --- | --- | 4.09 | 4.07 | +0.02 | 4.20 | 4.11 | +0.09 |
| H5/H2/CH ₃ | 5.57 | 5.98 | -0.41 | 5.52 | 5.73 | -0.21 | 7.60 | 7.65 | -0.05 | 7.60 | 7.65 | -0.05 |
| NH ₂ ^b | 8.09 | 8.05 | +0.04 | 8.33 | 8.65 | -0.32 | 7.24 | 7.32 | -0.08 | 7.24 | 7.28 | -0.04 |
| NH ₂ ^{ab} | 7.24 | 7.22 | +0.02 | 6.68 | 6.87 | -0.19 | 6.18 | 6.43 | -0.25 | 6.12 | 6.20 | -0.08 |
| | T5 | | | T6 | | | G7 | | | G8 | | |
| | δ_b | δ_f | $\Delta\delta$ | δ_b | δ_f | $\Delta\delta$ | δ_b | δ_f | $\Delta\delta$ | δ_b | δ_f | $\Delta\delta$ |
| H8/H6 | 7.10 | 7.16 | -0.06 | 7.18 | 7.27 | -0.09 | 7.76 | 7.84 | -0.08 | 7.72 | 7.82 | -0.10 |
| H1' | 5.82 | 5.90 | -0.08 | 5.67 | 5.79 | -0.12 | 5.55 | 5.66 | -0.10 | 5.98 | 6.15 | -0.17 |
| H2' | 1.92 | 1.96 | -0.04 | 1.86 | 1.98 | -0.12 | 2.62 | 2.50 | +0.12 | 2.34 | 2.39 | -0.05 |
| H2'' | 2.42 | 2.52 | -0.10 | 2.21 | 2.32 | -0.11 | --- | 2.66 | --- | 2.53 | 2.53 | 0.00 |
| H3' | 4.78 | 5.09 | -0.31 | | 4.85 | | 4.90 | 4.95 | -0.05 | 4.63 | 4.61 | +0.02 |
| H4' | 4.04 | 4.20 | -0.16 | | 4.12 | | 4.21 | 4.71 | -0.50 | 4.16 | 4.17 | -0.01 |
| H5' | | | | | | | 4.07 | 4.35 | -0.28 | | 4.23 | --- |
| H5'' | | | | | | | 3.82 | 4.07 | -0.25 | 3.83 | --- | -- |
| H5/H2/CH ₃ | 1.31 | 1.37 | -0.06 | 1.57 | 1.64 | -0.07 | | | | | | |
| NH ₂ ^b | | | | | | | 7.92 | 8.01 | -0.09 | 7.73 | 7.78 | -0.05 |
| NH ₂ ^{ab} | | | | | | | 6.43 | 6.43 | 0.00 | 6.82 | 6.93 | -0.09 |
| NH | 13.52 | 13.67 | -0.15 | 13.78 | 13.94 | -0.16 | 12.62 | 12.88 | -0.26 | | | |

+ve $\Delta\delta$ indicates downfield shift

-ve $\Delta\delta$ indicates upfield shift

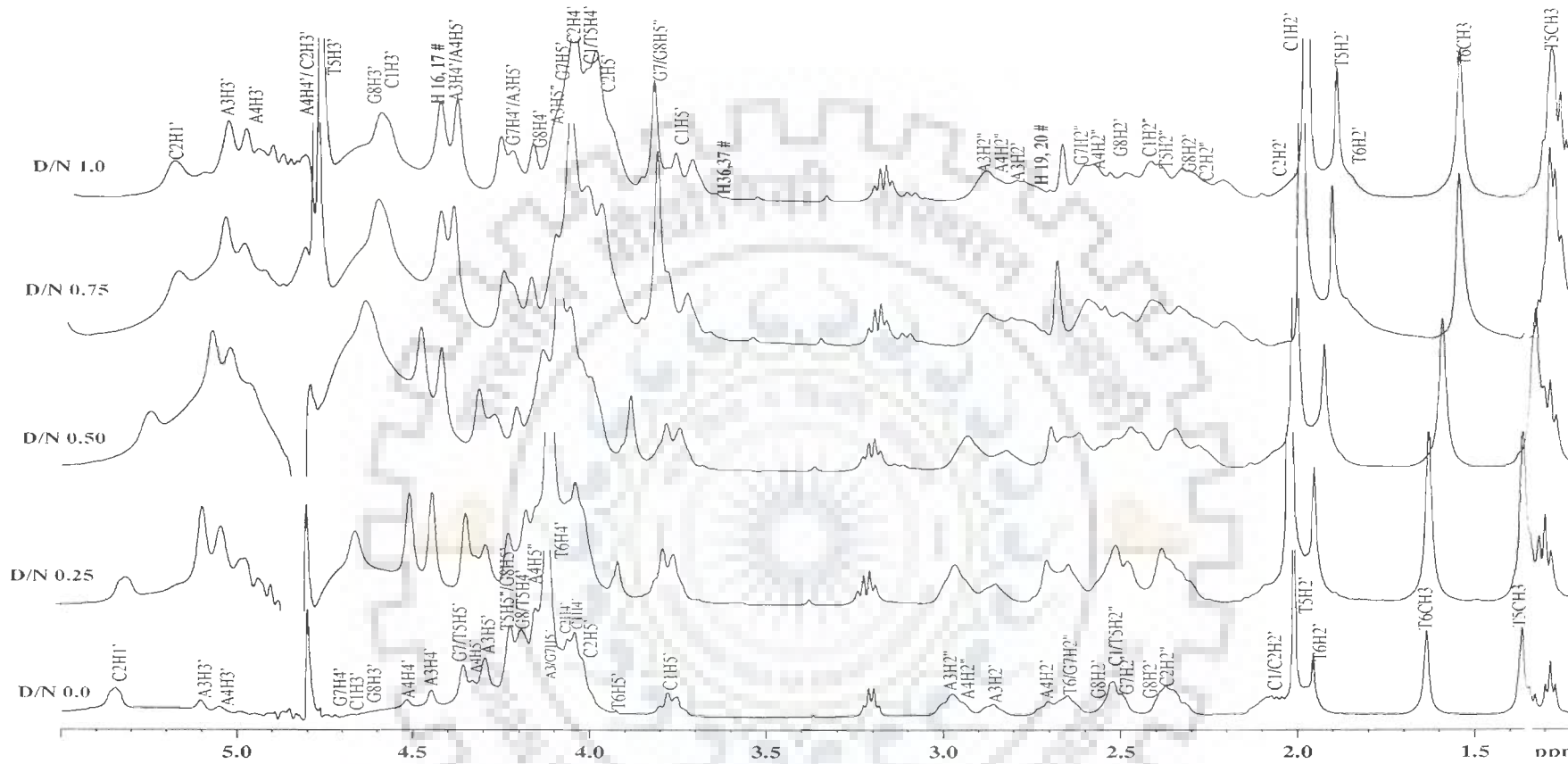


Figure 5.7 (a)

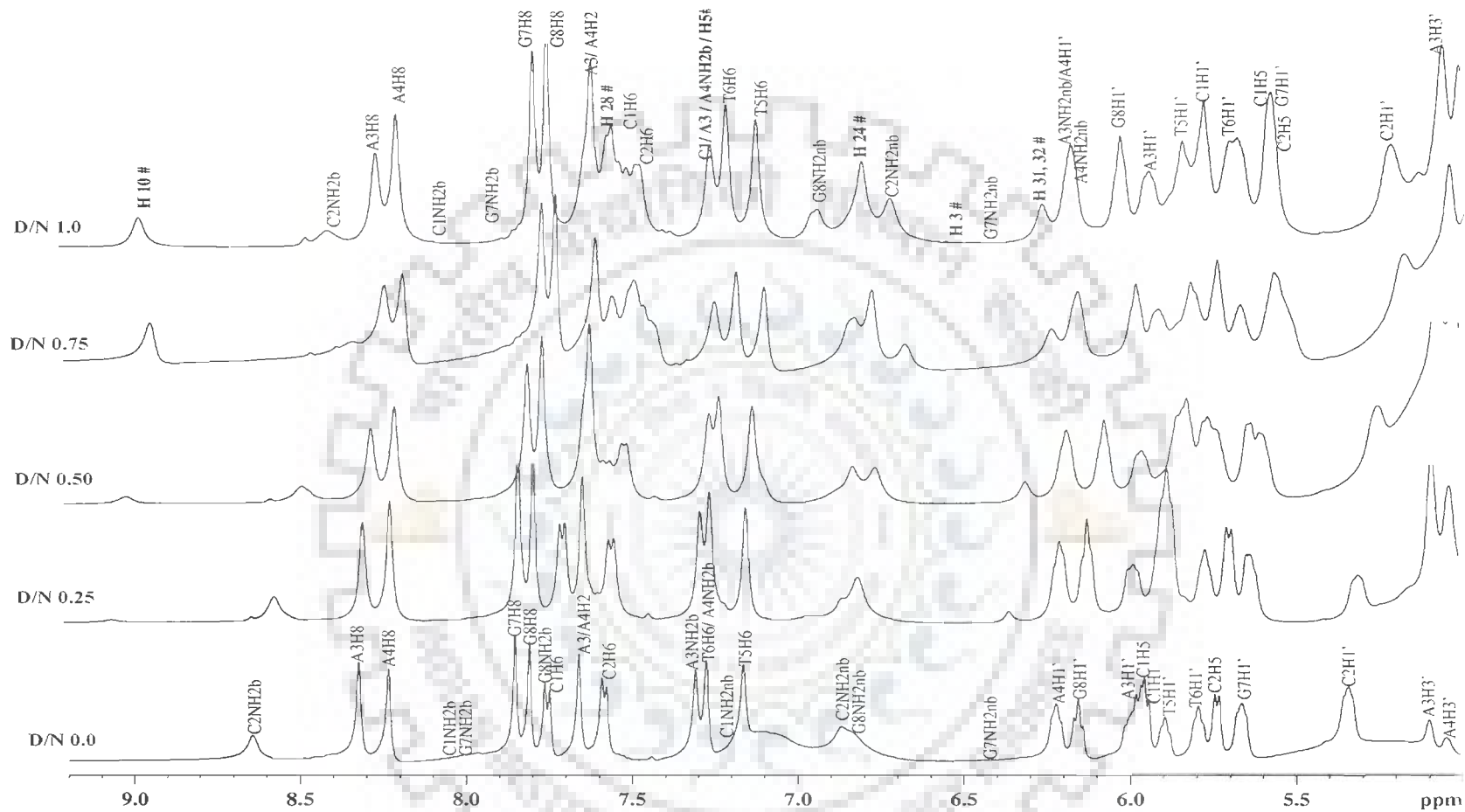


Figure 5.7 (b)

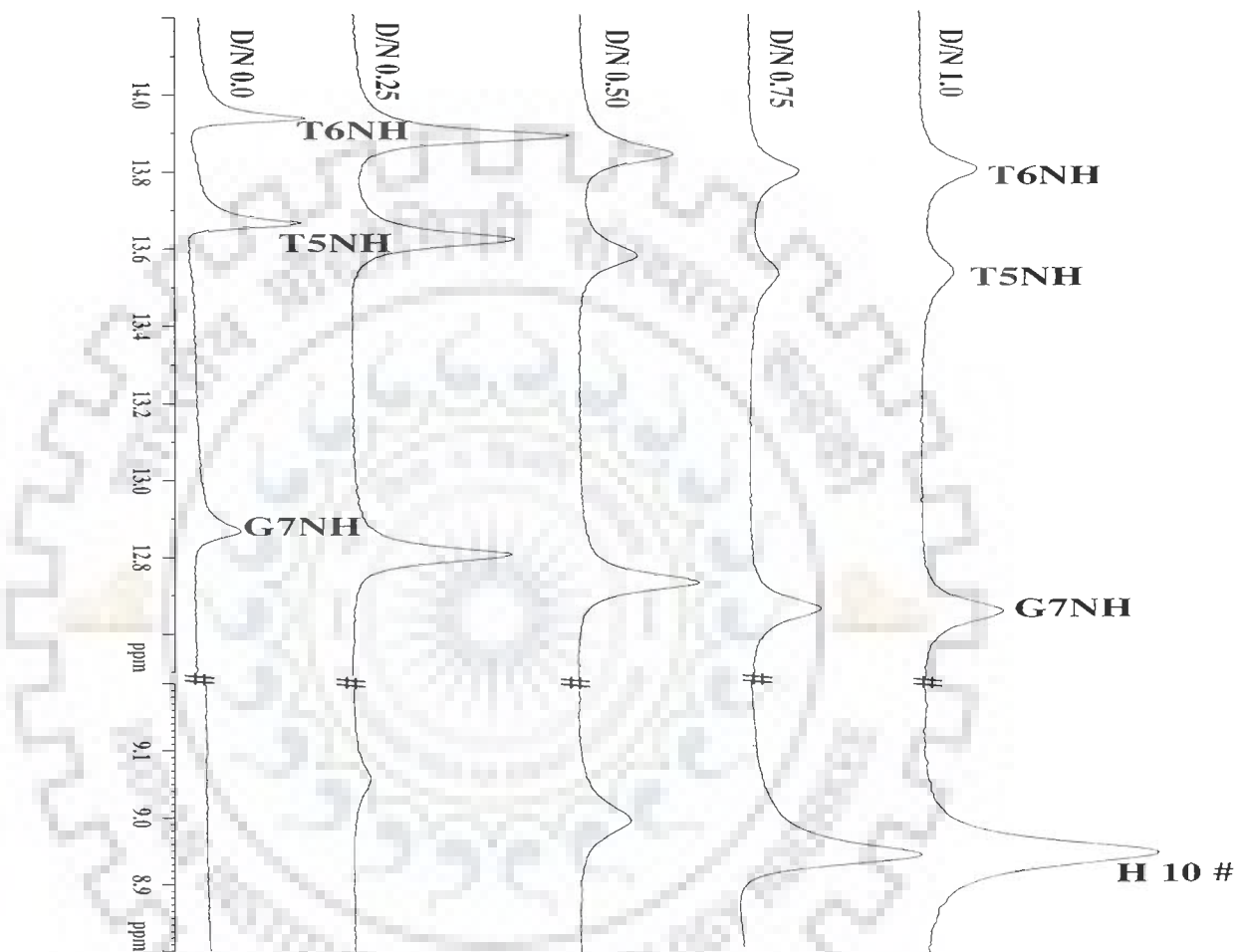


Figure 5.7 (c)

Figure 5.7 (a-c): Proton NMR spectra of complex of berberubine with d-(CCAATTGG)₂ as a function of D/N ratio at 298 K (# berberubine proton in berberubine-d-(CCAATTGG)₂ complex).

5.3.5 Structure of berberrubine-d-(CCAATTGG)₂ Complex

The 2D NOESY spectra of berberrubine-d-(CCAATTGG)₂ complex were investigated extensively at mixing time (τ_m) of 200 ms. The observation of NOEs between pairs of proton G7NH^b-C2NH₂^b, C2NH₂^{nb}; T6NH- A3NH₂^b, A3NH₂^{nb}, A3H2; and T5NH-A4NH₂^b, A4NH₂^{nb}, A4H2; establish Watson-Crick base pairing between C2-G7, T6-A3 and T5-A4 base pairs in the complex. This is further supported by presence of intrastrand sequential connectivity T5NH- A4NH₂^{nb} and interstrand sequential connectivities T6NH-C2NH₂^b, C2NH₂^{nb} (Table 5.9). The sequential connectivities G7NH-T6NH, T6NH-T5NH were also observed. The presence of all base H6/H8/CH₃ to sugar H1', H2', H2'' sequential NOE connectivities in DNA clearly prove that the base pairs do not open and hence the intercalative mode of binding is completely ruled out. All duplex pair peaks are found to be intact (Table 5.10 and 5.11).

Table 5.9: NOE connectivities observed in NOESY spectra for exchangeable protons of the berberrubine-d-(CCAATTGG)₂ complex at Drug/DNA ratio (D/N) = 1.0 at 298 K. The strong intense (ss), strong (s), medium (m), weak (w), very weakly (vw) intense cross peaks correspond to distances in the range ss 1.8 - 2.5 Å, s 2.5 - 3.0 Å, m 3.0 - 3.5 Å, w 3.5 - 4.0 Å, vw 4.0 - 5.0 Å, respectively.

| Cross peak | NOE Intensity | Cross peak | NOE Intensity |
|--|---------------|--|---------------|
| G7NH - C2NH ₂ ^b | vw | T6NH - C2NH ₂ ^{nb} | m |
| G7NH - C2NH ₂ ^{nb} | m | T6NH - C2NH ₂ ^b | m |
| A4NH ₂ ^b - T5NH | S | A3NH ₂ ^b - G7NH | vw |
| A4NH ₂ ^{nb} - T5NH | S | G7NH-T6NH | m |
| T5NH-A4H2 | S | T6NH-T5NH | m |
| A3NH ₂ ^b - T6NH | S | | |
| A3NH ₂ ^{nb} - T6NH | S | | |
| T6NH-A3H2 | S | | |

Table 5.10: Interproton distance (Å) obtained from intra nucleotide NOE connectivities (di) of base to sugar protons, sugar-sugar protons, and base to base protons of d-(CCAATTGG)₂ in berberrubine- d-(CCAATTGG)₂ complex at D N = 1.0 at 298 K estimated from NOESY spectra.

| Connectivities | Distance (Å) | Connectivities | Distance (Å) | Connectivities | Distance (Å) | Connectivities | Distance (Å) |
|----------------------|--------------|---------------------------------------|--------------|----------------|--------------|--------------------------|--------------|
| C1H6-H1' | 3.45 | C2H2''-H1' | 3.99 | A3H2'-H1' | 2.84 | A4H2-NH2 ^b | 3.61 |
| C1H6-H3' | 6.51 | C2H2''-H6 | 2.72 | A3H2'-H4' | 3.30 | A4H2''-H8 | 2.32 |
| C1HN2b-NH2nb | 5.99 | C2H2'-H1' | 3.95 | A3H2'-H8 | 2.38 | A4H2'-H1' | 2.33 |
| C1H2''-H1' | 2.85 | C2H2'-H6 | 2.60 | A3H3'-H8 | 2.75 | A4H2'-H8 | 2.42 |
| C1H2''-H4' | 2.75 | C2H3'-H6 | 2.42 | A3H4'-H1' | 3.36 | A4H2''-H1' | 2.71 |
| C1H2''-H6 | 2.34 | C2H4'-H1' | 4.32 | A3H4'-H8 | 2.63 | A4H3'-H8 | 2.87 |
| C1H2'-H1' | 2.26 | C2H4'-H6 | 2.49 | A3H8-H1' | 3.32 | A4H4'-H1' | 3.39 |
| C1H2'-H4' | 3.10 | C2H5-H6 | 2.25 | | | A4H4'-H8 | 7.08 |
| C1H2'-H6 | 2.24 | C2H5-NH2 ^b | 4.27 | | | A4H8-H1' | 4.08 |
| C1H3'-H1' | 3.80 | C2H5-NH2 ^{nb} | 3.62 | | | A4NH2 ^b -T5NH | 4.28 |
| C1H4'-H1' | 3.19 | C2H6-H1' | 5.71 | | | | |
| C1H5-H6 | 2.05 | C2H6-NH2 ^b | 5.27 | | | | |
| C1H6-H1' | 3.50 | C2NH2 ^{nb} -NH2 ^b | 3.62 | | | | |
| C1H6-H3' | 4.83 | | | | | | |
| C1H2''-H1' | 2.69 | | | | | | |
| C1H2''-H4' | 1.98 | | | | | | |
| C1H2''-H6 | 2.59 | | | | | | |
| C1H2'-H1' | 2.91 | | | | | | |
| C1H2'-H4' | 3.15 | | | | | | |
| C1H2'-H6 | 3.29 | | | | | | |
| C1H3'-H1' | 4.42 | | | | | | |
| C1H4'-H1' | 3.20 | | | | | | |
| C1H5-H6 | 2.05 | | | | | | |
| C1H6-H1' | 3.50 | | | | | | |
| C1H6-H3' | 4.83 | | | | | | |
| Connectivities | Distance (Å) | Connectivities | Distance (Å) | Connectivities | Distance (Å) | Connectivities | Distance (Å) |
| T5H1'-H6 | 3.84 | T6H2''-H1' | 2.25 | G7H2'-H1' | 2.76 | G8H2''-H1' | 2.76 |
| T5H2''-H1' | 2.14 | T6H2''-H6 | 2.85 | G7H2'-H8 | 2.33 | G8H2'-H1' | 2.85 |
| T5H2''-H6 | 3.19 | T6H2'-H1' | 2.50 | G7H2''-H1' | 5.11 | G8H3'-H1' | 3.97 |
| T5H2'-H1' | 3.23 | T6H2'-H6 | 2.89 | G7H3'-H1' | 3.22 | G8H3'-H8 | 3.61 |
| T5H2'-H6 | 3.21 | T6H6-CH ₃ | 2.85 | G7H3'-H8 | 3.31 | G8H4'-H1' | 3.50 |
| T5H3'-H1' | 3.72 | T6H6-H1' | 3.91 | G7H4'-H1' | 3.20 | G8H4'-H2'' | 2.29 |
| T5H3'-H6 | 3.63 | | | G7H4'-H2' | 2.98 | G8H4'-H2' | 2.32 |
| T5H4'-H1' | 2.99 | | | G7H8-H1' | 2.61 | G8H4'-H8 | 2.40 |
| T5H4'-H2'' | 2.33 | | | | | G8H8-H1' | 4.10 |
| T5H4'-H2' | 3.09 | | | | | G8H8-H2'' | 2.51 |
| T5H6-CH ₃ | 3.07 | | | | | G8H8-H2' | 3.41 |

Table 5.11: Interproton distance (Å) obtained from Sequential NOE connectivities (ds) of d-(CCAATTGG)₂ protons of the berberrubine-d-(CCAATTGG)₅ complex at D/N = 1.0 at 298 K estimated from NOESY spectra .

| Connectiviti es | Distan ce (Å) | Connectiviti es | Distan ce (Å) | Connectiviti es | Distan ce (Å) | Connectiviti es | Distan ce (Å) |
|-----------------------------|------------------|--------------------|------------------|--------------------|------------------|------------------------------|------------------|
| C1H1'-C2H6 | 5.07 | C2H2'- A3H8 | 4.22 | A3H1'- A4H8 | 3.08 | A4H1'- T5CH ₃ | 3.91 |
| C1H2'-C2H6 | 2.73 | C2H2''- A3H8 | 3.71 | A3H2''- A4H2' | 2.89 | A4H1''- T5H6 | 3.68 |
| | | C2H3'- A3H8 | 2.86 | | | A4H2''- T5H6 | 3.07 |
| | | C2H5'- C1H2'' | 4.09 | | | A4H2''- T5H2' | 5.92 |
| | | C2H6- C1H2'' | 3.47 | | | A4H3'- T5CH ₃ | 4.34 |
| | | C2H6- C1H2' | 2.39 | | | A4H3'- T5H6 | 2.50 |
| | | C2H6-A3H8 | 4.44 | | | A4H8- T5CH ₃ | 3.22 |
| | | | | | | A4NH2 ^b - T5NH | 4.28 |
| Connectiviti es | Distan ce (Å) | Connectiviti es | Distan ce (Å) | Connectiviti es | Distan ce (Å) | Connectiviti es | Distan ce (Å) |
| T5CH3- A4H2'' | 3.36 | T6H1'- G7H8 | 2.62 | G7H1'- G8H8 | 2.25 | G8H8- G7H2' | 2.38 |
| T5CH3- A4H2' | 3.43 | T6H2''- G7H8 | 1.97 | G7H3'- G8H8 | 2.38 | | |
| T5CH3- T6CH ₃ | 3.17 | T6H2'- G7H8 | 3.61 | | | | |
| T5H1'- T6CH ₃ | 3.80 | T6H6-G7H8 | 4.11 | | | | |
| T5H1'-T6H6 | 3.35 | T6NH- A3H2 | 3.91 | | | | |
| T5H2''- T6CH3 | 3.44 | | | | | | |
| T5H2''- T6H6 | 2.90 | | | | | | |
| T5H2'- T6CH3 | 3.21 | | | | | | |
| T5H3'- T6CH3 | 4.34 | | | | | | |
| T5H3'-T6H6 | 2.99 | | | | | | |
| T5H6- A4H2'' | 3.52 | | | | | | |
| T5NH- A4H2 | 4.04 | | | | | | |

The presence of more intense intra residue H6/H8-H2' than inter residue H6/H8-H2' shows the predominance of S-conformation for the deoxyribose ring. All the sequential connectivities between base and sugar protons H1', H2', H2'' were observed at all base pair steps. The NOE data thus confirm the existence of B-DNA duplex with no possibility of opening of base pairs. Hence intercalation mode of interaction between berberrubine and DNA in the drug-DNA complex is completely ruled out. Table 5.12 (a-b) shows the intramolecular and intermolecular NOE connectivities within the berberrubine molecule in the berberrubine-d-(CCAATTGG)₂ complex at D/N = 1.0.

The observed inter-drug cross peaks indicate that the two drug molecules are stacked over each other in an antiparallel orientation in the complex resulting in proximity of ring D protons with ring A protons (Table 5.12 (b)). H10 proton of berberrubine gives cross peaks with distantly placed protons H 24, H 28, H 31,32, H 3 and H 5 protons which can be attributed to rotation at N11-C15-C18-C21 torsional angle at ring B of berberrubine on binding to d-(CCAATTGG)₂ resulting in proximity of ring D protons with ring A protons. This suggests that the conformation of berberrubine changes on binding.

| Connectivities | NOE Distance (Å) |
|--------------------------|-------------------------|
| H 10-H 19, 20 | 3.69 |
| H10-H 16,17 | 2.89 |
| H 24-H 19,20 | 3.96 |
| H 24-H 16,17 | 2.91 |
| H 16, 17-H 19, 20 | 2.35 |
| H14-H28 | 3.92 |

Table 5.12 (a): Intra drug NOE connectivities and distances (Å) of berberrubine

| Connectivities | NOE Distances (Å) |
|-------------------|-------------------|
| H 10-H 24 | 4.39 |
| H 10-H 28 | 4.84 |
| H 10-H 5 | > 5 |
| H 10-H 31, 32 | 5.36 |
| H 10-H 14 | 4.67 |
| H 28-H 24 | 2.48 |
| H 28-H 19, 20 | 4.33 |
| H 28-H 31, 32 | 5.77 |
| H 28-H 24 | 2.62 |
| H 24-H 16, 17 | 4.30 |
| H 28-H 16, 17 | 4.44 |
| H 24-H 31, 32 | 3.87 |
| H 31, 32-H 19, 20 | 2.33 |
| H 14-H 31, 32 | 4.00 |
| H 16, 17-H 5 | 4.57 |
| H 16, 17-H 31, 32 | 4.02 |

Table 5.12 (b): Inter drug NOE connectivities and distances (Å) of berberrubine

Table 5.12 (a-b): Shows intra and Inter drug protons connectivities and distances (Å) of drug from NOESY spectra of berberrubine-d-(CCAATTGG)₂ complex at D/N = 1.0, at 298 K.

Some new intermolecular cross peaks, which were not present in free berberrubine (Tripathi et al., 2007), appeared in the NOESY spectrum of complex shown as # Figure 5.8 (a-h). The observed 19 inter-molecular NOEs connectivities of the drug protons H 10, H 31, 32, H 19, 20, H 24 and H 16, 17 with the sugar (H1', H2'/2'') and base (NH₂^{nb/h}, CH₃, A3/A4H2) shows that the ring B, C and ring D fit in the minor groove of the DNA and supports the minor groove mode of binding of berberrubine in the complex (Table 5.13).

Table 5.13: Connectivities and interprotons distances (Å) from NOESY spectra of berberrubine-d-(CCAATTGG)₂ complex at drug to nucleotide D/N = 1.0. at 298 K. The corresponding distances obtained from optimized rMD structure are also shown.

| Connectivities | DISTANCE (Å) Ref: C2H6-NH2b | Final rMD (Å) |
|-------------------|--------------------------------|------------------|
| H10- C1H6 | 3.93 | 5.17 (D1) |
| H10- T5H1' | 4.04 | 4.50 (D1) |
| H10- T6H1' | 7.29 | X |
| H10- C1H1' | 5.04 | X |
| H10-C1H5 | 4.98 | X |
| H10 - C2NH2ab | 6.53 | 6.28 (D2) |
| H10- C2NH2b | 6.20 | 6.05 (D2) |
| H10- A3/A4H2 | 4.02 | 4.64 (D2) |
| H10-G8NH2nb | 5.33 | 2.55 (D2) |
| H10-G8H1' | 7.38 | X |
| H31-32 -T5H2' | 3.52 | 4.08 (D2) |
| H31-32 -T5H2'' | 4.52 | 5.22 (D2) |
| H1617- A4NH2b | 4.60 | 5.82 (D2) |
| H16,17- A4H1' (O) | 3.02 | X |
| H16,17-A3/A4H2 | 4.23 | 4.49 (D2) |
| H16,17-A3H3' | 4.55 | X |
| H19,20-A3,A4H2 | 3.33 | 2.47 (D2) |
| H24-T5H1' | 3.77 | 5.42(D2) |
| H24-T6CH3 | 4.74 | 5.70 (D2) |

X= distances out of range in the final rMD structure of the complex

D1 and **D2** represent the individual berberrubine molecule in the final rMD structure of the berberrubine-d-(CCAATTGG)₂.

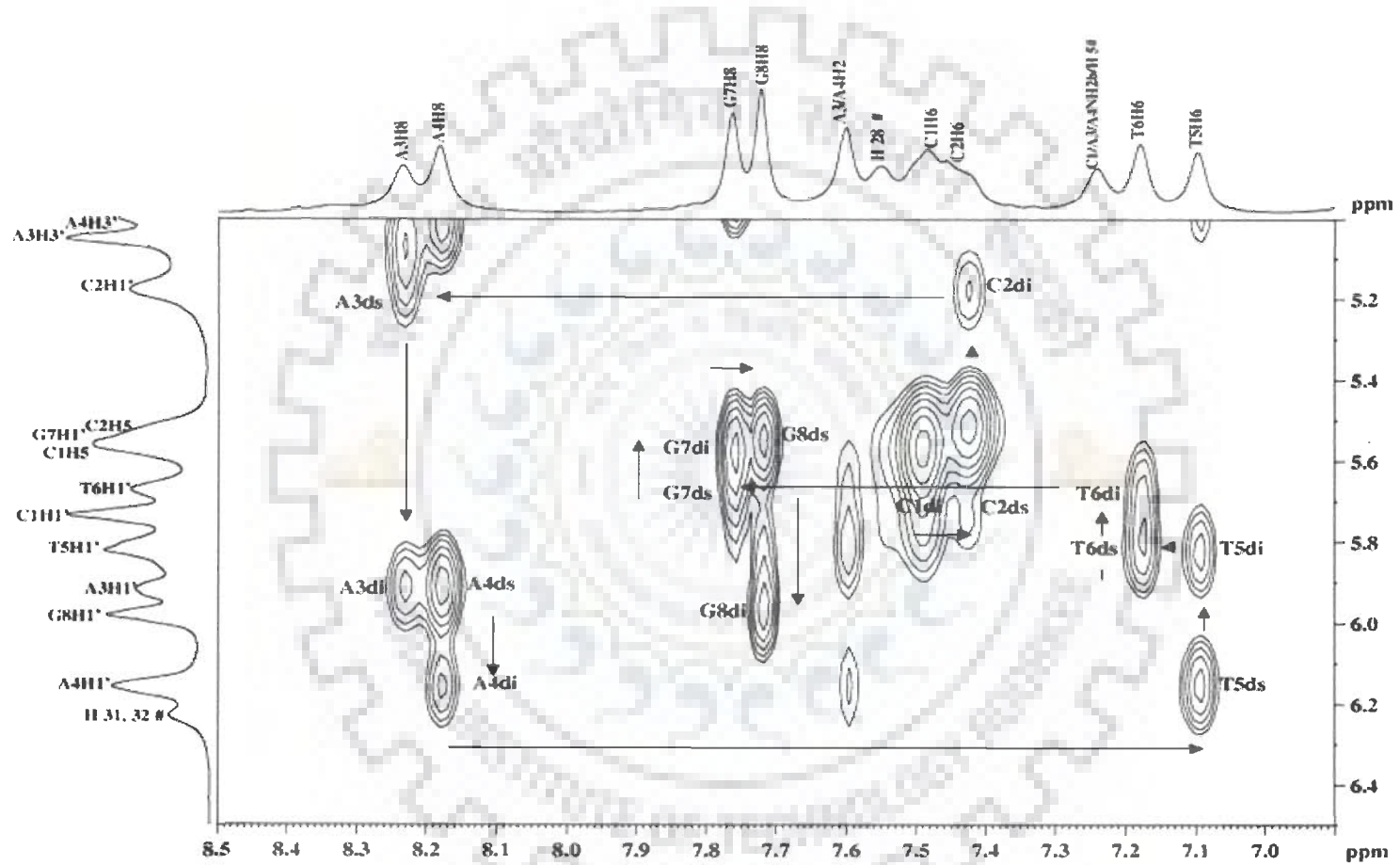


Figure 5.8 (a)

1H NOESY 200ms 298K
 CCAATTGG D/N =1.0

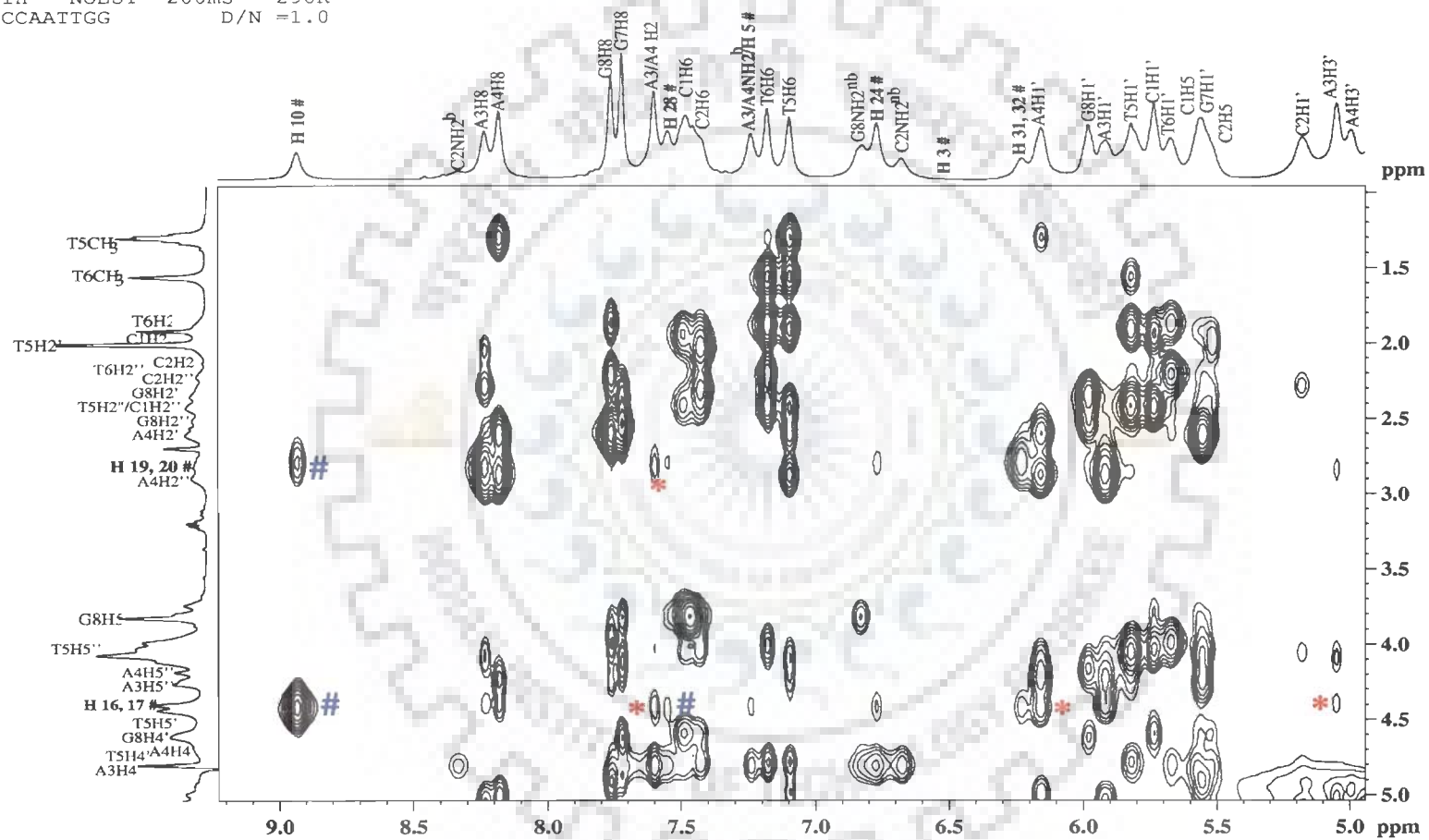


Figure 5.8 (b)

1H NOESY 200ms 298K
 CCAATTGG D/N =1.0

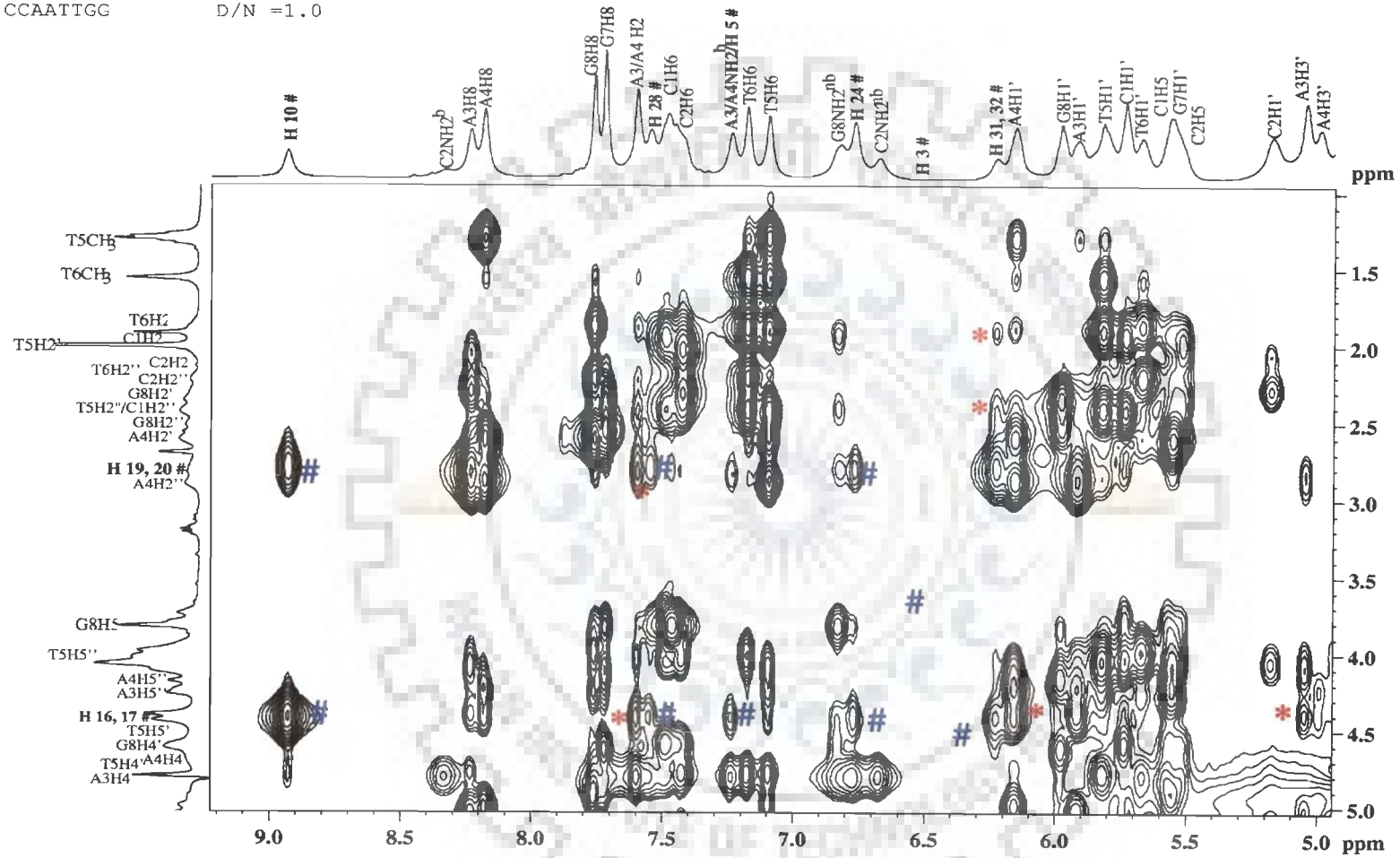


Figure 5.8 (b')

1H NOESY 200ms 298K
 CCAATTGG D/N =1.0

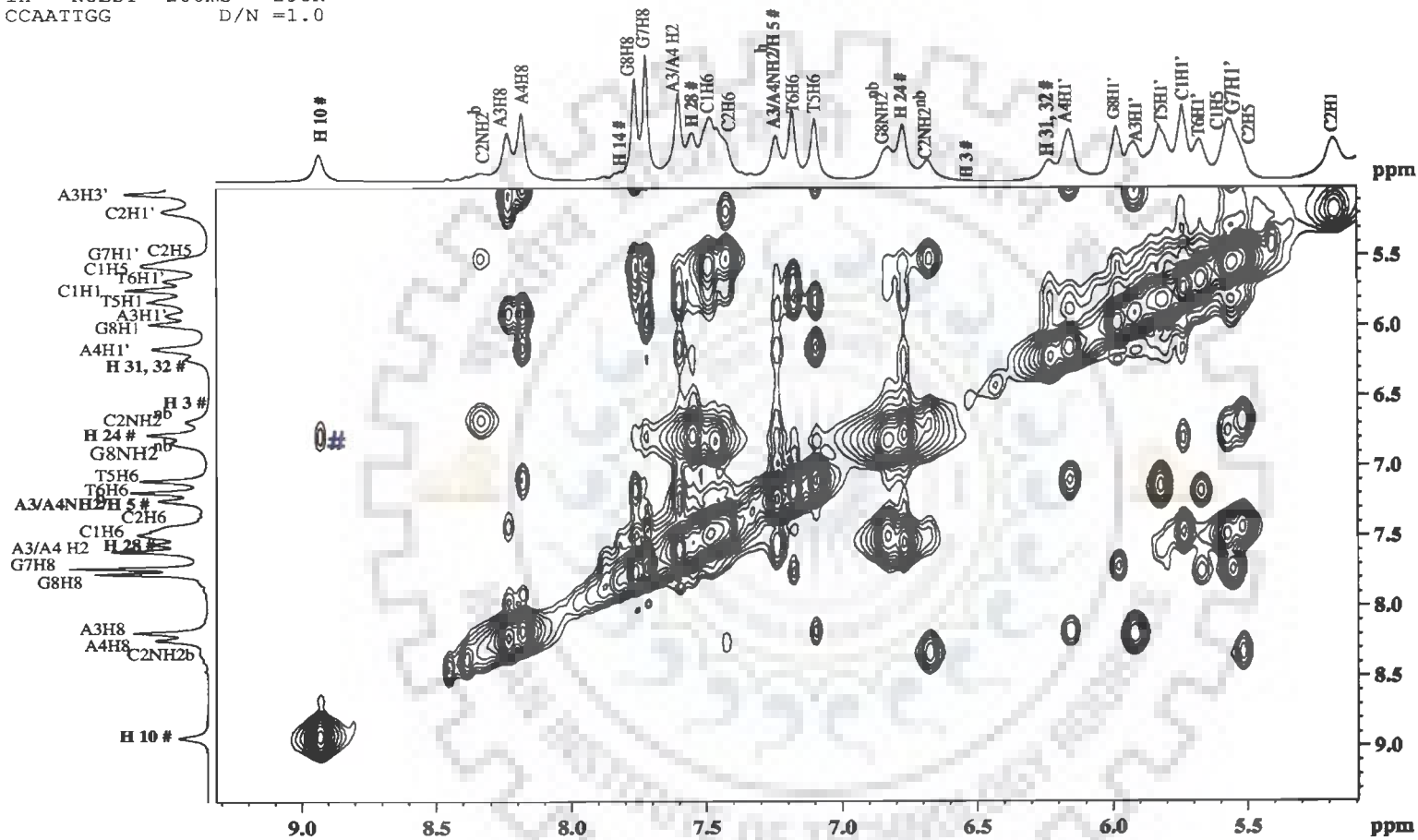


Figure 5.8 (c)

1H NOESY 200ms 298K
 CCAATTGG D/N = 1.0

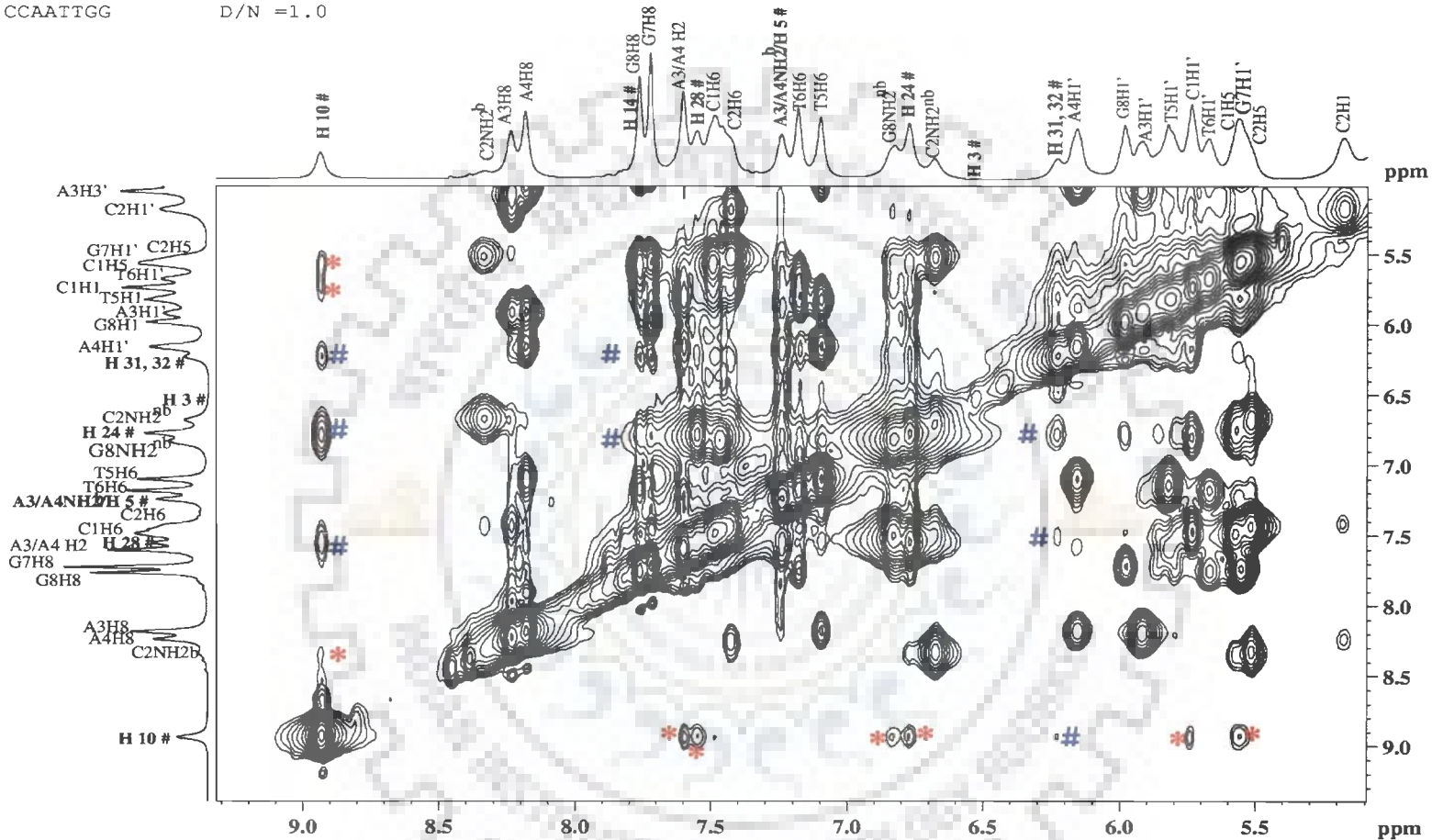


Figure 5.8 (c')

1H NOESY 200ms 298K
CCAATTGG D/N =1.0

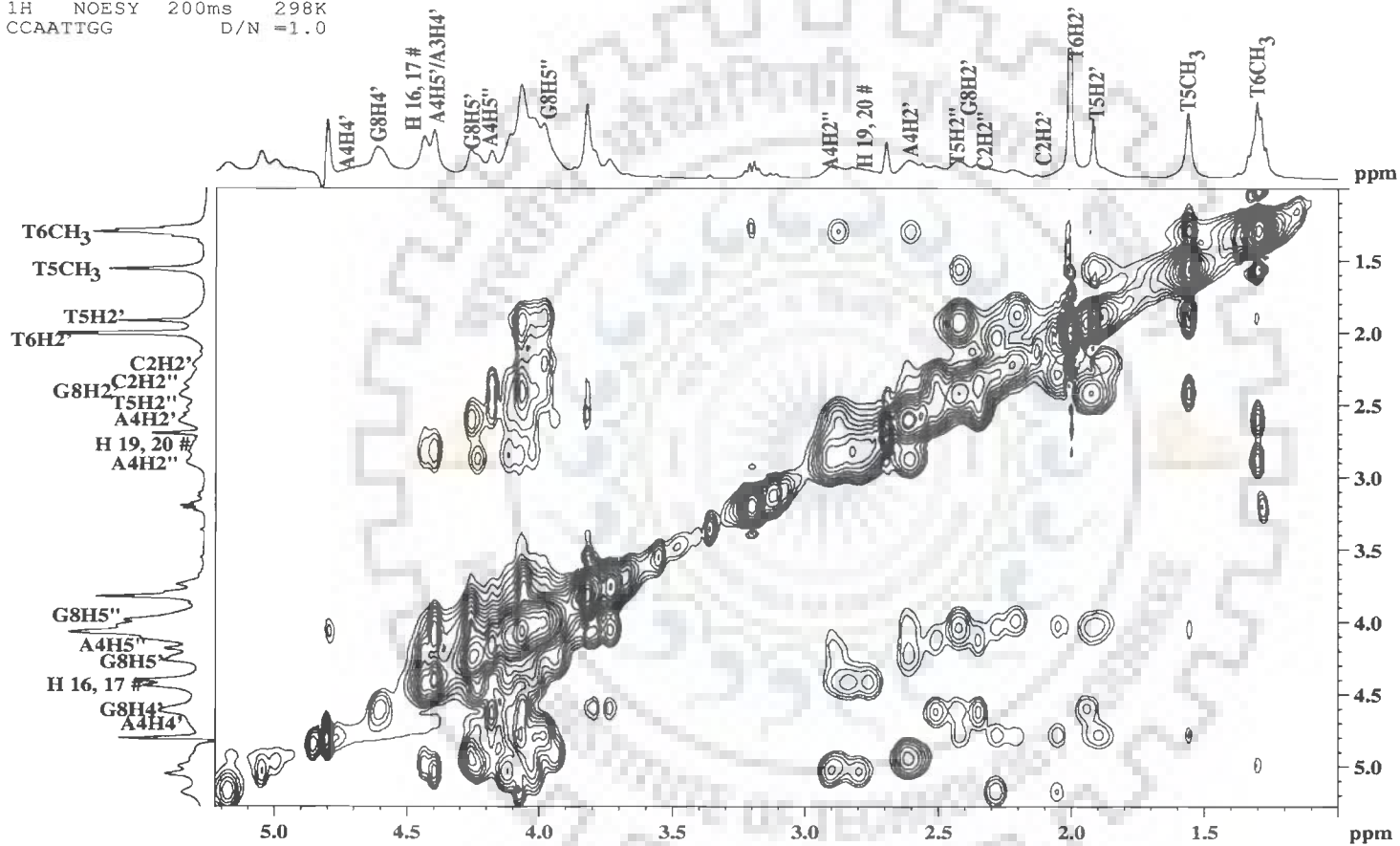


Figure 5.8 (d)

1H NOESY 200ms 298K
 CCAATTGG D/N =1.0

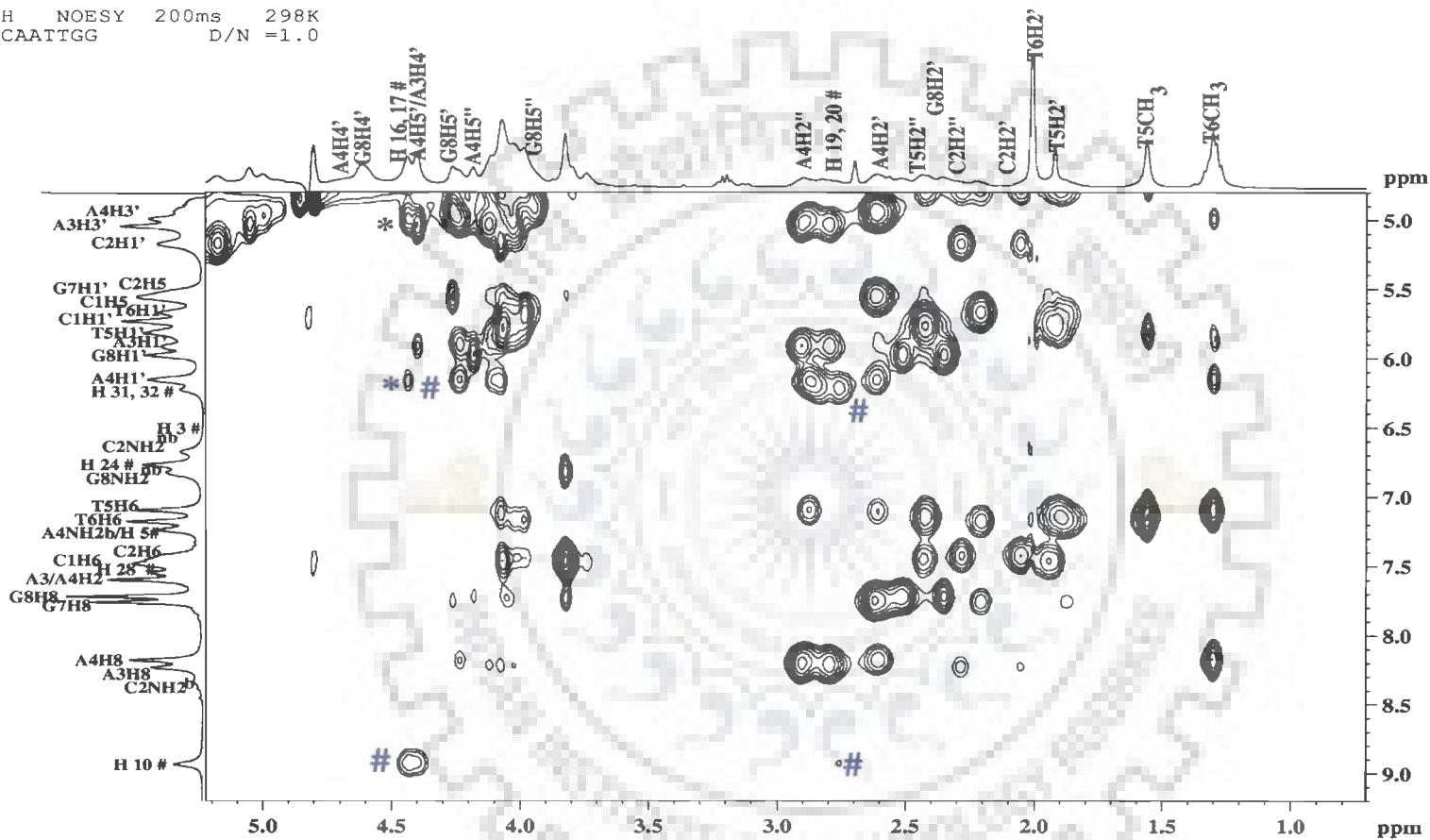


Figure 5.8 (e)

1H NOESY 200ms 283K
CCAATTGG IN H2O

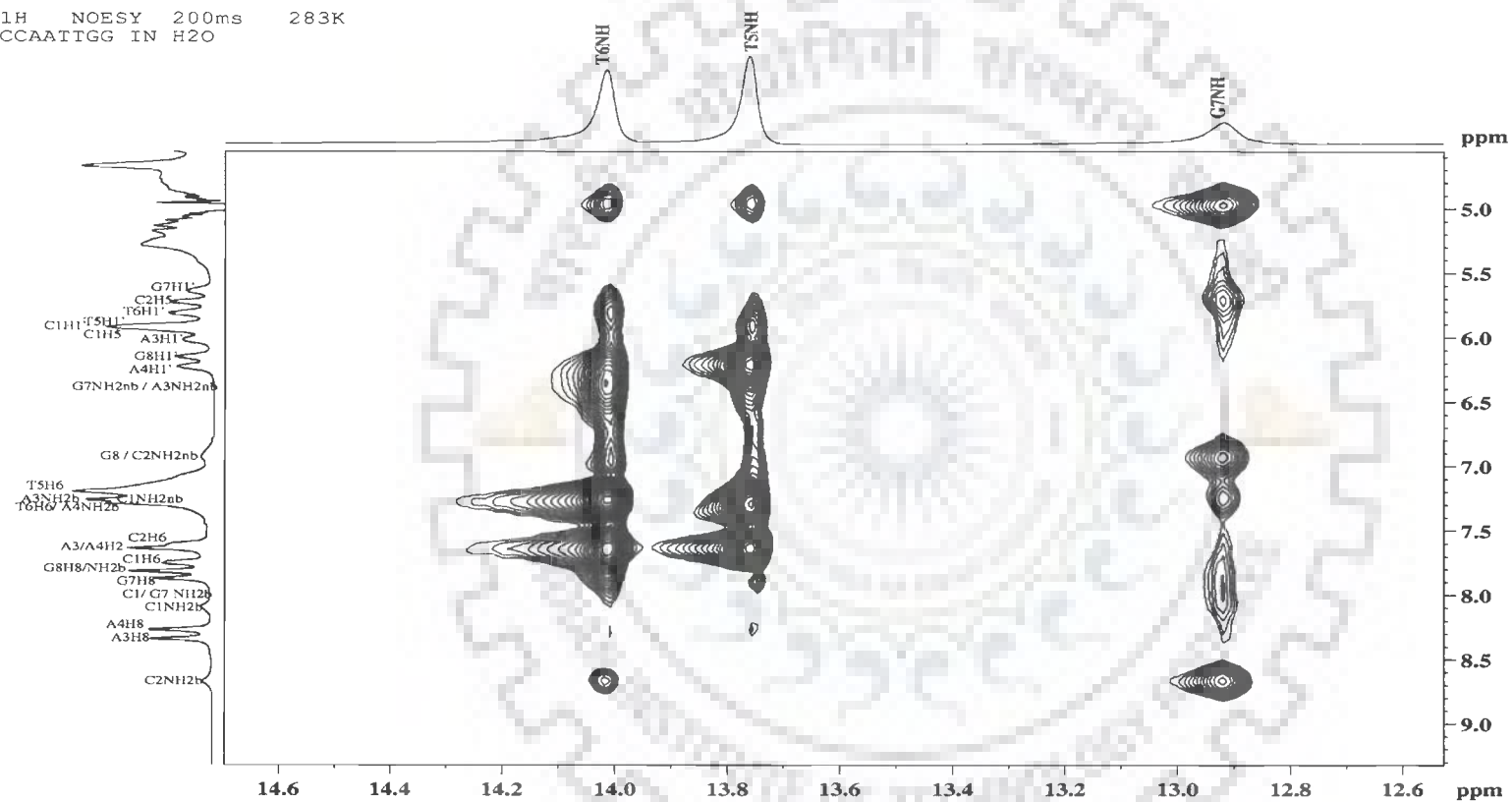


Figure 5.8 (f) Alone d-(CCAATTGG)₂ -NH region

1H NOESY 200ms 283K
CCAATTGG D/N=1.0 IN H2O

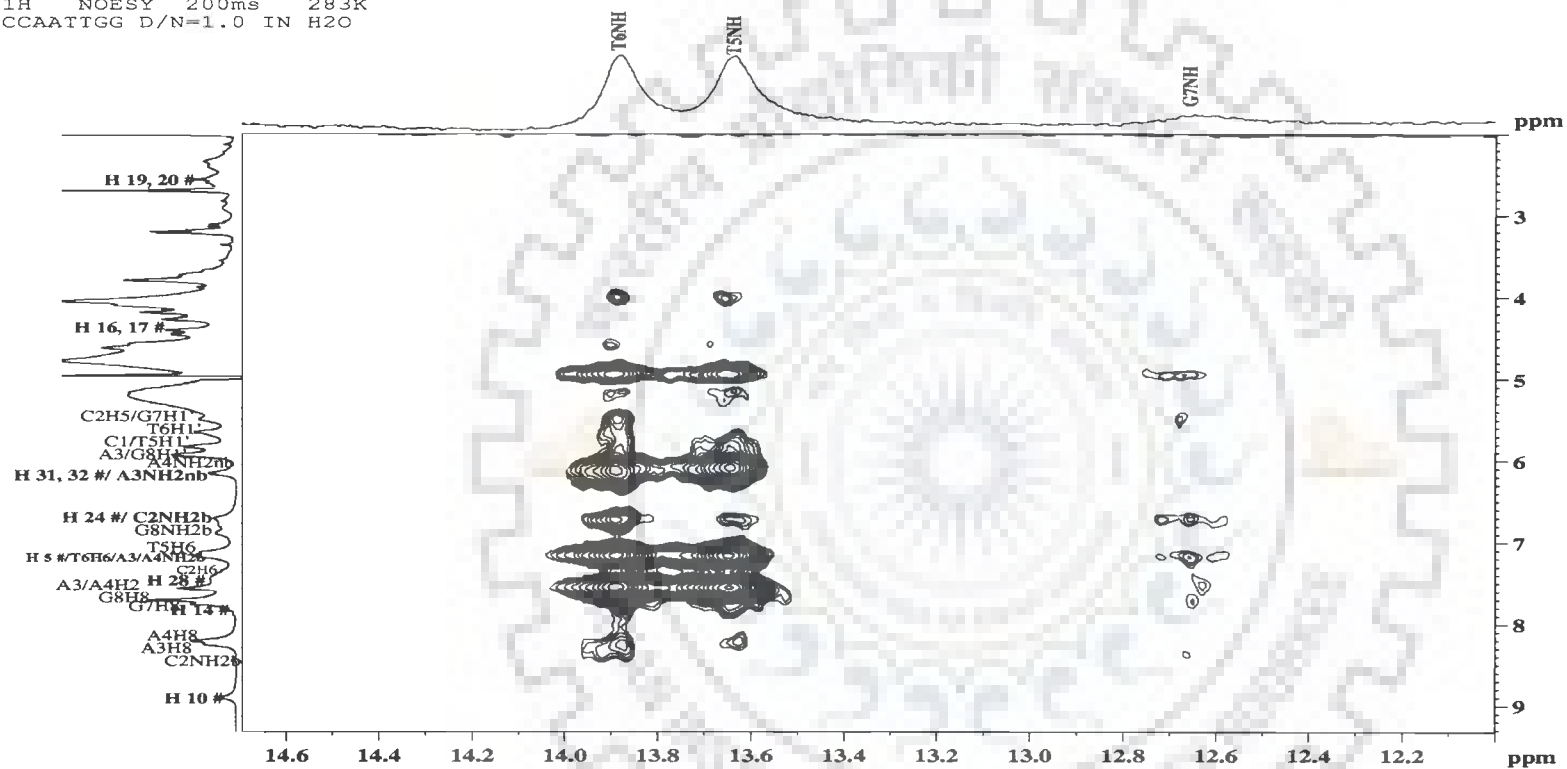


Figure 5.8 (g) Berberubine-d-(CCAATTGG)₂ Complex -NH region

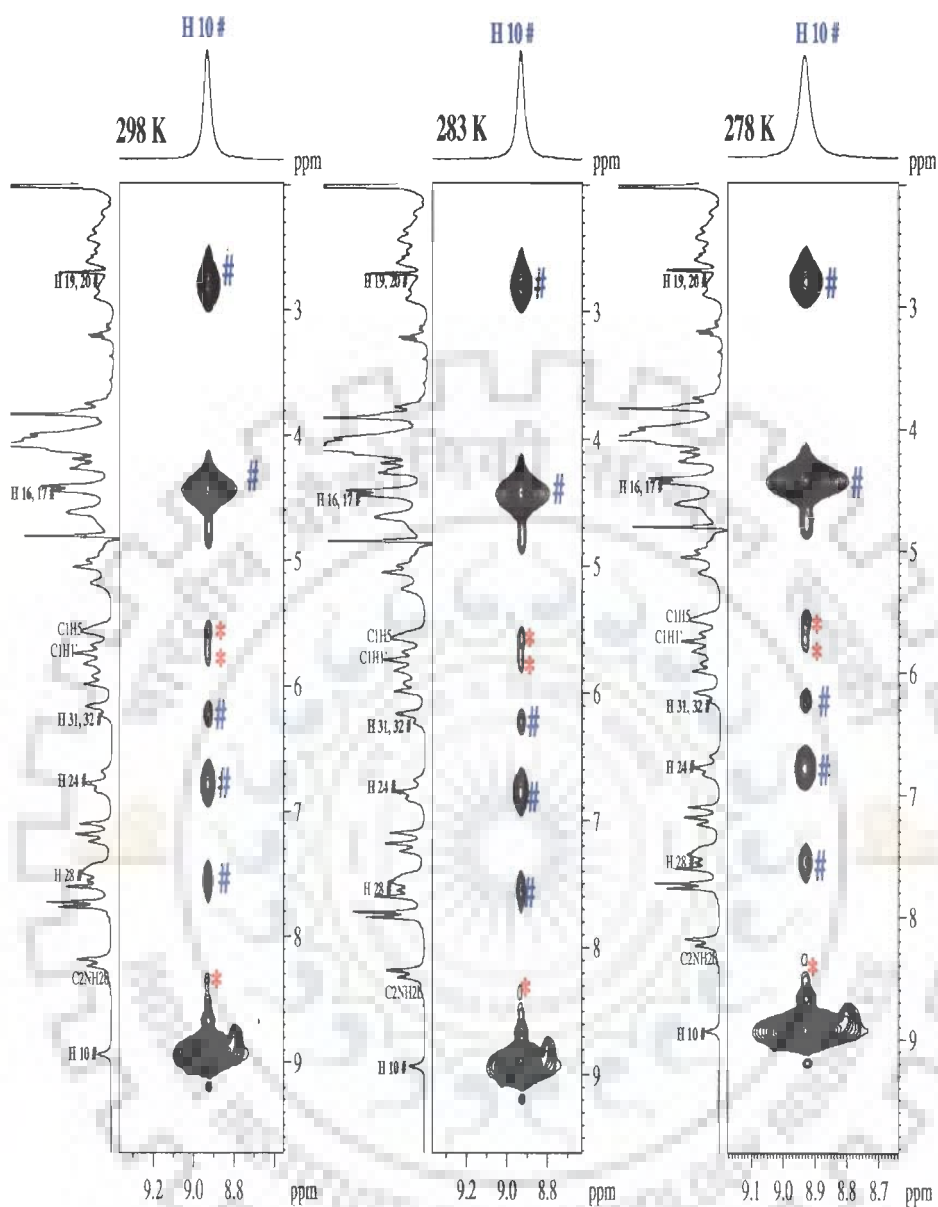


Figure 5.8 (h)

5.8 (a-h): Expansion of the specific regions of NOESY spectra of berberrubine complexed with $d\text{-(CCAATTGG)}_2$ to highlight specific connectivities (“#” represent inter molecular drug peaks berberrubine; “*” represent intermolecular peaks in berberrubine- $d\text{-(CCAATTGG)}_2$ complex).

The berberrubine-d-(CCAATTGG)₂ complex at the minor groove of the d-(CCAATTGG)₂ was stabilized via close contacts which involved specific van der Waals, hydrogen bond and electrostatic forces. Therefore overall binding of berberrubine with d-(CCAATTGG)₂ gave a clear evidence against intercalative binding on the basis of absence of large downfield shifts ($\delta > 1.5$ ppm) in phosphorus-31 NMR signals and presence of all base-sugar H1', H2', H2'' sequential NOE connectivities in the NMR spectra of complex.

5.4 Restrained Molecular Dynamics Simulations

The model of berberrubine d-(CCAATTGG)₂ complex built using the observed intra- and inter molecular NOEs (Table 5.12 (a-b) and 5.13) with berberrubine molecules placed antiparallel with respect to each other and located in the minor groove of d-(CCAATTGG)₂ by rMD simulations for 25ps is shown in figure 5.9. Resulting rMD structure was thoroughly analyzed with CURVES software, version 5.1 (Lavery and Sklenar, 1996) The structural characteristics of various rMD structures are discussed in the following sections:

An assessment of the refined structure after equilibration in terms of energetics which includes average Root Mean Square Deviation of energy with respect to atomic coordinates (RMSD); minor groove width and depth; the total potential energy and other energy terms for rMD structure generated by restrained Molecular Dynamics (rMD) are shown in Table 5.14 (a-b). Plot of some of the helicoidal parameters as a function of residue position in the duplex is shown in Figure 5.10 along with that for canonical structures of A-DNA, B-DNA, and uncomplexed d-(CCAATTGG)₂.

The overlap geometry at different base pair steps along the sequence in berberrubine-d-(CCAATTGG)_n is shown in figure 5.11. Base sequence dependent variations in helicoidal parameters are evident. The octamer in the complexed state with berberrubine adopts generally B-type conformation with little disruption in some of the parameters. Among the base pair-axis parameters, the X-displacement (dx) ~ 1 Å for all residues, which is close to a value of -0.7 Å observed in canonical B-DNA and uncomplexed structure of d-(CCAATTGG)₂. But small deviations at A3, A4, T5, T6 steps are apparent. The y-axis displacement (dy) varied within 0 to +20 Å along the sequence. The values of η for C1 and C2 residues are close to that of A-DNA but shift towards that for B-DNA for residues towards 3' end.

It was observed that berberrubine induced perturbations, manifesting more negative value for propeller, twist at C2, A3, A4 residues, and higher opening per base pair for the central AATT residues. These results suggest that the binding of berberine takes place at A3-T6 and A4-T5 base pairs thereby causing significant distortions in DNA helix while distortions are much less towards the 3' end of the DNA. In regular A-DNA and B-DNA geometries, global values of the inter base pair parameters shift (Dx), slide (Dy), roll (rho) and tilt (tau) are essentially zero. Among the inter base pair parameters rise, tilt, roll and twist showed variation at the A3-A4 and marginal variation along the base sequence. It is noted that overlap of bases at C1pC2, C3pA3 step was particularly low. The relatively less magnitude positive roll at A3pA4, T5pT6 and G7pG8 step indicate increased base stacking interactions which are clearly shown in Figure 5.10. The central AATT quartet of the NMR structure forms a tight stack.

Table 5.14 (a): Energy terms (K cal mol⁻¹) for starting structure and final rMD structure

| Structure | Total | P.E | K.E | Bond | Out of plane |
|-----------|----------|----------|---------|---------|--------------|
| Initial | 5455.306 | 4961.729 | 493.577 | 290.992 | 25.33 |
| Final | 2452.983 | 1962.983 | 490.00 | 102.303 | 13.579 |

Table 5.14 (b): Summary of Experimental restraints and statistical analysis of final structure generated by Restrained Molecular Dynamics (rMD).

| Parameter | No. of Distance Restraints |
|---------------------------|---|
| Intra residue | 106 |
| Inter residue | 66 |
| Inter molecular | 13 |
| Minor Groove width | Initial: 5.87 Final: 6.02 |
| Minor Groove depth | Initial: 4.59 Final: 5.23 |
| Average residue wise RMSD | C1=0.069; C2=0.056; A3=0.055; A4=0.049; T5=0.058; T6=0.0965; G7=0.0835; G8=0.0835 |

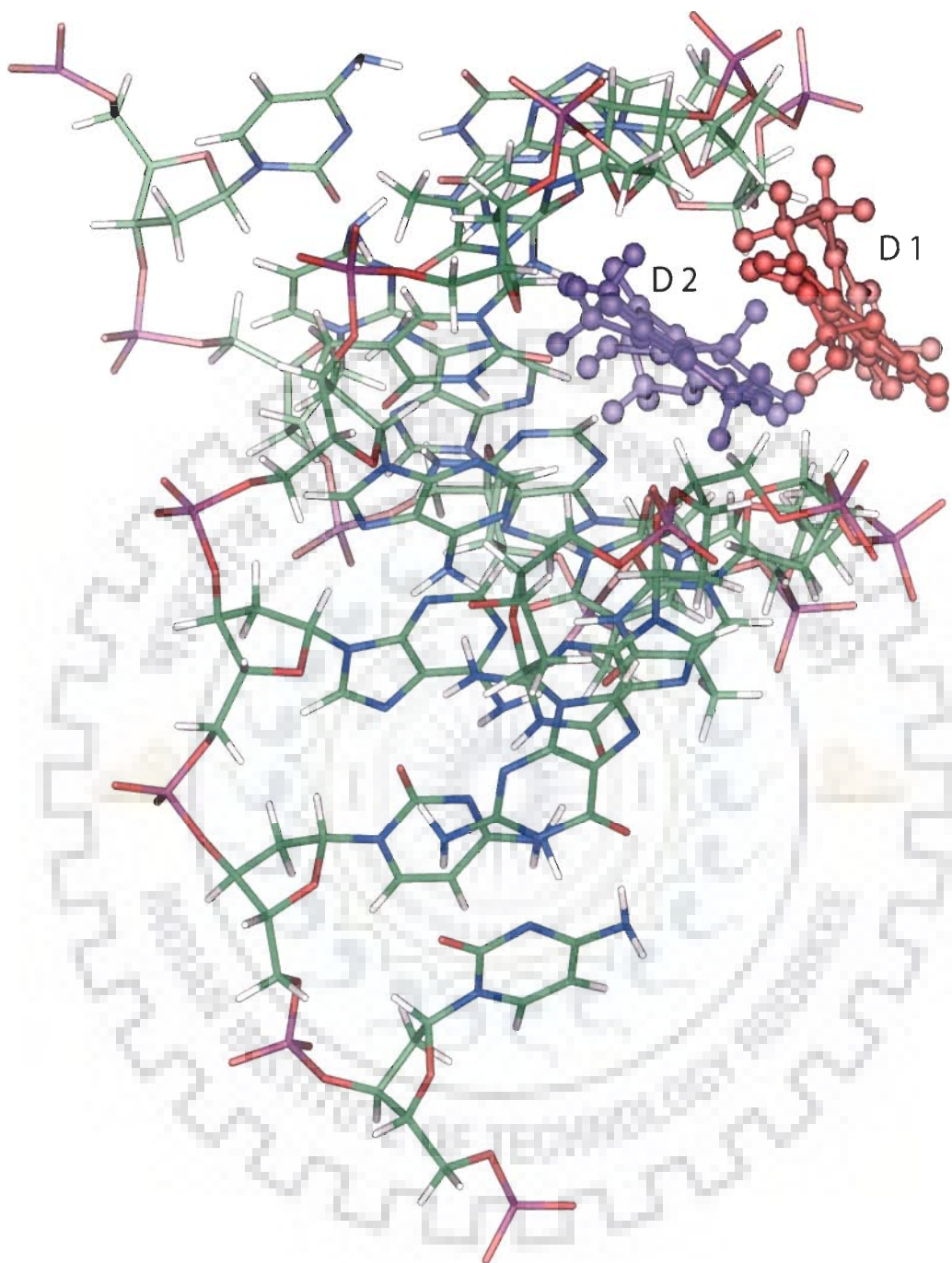


Figure 5.9: Shows the minimum energy conformation of the berberubine- $(\text{CCAATTGG})_2$ complex after rMD simulation by DISCOVER and INSIGHT

II

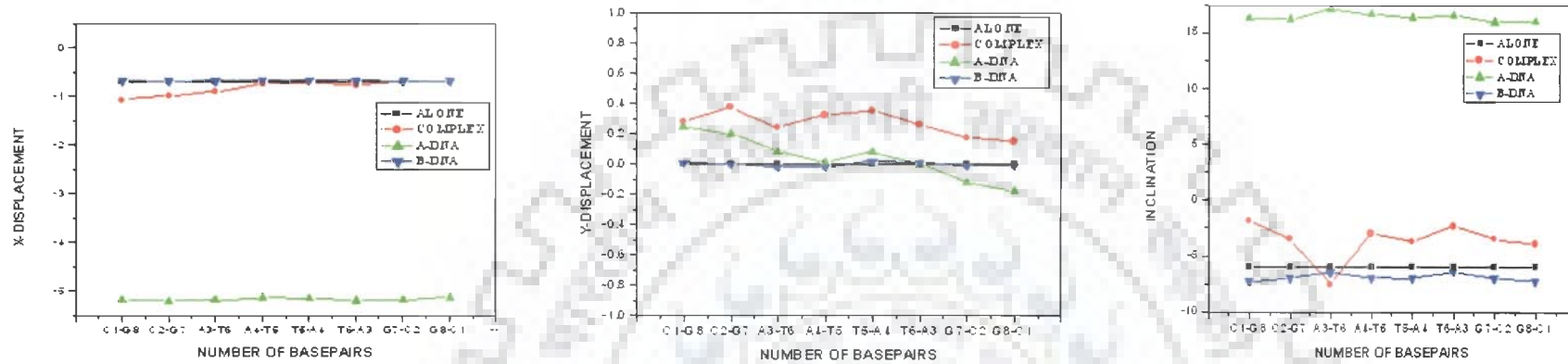
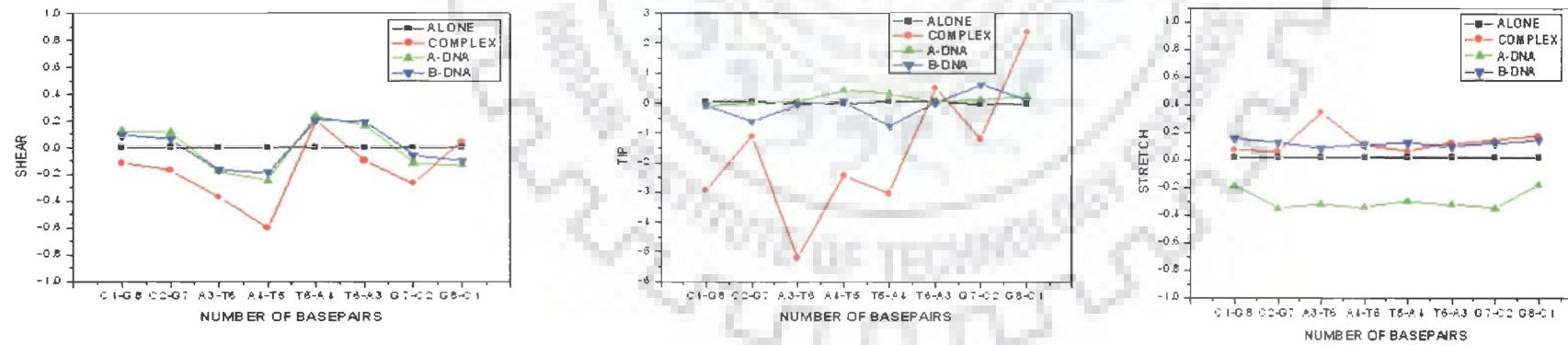


Figure 5.10 (a)



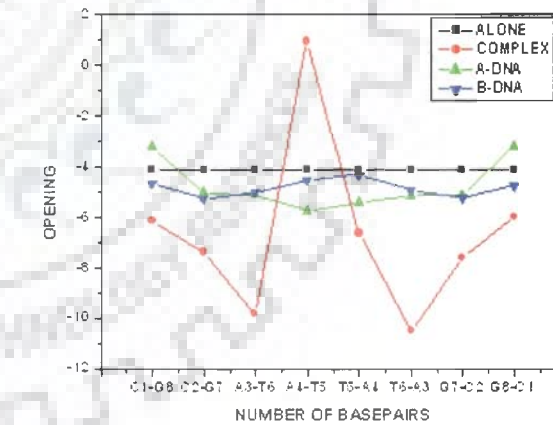
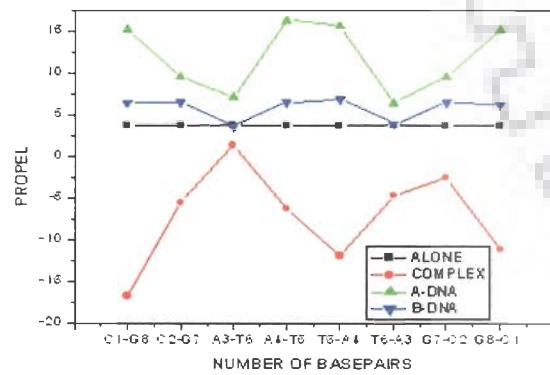
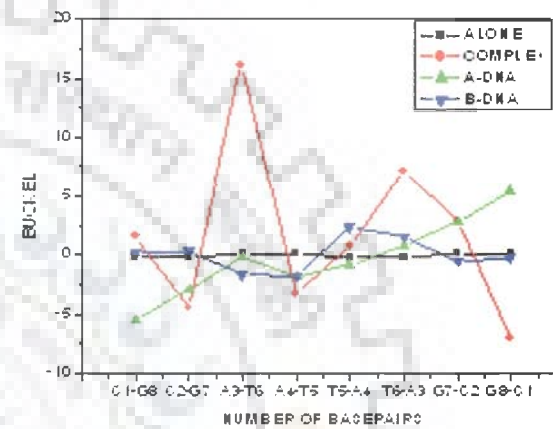
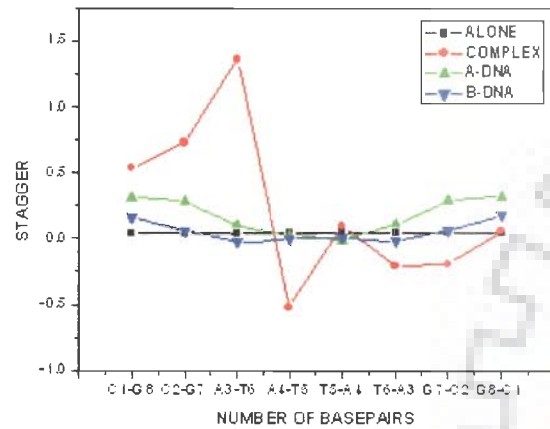


Figure 5.10 (a)

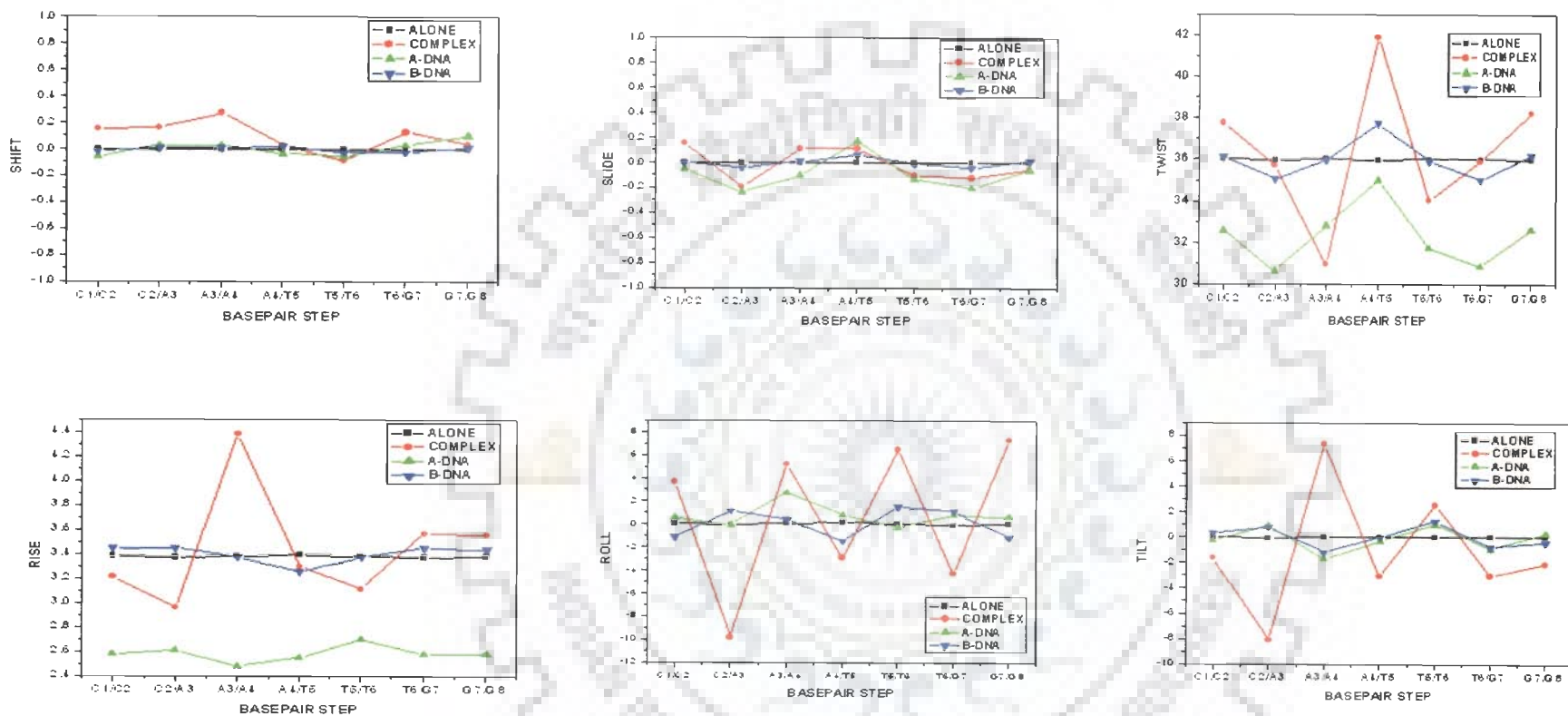


Figure 5.10 (b)

Figure 5.10: (a) and (b) Helical parameters for d-(CCAATTGG)₂ complexed with berberrubine calculated for structure obtained by restrained molecular dynamics simulation (ALONE DNA -■; COMPLEX DNA -■) and that for canonical A-DNA (▲) and B-DNA (▼).

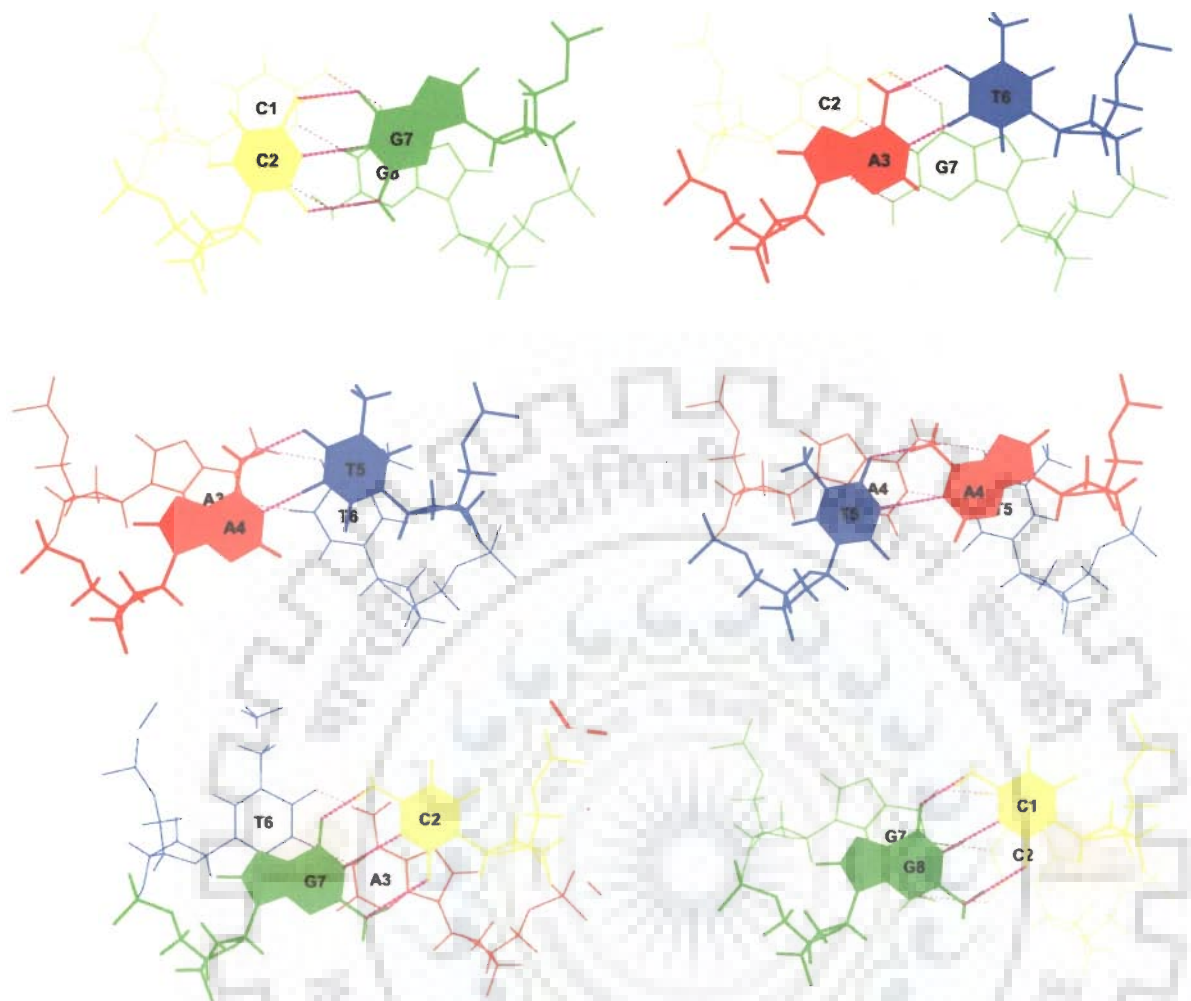


Figure 5.11: Stereo view of seven individual base pair steps viewed down the global helix axis showing stacking between adjacent base pairs in d-(CCAATTGG)₂

The variation of torsional angles with base sequence (Table 5.15 (a-b)) showed equivalence of the strands of duplex. Although the angles α through ξ showed variations with base sequence, they had values closer to B-DNA for most residues rather than to the corresponding A-DNA structure. The angle α varied in a narrow range of -40° to -65° and was smallest in negative magnitude for T5 base in rMD structures. The β angle was found either in -150 to -170° value appreciably with base

sequence and adopted a trans-conformation. The variation of γ was in the range 50°-70° except at 5' end where it was unusually large for crystal structure and adopted trans conformation. The angle δ reflects the deoxyribose puckering and adopted conformation between that of A-DNA and B-DNA

| <i>d(CCAATTGG)₂</i> | | | | | | | | | |
|--------------------------------|-----------|----------|-----------|----------|-----------|----------|-----------|----------|-----------|
| | | <i>a</i> | | <i>B</i> | | <i>Γ</i> | | <i>δ</i> | |
| Strand I | Strand II | Strand I | Strand II | Strand I | Strand II | Strand I | Strand II | Strand I | Strand II |
| C1 | G16 | -62.59 | | -158.8 | | 64.22 | 48.98 | 139.17 | 145.05 |
| C2 | G15 | -65.25 | -65.16 | -165.58 | -149.68 | 49.57 | -53.63 | 143.41 | 154.92 |
| A3 | T14 | -63.6 | 57.88 | -162.81 | 168.18 | 54.23 | 50.97 | 135.27 | 144.87 |
| A4 | T13 | -63.62 | -55.76 | -174.34 | -168.13 | 50.53 | 48.8 | 137.8 | 129.99 |
| T5 | A12 | -45.87 | -61.11 | -151.87 | -161.92 | 60.47 | 51.95 | 123.42 | 141.56 |
| T6 | A11 | -66.3 | -63.93 | -154.21 | -165.39 | 21.12 | 54.75 | 153.85 | 134.4 |
| G7 | C10 | -64.91 | -65.41 | -148.16 | -165.2 | 51.11 | 49.77 | 143.81 | 144.64 |
| G8 | C9 | | -62.9 | | -159.34 | 49.14 | 65.12 | 145.41 | 139.79 |
| B-DNA | | -63 | | 136 | | 54.0 | | 123 | |

Table 5.15 (a)

| <i>d(CCAATTGG)₂</i> | | | | | | | | | |
|--------------------------------|-----------|----------|-----------|----------|-----------|----------|-----------|----------|-----------|
| | | <i>ε</i> | | <i>Z</i> | | <i>χ</i> | | <i>P</i> | |
| Strand I | Strand II | Strand I | Strand II | Strand I | Strand II | Strand I | Strand II | Strand I | Strand II |
| C1 | G16 | 172.26 | | -97.09 | | -94.57 | -97.37 | 179.56 | 189.85 |
| C2 | G15 | 176.35 | 155.4 | -98.25 | -88.76 | -100.95 | -88.29 | 191.74 | 203.85 |
| A3 | T14 | 177.18 | -176.47 | -96.1 | -145.58 | -103.28 | -110.8 | 169.89 | 174.23 |
| A4 | T13 | 179.11 | 178.28 | -97.24 | -84.58 | -104.17 | -106.39 | 176.98 | 197.03 |
| T5 | A12 | 176.21 | 176.09 | -85.13 | -99.65 | -117.35 | -105.74 | 145.5 | 175.33 |
| T6 | A11 | 162.9 | 176.14 | -98.02 | -96.14 | -86.15 | -104.47 | 203.39 | 169.12 |
| G7 | C10 | 163.51 | 177 | -90.97 | -98.86 | -97.83 | -99.55 | 187.26 | 192.46 |
| G8 | C9 | | 173.41 | | -98.64 | -103.21 | -91.55 | 191.43 | 178.84 |
| BDNA | | -169 | | -108 | | -105 | | 162 | |

Table 5.15 (b)

Table 5.15 (a-b): Backbone torsional angles, pseudorotation phase angle and glycosidic bond rotation of the final rMD structure of berberrubine-*d(CCAATTGG)₂* complex.

In rMD structure δ was mostly found towards B-DNA ranging from 120° to 150° . The angle ϵ was in trans conformation for two alternating residues while ξ was closer to the corresponding value in B-DNA in both the structures. The value of P angle in structure resulting from our rMD was essentially consistent with the results of the NMR data explained above and shows that it lies in the range 138° - 178° .

5.5 CONCLUSION

Our results on addition of berberrubine to nucleic acid sequence up to D/N = 1.0 show that spectral lines shift gradually with a formation of specific complex having reduced diffusion constant with DNA intact as a right handed duplex structure with sugar in S conformation and glycosidic bond angle. The interaction mode is not intercalative as neither ^{31}P resonance shifts downfield nor sequence connectivities are broken at any step. On the other hand specific NOEs suggest binding at minor groove with electrostatic interaction specifically at A3pA4, A4pT5 and T5pT6 sites and van der waals contacts involving H 10, H 31, 32, H 16, 17 and H 24 protons of berberrubine with C2, A3, A4, T5, T6 sugar and base protons of DNA in the minor groove.

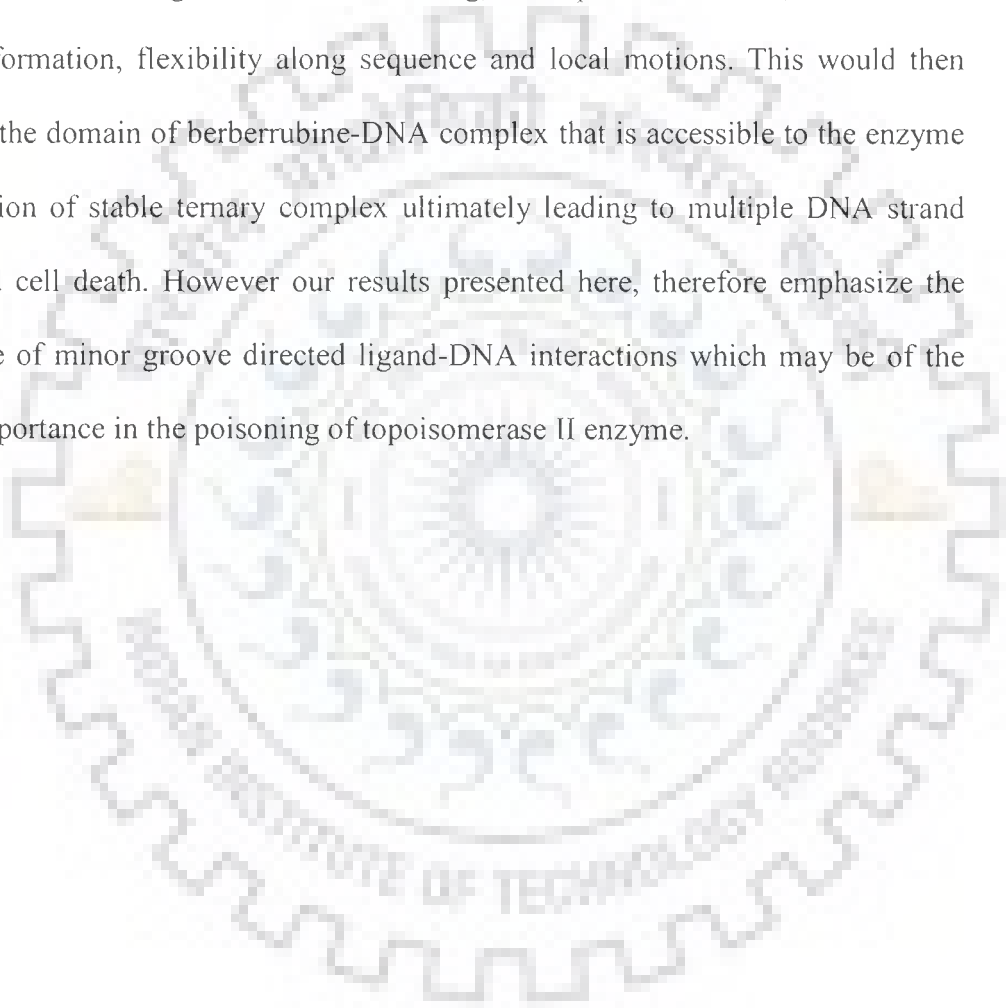
Several authors have reported the necessity of hydrogen bond formation between ligand and adenine H2 at the minor groove floor to establish minor groove binding (Jenkins et al., 1997; Lane et al., 1991). But we did not find any hydrogen bond between berberrubine and d-(CCAATTGG)₂ in the final rMD model. Absence of hydrogen bond in berberrubine binding to the minor groove of d-(CCAATTGG)₂ can be explained by extensive study done by Taberero et al. They studied extensively the role of ligand-DNA hydrogen bonds for 22 minor groove ligand-oligonucleotide crystal structures and found that the ligand cationic group did not

show a preference to hydrogen bonding suggesting that presence of hydrogen bond has less importance (Tabernero et al., 1996). This is also supported by several studies done with empirical force field, which showed the absence of any hydrogen bond formation and found that van der Waals terms are the dominant factor in minor groove binding (Chang et al., 1996). This view has been supported by Czarny et al by a combined solution binding and structural study on a series of bis-benzimidazole - DNA complexes, which showed that increasing the number of charged group did not significantly affect binding affinity whereas, increasing the number of contacts with the minor groove walls increased the ability to bind (Czarny et al., 1995).

Hence we conclude that interaction of berberrubine with DNA involves minor groove binding of ring B, C and D over CAATT segment without intercalation of drug chromophore between base pairs of DNA. Absence of large downfield shift of any phosphorus -31 NMR signals of A3pA4, A4pT5, T5pT6 phosphorus resonances presumably due to electrostatic interaction; presence of sequential base-sugar NOE connectivities; large upfield shift ($\Delta\delta$) in H 19, 20, H 10, H 14, H 24 and down field shift in H 31, 32 and H 3 protons of berberrubine; change in its conformation and observation of 19 intermolecular NOEs unambiguously establish the minor groove binding mode of interaction. The DNA conformation has also changed in a subtle way to accommodate binding of drug. The width and depth of minor groove has changed from 5.87 and 4.59 to 6.02 and 5.23 (Table 5.9 (b)) respectively on binding. Results on dynamics also support our study that the perturbations, manifesting more negative value for propeller, twist at C2, A3, A4 residues, and higher opening per base pair for the central AATT residues can be due to binding of the berberrubine at the minor groove (CAATT) region of the octamer.

Our results have important implications to the biological activity since DNA-binding is directly related to the poisoning of topoisomerase-II-enzyme. The results obtained also prove that it is the molecular structure that will be the diagnostic for identification of a specific drug-DNA complex as topoisomerase poison.

In this context the structure-conformation of berberrubine-DNA complexes spells out the role of ring B, C and D in binding, subsequent distortions, alterations in DNA conformation, flexibility along sequence and local motions. This would then determine the domain of berberrubine-DNA complex that is accessible to the enzyme for formation of stable ternary complex ultimately leading to multiple DNA strand breaks and cell death. However our results presented here, therefore emphasize the importance of minor groove directed ligand-DNA interactions which may be of the general importance in the poisoning of topoisomerase II enzyme.



Summary and Conclusions

Over the last two decades many strategies have been developed to design drugs to control diseases like cancer and diabetes mellitus. Advancement of in our understanding of these diseases at the molecular level has provided us with new effective armors to diagnose, combat and control the spread of these diseases. In this regard the understanding of the interaction of small molecules with macromolecules like protein or DNA has opened the doors for rational drug design against cancer and type 1 and 2 diabetes mellitus. A substantial body of research has been directed towards screening of drugs acting as stimulator of insulin (insulinotropic agent) or drugs which regenerate the injured pancreatic beta cells. At the same time, focus is on for developing and improvising the existing methodology to screen potent anticancer drugs from herbal origin. The present research work is directed towards screening components which shows insulinotropic properties. As well as screen phytochemical enriched fractions which targets topoisomerases and bind to specific nucleic acid sequence of oncogenes. Therefore, this work will allow us to screen both antidiabetic and antitumor agents.

To achieve the goal of screening drugs from herbal origin; we have used both *in vitro* and *in vivo* method to screen active insulinotropic agents phytochemical from *Cinnamomum zeylanicum* and antitumor components through topoisomerase I and II inhibition assay and restriction inhibition assay using specific restriction

endonucleases. In order to gain understanding of the mode of action berberrubine-a protoberberine analogue which is known to have antitumor potential we present here the structure-conformation of berberrubine d-(CCAATTGG)₂ complex based on 1D, 2D ¹H and ³¹P NMR spectroscopy measurements followed by restrained Molecular Dynamics simulations based on observed NOEs.

In conclusion, the data obtained from the present study indicates that:

(1) *Cinnamomum zeylanicum* aqueous extract contains bioactive molecules such as Saponins which may be beneficial as both hypoglycemic and anti-hyperglycemic agents. To the best of our knowledge, this is the first ever report on the role of Saponins from *Cinnamomum zeylanicum* aqueous extract in type I diabetes. It is necessary to identify and isolate the particular compound showing the desired effect from the *Cinnamomum zeylanicum* aqueous extract. However, the present study gives a preliminary indication that the Saponins rich fraction has potential to act at multiple sites of glucose regulatory pathways. Toxicity studies proved that the dose used in this investigation is safe for the animal as it did not show any change in morphological parameter. Considering all these facts, it is reasonable to undertake further studies on possible usefulness of saponin-rich *Cinnamomum zeylanicum* aqueous extract in the treatment of type I diabetes mellitus (T1DM).

(2) A simple and rapid method—Restriction Inhibition Assay (RIA) can be used to screen anticancer compounds, plant extracts and the active phytochemicals involved in binding with restriction sequences of *Eco*RI and *Hind*III in a relatively qualitative and quantitative manner. The results show that (a) mitoxantrone bind to *Hind*III restriction site at 220 μM concentration giving a direct evidence of the co-existence of concentration and sequence specificity for drug-DNA interaction, (b) the fraction II (saponins) rich fraction from *Cinnamomum zeylanicum* shows inhibition at

minimum concentration 15 µg/ml and 2.1 µg/ml for *Eco*RI and *Hind*III restriction endonucleases, respectively (c) the *Eco*RI and *Hind*III restriction sites were found repeatedly in the cDNA/mRNA and ESTs of BRCA2 early onset oncogene. These observations project the possible use of the screened phytochemical as an anticancer agent, targeting the expression of an oncogene (BRCA2). Through this study we postulate for the first time the use of restriction inhibition assay as a rapid and simple method to screen possible anticancer phytochemical from herbal plants.

(3) The aqueous extract of *Picrorrhiza kurroa* was effective in inhibiting both topoisomerases I and II α activity. The inhibition was dose dependent for the aqueous extract with IC values 25 µg and 50 µg for topoisomerases I and II α respectively. Our results support the earlier report of anti topoisomerase I and II α activity of *Picrorrhiza kurroa* (Joy et al., 1995). In this context we are reporting for the first time the anti human topoisomerases I and II activity of the aqueous extract of *Picrorrhiza kurroa*. The inhibitory mechanism of the extract is attributed to its ability to stabilize; 1) the covalent topoisomerase I–DNA complex and, 2) the topoisomerase I and II α -extract complexes. These mechanisms therefore restrict the reversal of intermediate relaxed form of enzyme-DNA complex to its native supercoiled form. This result encourages additional studies to identify and isolate the active principle involved in inhibiting topoisomerases from the aqueous extract of *Picrorrhiza kurroa*.

(4) The interaction of berberrubine with DNA involves minor groove binding of ring B, C and D over CAATT segment without intercalation of drug chromophore between base pairs of DNA. Absence of large downfield shift of any phosphorus -31 NMR signals of A3pA4, A4pT5, T5pT6 phosphorus resonances presumably due to electrostatic interaction; presence of sequential base-sugar NOE connectivities; large upfield shift ($\Delta\delta$) in H 19, 20, H 10, H 14, H 24 and down field shift in H 31, 32 and

H 3 protons of berberrubine; change in its conformation and observation of 19 intermolecular NOEs unambiguously establish the minor groove binding mode of interaction. The DNA conformation has also changed in a subtle way to accommodate binding of drug. The width and depth of minor groove has changed from 5.87 and 4.59 to 6.02 and 5.23, respectively on binding. Results on dynamics also support our study that the perturbations, manifesting more negative value for propeller, twist at C2, A3, A4 residues, and higher opening per base pair for the central AATT residues can be due to binding of the berberrubine at the minor groove (CAATT) region of the octamer. Our results have important implications to the biological activity since DNA-binding is directly related to the poisoning of topoisomerase II enzyme.

The results also prove that it is the molecular structure that will be the diagnostic for identification of a specific drug-DNA complex as topoisomerase poison. In this context the structure-conformation of berberrubine-DNA complexes spells out the role of ring B, C and D in binding, subsequent distortions, alterations in DNA conformation, flexibility along sequence and local motions. This would then determine the domain of berberrubine-DNA complex that is accessible to the enzyme for formation of stable ternary complex ultimately leading to multiple DNA strand breaks and cell death. However our results presented here, therefore emphasize the importance of minor groove directed ligand-DNA interactions which may be of the general importance in the poisoning of topoisomerase II enzyme.

REFERENCES

1. Adams, M.D., Kelley, J.M., Gocayne, J.D., Dubnick, M., Polymeropoulos, M.H., Xiao, H., Merril, C.R., Wu, A., Olde, B., Moreno, R.F., et al. 1991. Complementary DNA sequencing: expressed sequence tags and human genome project. *Science*, 21; 252 (5013): 1651-6.
2. Anderson, R.A., Broadhurst, C.L., Polansky, M.M., Schmidt, W.F., Khan, A., Flanagan, V.P., Schoene, N.W., & Graves, D.J. 2004. Isolation and characterization of polyphenol type-A polymers from cinnamon with insulin-like biological activity. *Journal of Agricultural and Food Chemistry*, 52, 65-70.
3. Ansari, R.A., Aswal, B.S., Chander, R., Dhawan, B.N. and Sharma, S.K. 1988. Hepatoprotective activity of kutkin, the iridoid glycoside mixture of *Picrorrhiza kurroa*. *Indian Journal of Medical Research*, 87, pp. 401-404.
4. Antarkar, D.S., Vaidya, A.B., Doshi, J.C., Ramesh, V. and Kale, N. 1988. A double blind clinical trial of Arogyawardhani, an Indian drug in acute viral hepatitis. *Indian Journal of Medical Research*, 72, pp. 588-593.
5. Bai, P.V., Krishnaswami, C.V., Chellamariappan, M., Kumar, G.V and Subramaniam, J.R. 1991. Glycosuria and diabetes mellitus in children and adolescents in south India. *Diabetes Res Clin Pract.*, (1-2):131-5.
6. Bai, P.V., Krishnaswami, C.V., Chellamarippan, M., Kumar, G.V., Subramaniam, J.R., Srivatwa, A., Subramanyam, B and Rao, M.B. 1995 Nov Prevalence of diabetes in the young in south India. *Indian*

- Pediatr. 1995 Nov, 32(11):1173-6.
7. Bailly, C., Rouier, S., Bernier, J. C and Waring, M. J. 1986. DNA recognition by two mitoxantrone analogues: influence of the hydroxyl groups. *FEBS letters*, 379, 269-272.
 8. Ballerini, P., Blaise, A., Busson-Le Coniat, M., Su, X.Y., Zucman-Rossi, J., Adam, M., van den Akker, J., Perot, C., Pellegrino, B and Landman-Parker, J (2002). HOX11L2 expression defines a clinical subtype of pediatric T-ALL associated with poor prognosis. *Blood*, 100, 3: 991-997.
 9. Barthwal R., Shrikant K., Mujeeb A. (1992) A 500 MHz Proton NMR Study of Interaction of Tripeptides Lys-Tyr-Lys and Lys-Phe-Lys with Deoxydinucleotide d-CpG." *Indian Journal of Biochemistry and Biophysics*, 29(5), 394-40.
 10. Barthwal R., Prashansa A., Tripathi A. N., Sharma U., Jagannathan N. R. and Govil G. Structural elucidation of 4'-epiadriamycin by nuclear magnetic resonance spectroscopy and comparison with adriamycin and daunomycin using quantum mechanical and restrained molecular dynamics approach. *Arch Biochem Biophys*. 2008, 474, 48-64.
 11. Barthwal, R., U. Sharma, N. Srivastava, M. Jain, P. Awasthi, M.Kaur, S. K. Barthwal,, G. Govil. 2006. Structure of Daunomycin complexed to d-TGATCA by two-dimensional nuclear magnetic resonance spectroscopy. *Eur. J. Med. Chem.*, 41, 27-29.
 12. Beckers, C.J.M., Keller, D.S. and Balch, W.E. 1987. Semi-intact cells permeable to macromolecules: use in reconstruction of protein transport from the endoplasmic reticulum to the Golgi complex. *Cell*, 50:523-534.

13. Bellomo, A., Mancinella, M., Troisi, G., Ettore, E. and Marigliano, V. 2007. Diabetes and metabolic syndrome (MS). *Arch Gerontol Geriatr.* 44(1): 61-67.
14. Benoist, C., O'Hare, K., Breathnach, R and Chambon, P (1980). The ovalbumin gene-sequence of putative control regions. *Nucleic Acids Res.*, 8, 1: 127-142.
15. Borghini, S., Vargiolu, M., Di Duca, M., Ravazzolo, R and Ceccherini, I (2006). Nuclear Factor Y Drives Basal Transcription of the Human TLX3, a Gene Overexpressed in T-Cell Acute Lymphocytic Leukemia. *Molecular Cancer Research* 4, 9: 635.
16. Borghini, Silvia., Vargiolu, Manuela., Duca, Marco, Di., Ravazzolo, Robert., Ceccherini, Isabella., 2006. Nuclear factor Y drives basal transcription of the human TLX3, a gene overexpressed in T-Cell Acute Lymphocytic Leukemia. *Mol. Cancer. Res.* 9, 635-643.
17. Boulikas T. 1996. Common structural features of replication origins in all life forms. *J. Cell. Biochem.* 60, 3: 297-316.
18. Broadhurst, C.L., Polansky, M.M., & Anderson, R.A. (2000). Insulin-like biological activity of culinary and medicinal plant aqueous extracts in vitro. *Journal of Agricultural and Food Chemistry*, 48, 849-852.
19. Brondum, E., Nilsson, H., and Aalkjaer, C. (2005). Functional abnormalities in isolated arteries from Goto-Kakizaki and streptozotocin-treated diabetic rat models. *Horm. Metab. Research*, 37, 56-60.

20. Bucher, P and Trifonov, E.N. 1988. CCAAT box revisited: bidirectionality, location and context. *Journal of biomolecular structure & dynamics* 5, 6: 1231.
21. Bucher, P. 1990. Weight matrix descriptions of four eukaryotic RNA polymerase II promoter elements derived from 502 unrelated promoter sequences. *J. Mol. Biol* 212, 4: 563.
22. Capranico, G., Binaschi, M.. 1998. DNA sequence selectivity of topoisomerases and topoisomerase poisons. *Biochim. Biophys. Acta.* 1400, 185-194.
23. Cave, H., Suciu, S., Preudhomme, C., Poppe, B., Robert, A., Uyttebroeck, A., Malet, M., Boutard, P., Benoit, Y and Mauvieux, L. 2004. Clinical significance of HOX11L2 expression linked to t (5; 14)(q35; q32), of HOX11 expression, and of SIL-TAL fusion in childhood T-cell malignancies: results of EORTC studies 58881 and 58951. *Blood* 103, 2: 442-450.
24. Chaires, J. B. 1998. Drug--DNA interactions. *Curr. Opin. Struct. Biol.*, 8, 3, 314-320.
25. Chaires, J. B. and Waring, M. J. 2001. *Drug-nucleic acid interactions*, Academic Press.
26. Chaires, J. B., K. R. Fox, J. E. Herrera, M. Britt and Waring, M. J. 1987. Site and sequence specificity of the Daunomycin-DNA interaction. *Biochemistry.* 26 (25), 8227-8236.

27. Chang DK and Cheng SF (1996). On the importance of van der Waals interaction in the groove binding of DNA with ligands: restrained molecular dynamics study. *Int J Biol Macromol* **19**, 4: 279-285.
28. Chen A.Y., Liu. L.F., 1994. DNA Topoisomerase: Essential Enzymes and Lethal Targets. *Annu. Rev. Pharmacol. Toxiol.* **34**, 191-218.
29. Chen, W.H., Qin, Y., Cai, Z., Chan, C.L., Luod, G.A., Jiang, Z.H., 2005. Spectrometric studies of cytotoxic protoberberine alkaloids binding to double-stranded DNA. *Bioorg. Med. Chem.* **13**, 1859-1866.
30. Cheung, A.T., Dayanandan, B., Lewis, J.T et al. 2000. Glucose dependent insulin release from genetically engineered K cells. *Science*; **290**:1959-62.
31. Coll, M., C. A. Fredrick, A. H. J. Wang and A. Rich. 1987. A bifurcated hydrogen-bonded conformation in the d(A.T) base pairs of the DNA dodecamer d(CGCAAATTTGCG) and its complex with distamycin. *Proc. Natl. Acad. Sci. USA.* **84**, 8385-8389.
32. Crothers, D.M and Shakked, Z. 1999. *Oxford Handbook of Nucleic Acid Structure.*
33. Czarny A, Boykin DW, Wood AA, Nunn CM, Neidle S, Zhao M and Wilson WD (1995). Analysis of van der Waals and electrostatic contributions in the interactions of minor groove binding benzimidazoles with DNA. *J Am Chem Soc* **117**, 16: 4716-4717.

34. Davidson MW, Lopp I, Alexander S and Wilson WD (1977). The interaction of plant alkaloids with DNA. II. Berberinium chloride. *Nucleic Acids Res* **4**, 8: 2697-2712.
35. Denny, W.A.; Baguley, B.C. 2003. Dual Topoisomerase I / II Inhibitors in Cancer Therapy. *Current Topics in Medicinal Chemistry*, Volume 3, Number 3, pp. 339-353(15).
36. Dickerson, R.E. 1992. DNA structure from A to Z. *Methods Enzymol* **211**: 67-111.
37. Dickerson, R. E., Bansal, M., Calladine, C. R., Diekmann, S., Hunter, W. N., Kennard, O., Lavery, R., Nelson, H. C. M., Olson, W. K., Saenger, W., Shakked, Z., Sklenar, H., Soumpasis, D. M., Tung, C.-S., von Kitzing, E., Wang, A. H.-J. & Zhurkin, V. B. (1989). Definitions and nomenclature of nucleic acid structure parameters, *J. Mol. Biol.* **205**, 787–791.
38. Diwan, R and Malpathak, N. (2009) Furanocoumarins: Novel topoisomerase I inhibitors from *Ruta graveolens* L. *Bioorganic & Medicinal Chemistry* **17**, 7052–7055.
39. Efrat S. 1998. Development of engineered pancreatic B-cell lines for cell therapy of diabetes. *Adv Drug Del. Rev.*, 33-45.
40. Efstratiadis, A., Posakony, J.W., Maniatis, T., Lawn, R.M., O'Connell, C., Spritz, R.A., DeRiel, J.K., Forget, B.G., Weissman, S.M and Slightom, J.L 1980. The structure and evolution of the human B-globin gene family. *Cell* **21**: 653-668.

41. Eidi, A., Eidi, M., & Esmacili, E. 2006. Antidiabetic effect of garlic (*Allium sativum* L.) in normal and streptozotocin-induced diabetic rats. *Phytomedicine*, 13(9–10), 624–629.
42. ESTs Factsheet. National Center for Biotechnology Information.
43. Ferrando, A.A., Herblot, S., Palomero, T., Hansen, M., Hoang, T., Fox, E.A and Look, A.T. 2004. Biallelic transcriptional activation of oncogenic transcription factors in T-cell acute lymphoblastic leukemia. *Am Soc Hematology*, 103 1909-1911.
44. Flier, J., Kulkarni, R.N., Kahan, C.E. 2001. Evidence of a circulating islet cell growth factor in insulin-resistant states. *PNAS*; 98: 7475-80.
45. Forrow, S. M., M. Lee, R. L. Souhami and J. A. Hartley. 1995. The effect of AT and GC sequence specific minor groove-binding agents on restriction endonucleases activity. *Chem. Biol. Interact.*, 96, 125-142.
46. Fox, K. R., M. J. Waring, and S. Neidle. 1986. DNA sequence preferences for the anti-cancer drug mitoxantrone and related anthraquinones revealed by DNase I footprinting. *FEBS.*, 202 (2), 289-294.
47. Frederick, C. A., William, L. D., Ughetto, G., van der Marel, G. A., Van Boom, J. H., A. Rich and Wang, A. 1990. *Structural comparison of Anticancer Drug-DNA Complexes: Adriamycin and Daunomycin. Biochemistry*, 29, 2538-2549.
48. Freudenreich, C.H., Krezuer, K.N., 1993. Mutational analysis of a type II topoisomerase cleavage site: distinct requirements for enzyme and inhibitors. *EMBO. J.* 12, 2085 -2097.

49. Frolich- Ammon, S.J., Osheroff, N., 1995. Topoisomerase Poisons. Harnessing other Dark Side of Enzyme Mechanism. *J. Bio. Chem.* 270, 21429-21432.
50. Gamemeltoft, S. 1984. Insulin receptors: binding kinetics and structure-function relationship of insulin. *Physiol Rev.*, 64:1321-1378.
51. Golden, S., Wals, P. A., & Okakima, F. 1979. Glycogen synthesis by hepatocytes from diabetic rats. *Biochemical Journal*, 182(3), 727-734.
52. Gomori, G. (1941). Observations with differential stains on human islets of Langerhans. *American Journal of Pathology*, 17(3), 395-406.
53. Grover, J.K., Yadav, S., & Vats, V. (2002). Medicinal plants of India with anti-diabetic potential. *Journal of Ethnopharmacology*, 81, 81-100.
54. Gunther U. L., Ludwig C., and Ruterjans H; NMRLAB-Advanced NMR data processing in MATLAB. *J. Magn. Reson.*, 2000, 145, 201.
55. Gupta, R. K., Kesari, A. N., Watal, G., Murthy, P. S., Chandra, R., & Maithal, K. 2005. Hypoglycemic and antidiabetic effect of aqueous extract of leaves of *Annona squamosa* (L) in experimental animal. *Current Science*, 88(1), 1244-1254.
56. Handa, S.S., Sharma, A. and Chakraborti, K.K., 1986. Natural products and plants as liver protecting drugs. *Fitoterapia* 58, pp. 307-351.
57. Hartge, M.M., Unger, T., Kintscher, U. 2007. The endothelium and vascular inflammation in diabetes. *Diab Vasc Dis Res.*, 4(2):84-88.
58. Haurman, V.A., Hilbrands, R., Pinkse, G.G., Gillard, P., Duinkerken, G., Van De Linde, P., van der Meer-Prins, P.M., Vestee-g-van der Voort

- Maarschalk, M.F., Verbeeck, K., Alizadeh, B.Z., Mathieu, C., Gorus, F.K., Roelen, D.L., Claas, F.H., Keymeulen, B., Pipeleers, D.G and Roep, B.O 2008. Cellular islet autoimmunity associates with clinical outcome of islet cell transplantation. PLoS, ONE, 3(6): 24-35.
59. Hengstler, J.G., Heimerdinger, C.K., Schiffer, B., Gebhard, S., Sagemuller, J., Tanner, B., Bolt, H.M., Oesch, F., 2002. Dietary topoisomerase II –poisons: contribution of soy product to infant leukemia?. EXCLI. J. 1, 8-14.
60. Hertzberg, R.P., M.J. Caranfa, S.M. Hecht. 1989. On the mechanism of topoisomerase I inhibition by camptothecin: evidence for binding to an enzyme–DNA complex, Biochemistry. 28, 4629–4638.
61. Hiromu, K., Katudi, O., & Nenokichi, H. (1974). Constituent of essential oils from *Cinnamomum loureirii*. Reports of the scientific research institute, 10, 47-50.
62. Holden, J. A. 2001. DNA topoisomerases as Anticancer Drug Targets: From the Laboratory to the Clinic pp. 1-25 (25). Curr. Med. Chem. Anti-Cancer Agents, 1, 1.
63. Hong, S.W., Kim, S.H., Jeun, J.A., Lee, S.J., Kim, S.U., Kim, J.H., 1996. Antimicrobial activity of 9-O-acyl- and 9-O- benzoyl-substituted berberrubines. Annu. Rev. Biochem. 65, 635-692.
64. Hong, S.W., Kim, S.H., Jeun, S.J., Kim, S.U., Kim, J.H., 2000. Antimicrobial activity of 9-O-acyl- and 9-O-benzoyl-substituted berberrubines. Planta Med. 66, 361-363.

65. Hong, S.W., Kim, S.H., Jeun, S.J., Kim, S.U., Kim, J.H., 2000. Antimicrobial activity of 9-O-acyl- and 9-O-benzoyl-substituted berberrubines. *Planta Med.* 66, 361-363.
66. Hoshi, A., Ikekawa, T., Ikeda, Y., Shirakawa, S., Tigo, M., 1976. Antitumor activity of berberrubine derivatives. *Gann.* 67, 321-325.
67. Hoshi, A., Ikekawa, T., Ikeda, Y., Shirakawa, S., Tigo, M., 1976. Antitumor activity of berberrubine derivatives. *Gann.* 67, 321-325.
68. Hosur, R.V., Govil, G and Miles, H.T. 1988. Application of two-dimensional NMR spectroscopy in the determination of solution conformation of nucleic acids. *Magnetic Resonance in Chemistry* 26, 927-944.
69. Hurman, V.A., Hilbrands, R., Pinkse, G.G., Gillard, P., Duinkerken, G., Van de Linde, P., Van der Meer-Prins, P.M., Versteeg-van der Voort Maarschalk, M.F., Verbeeck, K., Alizadeh, B.Z., Mathieu, C., Gorus, F.K., Roelen, D.L., Claas, F.H., Keymeulen, B., Pipeleers, D.G. and Roep, B.O. 2008. Cellular islet autoimmunity associates with clinical outcome of islet cell transplantation. *PLoS ONE*, 3(6):24-35.
70. Ibid Wall, M. E., M. C. Wani, C. E. Cook, K. H. Palmer, A. T. McPhail and G. A. Sim, 1966, "Plant antitumor agents. I. The isolation and structure of camptothecin, a novel alkaloidal leukemia and tumor inhibitor from *Camptotheca acuminata*." *Journal of the American Chemical Society.* 88: 3888-3890.

71. Ikekawa T and Ikeda Y (1982). Antitumor activity of 13-methyl-berberrubine derivatives. *J Pharmacobiodyn* 5, 7: 469-474.
72. Ikekawa, T., Ikeda, Y., 1982. Antitumor activity of 13-methyl-beberrubine derivatives. *J. Pharmacobiodyn.* 5, 469-474.
73. Inokuchi, J., Okabe, H., Yamauch, T., & Nagamatsu, A. (1984). Inhibitors of angiotensin converting enzyme in crude drugs. *Chemical and Pharmaceutical Bulletin*, 32, 3615-3619.
74. Ishida, R., Miki, T., Narita, T., Yui, R., Sato, M., Utsumi, K.R., Tanabe, K., Andoh, T., 1991. Inhibition of Intracellular Topoisomerase II by Antitumor Bis (2, 6-dioxopiperazine) Derivatives: Mode of Cell Growth Inhibition Distinct from that of Cleavable Complex-Forming Type Inhibitors. *Cancer Research*. 51, 4903-4908.
75. Iwasa, K., Kamigauchi, M., Ueki, M., Taniguchi, M., 1996. *Antibacterial activity and structural- activity relationships of berberine analog*. *Eur. J. Med. Chem.* 31, 469-478.
76. Jarvill-Taylor, K.J., Anderson, R.A., & Graves, D.J. (2001). A hydroxychalcone derived from cinnamon function as a mimetic for insulin in 3T3-L1 adipocytes. *Journal of American College of Nutrition*, 20, 327-336.
77. Jenkins TC and Lane AN (1997). AT selectivity and DNA minor groove binding: modelling, NMR and structural studies of the interactions of

- propamidine and pentamidine with d(CGCGAATTCGCG)₂. *Biochim Biophys Acta* **1350**, 2: 189-204.
78. Jeon, Y.W., Jung, J.W., Knag, M.R., Chung, I.K., Lee, W., 2002. NMR Studies on Antitumor Drug Candidates, Berberine and Berberrubine. *Bull. Korean. Chem. Soc.* **23**, 391-394.
79. Jeon, Young, Wook., Jung, Jin, Won., Kang, Miran., Chung, In, Kwon., Lee, Weontae., 2002. *NMR studies on antitumor drug candidates, berberine and berberrubine*. *Bull. Korean Chem. Soc.* **23**, 392- 394.
80. Joseph, J., Dandekar, D.S., Ramachandran, A.V. 1996. Dexamethasone-induced alterations in glucose tolerance and, insulin, glucagon and adrenalin responses during the first month in White Leghorn chicks. *Br Poult Sci.*, **37**(3):665-676.
81. Joshi B.S., Singh K.L. and Raja R. An approach for complete assignments of ¹H and ¹³C NMR spectra of pentacyclic triterpene. *Magn. Reson. Chem.*, 1999, **37**, 295.
82. Joy, K. L., N. V. Rajeshkumar, Girija Kuttan and Ramadasan Kuttan, 2000. Effect of *Picrorrhiza kurroa* extract on transplanted tumours and chemical carcinogenesis in mice, *Journal of Ethnopharmacology* **71**, 261–266.
83. Joy, K.L. and Kuttan, R., 1995. Antioxidant activity of selected plant extracts. *Amala Research Bulletin* **15**, pp. 68–71.
84. Joy, K.L. and Kuttan, R., 1999. Anti-diabetic activity of *Picrorrhiza kurroa* extract. *Journal of Ethnopharmacology* **167**, pp. 143–148.

85. Kang, M.R., Chung, I.K., 2002. Down-Regulation of DNA Topoisomerase II α in Human Colorectal Carcinoma Cells Resistant to a Protoberberine Alkaloid, Berberrubine. *Mol. Pharma.* 61, 879-884.
86. Kang, M.R., Chung, I.K., 2002. Down-Regulation of DNA Topoisomerase II α in Human Colorectal Carcinoma Cells Resistant to a Protoberberine Alkaloid, Berberrubine. *Mol. Pharma.* 61, 879-884.
87. Kasiviswanath, R., Ramesh, A., & Kumar, K. E. (2005). Hypoglycemic and antihyperglycemic effect of *Gmelina asaistica* Linn. In normal and alloxan induced diabetic rats. *Biological and Pharmaceutical Bulletin*, 28(4), 729–732.
88. Kenneth K. Wu & Youming Huan. (2008). Streptozotocin-Induced Diabetic Models UNIT 5.47 in Mice and Rats, *Current Protocols in Pharmacology*, 5.47.1-5.47.14
89. Khan QA, Elban MA, Hecht SM. The topopyrones poison human DNA topoisomerases I and II. *J Am Chem Soc.* 2008 Oct 1;130(39):12888-9.
90. Khardori, R and Pauza, M.E. (2003). Type 1 diabetes mellitus: Pathogenesis and advances in therapy, *Int. J. Diab. Dev. Countries* .Vol. 23
91. Kim, H.S.H., & Choung, S.Y. (2006). Anti-diabetic effect of cinnamon extract on blood glucose in db/db rats. *Journal of Ethnopharmacology*, 104, 119-123.

92. Kim, S.A., Kwon, Y., Kim, J.H., Muller, M.T., Chung, I.K., 1998. Introduction of Topoisomerase II-Mediated DNA Cleavage by a Protoberberine Alkaloid, Berberrubine. *Biochemistry*. 37, 16316-16324.
93. Kim, S.H., Lee, S.J., Lee, J.H., Sun, W.S., Kim, J.H., 2002. Antimicrobial activity of 9-O-acyl- and 9-O-alkylberberrubine derivatives. *Planta Med.* 68, 277-281.
94. Kim, S.H., Lee, S.J., Lee, J.H., Sun, W.S., Kim, J.H., 2002. Antimicrobial activity of 9-O-acyl- and 9-O-alkylberberrubine derivatives. *Planta Med.* 68, 277-281.
95. Kim, Sun Ahe., Kwon, Young ., Kim, Jung Han., Muller, Mark T. Chung, In Kwon., 1998. Induction of Topoisomerase II-Mediated DNA Cleavage by a Protoberberine Alkaloid, Berberrubine. *Biochemistry*. 37, 16316-16324.
96. King, H., Aubert, R.E., & Herman, W.H. (1998). Global burden of diabetes 1995-2025 prevalence, numerical estimates and projections. *Diabetes care*, 21, 1414-1431.
97. Klevit, R. R., D. E. Wemmer and B. R. Reid. 1986. ¹H NMR studies on the interaction between Distamycin A and a Symmetrical DNA Dodecamer. *Biochemistry*., 25, 3296-3303.
98. Kolb, H. (1987). Mouse models of insulin dependent diabetes: Low-dose streptozocin-induced diabetes and nonobese diabetic (NOD) mice. *Diabetes Metab. Rev*, 3, 751-778.

99. Krishnan, P., Bastow, K.F., 2000. The 9-position in Berberine analogs is an important determinant of DNA topoisomerase II inhibition. *Anticancer Drug Des.* 15, 255-264.
100. Krishnan, P., Bastow, K.F., 2000. The 9-position in Berberine analogs is an important determinant of DNA topoisomerase II inhibition. *Anticancer Drug Des.* 15, 255-264.
101. Kuo, C. L., Chou, C C., Yung, B.Y-M., 1995. *Berberine complexes with DNA in the berberine- induced apoptosis in human leukemic HL-60 cells.* *Cancer letter.* 93, 193-200.
102. Küpeli B, Alkibay T, Sinik Z, Karaođlan U, Bozkirli I. 2000. What is the optimal treatment for lower ureteral stones larger than 1 cm?, *Int J Urol.* 2000 May;7(5):167-71.
103. Kwok, Y., Zeng, Q., Hurley, L. H., 1998. Topoisomerase II-mediated site – directed alkylation of DNA by psorospermin and its use in mapping other topoisomerase II poison binding sites. *Proc. Natl Acad. Sci. USA.* 95, 13531-13536.
104. Lancelot, G. and Paquet, F. 2003. In: G.A. Webb, Editor, *Annual Reports on NMR Spectroscopy*, Elsevier Science Ltd., 170.
105. Lane AN, Jenkins TC, Brown T and Neidle S (1991). Interaction of berenil with the EcoRI dodecamer d (CGCGAATTCGCG) 2 in solution studied by NMR. *Biochemistry* 30, 5: 1372-1385.

106. Lavery R and Sklenar H (1996). CURVES 5.1 Helical analysis of irregular nucleic Acids. *Laboratory of Theoretical Biology. CNRS, Paris.*
107. Langer, L.G., Gupta, O.P. and Atal, C.K., 1981. Clinical trials of *Picrorrhiza kurroa* as immunomodulator. *Indian Journal of Pharmacology* 13, pp. 98–99.
108. Langlois, W.J. and Olefsky, J.M. 1994. Insulin Action, Effects on Gene Expression and Regulation, and Glucose Transport. In: *Molecular Biology of Diabetes* [Eds] Draznin, B. and Reith, D.L. Humana Press, 25-50.
109. Lee, H.C., Kim, S-J., Shin, H-C et al. 2000. Remission in models of type-1 diabetes by gene therapy using single chain insulin analogue. *Nature*; 408: 483-8.
110. Li TK, Bathory E, LaVoie EJ, Srinivasan AR, Olson WK, Sauers RR, Liu LF, Pilch DS. 2000. Human topoisomerase I poisoning by protoberberines: potential roles for both drug-DNA and drug-enzyme interactions. *Biochemistry*. 20;39(24):7107-16.
111. Li, T. K.; Liu, L. F. 2001. Cell Death Induced by Topoisomerase-Targeting Drugs. *Annu. Rev. Pharmacol. Toxicol.* 41, 53.
112. Li, T.K., Bathory, E., LaVoie, E. J., Srinivasan, A.R., Olson, W.K., Sauers, R.R., Liu, L. F, Pilch, D.S., 2000. Human topoisomerase I poisoning by protoberberines: potential roles for both drug-DNA and drug-enzyme interactions. *Biochemistry*. 39, 7107-16.
113. Li, Wen- You., Lu, Zu-Hong., 1998. *The Fluorescent Reaction between Berberine and DNA and the Fluorimetry of DNA*. *Microchemical Journal*. 60, 84-88.

114. M. Jain, S. K. Barthwal, R. Barthwal, G. Govil . Restrained Molecular Dynamics studies on Complex of adriamycin With DNA hexamer sequence d-CGATCG. *Arch. Biochem. Biophys.*, 2005, 439, 12-24.
115. Ma, J.; Jones, S.; Marshall, R.; Wu, X.; Hecht, S. DNA topoisomerase I inhibitors from *Rinorea anguifera*. *Bioorg. Med. Chem. Lett.* 2005, 15, 813.
116. Maiti, R., Jana, D., Das, U.K., & Ghosh, D. (2004). Antidiabetic effect of aqueous extract of seed of *Tamarindus indica* in streptozotocin-induced diabetes rats. *Journal of Ethnopharmacology*, 92, 85-91.
117. Mantovani R (1998). A survey of 178 NF-Y binding CCAAT boxes. *Nucleic Acids Res* 26, 5: 1135-1143.
118. Mantovani, R. 1998. A survey of 178 NF-Y binding CCAAT boxes. *Nucl. Acids Res.* 26, 1135-1143.
119. Marini, J.C, Levene, S.D, Crothers, D.M and Englund, P.T (1982). Bent helical structure in kinetoplast DNA. *Proc Nat Acad Sci U.S.A* 79, 24: 7664-7668.
120. Mathew, S; & Abraham, T.E. (2006). Studies on the antioxidant activities of cinnamon (*Cinnamomum verum*) bark extracts, through various in vitro models. *Food Chemistry*, 94, 520-528.
121. Mauvieux, L., Leymarie, V., Helias, C., Perrusson, N., Falkenrodt, A., Lioure, B., Lutz, P and Lessard, M. 2002. High incidence of Hox11L2 expression in children with T-ALL. *Leukemia* 16: 2417-2422.

122. Mazzini, S., Belluccin, M.C., Mondelli, R., 2003. Mode of Binding of the Cytotoxic Alkaloid Berberine with the Double Helix Oligonucleotide D(AAGAATTCTT)₂. *Bio. Inorg. & Med. Chem.* 11, 505-514.
123. Mittal, G.C., Saxena, S., Kanchan, S.K., Mangal, O.P., Dandiya, P.C., 1978. Clinical trials on bibarin in liver disorders with special reference to infective hepatitis. *The Indian Practitioner* August, 683-693.
124. Morran, M.P., Omenn, O.S., Pietropaolo, M. 2008. Immunology and genetics of type I diabetes. *Mt Sinai J Med.*, 75(4):314-327.
125. Mukherjee, K. L. (2003). Routine biochemical tests. In K. L. Mukherjee (Ed.). *Medical laboratory technology* (Vol. III, pp. 1124-1190). New Delhi: Tata McGraw-Hill Publishing Company Limited.
126. Nagaraj, S.H., Gasser, R.B., Ranganathan, S. (Jan 2007). "A hitchhiker's guide to expressed sequence tag (EST) analysis". *Brief. Bioinformatics* 8 (1): 6-21.
127. Neidle, S. 2001. DNA minor groove recognition by small molecules. *Nat. Prod. Rep.* 18, 291-309.
128. Newgard, C.B. 1994. Cellular engineering and gene therapy. *Strategies for insulin replacement in diabetes.* 43; 341-50.
129. Nussinov R (1985). Large helical conformational deviations from ideal B-DNA and prokaryotic regulatory sites. *J Theor Biol* 115, 2: 179-189.
130. Ogiso Y, Tomida A, Lei S, Omura S, Tsuruo T. 2000. Proteasome inhibition circumvents solid tumor resistance to topoisomerase II-directed drugs. *Cancer Res.* 1;60(9):2429-34.

131. Olson M et al. 1989. A common language for physical mapping of the human genome. *Science*. Sep 29; 245(4925):1434-5.
132. Panousis, C and Phillips, D. R. DNA sequence specificity of Mitoxantrone. *Nucl. acids Res.* 1994, 22 (8), 1342-1345.
133. Paquet, F., Boudvillain, M., Lancelot G and Leng, M. 1999. NMR solution structure of a DNA dodecamer containing a transplatin interstrand GN7-CN3 cross-link. *Nucleic Acids Res* 27, 21: 4261.
134. Park, H. S., Kim, E.H., Kang, M.R., Chung, I.K., Cheong, C., Lee, W., 2004.
135. Park, H., Kim, E.H., Kang, M.R., Chung, I.K., Cheong, C., Lee, W., 2004. Spectroscopic studies on interaction of Protoberberine with Deoxyoligonucleotide d(GCCGTCGTTTTACA)₂. *Bull. Korean Chem. Soc.* 25, 1559.
136. Park, H., Kim, E.H., Sung, Y.H., Kang, M.R., Chung, I.K., Cheong, C., Lee, W., 2004. DNA binding mode of the Isoquinoline Alkaloid Berberine with the deoxyoligonucleotide d(GCCGTCGTTTTACA)₂. *Bull. Korean Chem. Soc.* 25, 539-544.
137. Park, H., Kim, E.H., Sung, Y.H., Kang, M.R., Chung, I.K., Cheong, C., Lee, W., 2004. DNA binding mode of the Isoquinoline Alkaloid Berberine with the deoxyoligonucleotide d(GCCGTCGTTTTACA)₂. *Bull. Korean Chem. Soc.* 25, 539-544.

138. Patel, S., Doble, B.W., Macaulay, K., Inchausti, E.M., Drucker, D.I., Woodgett, J.R. 2008. Tissue-specific role of glycogen synthase kinase-3 β in glucose homeostasis and insulin action. *Mol Cell Biol.*, [In press].
139. Pelton J. G and D. E. Wemmer. 1990. Binding Modes of Distamycin A with d(CGCAAATTTGCG)₂ determined by Two Dimensional NMR. *J. Am. Chem. soc.*, 112, 1393-1399.
140. Pilch, D.S., Yu, C. Makhey, D., LaVoie, E.J., Srinivasan, A.R., Olson, W.K., Ross, Warren, E., 1985. *DNA topoisomerases as targets for cancer therapy*, *Biochemical Pharmacology*. 34, 4191-4195.
141. Pommier, Y. 2009. DNA Topoisomerase I Inhibitors: Chemistry, Biology and Interfacial Inhibition *Chem Rev.* 109(7): 2894–2902.
142. Qian, Y., Fritsch, B., Shirasawa, S., Chen, C.L., Choi, Y and Ma, Q. 2001. Formation of brainstem (nor) adrenergic centers and first-order relay visceral sensory neurons is dependent on homeodomain protein Rnx/Tlx3. *Genes & Development* 15, 19: 2533-2545.
143. Qin, B., Nagasaki, M., Ren, M., Bajotto, G., Oshida, Y., & Sato, Y. (2003). Cinnamon extract (traditional herb) potentiates in vivo insulin-regulated glucose utilization via enhancing insulin signaling in rats. *Diabetes Research and Clinical Practice*, 62, 139-148.
144. Quigley, G. J., Wang, A. H., Ughetto, G., Marel, G. V. D. Boom, J. H. V and Rich, A. 1980. Molecular structure of an anticancer drug-DNA complex: daunomycin plus d(CpGpTpApCpG). *Proc .Natl. Acad. Sci. USA.* 77 (12), 7204-7208.

145. Rafatro H, Ramanitrahasimbola D, Rasoanaivo P, Ratsimamanga-Urverg S, Rakoto-Ratsimamanga A, Frappier F. 2000 May. Reversal activity of the naturally occurring chemosensitizer malagashanine in *Plasmodium malariae*. *Biochem Pharmacol.* 1;59(9):1053-61.
146. Rajeshwari, M.R (1996). Tryptophan Intercalation In G, C Containing Polynucleotides: Z to B Conversion of Poly (d (G-5M C)) in Low Salt Induced By a Tetra Peptide. *J Biomol Struct Dyn* 14, 1: 25-30.
147. Ren, J., Chaires, J.B., 1999. Sequence and structural selectivity of nucleic acid binding ligands. *Biochemistry.* 38, 16067-75.
148. Resic-Lindehamner, S. Larsson, K., Ortqvist E., Carl son, A, Cederwall, E., Cilio, C.M., Ivarsson, S.A., Jonsson, B.A., Larsson, H.E., Lynch, K., Neiderud, J. Nilsson, A., Sjoblad, S. and Lernmark A. 2008. Temporal trends of HLA genotype frequencies of type 1 diabetes patients in Sweden from 1986 to 2005 suggest altered risk. *Acta Diabetol.*, [In press].
149. Ross.W.E., 1985. DNA Topoisomerase as a target for cancer therapy. *Biochemical pharmacology.* 34, 4191-4195.
150. Sadasivam, S., & Manikam, A. (1996). Carbohydrates. In S. Sadasivam & A. Manickam (Eds.), *Methods in biochemistry* (pp. 11–12). New Delhi: New Age International Pvt. Ltd.
151. Samy, R.P. and Gopalakrishnakone, P. 2007. Current status of herbal and their future perspectives. *Nature precedings.*, 1176: 1.
152. Sanger, R.P. and Gopalakrishnokone, P. 2007. Current status of herbal

and their future perspectives. *Nature Precedings.*, 1176.1.

153. Schemeller, T., Bruning, B. L., Wink, M., 1997. *Biochemical activities of berberine, palmatine and sanguinarine mediating chemical defence against microorganisms and herbivores.* *Phytochemistry.* 2, 257-266.
154. Sebastian A. Peter, Rebecca Johnson, Charles Taylor, Andrea Hanna, Patrick Roberts, Percival McNeil, Beverley Archer, Corrine SinQuee, and Paul Roberts. 2005. The Incidence and Prevalence of Type-1 Diabetes Mellitus, *Journal of the national medical association*, Vol. 97, No. 2
155. Sebastian Yakisich, J., Åke Side'n, Peter Eneroth, and Mabel Cruz. Disulfiram Is a Potent in Vitro Inhibitor of DNA Topoisomerases. *Biochemical and Biophysical Research Communications* 289, 586–590 (2001).
156. Sehested, M.; Jensen, P. B. Mapping of DNA topoisomerase II poisons (etoposide, clerocidin) and catalytic inhibitors (aclerubicin, ICRF-187) to four distinct steps in the topoisomerase II catalytic cycle. *Biochem. Pharmacol.* 1996, 51, 879.
157. Shafer R.H. Spectroscopic studies of the interaction of daunomycin with transfer RNA. *Biochem. Pharmacol.*, 1977, 26, 1729.
158. Shulman, R.G., Bloch, G. and Rothman, D.L. 1995. In vivo regulation of muscle glycogen synthase and the control of glycogen synthesis. *Proc Natl Acad Sci USA.*, 92:8535-8542.

159. Singh, M.P., Joseph, T., Kumar S., Bathini, Y. and Lown, J. W. Synthesis and Sequence –Specific DNA binding of a Topoisomerase Inhibitory Analog of Hoechst 33258 designed for altered base and sequence recognition. *Chem. Res. Toxicol.*, 1992, 5, 597-607.
160. Skorobogaty, A., White, R. J., Phillips, D.R and Reiss, J.A. 1988. Elucidation of the DNA sequence preferences of daunomycin. *Drug Des. Deliv*, 3(2), 125-152.
161. Spectroscopic Studies on Interaction of Protoberberines with the Deoxyoligonucleotide d(GCCGTCGTTTTACA)₂. *Bull. Korean Chem.Soc.* 2, 1559-1563.
162. Sutherland, D.E.R., Gruessner RWG, Dunn DL et al. 2001. Lessons learned from more than 1,000 pancreas transplants at a single institution. *Ann Surg*; 233: 463-501.
163. Taberner L, Bella J and Aleman C (1996). Hydrogen bond geometry in DNA-minor groove binding drug complexes. *Nucleic Acids Res* 24, 17: 3458-3466.
164. Tamborlane, W.V, Bonfig, W., Boland, E. 2001. Recent advances in treatment of youth with Type-1 diabetes: better care through technology. *Diabetic. Med*;18: 864-70.
165. Tanabe, K., Ikegami, Y., Ishida, R., Andoh, T., 1991. Inhibition of Topoisomerase II by Antitumor Agents Bis (2, 6 dioxopiperazine) Derivatives. *Cancer Research.* 51, 4903-4908.
166. The Writing Team for the Diabetes Control and Complications

Trial/Epidemiology of Diabetes Interventions and Complications Research Group: effect of intensive therapy on the microvascular complications of type 1 diabetes mellitus. *JAMA* 2002; 287: 2563-9.

167. Thivolet C. New Therapeutic approaches to type 1 diabetes: from prevention to cellular or gene therapies. *Clin Endocrinol* 2001; 55:565-74.
168. Tiwari, A.K. 2005. Wisdom of Ayurveda in perceiving diabetes: Engima of therapeutic recognition. *Current Science*, 88(7):1043-1051.
169. Tiwari, A.K. and Madhusudana, R. 2005. Diabetes mellitus and multiple therapeutic approaches of phytochemicals: Present status and future prospects. *Current Science*. 83(1):30-38.
170. Trist, H. and Phillips, D. R. 1989. In vitro transcription analysis of the role of flanking sequence on the DNA sequence specificity of Adriamycin. *Nucl. acids Res.* 17(10), 3673-3687.
171. Ulyanov, N.B., Ivanov VI, Minyat EE, Khomyakova EB, Petrova MV, Lesiak K and James, T.L (1998). A Pseudosquare Knot Structure of DNA in Solution†. *Biochemistry* 37, 37: 12715-12726.
172. Ulyanov, N.B., Mujeeb A, Du Z, Tonelli M, Parslow TG and James TL (2006). NMR structure of the full-length linear dimer of stem-loop-1 RNA in the HIV-1 dimer initiation site. *J Biol Chem* 281, 23: 16168-16177.
173. Verspohl, E.J., Bauner, K., & Neddermann, E. (2005). Antidiabetic Effect of *Cinnamomum cassia* and *Cinnamomum zeylanicum* In vivo and in vitro. *Phytotherapy Research*, 19, 203-206.

174. Vestergaard, H. (1999). Studies of gene expression and activity of hexokinase, phosphofructokinase and glycogen synthase in human skeletal muscle in states of altered insulin-stimulated glucose metabolism. *Dan. Med. Bull.*, 46, 13-34
175. Vogt, C., Ardehali, H., Iozzo, P., Yki-Jarvinen, H., Koval, J., Maezono, K., Pendergrass, M., Printz, R., Granner, D., DeFronzo, R. and Mandarino, L. 2000. Regulation of hexokinase II expression in human skeletal muscle in vivo. *Metabolism*, 49:814-818.
176. Wagner, H. 2005. Natural products chemistry and phytomedicine in the 21st century: New developments and challenges. *Pure Appl Chem.*, 77(1): 1-6.
177. Wagner, H., Blatt, S., Zgainski, E.M., & Scott, T. (1984). In: 2nd Ed., *Plant drug analysis. A thin layer chromatography atlas*, Springer. p.349.
178. Wahren, J., Felig, P., Cerasi, E. and Luft, R. 1972. Hepatic glucose and amino acid metabolism in diabetes. *Isr J Med Sci.*, 8:857-862.
179. Wang, A. H. J., Ughetto, G., Quigley, G. J., and Rich, A. Interaction between anthracycline antibiotic and DNA: Molecular structure of daunomycin complexed to d-CpGpTpApCpG at 1.2 Å resolution. *Biochemistry*, 1987, 26, 1152-1153.
180. Wang, H.; Mao, Y.; Chen, A. Y.; Zhou, N.; LaVoie, E. J.; Liu, L. F. Stimulation of topoisomerase II-mediated DNA damage via a mechanism involving protein thiolation. *Biochemistry*; 2001, 40, 3316.
181. Wijesekera, R.O. (1978). Historical overview of the cinnamon industry. *CRC Critical Reviews in Food Science and Nutrition*, 10, 1-30.

182. Wright CW, Marshali SJ, Russell PF, Anderson MM, Phillipson JD, Kirby GC, Warhurst DC and Schiff PL (2000). In vitro antiplasmodial, antiamebic, and cytotoxic activities of some monomeric isoquinoline alkaloids. *J Nat Prod* **63**, 12: 1638-1640.
183. Xia, M., & Laychok, S. C. (1993). Insulin secretion myoinositol transport and Na⁺-K ATPase in glucose desensitized rat islets. *Diabetes*, 42(10), 1392–1400.
184. Y.H. Hsiang, R. Hertzberg, S. Hecht, L.F. Liu, Camptothecin induces protein-linked DNA breaks via mammalian DNA topoisomerase I, *J. Biol. Chem.* 260 (1985) 14873–14878.
185. Yadav, S., Vats, V., Dhunnoo, Y., & Grover, J. K. (2002). Hypoglycemic and antihyperglycemic activity of *Murraya koenigii* leaves in diabetic rats. *Journal of Ethnopharmacology*, 82(2), 111–116.
186. Yki-Jarvinen, H. 1993. Action of insulin on glucose metabolism in vivo. *Baillieres Clin Endocrino/ Metab.*, 7:903-927.
187. Yonezawaa, Y., Tsuyoshi Tsuzukib, Takahiro Eitsukab, Teruo Miyazawab, Takahiko Hadac, Keisuke Uryuc, Chikako Murakami-Nakaia,1, Hiroshi Ikawaa, Isoko Kuriyamaa, Masaharu Takemurad, Masahiko Oshigee, Hiromi Yoshidaa,f, Kengo Sakaguchig, Yoshiyuki Mizushinaa,f, (2005). Inhibitory effect of conjugated eicosapentaenoic acid on human DNA topoisomerases I and II, *Archives of Biochemistry and Biophysics* 435, 197–206.
188. Zhou, B.N; Johnson, R.; Mattern, M.; Wang, X.; Hecht, S.; Beck, H.; Ortiz, A.; Kingston, D. J. 2000. Isolation and Biochemical Characterization of a

New Topoisomerase I Inhibitor from *Ocotea leucoxyloides*. *Nat. Prod.*, 63 (2),
217.

